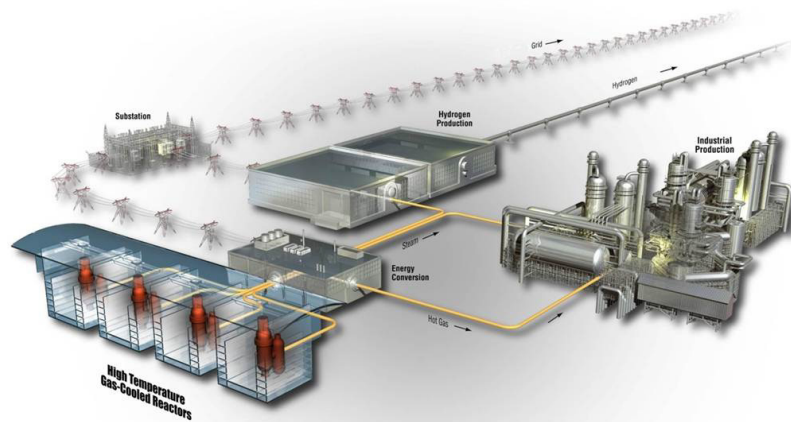




Radial Deconsolidation and Leach-Burn-Leach of Eight As-Irradiated AGR-3/4 TRISO Fuel Compacts

April 2024

John D Stempien and Lu Cai



*INL is a U.S. Department of Energy National Laboratory
operated by Battelle Energy Alliance, LLC*

DISCLAIMER

This information was prepared as an account of work sponsored by an agency of the U.S. Government. Neither the U.S. Government nor any agency thereof, nor any of their employees, makes any warranty, expressed or implied, or assumes any legal liability or responsibility for the accuracy, completeness, or usefulness, of any information, apparatus, product, or process disclosed, or represents that its use would not infringe privately owned rights. References herein to any specific commercial product, process, or service by trade name, trade mark, manufacturer, or otherwise, does not necessarily constitute or imply its endorsement, recommendation, or favoring by the U.S. Government or any agency thereof. The views and opinions of authors expressed herein do not necessarily state or reflect those of the U.S. Government or any agency thereof.

Radial Deconsolidation and Leach-Burn-Leach of Eight As-Irradiated AGR-3/4 TRISO Fuel Compacts

John D Stempien and Lu Cai

April 2024

**Idaho National Laboratory
Advanced Reactor Technologies
Idaho Falls, Idaho 83415**

<http://www.ART.INL.gov>

**Prepared for the
U.S. Department of Energy
Office of Nuclear Energy
Under DOE Idaho Operations Office
Contract DE-AC07-05ID14517**

Page intentionally left blank

INL ART Program

Radial Deconsolidation and Leach-Burn-Leach of Eight
As-Irradiated AGR-3/4 TRISO Fuel Compacts

INL/RPT-24-77357
Revision 0

April 2024

Technical Reviewer: (Confirmation of mathematical accuracy, and correctness of data and appropriateness of assumptions.)



Adriaan A. Riet, PhD
ART AGR Computational Scientist

4/1/2024

Date

Approved by:



Paul A. Demkowicz, PhD
ART AGR Fuels Technical Director

3/28/2024

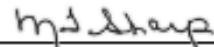
Date



Travis R. Mitchell
ART AGR Program Manager

4/1/2024

Date



Michelle T. Sharp
Idaho National Laboratory Quality Assurance

4/1/2024

Date

Page intentionally left blank

ABSTRACT

Eight as-irradiated AGR-3/4 fuel compacts were subjected to destructive post-irradiation examination via radial-deconsolidation-leach-burn leach (RDLBL) at Idaho National Laboratory (INL). The RDLBL process deconsolidated the compacts in multiple, radial steps, followed by a final, single-step axial deconsolidation. The samples generated at each step were analyzed for isotopes of key fission products and actinides. After each deconsolidation step, the compact volume was assessed, and this was used to normalize the measured quantity of nuclides of interest to give a volumetric concentration as a function of radial position within the compact. The total inventories of measured fission products and actinides and the radial-concentration profiles were compared among the eight compacts deconsolidated at INL and four other as-irradiated compacts examined at Oak Ridge National Laboratory (ORNL). The results were analyzed for the effects of irradiation temperature. These results will be used for comparisons with fission-product transport models and as input from which fission-product diffusivities can be calculated.

Page intentionally left blank

ACKNOWLEDGEMENTS

The examinations reported here were carried out over the course of 6 years, beginning in 2017. The preparations for these examinations, including the development of the methodologies and equipment, started even earlier. Philip Winston designed the in-cell radial-deconsolidation apparatus and jig for mounting the compact to the radial-deconsolidation rod. Staff at the Analytical Laboratory are acknowledged. Rodney Hudman and Richard Leavitt were the hot-cell technicians at the Analytical Laboratory responsible for mounting the compact to the rod, operating the deconsolidation apparatus, conducting caliper measurements when necessary, and carrying out the leach-burn-leach processes. Dr. Luiza Albuquerque and Dr. Magen Coleman were responsible for compiling and checking many of the data reports generated from the voluminous radiochemical measurements at Analytical Laboratory. David Laug was instrumental in sample transfers and project management support.

Page intentionally left blank

CONTENTS

ABSTRACT	ii
ACKNOWLEDGEMENTS	ii
ACRONYMS	xii
1. INTRODUCTION	1
1.1 Overall Program Purpose	1
1.2 Purpose of AGR-3/4	1
1.3 AGR-3/4 Fuel Description	1
2. SAMPLE SELECTION, EXPERIMENTAL PROCESSES, AND DATA PROCESSING	3
2.1 Sample Selection	3
2.2 Deconsolidation-Leach-Burn-Leach	4
2.2.1 Axial Deconsolidation	4
2.2.2 Radial Deconsolidation	5
2.3 Compact Dimensional Measurements by Image Analysis	9
2.4 Processing of Radiochemical Results	11
3. DIMENSIONAL RESULTS FROM COMPACT RADIAL DECONSOLIDATIONS	16
3.1 Compact 3-3	17
3.2 Compact 5-3	19
3.3 Compact 5-4	20
3.4 Compact 7-3	21
3.5 Compact 8-3	23
3.6 Compact 10-3	24
3.7 Compact 12-1	26
3.8 Compact 12-3	27
4. RESULTS AND DISCUSSION FROM RDLBL SOLUTIONS ANALYSES	29
4.1 Compact 3-3	30
4.1.1 Compact 3-3 Gamma-Emitter and Sr-90 Results	30
4.1.2 Compact 3-3 ICP-MS Results	32
4.1.3 Compact 3-3 Discussion	34
4.2 Compact 5-3	36
4.2.1 Compact 5-3 Gamma-Emitter and Sr-90 Results	36
4.2.2 Compact 5-3 ICP-MS Results	38
4.2.3 Compact 5-3 Discussion	40
4.3 Compact 5-4	41
4.3.1 Compact 5-4 Gamma-Emitter and Sr-90 Results	41
4.3.2 Compact 5-4 ICP-MS Results	42

4.3.3	Compact 5-4 Discussion	44
4.4	Compact 7-3	44
4.4.1	Compact 7-3 Gamma-Emitter and Sr-90 Results	44
4.4.2	Compact 7-3 ICP-MS Results	46
4.4.3	Compact 7-3 Discussion	48
4.5	Compact 8-3	48
4.5.1	Compact 8-3 Gamma-Emitter and Sr-90 Results	49
4.5.2	Compact 8-3 ICP-MS Results	50
4.5.3	Compact 8-3 Discussion	52
4.6	Compact 10-3	53
4.6.1	Compact 10-3 Gamma-Emitter and Sr-90 Results	53
4.6.2	Compact 10-3 ICP-MS Results	55
4.6.3	Compact 10-3 Discussion	56
4.7	Compact 12-1	57
4.7.1	Compact 12-1 Gamma-Emitter and Sr-90 Results	57
4.7.2	Compact 12-1 ICP-MS Results	59
4.7.3	Compact 12-1 Discussion	61
4.8	Compact 12-3	62
4.8.1	Compact 12-3 Gamma-Emitter and Sr-90 Results	62
4.8.2	Compact 12-3 ICP-MS Results	64
4.8.3	Compact 12-3 Discussion	66
5.	RADIAL URANIUM AND FISSION-PRODUCT-CONCENTRATION PROFILES	66
5.1	Compact 3-3 Radial Fission-Product Profiles	66
5.2	Compact 5-3 Radial Fission-Product Profiles	69
5.3	Compact 5-4 Radial Fission-Product Profiles	72
5.4	Compact 7-3 Radial Fission-Product Profiles	74
5.5	Compact 8-3 Radial Fission Product Profiles	77
5.6	Compact 10-3 Radial Fission-Product Profiles	80
5.7	Compact 12-1 Radial Fission-Product Profiles	82
5.8	Compact 12-3 Radial Fission-Product Profiles	85
5.9	Comparisons of Fission-Product Inventories and Radial Concentration Profiles	88
5.9.1	Total Fission-Product Inventories from RDLBL	88
5.9.2	Radial Fission-Product Concentration Profiles	92
6.	SUMMARY AND CONCLUSIONS	98
7.	REFERENCES	101
	Appendix A Additional RDLBL Data	106

FIGURES

Figure 1. Image of an AGR-3/4 fuel compact (left) and x-radiograph of a 2.5-mm-thick section taken from the center of an AGR-3/4 compact(right).....	2
Figure 2. Axial deconsolidation configuration.	5
Figure 3. Radial-deconsolidation apparatus and depiction of compact (x-ray image) indicating three radial segments and a central core with DTF particles.	6
Figure 4. Unirradiated AGR-3/4 compact mounted to deconsolidation rod with platinum-rhodium anode behind the compact.	7
Figure 5. Process-flow diagram for samples generated from RDLBL.	8
Figure 6. Axial deconsolidation (at left) of compact core remaining after radial deconsolidation.	9
Figure 7. Blue shading shows the compact region determined by FrameGrabber for Compact 3-3.....	10
Figure 8. Compact 3-3 reglued to the deconsolidation rod after the initial rod-compact bond failed.....	18
Figure 9. Compact 3-3 held by tweezers after the fourth segment of deconsolidation, after the compact had fallen off the deconsolidation rod.....	18
Figure 10. Frame 89 from video DSC_0073 taken of Compact 5-3 after the third segment of deconsolidation.	19
Figure 11. Frame 60 from the analysis of video DSC_0042 taken after the third radial deconsolidation segment of Compact 5-4.	20
Figure 12. Pre-deconsolidation photo taken through the hot cell window showing a piece of material missing from Compact 7-3.....	22
Figure 13. Frame 103 from video DSC_0064 taken after the second and final radial segment was obtained from Compact 7-3.	22
Figure 14. Screenshot from video DSC_0013 taken after the first segment was obtained from Compact 8-3.	24
Figure 15. (a) Compact 10-3 fell from the rod after it was initially epoxied before deconsolidation. There seemed to be a piece of compact that came off the top of the compact. (b) Scratches appear on the side of the compact. (c)The compact fell off the rod a second time during radial deconsolidation of Segment 2. (d) The compact fell off the rod a third time after radial Segment 3.....	25
Figure 16. Images of Compact 12-1 after it had been mounted to the rod, prior to the start of deconsolidation.	26
Figure 17. Frame 175 from analysis 11k_2_DSC_4613 after the 16 minutes of Segment 1 radial deconsolidation of Compact 12-1 was completed.....	27
Figure 18. (a) Epoxy and some compact material adhered to rod. (b) Compact showing the end formerly bonded to the rod. Photos taken through the hot cell window.	28
Figure 19. Analysis from Frame 1670 analyzed from video DSC_4475.	28
Figure 20. Compact 3-3 fission-product radial-concentration profiles in units of particle equivalents/mm ³	68
Figure 21. Compact 3-3 fission-product radial-concentration profiles in units of Bq/mm ³	68
Figure 22. Comparison of U-238 and Ce-144 radial-concentration profiles in Compact 3-3.	69

Figure 23. Compact 5-3 fission-product radial-concentration profiles in units of particle equivalents/mm ³	71
Figure 24. Compact 5-3 fission-product radial-concentration profiles in units of Bq/mm ³	71
Figure 25. Comparison of Ce-144 and U-238 radial-concentration profiles for Compact 5-3.....	72
Figure 26. Compact 5-4 fission-product radial-concentration profiles in units of particle equivalents/mm ³	73
Figure 27. Compact 5-4 fission-product radial-concentration profiles in units of Bq/mm ³	74
Figure 28. Comparison of Ce-144 and U-238 radial-concentration profiles for Compact 5-4.....	74
Figure 29. Compact 7-3 fission-product radial-concentration profiles in units of particle equivalents/mm ³	76
Figure 30. Compact 7-3 fission-product radial-concentration profiles in units of Bq/mm ³	76
Figure 31. Comparison of U-238 and Ce-144 radial-concentration profiles in Compact 7-3.	77
Figure 32. Compact 8-3 fission-product radial-concentration profiles in units of particle equivalent/mm ³	78
Figure 33. Compact 8-3 fission-product radial-concentration profiles in units of Bq/mm ³	79
Figure 34. Comparison of U-238 and Ce-144 radial-concentration profiles in Compact 8-3.	79
Figure 35. Radial concentrations of fission products in Compact 10-3 (uncorrected for particles accidentally broken) in units of Bq/mm ³	81
Figure 36. Radial concentrations of fission products in Compact 10-3 (uncorrected for particles accidentally broken) in units of particle equivalents/mm ³	81
Figure 37. Comparison of Ce-144 and U-238 radial-concentration profiles (uncorrected for particles accidentally broken) in Compact 10-3.	82
Figure 38. Radial concentrations of fission products in Compact 12-1 in units of particle equivalents/mm ³	84
Figure 39. Radial concentrations of fission products in Compact 12-1 in units of Bq/mm ³	84
Figure 40. Comparison of Ce-144 and total-uranium radial-concentration profiles in Compact 12-1.....	85
Figure 41. Compact 12-3 fission-product radial-concentration profiles in units of particle equivalents/mm ³	86
Figure 42. Compact 12-3 fission-product radial-concentration profiles in units of Bq/mm ³	87
Figure 43. Comparison of Ce-144 and U-238 radial-concentration profiles for Compact 12-3.....	87
Figure 44. Compact RDLBL and capsule mass-balance inventories as a function of calculated compact TAVA irradiation temperatures.	89
Figure 45. Total RDLBL inventories of Eu-154 and Sr-90 in AGR-3/4 fuel compacts outside of the SiC layer of TRISO-coated driver-fuel particles as a function of TAVA temperature.....	90
Figure 46. Particle equivalents of Cs-134 and Cs-137 as function of compact TAVA temperature.	92
Figure 47. The AGR-3/4 compact radial-concentration profiles for U-238.	94
Figure 48. The AGR-3/4 compact radial-concentration profiles for Ce-144.....	95
Figure 49. Radial-concentration profiles for Eu-154 in AGR-3/4 compacts.	96
Figure 50. The concentration of Sr-90 particle equivalents as function of compact radius.	97
Figure 51. The concentration of Cs-134 particle equivalents as function of compact radius.....	98

TABLES

Table 1. As-fabricated particle dimensions and standard deviations from Table A-2 of the “AGR-3/4 Irradiation Test Final As-Run Report” (Collin 2015a).....	3
Table 2. AGR-3/4 fuel compacts subject to as-irradiated radial deconsolidation and their irradiation properties.....	3
Table 3. Typical radial deconsolidation parameters.....	7
Table 4. Summary of video equipment and resolutions used for the eight compacts investigated here.....	10
Table 5. Combinations of threshold variables used for analyses in FrameGrabber.....	11
Table 6. Inventories of fission products and actinides calculated to have been produced in Compact 3-3.....	12
Table 7. Inventories of fission products and actinides calculated to have been produced in Compact 12-1.....	12
Table 8. Inventories of fission products and actinides calculated to have been produced in Compact 12-3.....	13
Table 9. Inventories of fission products and actinides calculated to have been produced in Compact 5-3.....	13
Table 10. Inventories of fission products and actinides calculated to have been produced in Compact 5-4.....	14
Table 11. Inventories of fission products and actinides calculated to have been produced in Compact 7-3.....	14
Table 12. Inventories of fission products and actinides calculated to have been produced in Compact 8-3.....	15
Table 13. Inventories of fission products and actinides calculated to have been produced in Compact 10-3.....	15
Table 14. Comparison of compact diameter measured by contact metrology and video analysis via FrameGrabber.....	17
Table 15. Summary of Compact 3-3 diameter change, new diameter after each segment of deconsolidation, and the volume of each segment.....	19
Table 16. Summary of Compact 5-3 diameter change, new diameter after a segment of deconsolidation, volume of the compact material removed, and the volume of the core remaining after the three segments of radial deconsolidation.....	20
Table 17. Summary of Compact 5-4 diameter change, new diameter after a segment of deconsolidation, volume of the compact material removed, and the volume of the core remaining after the three segments of radial deconsolidation.....	21
Table 18. Summary of Compact 7-3 diameter change, new diameter after a segment of deconsolidation, volume of the compact material removed, and the volume of the core remaining after the two segments of radial deconsolidation.....	23
Table 19. Summary of Compact 8-3 diameter change. See text for explanation of Segment 2 volume.....	24
Table 20. Summary of Compact 10-3 diameter change.....	25
Table 21. Summary of Compact 12-1 diameter change, new diameter after each segment of deconsolidation, and the volume of the compact material removed.....	27
Table 22. Summary of Compact 12-3 diameter change, new diameter after a segment of deconsolidation, and the volume of the compact material removed.....	29
Table 23. Particle-equivalent inventories measured in the solutions from the radial deconsolidation of Compact 3-3.....	30
Table 24. Relative error in the Compact 3-3 RDLBL results.....	31

Table 25. Particle equivalents for select actinides from ICP-MS of solutions from Compact 3-3 RDLBL.....	32
Table 26. Error in the Compact 3-3 ICP-MS results that were summarized in the preceding tables.	33
Table 27. Particle-equivalent inventories measured in the solutions from the radial deconsolidation of Compact 5-3.	36
Table 28. Relative error in the Compact 5-3 RDLBL results.	37
Table 29. Particle equivalents for select actinides from ICP-MS of solutions from Compact 5-3 RDLBL.....	38
Table 30. Relative error for select actinides from ICP-MS of solutions from Compact 5-3 RDLBL.	39
Table 31. Particle-equivalent inventories measured in the solutions from the radial deconsolidation of Compact 5-4.	41
Table 32. Relative error in the Compact 5-4 RDLBL results.	42
Table 33. Particle equivalents for select actinides from ICP-MS of solutions from Compact 5-4 RDLBL.....	43
Table 34. Relative error in the Compact 5-4 ICP-MS results given in the preceding table.....	43
Table 35. Particle-equivalent inventories measured in the solutions from the radial deconsolidation of Compact 7-3.	45
Table 36. Relative error in the Compact 7-3 RDLBL results.	46
Table 37. Particle equivalents for select actinides from ICP-MS of solutions from Compact 7-3 RDLBL.....	47
Table 38. Relative error in the Compact 7-3 ICP-MS results.	47
Table 39. Particle-equivalent inventories measured in the solutions from the radial deconsolidation of Compact 8-3.	49
Table 40. Relative error in the Compact 8-3 RDLBL results.	50
Table 41. Particle equivalents for select actinides from ICP-MS of solutions from Compact 8-3 RDLBL.....	50
Table 42. Relative error in the Compact 8-3 ICP-MS results given in the preceding tables.	51
Table 43. Particle-equivalent inventories measured in the solutions from the radial deconsolidation of Compact 10-3.	53
Table 44. Relative error for the RDLBL results from Compact 10-3.	54
Table 45. Particle equivalents for select actinides from ICP-MS of solutions from Compact 10-3 RDLBL.....	55
Table 46. Relative error in the Compact 10-3 U and Pu results given in Table 45.....	55
Table 47. Particle-equivalent inventories measured in the solutions from the radial deconsolidation of Compact 12-1.	57
Table 48. Relative error in the Compact 12-1 results.	58
Table 49. Uranium and plutonium measured from radial deconsolidation of Compact 12-1.....	59
Table 50. Relative error in the Compact 12-1 U and Pu measurements given in Table 49.	60
Table 51. Masses of spilled (and recovered) and unspilled particles and matrix debris from the axial deconsolidation of the core of Compact 12-3.	62
Table 52. Quantity of fission products measured in the solutions from the radial deconsolidation of Compact 12-3.	63
Table 53. Relative error for the results from the Compact 12-3 RDLBL.....	63

Table 54. Particle equivalents for select actinides from ICP-MS of solutions from Compact 12-3 RDLBL.....	64
Table 55. Relative error in ICP-MS results for Compact 12-3.	65
Table 56. Radial fission product and U-238 concentrations expressed in several units for Compact 3-3.....	67
Table 57. Relative error for the Compact 3-3 fission product and U-238 concentrations given in Table 56.	67
Table 58. Radial fission product and U-238 concentrations expressed in several units for each segment of Compact 5-3.	70
Table 59. Relative error in the Compact 5-3 concentrations given in Table 58.....	70
Table 60. Radial fission-product and U-238 concentrations expressed in several units for each segment of Compact 5-4.	73
Table 61. Relative error in the Compact 5-4 concentrations given in Table 60.....	73
Table 62. Radial fission product and U-238 concentrations expressed in several units for Compact 7-3.....	75
Table 63. Error for the Compact 7-3 fission product concentrations given in Table 62.	75
Table 64. Radial fission product and U-238 concentrations for Compact 8-3.	78
Table 65. Uncertainty for the Compact 8-3 fission product and U-238 concentrations given in Table 64.....	78
Table 66. Radial fission-product and U-238 concentrations for each segment of Compact 10-3.	80
Table 67. Error in the Compact 10-3 radial fission-product concentrations given in Table 66.	80
Table 68. Radial fission-product and uranium concentrations for each segment of Compact 12-1.	83
Table 69. Error in the Compact 12-1 radial fission-product and uranium concentrations given in Table 68.	83
Table 70. Radial fission-product and U-238 concentrations for each segment of Compact 12-3.	85
Table 71. Uncertainties in the Compact 12-3 concentrations given in Table 70.	86
Table 72. List of all as-irradiated AGR-3/4 compacts analyzed at INL and ORNL and whether corrections were applied to their results to account for accidental particle damage.....	88
Table 73. Activities of fission products measured in the solutions from RDLBL of Compact 3-3.	106
Table 74. Fraction (M/C) of the compact inventory of fission products measured in the solutions from RDLBL of Compact 3-3.....	107
Table 75. Masses for select actinides from ICP-MS analyses of solutions from Compact 3-3 RDLBL.....	108
Table 76. Compact fractions for select actinides from ICP-MS of solutions from Compact 3-3 RDLBL.....	109
Table 77. Activities of fission products measured in the solutions from RDLBL of Compact 5-3.....	110
Table 78. Fraction (M/C) of the compact inventory of fission products measured in the solutions from RDLBL of Compact 5-3.....	111
Table 79. Masses for select actinides from ICP-MS of solutions from Compact 5-3 RDLBL.	112
Table 80. Compact fractions for select actinides from ICP-MS of solutions from Compact 5-3 RDLBL.....	113
Table 81. Activities of fission products measured in the solutions from RDLBL of Compact 5-4.....	114
Table 82. Fraction (M/C) of the compact inventory of fission products measured in the solutions from RDLBL of Compact 5-4.....	115
Table 83. Masses for select actinides from ICP-MS of solutions from Compact 5-4 RDLBL.	116

Table 84. Compact fractions for select actinides from ICP-MS of solutions from Compact 5-4 RDLBL.....	116
Table 85. Activities of fission products measured in the solutions from RDLBL of Compact 7-3.....	117
Table 86. Fraction (M/C) of the compact inventory of fission products measured in the solutions from RDLBL of Compact 7-3.....	118
Table 87. Masses for select actinides from ICP-MS of solutions from Compact 7-3 RDLBL.	119
Table 88. Compact fractions for select actinides from ICP-MS of solutions from Compact 7-3 RDLBL.....	120
Table 89. Activities of fission products measured in the solutions from the RDLBL of Compact 8-3.	120
Table 90. Fraction (M/C) of the compact inventory of fission products measured in the solutions from RDLBL of Compact 8-3.....	121
Table 91. Masses for select actinides from ICP-MS of solutions from Compact 8-3 RDLBL.	122
Table 92. Compact fractions for select actinides from ICP-MS of solutions from Compact 8-3 RDLBL.....	123
Table 93. Activities of fission products measured in the solutions from RDLBL of Compact 10-3.....	123
Table 94. Fraction (M/C) of the compact inventory of fission products measured in the solutions from the radial deconsolidation of Compact 10-3.	124
Table 95. Masses for select actinides from ICP-MS of solutions from Compact 10-3 RDLBL.	125
Table 96. Compact fraction for select actinides from ICP-MS of solutions from Compact 10-3 RDLBL.	126
Table 97. Activities of fission products measured in the solutions from RDLBL of Compact 12-1.....	127
Table 98. Fraction (M/C) of the compact inventory of fission products measured in the solutions from the radial deconsolidation of Compact 12-1.	128
Table 99. Activities of fission products measured in the solutions from the radial deconsolidation of Compact 12-3.....	129
Table 100. Fraction of fission products measured in the solutions from the radial deconsolidation of Compact 12-3 compared to the calculated inventory (M/C).	129
Table 101. Masses of select actinides from ICP-MS analysis of Compact 12-3 RDLBL.....	130
Table 102. Compact fractions for select actinides from ICP-MS analysis of Compact 12-3 RDLBL.	131

ACRONYMS

AGR	Advanced Gas Reactor
AL	Analytical Laboratory
ART	Advanced Reactor Technologies
ATR	Advanced Test Reactor
C	Calculated value
DC	direct current
DLBL	Deconsolidation leach burn leach
DTF	Designed-to-fail
EOI	End of irradiation
FACS	Fuel Accident Condition Simulator
FIMA	Fissions per initial metal atom
HDPE	high-density polyethylene
HFEF	Hot Fuels Examination Facility
HTGR	High-temperature gas-cooled reactor
ICP-MS	Inductively coupled plasma mass-spectrometry
INL	Idaho National Laboratory
IPyC	Inner pyrolytic carbon
M	Measured value
M/C	Measured-to-calculated ratio
MDA	Minimum detectable activity
OPyC	Outer pyrolytic carbon
ORNL	Oak Ridge National Laboratory
PyC	pyrolytic carbon
PIE	Post-irradiation examination
RDLBL	Radial-deconsolidation leach burn leach
SiC	silicon carbide
TA	Time-averaged
TAVA	Time-average volume-average
TRISO	Tristructural isotropic
UCO	Uranium oxycarbide (a heterogeneous mixture of uranium carbide and uranium oxide)

Page intentionally left blank

Radial Deconsolidation and Leach-Burn-Leach of Eight As-Irradiated AGR-3/4 TRISO Fuel Compacts

1. INTRODUCTION

1.1 Overall Program Purpose

The Advanced Gas Reactor (AGR) Fuel Development and Qualification Program was established to perform research and development on tristructural isotropic (TRISO) coated-particle fuel to support deployment of a high-temperature gas-cooled reactor (HTGR). This work continues as part of the Advanced Reactor Technologies (ART) Program. The overarching goal of the ART AGR program is to provide a data set to support TRISO fuel qualification and the licensing and operation of HTGRs. To achieve these goals, the program includes the elements of fuel fabrication, irradiation, post-irradiation examination (PIE) and high-temperature tests, fuel performance modeling, and fission product transport (Idaho National Laboratory 2022). The fourth and final AGR TRISO fuel irradiation was completed at the Advanced Test Reactor (ATR) at Idaho National Laboratory (INL) in July 2020.

1.2 Purpose of AGR-3/4

The AGR-1 and AGR-2 experiments focused on the performance of high-quality TRISO fuel, and PIE focused on quantifying the very small rates of SiC and TRISO coating failures. In contrast, the AGR-3/4 experiment was primarily a fission-product-transport experiment focused on observing the migration of fission products throughout fuel and nuclear-grade graphites. Following irradiation, measurements of the fission-product concentration profiles (both axially and radially) within AGR-3/4 samples (primarily the graphite rings and compacts) has constituted the bulk of PIE (Stempien et al. 2018; Stempien 2021; Harp, Stempien, and Demkowicz 2021; Riet 2022). These data are being used to support refinement of fission-product-transport models and HTGR source-term analyses (Riet and Stempien 2022, Riet 2023).

1.3 AGR-3/4 Fuel Description

The cylindrical AGR-3/4 fuel compacts contained TRISO-coated driver-fuel particles, similar to AGR-1 baseline fuel (Collin 2015a; Hunn and Lowden 2007; Hunn et al. 2014) and designed-to-fail (DTF) particles to intentionally release fission products during irradiation to migrate through the surrounding cylindrical rings of graphitic matrix and nuclear-grade graphite. Each AGR-3/4 compact contained 20 DTF particles in addition to the approximately 1,898 TRISO-coated “driver” fuel particles. DTF fuel kernels were coated only with a thin (20- μm -thick) pyrocarbon layer. This layer was intentionally fabricated with high anisotropy, such that it would be likely to fail during the irradiation (Collin 2015a; Hunn and Miller 2009; and Kercher et al. 2011), resulting in 20 exposed fuel kernels per compact. As shown at right in Figure 1, the DTF particles (highlighted in red) were aligned roughly along the compact radial centerline. DTF particles provided a known source of fission products to migrate radially outward in the compacts and into the surrounding concentric rings of graphite and/or matrix material. It was expected that intact DTF particles would behave like TRISO particles with SiC layer failures (releasing substantial Cs, but retaining fission gases), and failed DTF particles (DTF particles with breached pyrocarbon layers) would behave like TRISO particles with failed TRISO coatings (releasing both Cs and fission gases).

The white particles in Figure 1 are the driver particles. AGR-3/4 driver-particle fuel kernels were fully TRISO-coated with buffer layer, inner pyrolytic carbon layer (IPyC), silicon carbide layer (SiC), and outer pyrolytic carbon layer (OPyC) characteristics similar to the Baseline fuel from the AGR-1 experiment (Collin 2015b; Hunn and Lowden 2007). Both the AGR-3/4 driver and DTF fuel particles contain UCO fuel kernels (approximately 350 μm in diameter) manufactured at BWXT (formerly BWX Technologies Nuclear Operations Group). The U-235 enrichment was 19.7 wt%. The DTF pyrocarbon coating and the driver fuel TRISO coatings were applied to the kernels at Oak Ridge National Laboratory (ORNL). Driver particle and DTF particle properties were summarized by Collin (2015a). Complete kernel and particle characterization and fabrication data were compiled in several AGR-program reports and publications (Kercher and Hunn 2006; Hunn and Lowden 2007; Hunn and Miller 2009; Kercher et al., 2011). Driver fuel particles and DTF particles had average dimensions summarized in Table 1.

AGR-3/4 driver and DTF particles were over-coated with a precursor to graphitic-matrix material and formed into cylindrical fuel compacts at ORNL. The compact graphitic-matrix material is composed of multiple types of graphite and a carbonized phenolic resin. Compacts were nominally 12.3 mm in diameter and 12.5 mm long (in contrast to the AGR-1 and AGR-2 compacts, which were approximately 12.3 mm in diameter and 25 mm long). A summary of AGR-3/4 fuel compact properties is provided in the AGR-3/4 Final As-Run Report (Collin 2015a). Detailed characterization data of the as-fabricated compacts have been compiled in an AGR-program report (Hunn, Trammel, and Montgomery 2011).

Each compact has a unique identifier denoting its position in the irradiation test train. In the X-Y compact naming convention, X denotes the capsule number, and Y denotes the level of the compact within the capsule (with Level 1 at the bottom and Level 4 at the top of the capsule). In AGR-3/4 there were four compacts per capsule. Thus, for example, Compact 3-3 is the third compact from the bottom of Capsule 3, and Compact 12-1 is the bottom compact from Capsule 12.

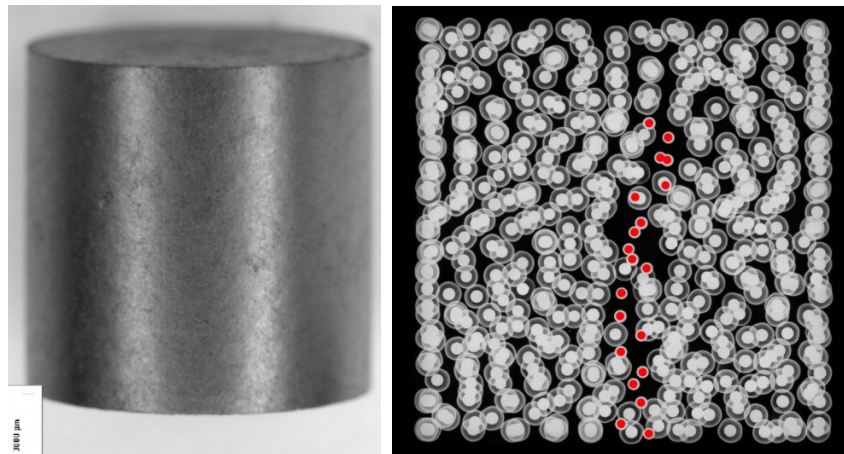


Figure 1. Image of an AGR-3/4 fuel compact (left) and x-radiograph of a 2.5-mm-thick section taken from the center of an AGR-3/4 compact(right) (Hunn, Trammell, and Montgomery 2011). DTF particles are highlighted with red dots in the x-ray image.

Table 1. As-fabricated particle dimensions and standard deviations from Table A-2 of the “AGR-3/4 Irradiation Test Final As-Run Report” (Collin 2015a).

DTF Particle Properties	
Kernel diameter (μm)	357.3 ±10.5
DTF pyrocarbon thickness (μm)	20.0 ±9
DTF particle overall diameter (μm)	400.0 ±9.2
Driver Particle Properties	
Kernel diameter (μm)	357.3 ±10.5
Buffer thickness (μm)	109.7 ±7.7
IPyC thickness (μm)	40.4 ±2.3
SiC thickness (μm)	33.5 ±1.1
OPyC thickness (μm)	41.3 ±2.1
Driver particle overall diameter (μm)	818.9 ±14.2

2. SAMPLE SELECTION, EXPERIMENTAL PROCESSES, AND DATA PROCESSING

2.1 Sample Selection

Table 2 lists all eight of the compacts that have undergone radial deconsolidation in the as-irradiated state at INL. Additional compacts have undergone radial deconsolidation at INL after heating tests were performed in the fuel accident condition simulator (FACS) furnace. The results from INL’s post-FACS radial deconsolidations will be reported separately. Another group of compacts was shipped to ORNL for as-irradiated or post-FACS radial deconsolidation, and those results have already been reported (Hunn et al. 2020, Helmreich et al. 2021, Helmreich et al. 2022).

Table 2. AGR-3/4 fuel compacts subject to as-irradiated radial deconsolidation and their irradiation properties. This information was summarized by Collin (2015a), but the neutronic and thermal calculations were performed by Sterbentz (2015) and Hawkes (2016), respectively.

Compact	Burnup (% FIMA)	Neutron Fluence (10^{25} n/m ² , E>0.18 MeV)	Time-Average Volume-Average (TAVA) Temperature (°C)	Time-Average Minimum Temperature (°C)	Time-Average Peak Temperature (°C)
3-3	12.73	4.28	1205	1170	1242
5-3	14.92	5.22	1050	1001	1102
5-4	14.98	5.23	989	858	1084
7-3	15.00	5.27	1376	1335	1418
8-3	14.54	5.07	1213	1171	1257
10-3	11.75	3.89	1210	1174	1248
12-1	5.87	1.8	849	802	883
12-3	5.17	1.41	864	844	884

2.2 Deconsolidation-Leach-Burn-Leach

Each as-irradiated AGR-3/4 fuel compact was subjected to multiple deconsolidation-leach-burn-leach (DLBL) operations as described below. The basic DLBL method used has been detailed in various PIE reports (e.g., Hunn et al. 2013; Stempien 2020). Actinides and fission products not contained within the boundary of normally retentive SiC layers were subject to dissolution in the DLBL leachates (contingent upon the individual fission-product solubilities and the ability of the acid to access their location). The dissolved actinides and fission products included those that (a) had migrated through normal SiC, but were still retained within the compact, (b) were related to uranium contamination present in the compact matrix and/or OPyC at the time the compact was fabricated, (c) were externally introduced by contamination from sources present in the hot cell, (d) were from particles with compromised SiC (with or without other compromised coatings), and (e) were from the DTF particles.

There are two methods of compact deconsolidation, axial and radial. The axial process deconsolidates the compact in a single step. The radial process deconsolidates the compact in multiple, radial steps, followed by a final single-step axial deconsolidation of the remaining material.

2.2.1 Axial Deconsolidation

The following is a brief discussion of traditional (axial) fuel compact DLBL. Additional discussion is available in Appendix B of Stempien (2020). Figure 2 illustrates the basic setup used for axial deconsolidations. The very bottom portion of the compact is immersed in nitric acid, but most of the compact is above the level of the acid at the start of the deconsolidation. A cathode wire is placed in the acid, and an anode wire is put in contact with the top of the compact that is above the level of the acid. A voltage is then applied to the cathode and anode wires, and the acid acts as an electrolyte to complete the circuit. Oxidation of the compact breaks up the compact matrix, TRISO particles are liberated, and TRISO particles and debris from the matrix are collected on a porous, fused silica frit (also referred to as a thimble) at the bottom of the apparatus. In this axial deconsolidation, the compact matrix is disintegrated from the bottom to the top. Some of the fission-product inventory in the matrix material outside of the particle OPyC layers will be dissolved in the deconsolidation solution. The deconsolidation solution is then analyzed for gamma-emitting fission products and undergoes analysis for beta-emitting Sr-90. The TRISO particles and matrix debris collected on the thimble frit are rinsed, dried, and leached twice in hot nitric acid to dissolve fission products. Following these two pre-burn leaches, the particles and matrix debris are oxidized (“burned”) in air at 750°C in a muffle furnace until the OPyC layer of the particles has been removed via oxidation. After this burn step, the particles and any remaining ash are leached twice. The two pre- and post-burn leaches are analyzed for gamma-emitting fission products and Sr-90. Inductively coupled plasma mass-spectrometry (ICP-MS) analysis is also performed on the solutions (primarily to quantify actinide inventory).

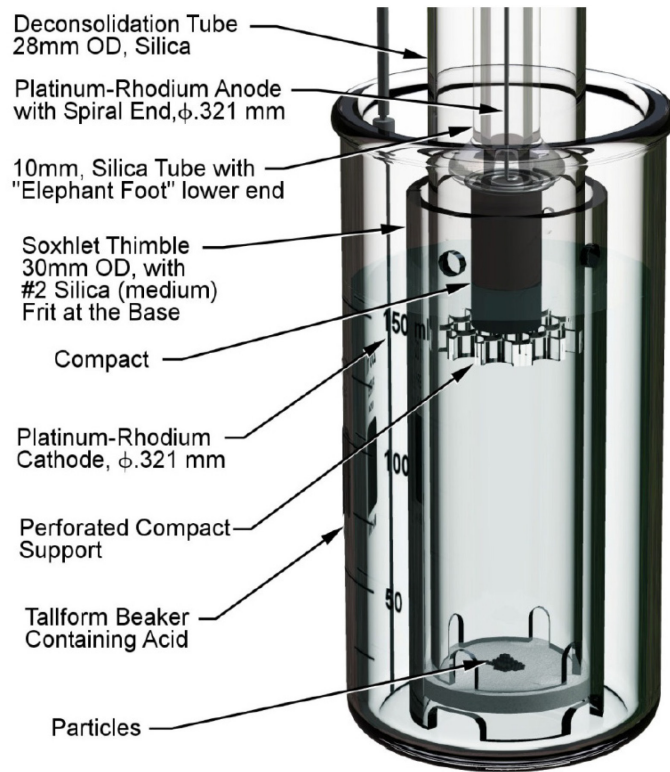


Figure 2. Axial deconsolidation configuration.

2.2.2 Radial Deconsolidation

Radial deconsolidation-leach-burn leach (RDLBL) has three benefits over a one-step axial deconsolidation. First, RDLBL enables measurements of the radial fission-product-concentration profile within a compact outside of the TRISO SiC layer. Second, RDLBL allows collection and analysis of particles from specific radial regions of a compact. Temperature gradients in compacts during irradiation may result in differences in fission-product retention between particles from different radial zones. It might be possible to observe such differences by separately analyzing the particles recovered from the different radial zones. Third, RDLBL allows radial segments of the compact to be removed without disturbing the DTF particles located approximately in the center of the compact. If failed DTF particles were deconsolidated along with other portions of the compact, the fission-product inventory of the OPyC and compact matrix would be difficult or impossible to distinguish from that still retained in the DTF fuel kernels.

Figure 3 shows the first iteration of the radial-deconsolidation apparatus developed at INL that was installed in Cell 5 at the Analytical Laboratory (AL). One end of the compact was epoxied to one end of a 6-mm diameter, hollow stainless-steel shaft (referred to here as a “rod”) using AA-CARB 61 conductive epoxy from Atom Adhesives. To mount the compact to the rod, the rod and its remote manipulator handle were set into a jig (INL 2017d). The epoxy was mixed outside the cell and loaded into a 1-mL syringe that was transferred into the hot cell and connected to the hollow rod, allowing the epoxy to be pumped into the gap between the rod and the compact. On the other end of the rod was a gear driven at 10 revolutions per minute by a direct current (DC) electric gearmotor (INL 2017b). A platinum wire was also epoxied into the rod such that it protruded from the compact-epoxy interface. This Pt wire facilitated electrical contact for the axial deconsolidation of the compact core that remained after the radial deconsolidation had been completed. The remote handle with the gear and compact attached was then positioned in the main deconsolidation drive apparatus and latched into place to engage the drive gear (INL 2017b). With the compact and the stainless-steel deconsolidation rod in place, a micrometer was used to lower the height of the rod and compact so that the rod was just within the mouth of the

beaker (Figure 4). More recently, the micrometer was replaced by a simple threaded knob to allow easier height adjustments. Figure 4 shows that the platinum-rhodium anode screen behind the compact was fixed to a high-density polyethylene (HDPE) paddle (called a “drag paddle” in [INL 2017c]), and the screen/paddle was adjusted by insertion of an HDPE wedge (INL 2017a) behind the paddle so that the screen made consistent, even contact with the compact (INL 2017a, INL 2017c).

The electrical leads to the platinum-rhodium anode screen and the cathode wire (inserted in the space between the walls of the thimble and the beaker) were connected to a DC power supply. Then, the compact rotation was started, and the top of the compact was rotated toward the anode screen. With the anode and cathode leads connected, the anode in contact with the compact, and the compact rotating, 8M nitric acid was added to the beaker, which also fills the thimble through the porous frit in the bottom of the thimble and the holes toward the top of the thimble. Acid was added until it just contacted the compact. With a complete electrical circuit between the anode, cathode, compact, and nitric acid, contact between the compact and the anode screen helped remove deconsolidated matrix material, allowing particles to come loose and fall to the bottom of the thimble. The DC power supply was operated in current-control mode (constant-voltage mode), and the voltage was adjusted manually such that the electrical power applied to the compact during deconsolidation was less than 10 W. The current (and total power) often varied as compact deconsolidation progressed. Towards the end of a radial deconsolidation, as the compact diameter approached that of the deconsolidation rod, the voltage might be constant at 7.5 V, but the applied current might vary from 0.1 to 1.5 A. Significant process development for the RDLBL method was performed at ORNL (Helmreich et al. 2015) and at INL. Parameters investigated by Helmreich et al. included nitric-acid concentration, speed of compact rotation, contact force between the compact and a platinum-rhodium screen serving as the anode, and the current applied to the compact. Development work at INL focused on designing a radial-deconsolidation apparatus to function in a hot cell that could be operated with hot cell manipulators. Typical parameters used for the radial deconsolidations are summarized in Table 3.

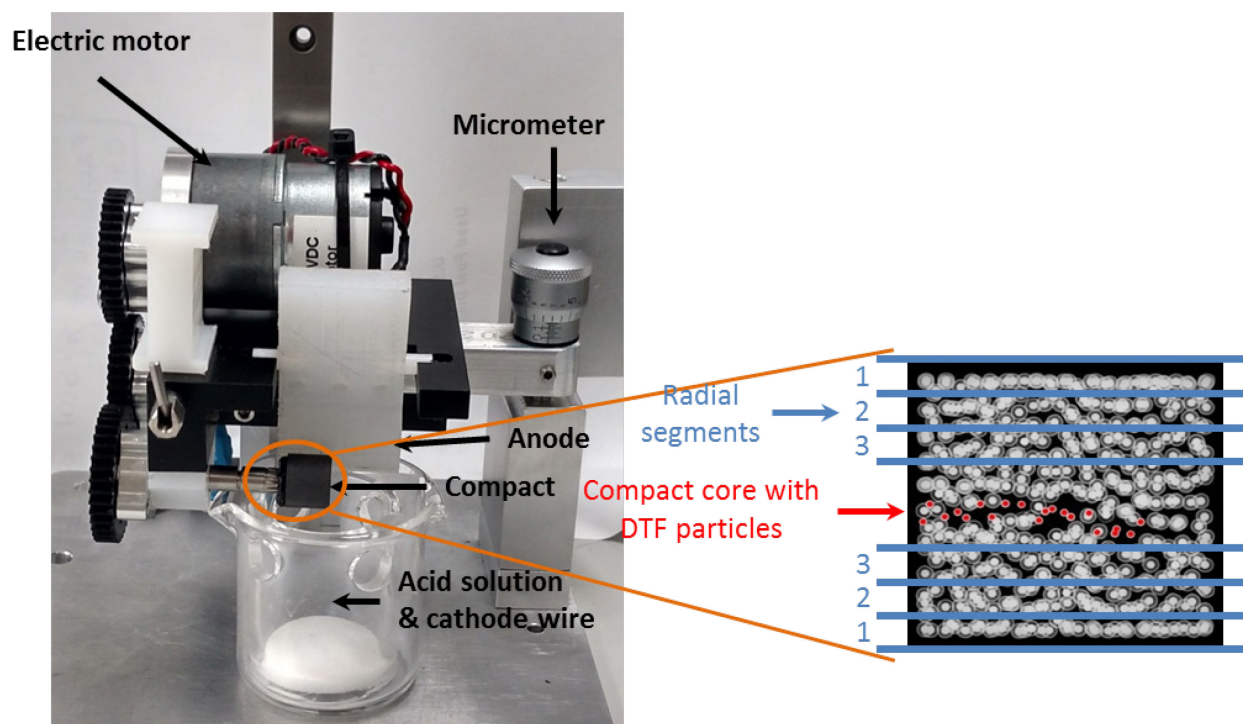


Figure 3. Radial-deconsolidation apparatus and depiction of compact (x-ray image) indicating three radial segments and a central core with DTF particles.

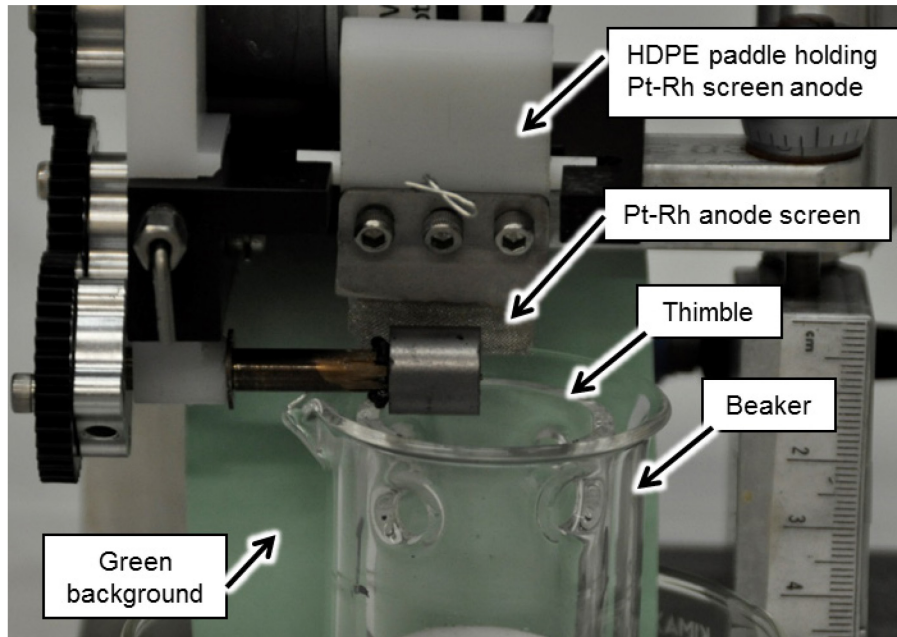


Figure 4. Unirradiated AGR-3/4 compact mounted to deconsolidation rod with platinum-rhodium anode behind the compact. The green screen behind the deconsolidation rod aided image analysis. A darker green background than is shown here was ultimately used in the hot cell.

Each step of the electrolytic radial deconsolidation proceeded for a period of time (typically 15 to 20 minutes to remove approximately 0.5–1 mm of the compact diameter). Then, the deconsolidation solution was changed, and a new thimble was put in place. The compact diameter was determined at the conclusion of each radial deconsolidation step (see Section 2.3). For each step of the deconsolidation, a deconsolidation solution and the particles and matrix debris collected in each thimble were stored in separate labeled containers to be analyzed separately. Up to four 15 to 20-minute segments of radial deconsolidation were used. After three to four segments, enough compact material had been removed that the epoxy holding the compact to the rod (and/or the deconsolidation rod itself) began to come in contact with the anode screen, and the compact itself was no longer in uniform contact with the anode screen. At this point, the radial portion of the deconsolidation was halted. Figure 5 depicts a process flow chart showing the samples generated from compact radial deconsolidation (solutions and thimbles of particles/matrix debris) and the analyses performed for each of these samples. Leach-burn-leach of the thimble material from each radial segment was performed, and a random sample of 30 TRISO-coated driver particles from each thimble was selected for individual visual inspection and gamma counting.

Table 3. Typical radial deconsolidation parameters.

Parameter	Value
Compact rotational speed	10 rpm
Nitric acid concentration	8M
Applied electrical current	1.0 to 1.5 A
Applied electrical voltage	7.0 to 8.0 V
Applied electrical power (voltage × current)	≤ 10 W

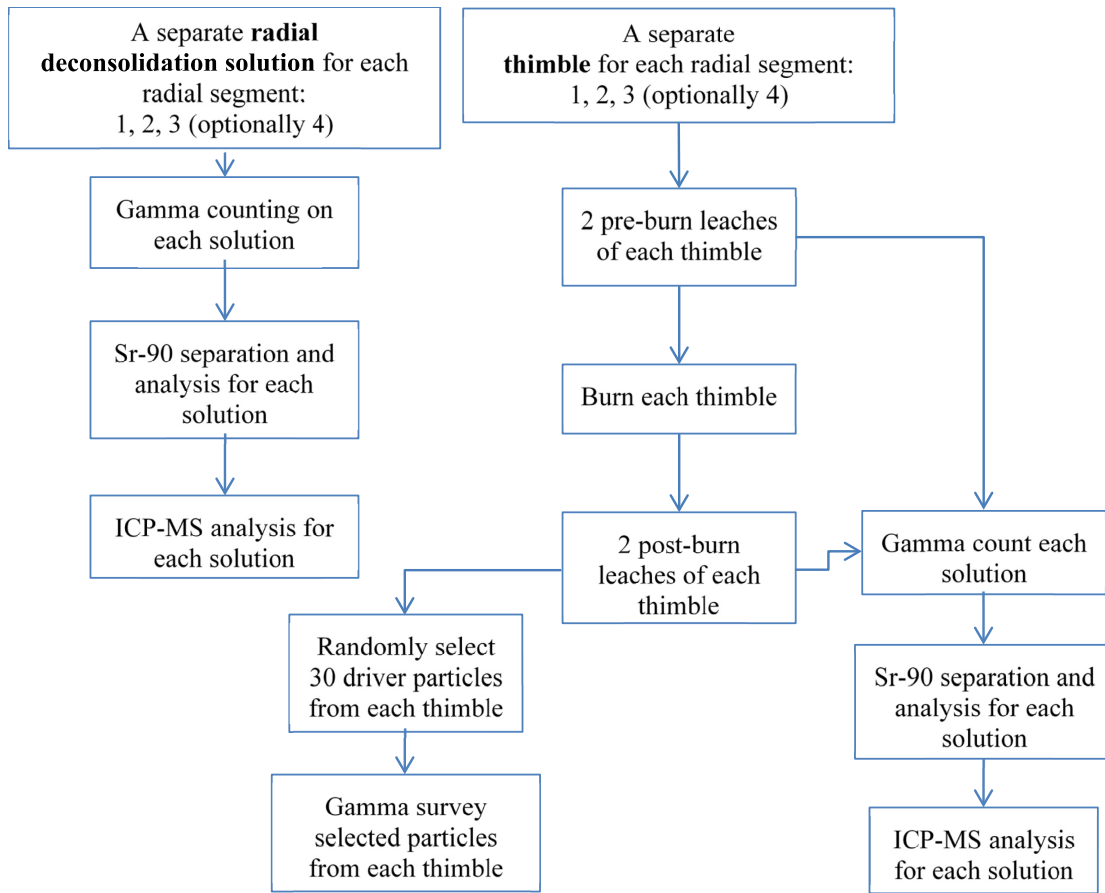


Figure 5. Process-flow diagram for samples generated from RDLBL.

After the radial-deconsolidation steps were completed, the compact, radial-deconsolidation rod and the gear attached to the deconsolidation rod were removed from the radial-deconsolidation apparatus, and an axial deconsolidation of the remaining compact core was performed in a manner similar to the single-step axial deconsolidation procedure described in Section 2.2.1. The compact-epoxy-rod bond was often weakened after a period of deconsolidation. If the compact core had inadvertently separated from the shaft, the standard axial deconsolidation technique with the elephant-foot anode and deconsolidation tube was used (see Figure 2). Figure 6 shows the axial deconsolidation of a compact core still attached to the deconsolidation rod after three radial segments had been collected. Here, the Pt wire that was embedded in the epoxy at the compact-rod interface is attached to the power supply via an alligator clip. In the process depicted in Figure 6, the acid level in the beaker was varied to maintain the circuit as the deconsolidation progressed. In the axial deconsolidation step, the compact core was deconsolidated in one step, so there is only one thimble and one deconsolidation solution from this part of the process. The deconsolidation solution and the material collected in the thimble went through the same analyses shown in Figure 5 for the radial segments. In the development phase of the radial-deconsolidation processes, sieving the thimble material was attempted to locate intact DTF particles. No DTF particles were successfully recovered at any stage of the development testing using unirradiated AGR-3/4 compacts. As a result, sieving was not performed during irradiated-compact deconsolidations, and no DTF particles were recovered from irradiated compacts.

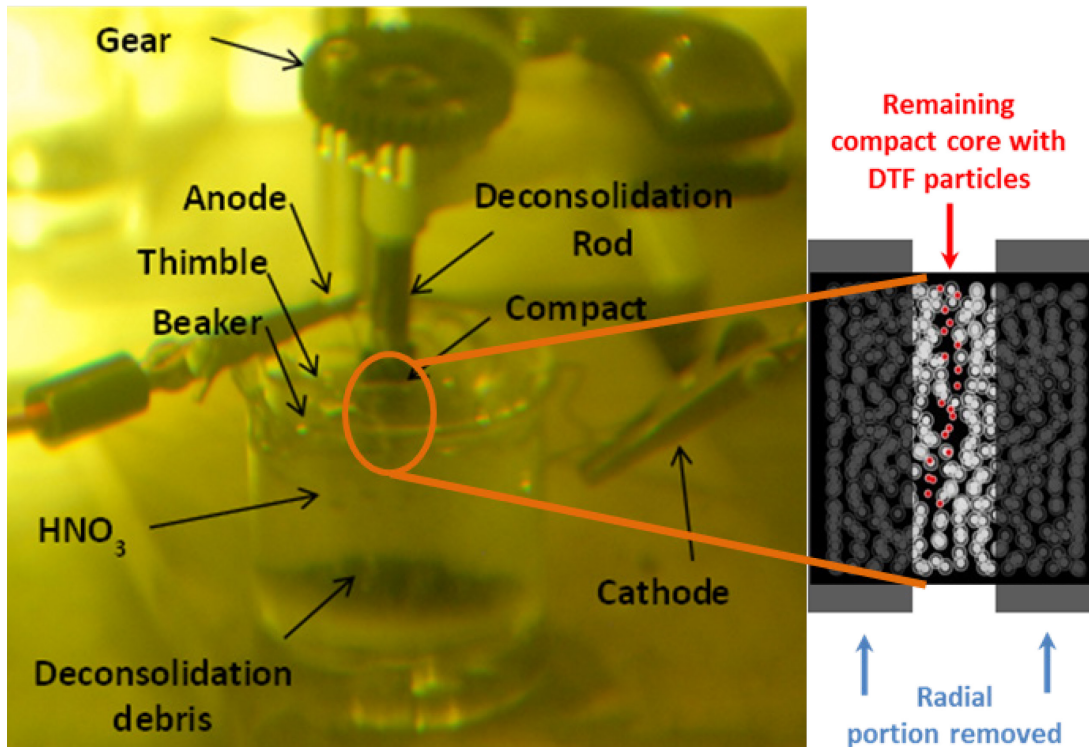


Figure 6. Axial deconsolidation (at left) of compact core remaining after radial deconsolidation. At right, X-radiograph of an AGR-3/4 compact with a depiction of the core remaining after radial deconsolidation.

2.3 Compact Dimensional Measurements by Image Analysis

The main goal of the AGR-3/4 experiment was the study fission product transport in TRISO fuels and related materials via the measurement of spatial variations in fission-product concentrations in compacts and graphite and the derivation of new transport parameters for use in predictive models. To get concentration profiles in the fuel compacts, the fission-product content in multiple radial segments in the compacts was measured (using the processes described in Section 2.1), and the diameter of the compact must be known at the beginning of radial deconsolidation and at the end of each segment of radial deconsolidation (using the procedures discussed in this section). The development work performed at ORNL produced a program called FrameGrabber (written in MATLAB) for measuring the diameter of a compact by analyzing video captured while the compact rotated (Helmreich et al. 2015). FrameGrabber was used during benchtop development work at INL; however, the program proved difficult to use with video captured through the hot-cell window at AL. FrameGrabber was rewritten by Helmreich, and the version dubbed FrameGrabber v11 has proven to be easier to use for analysis of video captured in the hot-cell environment.

The cameras, resolutions, and lenses used to acquire video and still images of the radial deconsolidations of the eight compacts are summarized in Table 4. Videos of the first three radial deconsolidations were captured on a Nikon D5000 digital camera using an 80–400 mm zoom lens operated at full zoom. Videos were acquired at a resolution of 1280×720 pixels at 24 frames per second (144 frames per rotation of the compact). Videos of the next five radial deconsolidations were captured using a Nikon D3400 digital camera. The first two of the five exams utilized the same 80–400 mm zoom lens operated at full zoom, and the last three utilized a 100–500 mm zoom lens operated at maximum zoom. Videos from the D3400 were acquired at a resolution of 1920×1080 pixels at 24 frames per second. A circular polarizer was used in some instances to reduce reflections caused by the hot-cell windows or from liquid remaining on the compact after a deconsolidation step. Detailed instructions for setting up the deconsolidation apparatus, lighting, and camera to effectively capture videos of the rotating compact through the hot cell window were discussed previously (Stempien 2017).

Table 4. Summary of video equipment and resolutions used for the eight compacts investigated here.

Compact	Camera	Lens	Video Resolution	Frames/second
3-3	Nikon D5000	Nikon 80–400 mm zoom	1280×720	24
12-1				
12-3				
5-3	Nikon D3400	Nikon 100–500 mm zoom	1920×1080	
5-4				
7-3				
8-3				
10-3				

The use of FrameGrabber v11.0 to process the videos and measure the diameter of the compact at each step of the radial deconsolidation was discussed by Stempien (2017). In short, a video is imported into FrameGrabber. The user is prompted to define a rectangular-shaped region around the rod and a separate rectangular region around the compact using a cursor controlled by a typical computer mouse. FrameGrabber then locates the edges of the rod and compact within the specified regions for a user-defined number of frames from the video. For each frame analyzed, FrameGrabber generates an image of that frame with overlays of the boundaries of the compact that it has determined and linear projections of the upper and lower edges and center of the deconsolidation rod. An example of a frame with the overlay and projections generated by FrameGrabber is given in Figure 7 for Frame 146 from analysis “11k_2_DSC_4739” from Compact 3-3. The known diameter of the rod (6 mm) is used as a standard to determine the diameter of the compact. For a given frame, the output diameter is the average diameter along the length of the compact. FrameGrabber repeats this process for each specified frame of the video. Videos were typically 30 seconds long, meaning that five full rotations of the compact were captured. Ten frames per rotation (for a total of 50 frames) were then analyzed in FrameGrabber. Because the user-defined region around the rod and compact can vary slightly in size from one analysis to the next, the 50 frames were analyzed three different times. The diameters determined from the three different analyses of each of the 50 analyzed frames were averaged, and a standard deviation was determined from that population. Knowing the length of the compact from metrology (Stempien et al. 2016) and the compact diameter determined from this image analysis, the volume of the radial deconsolidation segment was calculated. This process was performed for videos taken prior to the start of radial deconsolidation and for videos taken at the end of each approximately 15–20-minute segment of radial deconsolidation.

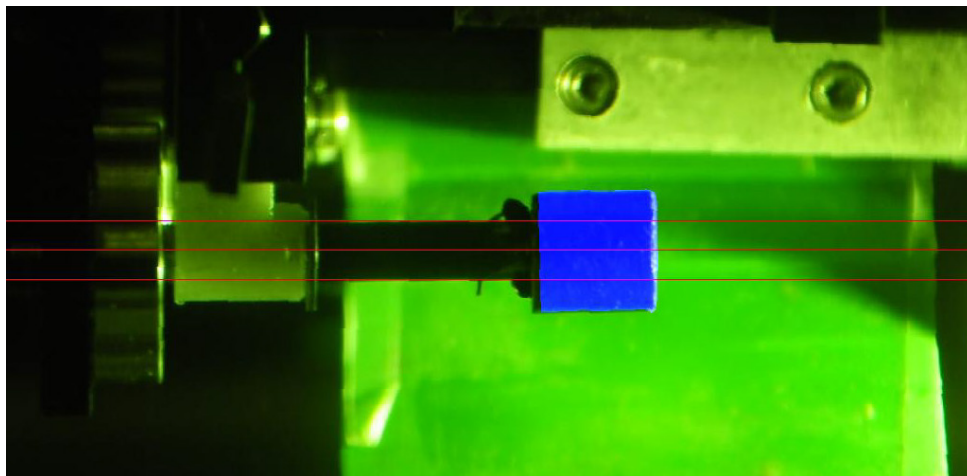


Figure 7. Blue shading shows the compact region determined by FrameGrabber for Compact 3-3. (Frame 146 from analysis 11k_2_DSC_4739). Red lines denote the deconsolidation-rod’s center and upper and lower edges.

FrameGrabber has adjustments that can be made to tune the program for different lighting conditions. These adjustments are made using four variables called: “num_rod_thresh,” “num_com_thresh,” “keep_rod_thresh,” and “keep_com_thresh.” The variables “num_rod_thresh” and “num_com_thresh” set the number of segmentation thresholds (up to 20) that the user-defined boxed regions will be divided into, based on the brightness of the green channel minus the red channel and minus the blue channel (Helmreich 2015). The second set of variables (keep_rod_thresh and keep_com_thresh) sets the number of the calculated thresholds (set by the first set of variables) that will be retained and used in the measurement. The second set of variables must be less than or equal to the values in the first set. In Table 5, the default values for these variables are summarized along with other combinations of these variables that produced reasonable results for videos taken through the hot-cell window.

Table 5. Combinations of threshold variables used for analyses in FrameGrabber.

	v11 Default	v11e	v11h	v11j	v11k	v11t	v11x	v11y
num_rod_thresh	2	3	3	3	3	11	9	5
num_com_thresh	2	4	7	9	9	3	9	9
keep_rod_thresh	1	2	2	2	2	4	4	1
keep_com_thresh	1	2	3	3	4	2	3	3

2.4 Processing of Radiochemical Results

RDLBL is used to measure gamma-emitting fission products, beta-emitting Sr-90, and actinides outside of the TRISO SiC layers and to compare these measured quantities to inventories calculated via physics calculations to have been produced in the compact during irradiation. Fission-product activities measured in the RDLBL solutions were decay-corrected back to the end of irradiation (EOI, April 12, 2014, 5:00 AM MST) plus one day (April 13, 2014, 5:00 AM MST) using the equation:

$$A = A_0 e^{-\lambda t} \quad (1)$$

where A is the activity at time t , A_0 is the activity at $t = 0$, and λ is the decay constant ($\lambda = \ln(2)/t_{1/2}$, and $t_{1/2}$ is the half-life). Isotope half-lives were taken from the ENDF/B-VII.1 library. The uranium and plutonium nuclides measured via mass spectrometry were not decay-corrected, and their measured quantities were compared to the calculated inventories at EOI + 1 year. The reference time of EOI plus one year was selected to account for the appreciable production of some stable nuclides of interest during the first year after the irradiation. After the first year, inventory changes in these nuclides were deemed insignificant (Hunn et al. 2013, Table 1). To compute the fraction of the compact inventory measured in the solutions (sometimes referred to as the measured-to-calculated ratio or [M/C]), the measured fission-product and actinide values were divided by the inventories predicted by physics calculations to exist in the compacts at the reference times (Sterbentz 2015). Table 6 through Table 13 give the calculated inventories of fission products and actinides in Compacts 3-3, 5-3, 5-4, 7-3, 8-3, 10-3, 12-1, and 12-3. Ce-144 is detected by measuring the short-lived Pr-144 nuclide that is the daughter of Ce-144 decay and is in secular equilibrium with Ce-144. Similarly, Ru-106 is measured by detecting Rh-106, which has a short half-life and is in secular equilibrium with Ru-106. The nomenclature used in the tables reflects this.

For gamma-emitting nuclides, the staff at AL stated that a minimum 3% two-sigma error was applied for all measurements; however, the reported error could be higher based on gamma-ray counting statistics. For beta-emitting Sr-90, a minimum of 2% error at two-sigma was applied; however, the reported error could have been higher due to counting statistics. Where multiple measurements were added together (for example to sum the total Cs-134 measured from all the different RDLBL steps), the errors from the individual measurements were combined by adding them in quadrature. In instances where no activity was detected for a given nuclide, minimum detectable activities (MDAs) were reported. Like the measured activities, these MDAs were also decay-corrected, and were denoted by “<”. These MDAs were considered an upper bound on the activity of a given nuclide but were treated as zero (MDA = 0) any time activities were summed.

For the measurements made via ICP-MS, the uncertainty was estimated at AL using the GUM Workbench Pro Version 2.4.1.406 computer program. In samples where the uncertainty in the signal intensity was small, the uncertainties from the instrument calibration, sample weights, and dilutions dominated, and the estimated total uncertainty was reported as 5% at two-sigma. This value (5%) was the lowest reported uncertainty in any of the ICP-MS results from AL. For measurements where uncertainty in the signal intensity was greater than 5%, which occurred when the analyte concentration was low (closer to the instrument's detection limits), the uncertainty was rounded up to the nearest 10%. Where multiple measurements were added together (for example to sum the total U-238 measured from all the different RDLBL steps), the errors from the individual measurements were combined by adding them in quadrature. In instances where a given analyte was not detected, a minimum detectable mass was reported. These were denoted by "<". These less-than values were considered an upper bound on the quantity of a given nuclide but were treated as zero any time values from multiple RDBL steps were summed.

Table 6. Inventories of fission products and actinides calculated to have been produced in Compact 3-3.

Isotope	Inventory (Bq) at EOI + 1 Day
Ag-110m	7.09E+07
Ce-144	9.69E+10
Cs-134	7.02E+09
Cs-137	6.39E+09
Eu-154	2.28E+08
Eu-155	1.54E+08
Ru-106	2.02E+10
Sb-125	4.93E+08
Sr-90	5.57E+09
Isotope	Inventory (g) at EOI + 1 Year
U-234	4.52E-04
U-235	3.10E-02
U-236	9.93E-03
U-238	3.43E-01
Pu-239	5.04E-03
Pu-240	1.79E-03

Table 7. Inventories of fission products and actinides calculated to have been produced in Compact 12-1.

Isotope	Inventory (Bq) at EOI + 1 Day
Ag-110m	7.87E+06
Ce-144	4.78E+10
Cs-134	1.27E+09
Cs-137	2.93E+09
Eu-154	4.31E+07
Eu-155	4.87E+07
Ru-106	6.16E+09
Sb-125	2.02E+08
Sr-90	2.71E+09

Isotope	Inventory (g) at EOI + 1 Year
U-234	5.54E-04
U-235	5.96E-02
U-236	5.58E-03
U-238	3.53E-01
Pu-239	4.00E-03
Pu-240	7.16E-04

Table 8. Inventories of fission products and actinides calculated to have been produced in Compact 12-3.

Isotope	Inventory (Bq) at EOI + 1 Day
Ag-110m	4.93E+06
Ce-144	4.25E+10
Cs-134	9.46E+08
Cs-137	2.58E+09
Eu-154	3.17E+07
Eu-155	4.23E+07
Ru-106	4.97E+09
Sb-125	1.73E+08
Sr-90	2.42E+09
Isotope	Inventory (g) at EOI + 1 Year
U-234	5.66E-04
U-235	6.28E-02
U-236	5.02E-03
U-238	3.54E-01
Pu-239	3.32E-03
Pu-240	5.34E-04

Table 9. Inventories of fission products and actinides calculated to have been produced in Compact 5-3.

Isotope	Inventory (Bq) at EOI + 1 Day
Ag-110m	1.16E+08
Ce-144	1.11E+11
Cs-134	1.01E+10
Cs-137	7.49E+09
Eu-154	3.11E+08
Eu-155	2.04E+08
Ru-106	2.65E+10
Sb-125	5.96E+08
Sr-90	6.40E+09

Isotope	Inventory (g) at EOI + 1 Year
U-234	4.15E-04
U-235	2.33E-02
U-236	1.09E-02
U-238	3.39E-01
Pu-239	4.99E-03
Pu-240	1.94E-03

Table 10. Inventories of fission products and actinides calculated to have been produced in Compact 5-4.

Isotope	Inventory (Bq) at EOI + 1 Day
Ag-110m	1.18E+08
Ce-144	1.12E+11
Cs-134	1.01E+10
Cs-137	7.52E+09
Eu-154	3.14E+08
Eu-155	2.06E+08
Ru-106	2.71E+10
Sb-125	6.03E+08
Sr-90	6.41E+09
Isotope	Inventory (g) at EOI + 1 Year
U-234	4.16E-04
U-235	2.33E-02
U-236	1.09E-02
U-238	3.38E-01
Pu-239	5.25E-03
Pu-240	2.00E-03

Table 11. Inventories of fission products and actinides calculated to have been produced in Compact 7-3.

Isotope	Inventory (Bq) at EOI + 1 Day
Ag-110m	1.19E+08
Ce-144	1.12E+11
Cs-134	1.02E+10
Cs-137	7.55E+09
Eu-154	3.11E+08
Eu-155	2.06E+08
Ru-106	2.68E+10
Sb-125	6.01E+08
Sr-90	6.44E+09

Isotope	Inventory (g) at EOI + 1 Year
U-234	4.15E-04
U-235	2.30E-02
U-236	1.10E-02
U-238	3.39E-01
Pu-239	4.99E-03
Pu-240	1.99E-03

Table 12. Inventories of fission products and actinides calculated to have been produced in Compact 8-3.

Isotope	Inventory (Bq) at EOI + 1 Day
Ag-110m	1.07E+08
Ce-144	1.09E+11
Cs-134	9.40E+09
Cs-137	7.30E+09
Eu-154	2.93E+08
Eu-155	1.95E+08
Ru-106	2.52E+10
Sb-125	5.78E+08
Sr-90	6.27E+09
Isotope	Inventory (g) at EOI + 1 Year
U-234	4.22E-04
U-235	2.45E-02
U-236	1.08E-02
U-238	3.39E-01
Pu-239	5.01E-03
Pu-240	1.96E-03

Table 13. Inventories of fission products and actinides calculated to have been produced in Compact 10-3.

Isotope	Inventory (Bq) at EOI + 1 Day
Ag-110m	5.55E+07
Ce-144	9.05E+10
Cs-134	5.85E+09
Cs-137	5.89E+09
Eu-154	1.92E+08
Eu-155	1.33E+08
Ru-106	1.76E+10
Sb-125	4.49E+08
Sr-90	5.19E+09

Isotope	Inventory (g) at EOI + 1 Year
U-234	4.68E-04
U-235	3.47E-02
U-236	9.42E-03
U-238	3.44E-01
Pu-239	5.00E-03
Pu-240	1.69E-03

3. DIMENSIONAL RESULTS FROM COMPACT RADIAL DECONSOLIDATIONS

The compact dimensions were obtained through video analysis, as described in Section 2.3. Comparisons of the pre-deconsolidation diameters determined via contact metrology (Stempien et al. 2016) and the pre-deconsolidation diameters determined from video analyses are made in Table 14. The results from both measurements are similar, with 3.5% being the maximum bias and the rest remaining within a $\pm 1.2\%$ difference. There was no consistent bias in the pre-deconsolidation diameter determinations among the compacts. Furthermore, there is no reason to suspect that the pre-deconsolidation bias would be the same for any of the radial-deconsolidation segments. The camera and lighting had to be moved out of the way in between every segment to allow the hot-cell operator to position the glassware, electrodes, and compact, and recover the thimble and deconsolidations solutions. While all attempts were made to set up the lighting in a consistent manner, variations were noticeable when it came time to process the videos, and FrameGrabber parameters (see Table 5) were frequently adjusted from one segment to another. Additionally, the compact surface was moist in between each segment, which increased the reflectivity of the compact, and adjustments to the camera and lighting setup were used to reduce light reflection from the compact. No attempts to adjust the diameters for biases were made.

In prior trials with unirradiated compacts, it was observed that the first 2 minutes of a radial deconsolidation can cause the compact diameter to increase by up to 0.4 mm, and a reduction in volume may not be apparent for at least the first 4 minutes (Helmreich 2015). That observation was made by taking video during the entire deconsolidation of unirradiated compacts in a clean (non-radioactive) laboratory environment. In the hot cell environment, it was impossible to collect video suitable for analysis. Thus, whether this effect occurred or the extent of this kind of effect could not be determined for the irradiated fuel compacts.

The dimensions of Compacts 3-3, 12-1, and 12-3 were analyzed by Stempien (2017). The results of those analyses will be reproduced here, but the reader is directed to that report for additional figures and more-detailed discussions of those dimensional results (Stempien 2017). The results of the dimensional analyses of Compacts 5-3, 5-4, 7-3, 8-3, and 10-3 will be presented and discussed in the following subsections.

Table 14. Comparison of compact diameter measured by contact metrology and video analysis via FrameGrabber.

Compact	Diameter before deconsolidation		Video bias (%)
	Contact metrology (mm)	Video analysis (mm)	
3-3	12.124 ± 0.0058	12.146 ± 0.140	0.18%
5-3	12.164 ± 0.0050	12.155 ± 0.075	-0.07%
5-4	12.192 ± 0	12.295 ± 0.119	0.84%
7-3	12.071 ± 0.0081	11.940 ± 0.136	-1.09%
8-3	12.139 ± 0.0050	12.28 ± 0.06	1.16%
10-3	12.141 ± 0	12.571 ± 0.076	3.54%
12-1	12.256 ± 0	12.207 ± 0.136	-0.40%
12-3	12.254 ± 0.0086	12.288 ± 0.149	0.28%

3.1 Compact 3-3

Compact 3-3 had an as-irradiated diameter of 12.124 ± 0.0058 mm (Stempien et al. 2016). The initial mount of Compact 3-3 to the deconsolidation rod failed prior to the start of deconsolidation, leaving all of the epoxy on the compact and none on the rod. The residual epoxy on the compact was chipped off using manipulators in the hot cell, but some of the compact matrix (and possibly a couple of particles) came off along with the epoxy. The undamaged end of the compact was glued to the rod and radial deconsolidation proceeded. Figure 8 shows the compact remounted to the rod, with the damaged end facing out.

Four radial segments were obtained from this compact. Segments 1 and 2 used 15-minute-long periods of deconsolidation. Segment 3 used 16 minutes of deconsolidation, and the compact fell off the rod after 15 minutes during the fourth deconsolidation segment. Had the compact not fallen from the rod, the fourth segment would have been run until the compact lost consistent contact with the platinum anode screen. Rounding of the compact at the unglued end was noted and became more pronounced as radial deconsolidation progressed. The diameter of the compact was measured by using FrameGrabber v11x to analyze videos taken after Segments 1 through 3. Because the compact fell off the deconsolidation rod after the fourth segment, the diameter of the compact was measured by contact measurements using analog calipers. Two caliper measurements were taken at each of three locations along the length of the compact. Figure 9 shows Compact 3-3 held between tweezers and denotes the approximate locations of caliper diameter measurements. Table 15 summarizes the dimensions and volumes of the compact at each segment of the deconsolidation process. The standard deviations in this table are from the variation in the measured diameters from the multiple frames analyzed with FrameGrabber v11x. These do not account for any systematic error, which may be significant (estimated to be on the order of 10%).

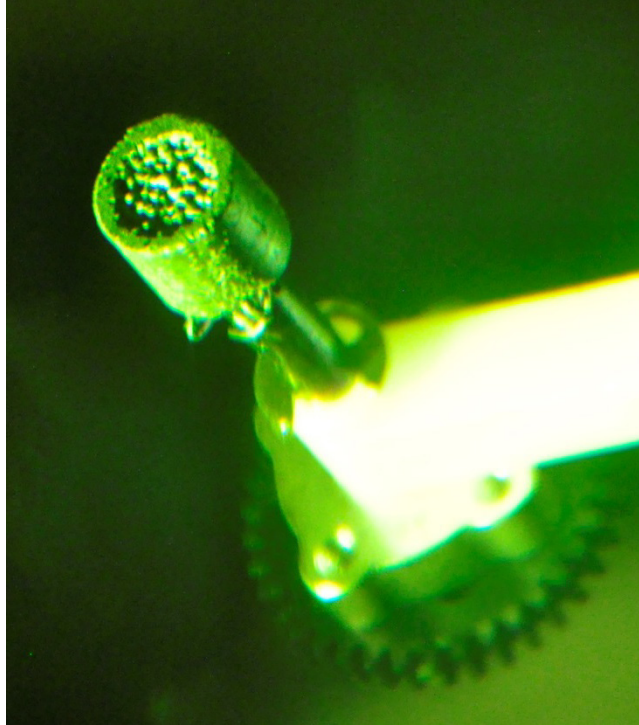


Figure 8. Compact 3-3 reglued to the deconsolidation rod after the initial rod-compact bond failed. The free end of the compact shows where some compact matrix pulled away when the first bond failed, exposing some particles.

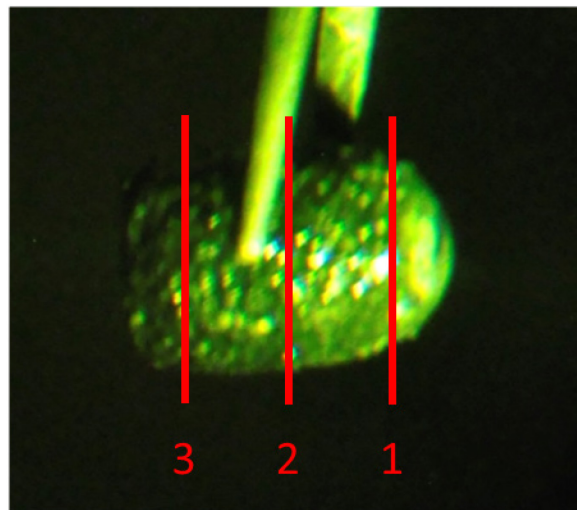


Figure 9. Compact 3-3 held by tweezers after the fourth segment of deconsolidation, after the compact had fallen off the deconsolidation rod. Approximate locations of caliper measurements marked Numbers 1 through 3.

Table 15. Summary of Compact 3-3 diameter change, new diameter after each segment of deconsolidation, and the volume of each segment. The volume of the core remaining after the four segments of radial deconsolidation is also given.

	Segment 1	Segment 2	Segment 3	Segment 4	Core
Radial Deconsolidation Time (min)	15	15	16	15	–
Diameter Reduction (mm)	1.005	0.951	0.468	0.674	–
Std Dev of Diameter Reduction	0.227	0.211	0.217	0.290	–
New Diameter (mm)	11.119	10.168	9.701	9.027	–
New Diameter Std Dev	0.227	0.277	0.244	0.223	–
Segment Volume (mm ³)	228.582	202.950	95.407	127.765	797.351
Segment Volume Std Dev	34.932	47.719	36.451	37.443	27.856

3.2 Compact 5-3

Compact 5-3 had an as-irradiated diameter of 12.164 ± 0.005 mm (Stempien et al. 2016). Three radial segments were obtained from Compact 5-3. To obtain the first segment, the deconsolidation proceeded for 12 minutes and 10 seconds. Segment two ran for 15 minutes, and the third segment ran for over 45 minutes. The third segment deconsolidation was stopped when consistent contact between the compact and the anode screen could not be maintained because the excess epoxy used to mount the compact to the deconsolidation rod began to contact the screen. FrameGrabber v11h was used to analyze the video captured after radial Segment 1, and v11g was used for Segments 2 and 3. Figure 10 shows a frame from the image analysis of a video taken after Segment 3 was completed. Table 16 summarizes the times, dimensions, and volumes for Compact 5-3 after each of the three radial segments.

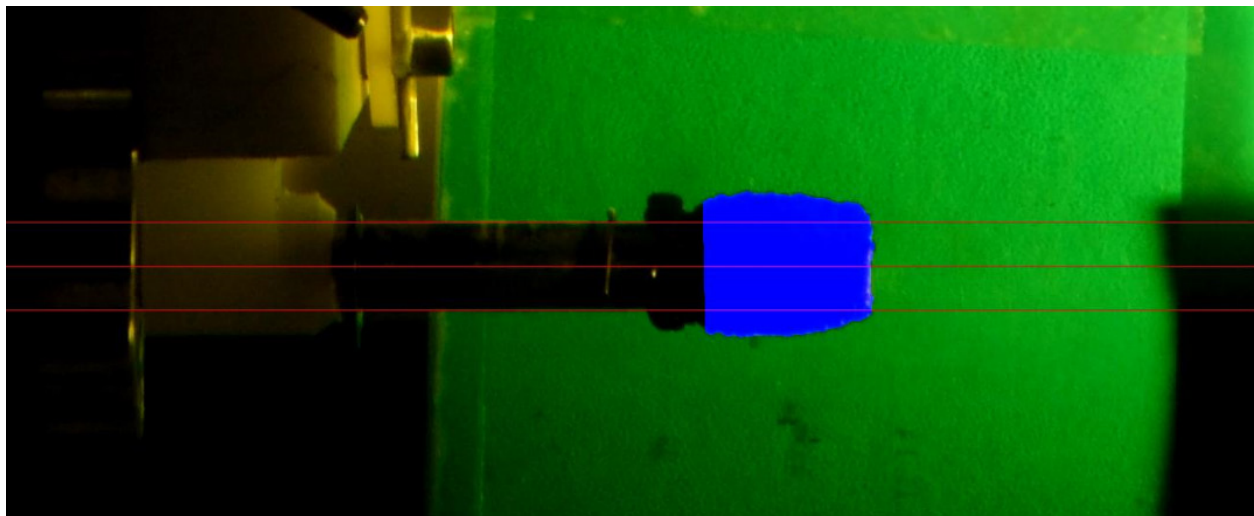


Figure 10. Frame 89 from video DSC_0073 taken of Compact 5-3 after the third segment of deconsolidation.

Table 16. Summary of Compact 5-3 diameter change, new diameter after a segment of deconsolidation, volume of the compact material removed, and the volume of the core remaining after the three segments of radial deconsolidation.

	Segment 1	Segment 2	Segment 3	Core
Deconsolidation Time (min)	12.17	15	45.37	–
Diameter Reduction (mm)	0.285	0.557	2.101	–
Std Dev of Diameter Reduction	0.154	0.190	0.180	–
New Diameter (mm)	11.879	11.322	9.221	–
New Diameter Std Dev	0.154	0.233	0.224	–
Segment Volume (mm ³)	67.377	125.227	422.853	837.154
Segment Volume Std Dev	25.534	43.002	35.605	40.648

3.3 Compact 5-4

Compact 5-4 had an as-irradiated diameter of 12.192 mm (Stempien et al. 2016). The set of triplicate, as-irradiated-diameter measurements all read 12.192 mm; therefore, there is no standard deviation available from repeating the measurements. Three radial segments were obtained for Compact 5-4. Segments 1 and 2 were each 15.5 minutes long. The third segment ran for just under 42 minutes. Segments 1 and 3 were analyzed using FrameGrabber v11j, and Segment 2 was analyzed using FrameGrabber v11w. Figure 11 shows an image from the analysis of a video taken after the third and final radial segment. Table 17 summarizes the dimensions and volumes for each segment and the remaining core.

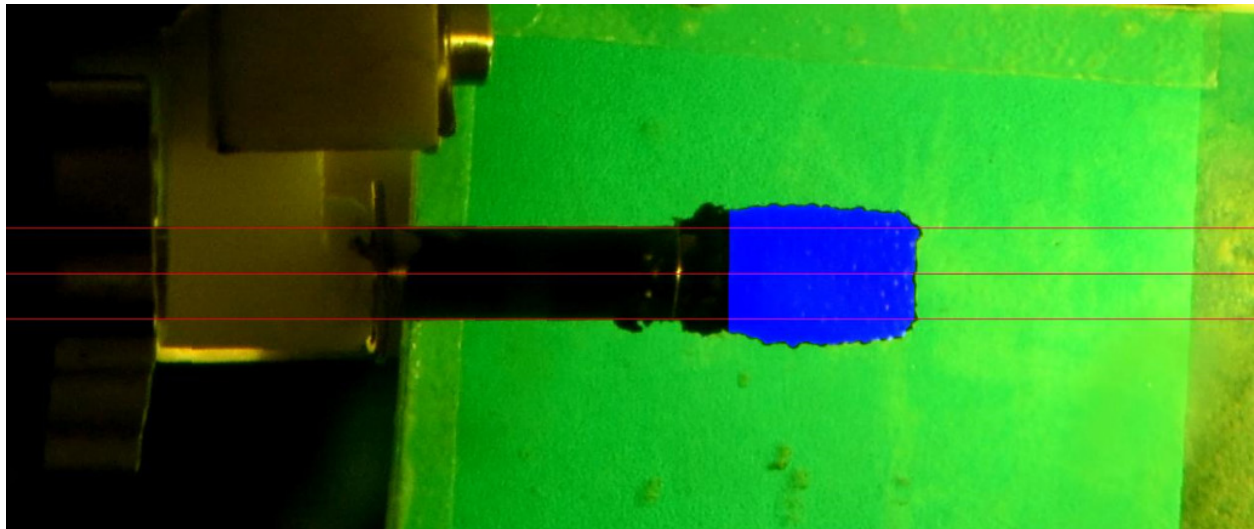


Figure 11. Frame 60 from the analysis of video DSC_0042 taken after the third radial deconsolidation segment of Compact 5-4.

Table 17. Summary of Compact 5-4 diameter change, new diameter after a segment of deconsolidation, volume of the compact material removed, and the volume of the core remaining after the three segments of radial deconsolidation.

	Segment 1	Segment 2	Segment 3	Core
Deconsolidation Time (min)	15.5	15.5	41.8	–
Diameter Reduction (mm)	0.442	1.118	2.018	–
Std Dev of Diameter Reduction	0.210	0.187	0.222	–
New Diameter (mm)	11.750	10.631	8.613	–
New Diameter Std Dev	0.210	0.255	0.233	–
Segment Volume (mm ³)	104.484	270.742	404.776	731.826
Segment Volume Std Dev	34.492	47.468	29.913	39.589

3.4 Compact 7-3

Compact 7-3 had an as-irradiated diameter of 12.071 ± 0.008 mm (Stempien et al. 2016). Prior to the start of the deconsolidation, Compact 7-3 suffered a chip and loss of material, including some particles, when it was transferred from the Hot Fuel Examination Facility (HFEF) to AL for RDLBL. Figure 12 shows the chip and the particles exposed as a result. Only two radial segments were obtained from the radial deconsolidation of Compact 7-3. This is at least partly due to there being minimal excess epoxy to interfere with compact-anode contact. Such interference on other compacts resulted in uneven material removal, and in some cases, the amount of excess epoxy was large enough to cause interference as early as Segment 1 of the radial deconsolidation. While, the rate of material removal was not quantified, it may also be that the irradiation history of the compacts affected the deconsolidation rate, and Compact 7-3 had a higher irradiation temperature more than 150°C hotter than the second hottest compact. FrameGrabber v11j was used to analyze the dimensions of the compact following the completion of radial Segments 1 and 2. Figure 13 shows a frame analyzed after the second radial segment had been completed. Compared to prior radial deconsolidations, this radial deconsolidation removed much more compact material, and the diameter of the remaining compact core was 7.8 mm. Of the prior deconsolidations, where the desired three or four radial segments were obtained, the remaining compact cores ranged in diameter from 8.6 to 9.2 mm. Table 18 summarizes the dimensions and volumes for each segment and the remaining core.



Figure 12. Pre-deconsolidation photo taken through the hot cell window showing a piece of material missing from Compact 7-3. The compact was pneumatically rabbited from HFEEF to AL, and the piece was missing when the compact was removed from the rabbit at AL.

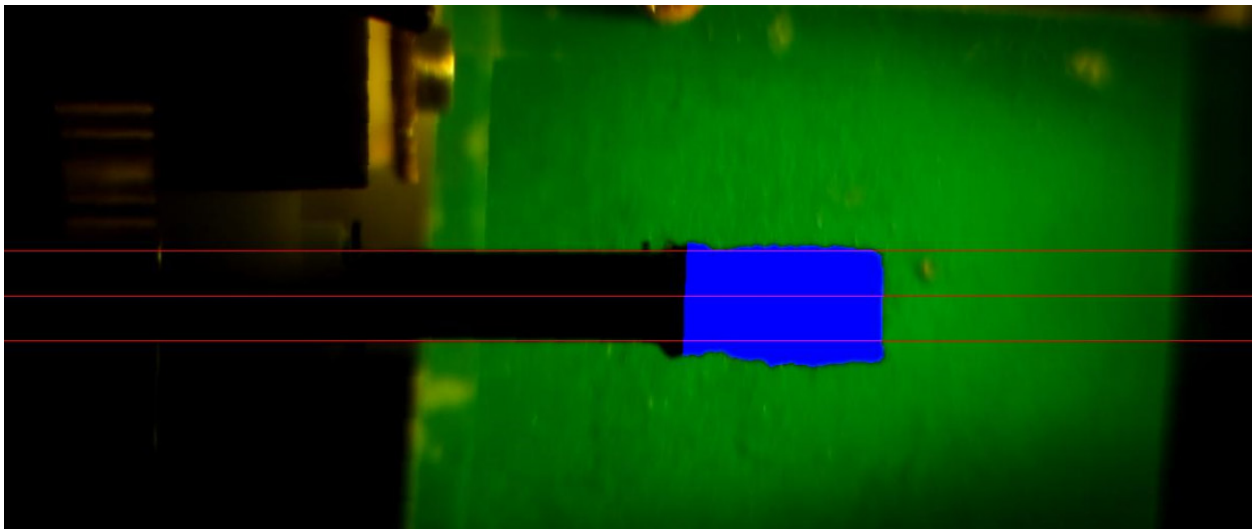


Figure 13. Frame 103 from video DSC_0064 taken after the second and final radial segment was obtained from Compact 7-3.

Table 18. Summary of Compact 7-3 diameter change, new diameter after a segment of deconsolidation, volume of the compact material removed, and the volume of the core remaining after the two segments of radial deconsolidation.

	Segment 1	Segment 2	Core
Deconsolidation Time (min)	19	18.5	–
Diameter Reduction (mm)	1.725	2.425	–
Std Dev of Diameter Reduction	0.198	0.205	–
New Diameter (mm)	10.215	7.790	–
New Diameter Std Dev	0.198	0.251	–
Segment Volume (mm ³)	407.559	430.254	597.947
Segment Volume Std Dev	28.217	34.057	38.472

3.5 Compact 8-3

Compact 8-3 fell off the rod after only two radial segments had been obtained, and it was not reattached. The baseline pre-deconsolidation diameter (12.28 ± 0.06 mm) from the video analysis (using FrameGrabber v11w) was compared to the results from contact metrology (12.139 ± 0.005 mm) (Stempien, 2016), giving a bias of +0.137 mm (1.16%) for the video-based diameter compared to the metrology diameter. The diameter after the first radial deconsolidation segment was 12.44 mm from the video analysis. This is considerably larger than either of the pre-deconsolidation diameters from contact metrology and video: 0.17 mm larger than the pre-deconsolidation video-based diameter and 0.30 mm larger than the contact metrology diameter. Figure 14 shows a screenshot from video DSC_0013 after the Segment 1. From the images, it is clear that material was removed from the fuel compact; however, the apparent increase in compact diameter means that the volume of the material removed cannot be determined from the video analysis. The top part of the compact in the screenshot seems smoother than the bottom part, which indicates the radial deconsolidation did not efficiently remove surface material around the entire circumference of the compact. Thus, a portion of the compact exterior appears largely untouched. As discussed at the beginning of Section 3, when radial deconsolidations of unirradiated compacts were performed to develop the radial deconsolidation methodology, it was found that the first 2 minutes of a radial deconsolidation can cause the compact diameter to increase by up to 0.4 mm, and a reduction in diameter may not be noticeable until at least 4 minutes (Helmreich et al. 2015). It is not clear if this kind of effect was active in Compact 8-3 or other irradiated AGR-3/4 compacts. Despite Segment 1 from the Compact 8-3 radial deconsolidation's being collected over the course of 12 minutes, its diameter was larger than when it started.

After Compact 8-3 fell off during the Segment 2 deconsolidation, the diameter was measured three times in the middle and once at each end of the compact by caliper. Given that the volume of material removed in Segment 1 could not be determined, the volume of Segment 2 was calculated by comparing the pre-deconsolidation volume and the post-Segment 2 volume. Thus, for this compact, only one radial volume and the core volume are known. The fission-product inventory from the leach-burn leach of the particles and matrix material from Segment 1 will be combined with that from Segment 2 and normalized by this radial volume in Section 4.5. Table 19 summarizes these volumes.

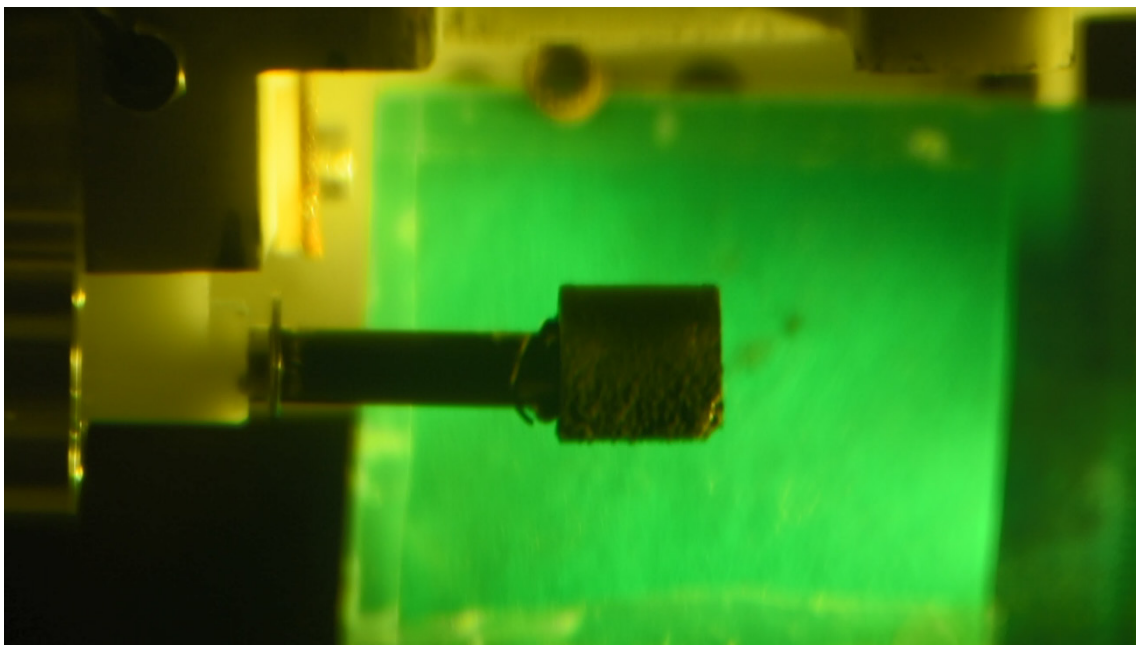


Figure 14. Screenshot from video DSC_0013 taken after the first segment was obtained from Compact 8-3.

Table 19. Summary of Compact 8-3 diameter change. See text for explanation of Segment 2 volume.

	Segment 1	Segment 2	Core
Deconsolidation Time (min)	12	17.25	–
Diameter Reduction (mm)	N/A	N/A	–
Std Dev of Diameter Reduction	N/A	N/A	–
New Diameter (mm)	11.43 ^a		–
New Diameter Std Dev	0.15 ^a		–
Segment Volume (mm ³)	163.845 ^a		1280.972
Segment Volume Std Dev	32.580 ^a		32.559

a. Segment 1 diameter and volume not determined. Dimensions listed were determined after Segment 2 radial deconsolidation.

3.6 Compact 10-3

Compact 10-3 fell off the rod three times. When it fell off after the initial mounting, a piece was peeled off the top end (Figure 15a). Scrapes were also observed on the side of the compact (Figure 15b). The first segment was deconsolidated over the course of 65 minutes. A longer time was used because contact between the compact and the anode screen was inconsistent, and the rate of deconsolidation was slower than usual. The compact fell off again after 26 minutes of deconsolidating Segment 2 (Figure 15c). After reattaching it, the compact underwent deconsolidation an additional 9 minutes of deconsolidation as part of Segment 2 work. The compact fell from the rod once more after 12.5 minutes of deconsolidation for Segment 3 (Figure 15d). Video was obtained at this point by placing the compact on top of a beaker next to the rod so that video analysis could be performed on the static (non-rotating) compact.

The baseline pre-deconsolidation diameter (12.571 ± 0.076 mm) from the video analysis (using FrameGrabber v11y) was slightly larger than the results from contact metrology (12.1412 ± 0.000 mm) (Stempien 2016). The resulting diameter after the first deconsolidation (12.501 ± 0.086 mm) from the video analysis was very close to the pre-deconsolidation diameter from the video analysis. Like Compact 8-3, the Compact 10-3 Segments 1 and 2 were combined into a single segment (Figure 15) to reduce the uncertainty on the volumes those segments. Table 20 summarizes the dimensions and volumes for each segment and the remaining core.

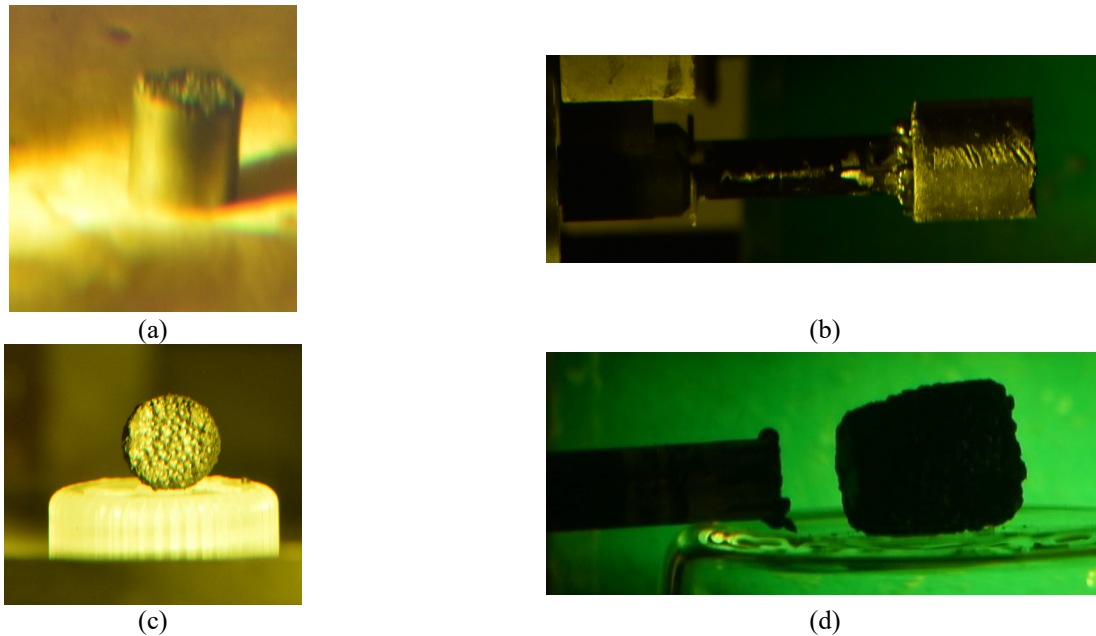


Figure 15. (a) Compact 10-3 fell from the rod after it was initially epoxied before deconsolidation. There seemed to be a piece of compact that came off the top of the compact. (b) Scratches appear on the side of the compact. (c) The compact fell off the rod a second time during radial deconsolidation of Segment 2. (d) The compact fell off the rod a third time after radial Segment 3.

Table 20. Summary of Compact 10-3 diameter change. Segment 1 was deconsolidated for 65 minutes and showed little discernible change in diameter; therefore, it was combined with Segment 2 (deconsolidated for a total of 35 minutes).

	Segments 1+2	Segment 3	Core
Deconsolidation Time (min)	See caption	12.5	–
Diameter Reduction (mm)	0.444	0.665	–
Std Dev of Diameter Reduction	0.20	0.21	–
New Diameter (mm)	12.127	11.462	–
New Diameter Std Dev	0.186	0.096	–
Segment Volume (mm ³)	107.25	153.38	1285.62
Segment Volume Std Dev	47.93	49.11	21.60

3.7 Compact 12-1

Some scuffing and chips around the top and bottom rims of the compact were noted prior to the start of the deconsolidation. In Figure 16, the white arrows denote chips of missing material, and the gray arrow denotes scuffs. The scuffing likely occurred when the deconsolidation apparatus was set up and the correct meshing of the gears for rotating the compact was tested with the anode screen in place, such that the compact could rub against it. It does not appear that these scuffs are deep enough to damage fuel particles. The chips, however, were deeper and could have uncovered some underlying particles. If the coatings on any particles had been broken, that damage would appear in the DLBL solutions as elevated concentrations of actinides and fission products.

Compact 12-1 had an as-irradiated diameter of 12.256 mm, ± 0.000 mm (Stempien et al. 2016). The first segment of the radial deconsolidation of Compact 12-1 was 16 minutes long. Figure 17 shows a frame of the video analysis after the first 16 minutes of radial deconsolidation. The second segment of deconsolidation ran for a total of 23 minutes. After the first 7.5 minutes of the second segment of deconsolidation, very little material had been removed, and the characteristic bubbling at the cathode wire had stopped. The deconsolidation was then paused, the wires and leads were repositioned, and the deconsolidation was restarted. Upon resuming, bubbling was visible, and compact material was being collected in the thimble. The deconsolidation was resumed for an additional 15.5 minutes. A third segment of radial deconsolidation was run for 15 minutes; however, the compact fell off the rod while the apparatus was being positioned for video collection after those 15 minutes. Using calipers, the compact was measured once at each of three locations along its length. The diameters after Segments 1 and 2 were determined via video analysis using FrameGrabber v11k. The compact dimensions determined after the three segments of radial deconsolidation are summarized in Table 21. There was some uneven removal of material from the compact because the excess epoxy extended beyond the diameter of the compact and interfered with the compact-screen contact. Similar interferences were not uncommon during radial deconsolidation of other fuel compacts.

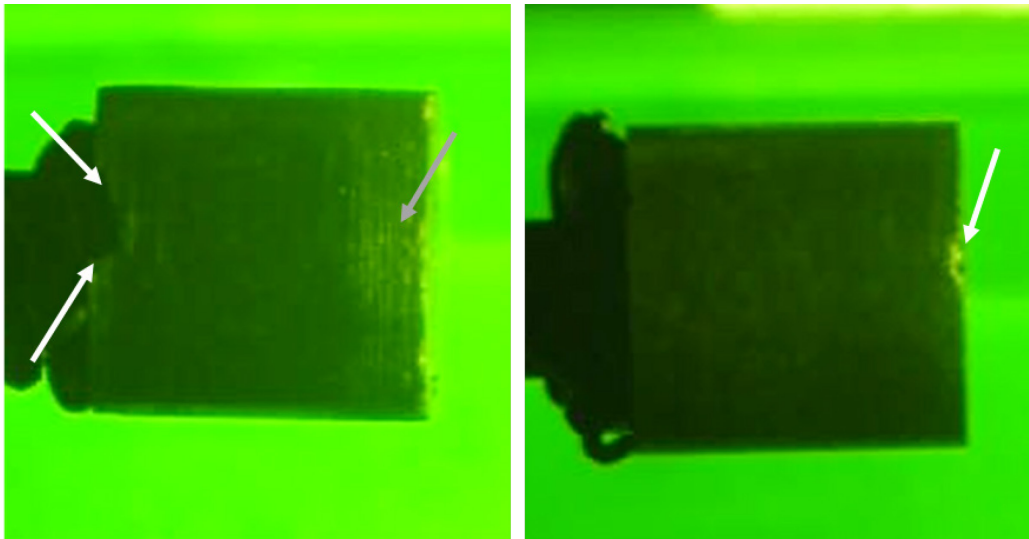


Figure 16. Images of Compact 12-1 after it had been mounted to the rod, prior to the start of deconsolidation. White arrows show where chips of material are missing. Gray arrow shows scuffing.

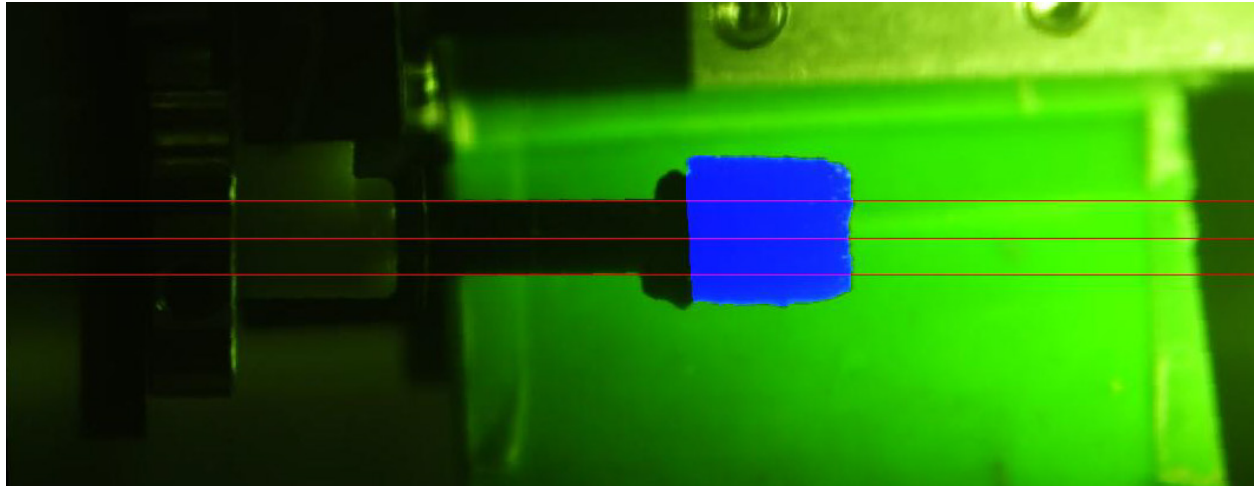


Figure 17. Frame 175 from analysis 11k_2_DSC_4613 after the 16 minutes of Segment 1 radial deconsolidation of Compact 12-1 was completed.

Table 21. Summary of Compact 12-1 diameter change, new diameter after each segment of deconsolidation, and the volume of the compact material removed. The volume of the core remaining after the three segments of radial deconsolidation is also given.

	Segment 1	Segment 2	Segment 3	Core
Deconsolidation Time (min)	16	15.5	15	–
Diameter Reduction (mm)	0.741	0.287	1.999	–
Std Dev of Diameter Reduction	0.221	0.217	0.288	–
New Diameter (mm)	11.515	11.227	9.229	–
New Diameter Std Dev	0.222	0.279	0.258	–
Segment Volume (mm ³)	172.438	53.004	389.440	833.435
Segment Volume Std Dev	35.330	51.407	38.531	32.950

3.8 Compact 12-3

Compact 12-3 had an as-irradiated diameter of 12.254 ± 0.000 mm (Stempien et al. 2016). After obtaining a pre-deconsolidation diameter for the compact via video analysis, a 15-minute period of radial deconsolidation was performed. Then, the compact was inadvertently knocked from the rod after the first segment of deconsolidation was completed, but before the diameter could be measured. Figure 18a shows that epoxy and some compact material adhered to the rod after the compact was dislodged. The star-shaped appearance in the epoxy is from small slits in the deconsolidation rod that were intended to allow some epoxy to seep through and increase the compact-epoxy-bond surface area. A thin portion of the compact surface that appears to be limited to compact graphitic-matrix material remains adhered to the epoxy in Figure 18a. Figure 18b shows a photo of the end of the compact that was attached to the deconsolidation rod. An outline matching the shape of the epoxy is visible on this end of the compact.

The compact was remounted to the rod (using the procedures and equipment used to mount it the first time), and video was obtained of the rotating compact. Figure 19 shows a frame of a video acquired after remounting the compact to the rod. Remounting the compact was successful for purposes of measuring the compact after the first (and only) segment of radial deconsolidation; however, the mounting jig could only center an as-irradiated compact on the rod. The remounted compact would not be centered on the rod, and any subsequent radial deconsolidation steps would not remove material uniformly from the compact. Thus, no further radial segments were obtained for this compact. The mounting jig was subsequently redesigned to effectively center compacts of any diameter, and this proved useful as instance of compact-rod detachment occurred during RDLBL of other compacts. Table 22 summarizes the dimensions and volumes of the compact for Segment 1 and the remaining core.

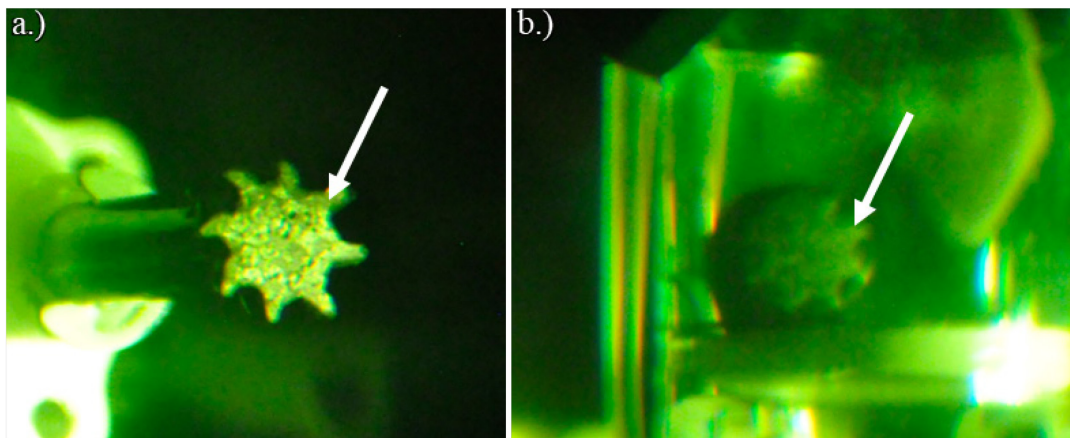


Figure 18. (a) Epoxy and some compact material adhered to rod. (b) Compact showing the end formerly bonded to the rod. Photos taken through the hot cell window.

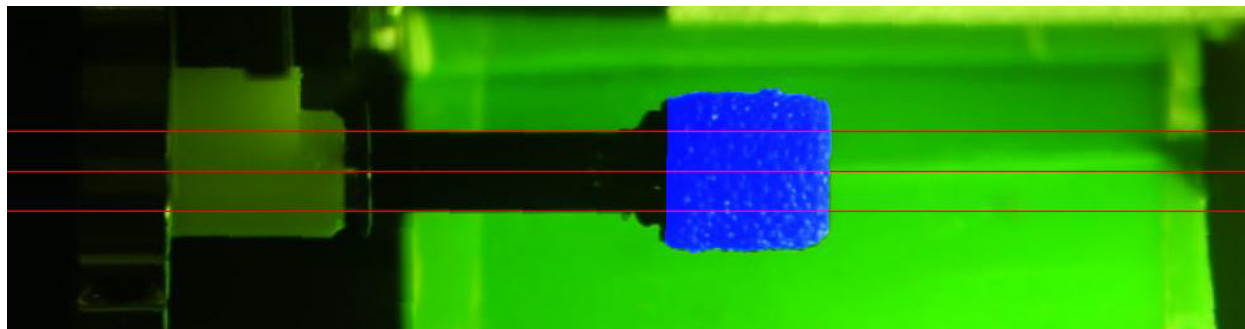


Figure 19. Analysis from Frame 1670 analyzed from video DSC_4475. Video was taken after re-gluing compact to rod after the first and only segment of radial deconsolidation.

Table 22. Summary of Compact 12-3 diameter change, new diameter after a segment of deconsolidation, and the volume of the compact material removed. The volume of the core remaining after the one segment of radial deconsolidation is also given.

	Segment 1	Core
Radial deconsolidation time (min)	15	–
Diameter Reduction (mm)	0.617	–
Diameter Reduction Std Dev (\pm mm)	0.188	–
New Diameter (mm)	11.637	–
New Diameter Std Dev (\pm mm)	0.188	–
Segment Volume (mm ³)	144.336	1325.088
Segment Volume Std Dev (\pm mm)	30.327	30.274

4. RESULTS AND DISCUSSION FROM RDLBL SOLUTIONS ANALYSES

RDLBL generates a deconsolidation solution, two pre-burn leach solutions, and two post-burn leach solutions for each radial segment and the compact core that remains after the radial segments have been taken. Each of these solutions was analyzed by gamma spectrometry, strontium separation and gas proportional counting, and ICP-MS. Thus, for a compact where three radial segments were obtained, a total of 20 solutions were analyzed. Triplicate analyses of each solution were typically (though not always) performed, resulting in up to 60 datasets per compact, not including blanks.^a Decay corrections, measured-to-calculated comparisons, and propagation of errors were discussed in Section 2.4.

Actinides and fission products not contained within the boundary of normally retentive SiC layers of the driver particles were subject to dissolution in the RDLBL leachates. The dissolved actinides and fission products included those that had (a) migrated out of the DTF particles into the surrounding compact matrix, (b) were retained in the DTF kernels that were leached during DLBL, (c) migrated through the SiC layer in the TRISO-coated driver particles and into the compact matrix, (d) were related to uranium contamination present in the compact matrix and/or OPyC at the time the compact was fabricated, (e) were externally introduced by contamination from sources present in the hot cell, and (f) were from TRISO-coated particles with damaged SiC (possibly, but not necessarily, including pyrolytic carbon [PyC] damage).

Potential sources of damaged driver particles include in-pile failure, as-fabricated defects, and those accidentally damaged by the RDLBL process. In instances where driver particles were deemed to have been damaged by the RDLBL process, attempts were made to correct the results for this damage. Generally, a determination on the number of damaged driver particles f (an integer) was made based on the quantities of U and Ce and when in the RDLBL process these quantities were detected. (In some cases, other nuclides were also considered in the enumeration of damaged driver particles.) If the inventory i of a given nuclide in the step of the process found to have damaged driver particles was $\geq f$ particle equivalents, f particle equivalents were subtracted from that inventory to give a corrected inventory $i_c = i - f$. If the inventory of a given nuclide in the step where the damaged particles were determined was $< f$ particle equivalents, then the corrected inventory i_c was set to zero. Each instance where a correction was made will be discussed specifically and in detail in the sections that follow.

^a Typically, 30 TRISO-coated driver particles from each segment of a radial deconsolidation from each compact were picked at random and gamma counted. Those results are not included in this report.

4.1 Compact 3-3

Compact 3-3 had four radial segments in addition to the core. This means a total of 25 distinct solutions were analyzed for Compact 3-3. Duplicate analyses of the solutions were not performed for this particular compact. Section 3.1 described the difficulties encountered with the deconsolidation of this compact. The compact fell from the deconsolidation rod before deconsolidation started. This pulled off the matrix at one end of the compact, exposing an entire face of particles. The compact was reattached. Then the compact fell from the rod again after the fourth radial segment was obtained. The compact was handled with metal tweezers and measured with analog calipers. It is thought that the matrix damage sustained prior to the start of the first segment of RDLBL and the perhaps ill-advised handling following the fourth segment RDLBL caused accidental damage to a number of driver particles. As Section 4.1.3 discusses, a number of the TRISO-coated driver particles were damaged during the deconsolidation, and this makes it impossible to distinguish the inventory of some fission products released from the DTF particles from that contributed by accidental damage to the driver particles.

4.1.1 Compact 3-3 Gamma-Emitter and Sr-90 Results

The total inventories of selected gamma-emitting fission products and beta-emitting Sr-90 measured in the compact outside of the driver-fuel SiC layer for each segment of the radial deconsolidation are summarized in Table 23. Additional results in units of activity and in terms of the fraction of the compact inventory of fission products can be found in Table 73 and Table 74 of Appendix A.1. Table 24 gives the relative error for these results.

Table 23. Particle-equivalent inventories measured in the solutions from the radial deconsolidation of Compact 3-3. All values were decay-corrected to EOI + 1 day and compared to the physics predictions using the same reference date (EOI + 1d).

Particle Equivalents		Ag-110m	Ce-144	Cs-134	Cs-137	Eu-154	Eu-155	Ru-106	Sb-125	Sr-90
Segment #1	Decon	<1.0E+0	9.09E-1	8.15E-2	1.68E-1	7.14E-1	7.68E-1	7.47E-1	5.23E-1	3.23E-1
	Pre-burn leach 1	<3.1E+0	5.18E-3	1.87E-1	2.67E-1	1.69E-1	1.52E-1	8.62E-2	<1.0E-1	1.22E+0
	Pre-burn leach 2	<4.0E+0	1.20E+0	5.17E-1	1.42E+0	6.59E-1	8.31E-1	8.37E-1	<1.4E-1	9.39E-3
	Post-burn leach 1	<4.0E+0	6.30E-2	4.50E-1	6.56E-1	1.35E+0	1.68E+0	<1.1E-1	1.80E-1	1.04E-2
	Post-burn leach 2	<1.0E+0	<1.5E-3	7.30E-3	2.44E-2	2.17E-2	<2.3E-2	<7.1E-3	<2.9E-2	4.75E-3
	SUM (MDA = 0)	0	2.18	1.24	2.54	2.92	3.44	1.67	7.03E-1	1.56
Segment #2	Decon	<1.0E+0	4.54E-2	6.33E-2	1.77E-1	3.31E-1	3.97E-1	5.93E-1	7.13E-2	4.61E-1
	Pre-burn leach 1	<1.0E+0	<3.6E-3	1.57E-3	9.14E-3	1.18E-1	1.26E-1	6.54E-2	<2.9E-2	6.56E-2
	Pre-burn leach 2	<1.0E+0	1.17E-2	1.56E-2	1.18E-1	<2.9E-2	<9.2E-2	3.31E-2	2.81E-2	6.24E-2
	Post-burn leach 1	<1.9E+0	3.65E-2	2.42E-3	1.37E-2	9.70E-1	1.20E+0	<2.1E-2	5.83E-2	5.63E-1
	Post-burn leach 2	<1.0E+0	<1.5E-3	<7.1E-4	6.94E-3	<1.6E-2	<4.6E-2	<1.1E-2	<1.4E-2	7.92E-3
	SUM (MDA = 0)	0	9.36E-2	8.29E-2	3.24E-1	1.42	1.72	6.91E-1	1.58E-1	1.16
Segment #3	Decon	<1.0E+0	6.06E-2	6.43E-2	1.91E-1	1.48E-1	2.34E-1	5.50E-1	7.47E-2	3.25E-1
	Pre-burn leach 1	<8.1E-1	<1.5E-3	2.12E-3	2.44E-2	4.53E-2	5.38E-2	2.42E-2	<2.9E-2	2.68E-2
	Pre-burn leach 2	<8.1E-1	<1.5E-3	3.71E-4	5.02E-3	<1.6E-2	<4.6E-2	<1.1E-3	<1.4E-2	6.37E-3
	Post-burn leach 1	<1.0E+0	9.17E-3	5.24E-4	1.42E-3	2.50E-1	3.20E-1	<1.1E-2	<1.4E-2	1.55E-1
	Post-burn leach 2	<7.1E-1	7.09E-3	3.94E-4	1.35E-3	1.86E-1	2.31E-1	<7.1E-3	<1.4E-2	1.09E-1
	SUM (MDA = 0)	0	7.68E-2	6.77E-2	2.23E-1	6.29E-1	8.38E-1	5.74E-1	7.47E-2	6.23E-1

Particle Equivalents		Ag-110m	Ce-144	Cs-134	Cs-137	Eu-154	Eu-155	Ru-106	Sb-125	Sr-90
Segment #4	Decon	<1.0E+1	5.04E-1	6.31E-1	1.83E+0	1.69E+0	2.31E+0	3.85E+0	7.13E-1	3.08E+0
	Pre-burn leach 1	<1.0E+0	<3.6E-3	1.87E-3	1.77E-2	1.04E-1	1.17E-1	4.36E-2	<2.9E-2	5.33E-2
	Pre-burn leach 2	<7.1E-1	<1.5E-3	<3.1E-4	7.34E-4	5.31E-2	5.67E-2	<7.1E-3	<1.4E-2	7.93E-3
	Post-burn leach 1	<7.1E-1	<3.6E-3	<7.1E-4	8.61E-4	3.73E-1	4.46E-1	<7.1E-3	3.11E-2	2.11E-1
	Post-burn leach 2	<5.0E-1	<7.3E-4	<3.1E-4	9.36E-4	<9.4E-3	<9.2E-3	<3.5E-3	<8.6E-3	3.82E-3
	SUM (MDA = 0)	0	5.04E-1	6.32E-1	1.85	2.22	2.93	3.89	7.44E-1	3.36
Core	Decon	<5.9E+0	5.31E+0	1.37E+0	3.50E+0	2.24E+0	3.62E+0	4.60E+0	1.93E+0	5.51E+0
	Pre-burn leach 1	<1.9E+1	7.79E+0	2.87E+0	3.79E+0	3.47E+0	3.20E+0	1.24E+1	1.95E+0	4.75E+0
	Pre-burn leach 2	<4.0E+0	5.49E-1	6.48E-1	9.01E-1	3.77E-1	3.61E-1	4.43E-1	5.45E-1	5.66E-1
	Post-burn leach 1	<8.1E+0	1.14E+1	8.57E-1	1.19E+0	7.68E+0	9.51E+0	3.15E-1	4.81E+0	5.76E+0
	Post-burn leach 2	<1.9E+0	1.03E-1	6.14E-2	9.17E-2	1.31E-1	1.26E-1	1.91E-1	3.36E-1	5.97E-2
	SUM (MDA = 0)	0	2.52E+1	5.81E+0	9.47E+0	1.39E+1	1.68E+1	1.80E+1	9.57E+0	1.67E+1
Compact TOTAL (MDA = 0)		0	28.01	7.84	14.40	21.09	25.74	24.79	11.25	23.36

Table 24. Relative error in the Compact 3-3 RDLBL results. The errors in the “sum” rows were computed by propagating the error from all the RDLBL steps.

Uncertainty		Ag-110m	Ce-144	Cs-134	Cs-137	Eu-154	Eu-155	Ru-106	Sb-125	Sr-90
Segment #1	Decon	N/A	5.0%	3.0%	6.0%	3.0%	6.0%	5.0%	4.0%	2.0%
	Pre-burn leach 1	N/A	25.0%	3.0%	6.0%	3.0%	15.0%	11.0%	N/A	2.0%
	Pre-burn leach 2	N/A	3.0%	3.0%	3.0%	3.0%	7.0%	3.0%	N/A	2.0%
	Post-burn leach 1	N/A	9.0%	3.0%	3.0%	3.0%	4.0%	N/A	4.0%	2.0%
	Post-burn leach 2	N/A	N/A	3.0%	3.0%	3.0%	N/A	N/A	N/A	2.0%
	SUM (MDA = 0)	N/A	2.7%	1.7%	2.0%	1.7%	3.0%	2.8%	3.2%	1.6%
Segment #2	Decon	N/A	10.0%	3.0%	6.0%	3.0%	7.0%	5.0%	11.0%	2.0%
	Pre-burn leach 1	N/A	N/A	10.0%	3.0%	3.0%	9.0%	4.0%	N/A	2.0%
	Pre-burn leach 2	N/A	9.0%	3.0%	3.0%	N/A	N/A	17.0%	27.0%	2.0%
	Post-burn leach 1	N/A	6.0%	3.0%	3.0%	3.0%	3.0%	N/A	7.0%	2.0%
	Post-burn leach 2	N/A	N/A	N/A	3.0%	N/A	N/A	N/A	N/A	2.0%
	SUM (MDA = 0)	N/A	5.7%	2.4%	3.4%	2.2%	2.7%	4.4%	7.4%	1.3%
Segment #3	Decon	N/A	8.0%	3.0%	6.0%	4.0%	8.0%	5.0%	11.0%	2.0%
	Pre-burn leach 1	N/A	N/A	7.0%	3.0%	3.0%	19.0%	6.0%	N/A	2.0%
	Pre-burn leach 2	N/A	N/A	17.0%	3.0%	N/A	N/A	N/A	N/A	2.0%
	Post-burn leach 1	N/A	8.0%	3.0%	8.0%	3.0%	5.0%	N/A	N/A	2.0%
	Post-burn leach 2	N/A	8.0%	4.0%	7.0%	3.0%	6.0%	N/A	N/A	2.0%
	SUM (MDA = 0)	N/A	6.6%	2.9%	5.2%	1.8%	3.6%	4.8%	11.0%	1.2%
Segment #4	Decon	N/A	11.0%	3.0%	6.0%	4.0%	8.0%	5.0%	12.0%	2.0%
	Pre-burn leach 1	N/A	N/A	4.0%	3.0%	3.0%	11.0%	5.0%	N/A	2.0%
	Pre-burn leach 2	N/A	N/A	N/A	9.0%	3.0%	14.0%	N/A	N/A	2.0%
	Post-burn leach 1	N/A	N/A	N/A	3.0%	3.0%	4.0%	N/A	3.0%	2.0%
	Post-burn leach 2	N/A	N/A	N/A	7.0%	N/A	N/A	N/A	N/A	2.0%
	SUM (MDA = 0)	N/A	11.0%	3.0%	5.9%	3.1%	6.4%	5.0%	11.5%	1.8%

Uncertainty		Ag-110m	Ce-144	Cs-134	Cs-137	Eu-154	Eu-155	Ru-106	Sb-125	Sr-90
Core	Decon	N/A	5.0%	3.0%	6.0%	3.0%	6.0%	4.0%	4.0%	2.0%
	Pre-burn leach 1	N/A	6.0%	3.0%	4.0%	4.0%	12.0%	3.0%	16.0%	2.0%
	Pre-burn leach 2	N/A	3.0%	3.0%	3.0%	3.0%	12.0%	4.0%	6.0%	2.0%
	Post-burn leach 1	N/A	3.0%	3.0%	3.0%	3.0%	3.0%	5.0%	3.0%	2.0%
	Post-burn leach 2	N/A	5.0%	3.0%	3.0%	3.0%	15.0%	4.0%	4.0%	2.0%
	SUM (MDA = 0)	N/A	2.5%	1.7%	2.8%	2.0%	3.1%	2.3%	3.7%	1.1%
Compact TOTAL (MDA = 0)		N/A	2.3%	1.3%	2.0%	1.4%	2.2%	1.9%	3.2%	0.8%

4.1.2 Compact 3-3 ICP-MS Results

ICP-MS was used to measure actinides in the RDLBL solutions. Intact TRISO particles will retain all actinides during the DLBL process, but exposed kernels, such as in the DTF particles or in damaged TRISO-coated particles, will be subject to leaching. Table 25 summarizes the actinide content measured from the RDLBL of Compact 3-3, and Table 26 gives the error in the measurement values. Additional tables (Table 75 and Table 76) in Appendix A1 provides these results in units of mass and compact fraction.

Table 25. Particle equivalents for select actinides from ICP-MS of solutions from Compact 3-3 RDLBL.

		Particle Equivalents					
		Pu-239	Pu-240	U-234	U-235	U-236	U-238
Segment #1	Decon	<2.7E+0	<1.1E+0	<1.3E+1	1.14	<1.2E+0	1.05
	Pre-burn leach 1	<1.3E+1	<6.3E+0	<7.3E+1	<1.4E+0	<5.8E-1	<8.4E-2
	Pre-burn leach 2	<8.8E+0	<4.2E+0	<5.2E+1	2.49	1.62	2.58
	Post-burn leach 1	<1.1E+1	<5.4E+0	<5.9E+1	<1.1E+0	<5.8E-1	<6.7E-2
	Post-burn leach 2	<1.2E+1	<5.4E+0	<6.3E+1	<1.2E+0	<5.8E-1	<7.3E-2
	Total (MDA = 0)	0	0	0	3.63	1.62	3.63
Segment #2	Decon	<2.7E+0	<1.1E+0	<1.3E+1	0.91	0.78	0.82
	Pre-burn leach 1	<1.1E+1	<5.4E+0	<6.3E+1	<1.2E+0	<5.8E-1	<7.3E-2
	Pre-burn leach 2	<1.3E+1	<6.3E+0	<7.3E+1	<1.4E+0	<7.7E-1	<1.1E-1
	Post-burn leach 1	<1.0E+1	<5.4E+0	<5.9E+1	<1.1E+0	<5.8E-1	<6.7E-2
	Post-burn leach 2	<1.2E+1	<5.4E+0	<6.7E+1	<1.3E+0	<5.8E-1	<7.9E-2
	Total (MDA = 0)	0	0	0	0.91	0.78	0.82
Segment #3	Decon	0.53	0.40	0.88	0.94	0.89	0.90
	Pre-burn leach 1	<1.1E-1	<2.1E-2	<4.2E-1	0.02	<1.2E-2	0.01
	Pre-burn leach 2	<1.1E-1	<2.1E-2	<8.4E-1	<6.1E-3	<1.6E-2	0.01
	Post-burn leach 1	<1.1E-1	<5.4E-2	<4.2E-1	<6.1E-3	<1.3E-2	0.01
	Post-burn leach 2	<8.4E+0	<4.2E+0	<4.6E+1	<8.6E-1	<3.8E-1	<5.6E-2
	Total (MDA = 0)	0.53	0.40	0.88	0.96	0.89	0.92
Segment #4	Decon	0.44	0.34	<8.4E-1	0.67	0.64	0.65
	Pre-burn leach 1	<2.3E-1	<3.3E-1	<2.9E+0	<4.4E-2	<5.8E-2	0.02
	Pre-burn leach 2	<1.9E-1	<2.1E-1	<2.5E+0	<3.6E-2	<3.8E-2	<5.0E-3
	Post-burn leach 1	<1.9E-1	<2.1E-1	<2.5E+0	<3.1E-2	<3.8E-2	0.01
	Post-burn leach 2	<3.8E-2	<7.5E-2	<2.9E-1	<6.1E-3	<7.7E-3	<1.1E-3
	Total (MDA = 0)	0.44	0.34	0	0.67	0.64	0.68

		Particle Equivalents					
		Pu-239	Pu-240	U-234	U-235	U-236	U-238
Core	Decon	11.45	10.35	<2.5E+1	17.79	17.09	17.13
	Pre-burn leach 1	10.76	11.14	<4.2E+1	10.44	9.93	9.91
	Pre-burn leach 2	0.27	0.33	<1.7E-1	0.12	0.12	0.12
	Post-burn leach 1	4.11	5.94	<2.5E-1	0.15	<1.6E-1	0.14
	Post-burn leach 2	0.06	<8.6E-2	<8.4E-2	<5.6E-3	<1.9E-2	<3.5E-3
	Total (MDA = 0)	26.65	27.76	0	28.49	27.13	27.31
Compact Total (MDA) = 0		27.63	28.50	0.88	34.65	31.06	33.35

Table 26. Error in the Compact 3-3 ICP-MS results that were summarized in the preceding tables.

		% Error					
		Pu-239	Pu-240	U-234	U-235	U-236	U-238
Segment #1	Decon	N/A	N/A	N/A	25%	N/A	10%
	Pre-burn leach 1	N/A	N/A	N/A	N/A	N/A	N/A
	Pre-burn leach 2	N/A	N/A	N/A	20%	20%	10%
	Post-burn leach 1	N/A	N/A	N/A	N/A	N/A	N/A
	Post-burn leach 2	N/A	N/A	N/A	N/A	N/A	N/A
	Total (MDA = 0)	N/A	N/A	N/A	15.8%	20.0%	7.7%
Segment #2	Decon	N/A	N/A	N/A	15%	15%	10%
	Pre-burn leach 1	N/A	N/A	N/A	N/A	N/A	N/A
	Pre-burn leach 2	N/A	N/A	N/A	N/A	N/A	N/A
	Post-burn leach 1	N/A	N/A	N/A	N/A	N/A	N/A
	Post-burn leach 2	N/A	N/A	N/A	N/A	N/A	N/A
	Total (MDA = 0)	N/A	N/A	N/A	15.0%	15.0%	10.0%
Segment #3	Decon	5%	10%	15%	15%	15%	10%
	Pre-burn leach 1	N/A	N/A	N/A	35%	N/A	20%
	Pre-burn leach 2	N/A	N/A	N/A	N/A	N/A	25%
	Post-burn leach 1	N/A	N/A	N/A	N/A	N/A	25%
	Post-burn leach 2	N/A	N/A	N/A	N/A	N/A	N/A
	Total (MDA = 0)	5.0%	10.0%	15.0%	14.7%	15.0%	9.7%
Segment #4	Decon	10%	15%	N/A	5%	10%	5%
	Pre-burn leach 1	N/A	N/A	N/A	N/A	N/A	15%
	Pre-burn leach 2	N/A	N/A	N/A	N/A	N/A	N/A
	Post-burn leach 1	N/A	N/A	N/A	N/A	N/A	15%
	Post-burn leach 2	N/A	N/A	N/A	N/A	N/A	N/A
	Total (MDA = 0)	10.0%	15.0%	N/A	5.0%	10.0%	4.8%

		% Error					
		Pu-239	Pu-240	U-234	U-235	U-236	U-238
Core	Decon	5%	15%	N/A	5%	10%	5%
	Pre-burn leach 1	25%	30%	N/A	10%	15%	10%
	Pre-burn leach 2	20%	35%	N/A	25%	35%	5%
	Post-burn leach 1	10%	5%	N/A	15%	N/A	10%
	Post-burn leach 2	35%	N/A	N/A	N/A	N/A	N/A
	Total (MDA = 0)	10.4%	15.0%	N/A	5.0%	10.0%	4.8%
Compact Total (MDA) = 0		10.1%	14.6%	15.0%	4.5%	8.8%	4.0%

4.1.3 Compact 3-3 Discussion

Ideally, the radial deconsolidation process would not damage the fuel compact or TRISO particles; however, this was not the case for Compact 3-3. Compact 3-3 was mounted to the deconsolidation rod using epoxy, and it was inadvertently dislodged from the rod prior to the start of the deconsolidation. This separation was a clean separation between the epoxy and the rod that left all the epoxy adhered to the compact. Before attempting to reattach the compact to the rod using the centering fixture, attempts were made to remove the epoxy. Unfortunately, this caused some of the compact, and potentially some particles, to pull off and remain with the epoxy (see Figure 8). This exposed many particles on one of the flat faces of the compact. The elevated quantities of certain fission products and actinides measured in the DLBL solutions support the conclusion that some of the TRISO-coated driver particles were damaged as a result of this and subsequent handling steps. Because this damage seems to have occurred prior to or during the deconsolidation step in Segments 1–4, it is impossible to distinguish the fission-product inventories that originated in the DTF particles from those that were introduced from accidental damage to some of the driver particles. If damage had occurred after the deconsolidation step, valid corrections could have been applied. The core also appears to have five to seven damaged particles, but because those occurred in the presence of 20 DTF particles, it is not clear exactly when in the core DLBL process this damage occurred. After the compact was dislodged from the rod after the fourth segment, it was handled with metal tweezers and calipers. This handling may have damaged some of the exposed particles that were subsequently leached during the deconsolidation of the remaining core.

Given the extent of damage to the driver particles, it is not possible to correct the results for this accidental damage in Compact 3-3. However, some of the following sections (such as Section 4.2 for Compact 5-3), detail cases of accidental damage that could be clearly linked to a single particle and a single step of the DLBL. In those cases, corrections could be reasonably applied to subtract the radionuclide inventory of the damaged driver particle from the rest of the radionuclide inventory.

Table 25 shows that 33.4 particle equivalents of U-238 were detected, in total, from the DLBL of Compact 3-3. In a compact with 20 DTF particles and no damaged TRISO-coated driver particles, approximately 20 particle equivalents of uranium are all that would be expected based on the assumption that the uranium in the DTF kernels was retained in the compact. For example, Compact 5-4 was not damaged during deconsolidation, and 19.5 particle equivalents of U-238 were measured, in total, from its deconsolidation. Compacts 5-3 and 7-3 each had one particle damaged during the post-burn leaches of their first segments, and a total of 19.5 and 21.0 particle equivalents of U-238 were measured in their deconsolidations, respectively. After correcting for the accidental particle damage, the total U-238 measured in Compacts 5-3 and 7-3 was 18.6 and 20.0, respectively. Based on comparing the amount of U-238 measured in Compact 3-3 to that measured in other compacts, 13 or 14 TRISO-coated driver particles are believed to have been damaged during the process of handling the compact, preparing it for radial deconsolidation, re-attaching it to the deconsolidation rod, and attempting to measure the diameter of the compact following the fourth radial segment. This allowed the contents of the kernels of the damaged particles (both actinides and fission products) to be leached. It is not known why the Pu-239, Pu-240,

and U-234 were below detection in Segments 1 and 2 when significant amounts of U-235 and U-238 were measurable.

Aside from looking at the total inventories of actinides and fission products, accidental TRISO particle damage can be assessed from one step to another in Table 25. In the deconsolidation of Segment 1, approximately one particle equivalent of U-235 and U-238 was measured. This is indicative of a particle that was broken prior to or during the Segment 1 deconsolidation. It seems reasonable to attribute this broken particle to the compact-rod detachment and reattachment that happened before the Segment 1 radial deconsolidation even started.

Next, approximately 2.5 particle equivalents of U-235 and U-238 were measured in the Segment-1 pre-burn-leach #2. This indicates that the OPyC, SiC, and IPyC were broken in two or three particles at this stage. It is unusual to see this much uranium in a second pre-burn leach. It is not clear what caused this. Perhaps coatings were partially damaged during the problems encountered with mounting and remounting the compact to the rod or from mechanical contact with the RDLBL screen or some other handling error. In that scenario, the partially damaged coatings would have completely failed during the second pre-burn leach. Given AGR-3/4 TRISO particles are of the same specification as AGR-1, which saw very low rates of in-pile SiC (Demkowicz et al. 2015), it is extremely unlikely that in-pile SiC failure contributed to this. It is not the result of irradiation-induced TRISO failure because failed-TRISO particles would have had the majority of their contents leached into the deconsolidation solution such that little material was left to leach in the subsequent pre-burn leaches.

One particle was damaged in the deconsolidation steps of Segments 2, 3, and 4. In the core of Compact 3-3, most of the uranium was measured in the deconsolidation and first pre-burn leach solutions, amounting to about 27 and 28.5 particle equivalents of U-238 and U-235, respectively. About 20 particle equivalents were expected in the core based on the assumption of little uranium migration out of the DTF kernels; therefore, the additional particle equivalents are attributed to accidental damage done to the driver particles, either during the mounting and remounting processes performed prior to the start of the deconsolidation of the first segment, the deconsolidation of the core segment itself, damage from the first core pre-burn leach, or damage from using calipers to measure the compact dimensions when it fell from the rod a second time after the fourth segment had been obtained (see Figure 9).

Accidental particle damage in Compact 3-3 is also apparent in comparisons of the quantities of certain gamma-emitting fission products (e.g., Ce-144 and Ru-106) measured in the Compact 3-3 DLBL solutions. Assuming Ce and Ru are generally retained in the compact, quantities >20 particle equivalents indicate driver-particle damage. Table 23 shows 28.0 particle equivalents of Ce-144 from the deconsolidation of Compact 3-3 (compared to 33.4 particle equivalents of U-238 in Table 25). In comparison, undamaged Compact 5-4 had a total of 20.4 particle equivalents of Ce-144 in its DLBL solutions. In Compact 5-3, after correcting for a particle damaged during the first post-burn leach of the first radial segment, there were 19.6 particle equivalents of Ce-144 (20.5 before applying the correction). Similarly, there were 20.7 particle equivalents of Ce-144 in Compact 7-3 (21.7 before applying the correction). The recovery of Ru-106 from Compact 3-3 was 24.8 particle equivalents, which is in relatively good agreement with the amount of Ce-144 measured. Generally, the recovery of Ru-106 via acid leaching can be incomplete relative to actinide recovery from the same samples. This is relatively common among other RDLBL and traditional DLBL results (Helmreich et al. 2022, Stempien et al. 2021). Therefore, measuring >20 particle equivalents of Ru-106 is another indication of damaged TRISO-coated particles.

Cesium recovery from a DLBL is not the most reliable indicator of exposed kernels because cesium can be lost (driven out of the sample) during the burn steps, or if the kernel was exposed in-pile, the Cs could have been lost during irradiation. Europium and Sr can be released in small quantities through intact TRISO coatings (especially at higher irradiation temperatures above about 1,100°C [Stempien et al. 2018]), but these elements generally are well-retained within the compact matrix even if they diffuse through the TRISO coatings. This can make it impossible to determine the quantity of Eu or Sr via small diffusive release through intact coatings from

the much larger quantity from the DTF particles. Thus, as indicators of the number of exposed kernels, Eu and Sr are less effective than Ce, Ru, and U.

4.2 Compact 5-3

This compact was deconsolidated in three radial segments, and the remaining core was deconsolidated in a single step. Thus, there were four distinct volumes of Compact 5-3 that were analyzed as part of its DLBL. The compact appeared normal prior to beginning the deconsolidation, with only some light scuffing around the edge of the unbonded end of the compact. The compact remained bonded to the rod for the entire deconsolidation. Section 4.2.3 discusses what appears to be a TRISO-coated particle in Segment 1 with a SiC failure that was leached in the first post-burn leach step.

4.2.1 Compact 5-3 Gamma-Emitter and Sr-90 Results

The total amounts of selected fission products measured in the compact outside of the driver fuel SiC layer for each segment of the radial deconsolidation are summarized in Table 27 in terms of the number of particle-equivalent inventories. As detailed in Section 4.2.3, the values in the first post-burn leach of Segment 1 were corrected by up to one particle equivalent to account for a particle that was damaged during Segment 1 post-burn-leach 1. Table 27 presents both uncorrected and corrected values. Table 28 gives the relative errors of these values. Additional tables (Table 77 and Table 78) in Appendix A.2 give the same results in units of activity and compact fraction.

Table 27. Particle-equivalent inventories measured in the solutions from the radial deconsolidation of Compact 5-3. All values were decay-corrected to EOI + 1 day and compared to physics predictions at the same reference date.

Particle Equivalents		Ag-110m	Ce-144	Cs-134	Cs-137	Eu-154	Eu-155	Ru-106	Sb-125	Sr-90
Segment #1	Decon	<6	<4E-02	5.58E-01	6.39E-01	<2E-02	<1E-01	<8E-02	<2E-01	5.74E-03
	Pre-burn leach 1	<6	<1E-02	7.30E-02	1.08E-01	<2E-02	<4E-02	<6E-02	<6E-02	1.76E-03
	Pre-burn leach 2	<6	<1E-02	9.57E-03	1.38E-02	<2E-02	<8E-02	<2E-02	<4E-02	6.64E-04
	Post-burn leach 1	<6	9.33E-01	4.15E-01	5.91E-01	7.59E-01	8.77E-01	<2E-01	4.06E-01	1.02E+00
	Post-burn leach 1*	<6	0	0	0	0	0	0	0	2.18E-02
	Post-burn leach 2	<6	<1E-02	3.12E-03	3.19E-03	<1E-02	<8E-02	1.30E-02	3.99E-02	1.39E-03
	SUM (MDA = 0)	0	9.33E-01	1.06E+00	1.35E+00	7.59E-01	8.77E-01	1.30E-02	4.46E-01	1.03E+00
	SUM (MDA = 0)*	0	0	6.44E-01	7.64E-01	0	0	1.30E-02	3.99E-02	3.14E-02
Segment #2	Decon	<4	1.15E-02	2.62E-01	4.15E-01	<1E-02	<8E-02	<8E-02	<8E-02	7.87E-03
	Pre-burn leach 1	<4	<1E-02	5.20E-02	7.53E-02	<2E-02	<8E-02	<8E-02	<8E-02	1.18E-03
	Pre-burn leach 2	<2	<1E-02	8.43E-03	1.13E-02	<1E-02	<4E-02	<2E-02	<4E-02	3.01E-04
	Post-burn leach 1	<4	<1E-02	8.12E-02	1.13E-01	2.28E-02	<8E-02	<8E-02	<8E-02	5.86E-04
	Post-burn leach 2	<2	<6E-03	9.64E-04	1.49E-03	<1E-02	<4E-02	<2E-02	<1E-02	1.87E-04
	SUM (MDA = 0)	0	1.15E-02	4.04E-01	6.17E-01	2.28E-02	0	0	0	1.01E-02
Segment #3	Decon	<6	5.02E-02	6.55E-01	1.08	4.41E-02	8.58E-02	<2E-01	<1E-01	1.69E-01
	Pre-burn leach 1	<2	<1E-02	6.27E-02	9.08E-02	<2E-02	<8E-02	<8E-02	<8E-02	8.98E-04
	Pre-burn leach 2	<2	<1E-02	8.22E-03	1.20E-02	<1E-02	<4E-02	<2E-02	<4E-02	3.04E-04
	Post-burn leach 1	<6	1.15	7.95E-01	1.19	9.32E-01	1.12	7.96E-02	5.05E-01	2.14
	Post-burn leach 2	<4	6.10E-03	6.31E-03	9.23E-03	<2E-02	<8E-02	4.10E-02	6.02E-02	2.44E-03
	SUM (MDA = 0)	0	1.20	1.53	2.37	9.76E-01	1.20	1.21E-01	5.66E-01	2.31

Particle Equivalents		Ag-110m	Ce-144	Cs-134	Cs-137	Eu-154	Eu-155	Ru-106	Sb-125	Sr-90
Core	Decon	<2E+01	9.54	1.22	2.97	6.04	7.48	4.18	3.50	7.19
	Pre-burn leach 1	<2E+01	7.76	4.58E-01	1.13	4.23	5.10	4.49	1.74	6.44
	Pre-burn leach 2	<4	3.92E-02	1.95E-02	3.07E-02	7.08E-02	6.29E-02	3.22E-01	6.91E-01	1.30E-01
	Post-burn leach 1	<1E+01	1.05	2.14E-01	3.72E-01	3.19	3.76	5.45E-01	4.13	6.46
	Post-burn leach 2	<4	6.28E-03	8.00E-03	1.61E-02	<2E-02	<8E-02	9.19E-02	3.96E-01	1.10E-02
	SUM (MDA = 0)	0	1.84E+01	1.92	4.53	1.35E+01	1.64E+01	9.63	1.05E+01	2.02E+01
Compact TOTAL (MDA = 0)		0	20.54	4.91	8.87	15.29	18.49	9.76	11.47	23.58
Compact TOTAL (MDA = 0)*		0	19.61	4.49	8.28	14.53	17.61	9.76	11.06	22.58
*Corrected for apparent particle damage in Segment 1 post-burn leach 1.										

Table 28. Relative error in the Compact 5-3 RDLBL results. The errors in the “sum” rows were computed by propagating the error from all the RDLBL steps.

Uncertainty		Ag-110m	Ce-144	Cs-134	Cs-137	Eu-154	Eu-155	Ru-106	Sb-125	Sr-90
Segment #1	Decon	N/A	N/A	3.0%	3.0%	N/A	N/A	N/A	N/A	2.0%
	Pre-burn leach 1	N/A	N/A	3.0%	3.0%	N/A	N/A	N/A	N/A	4.3%
	Pre-burn leach 2	N/A	N/A	3.3%	2.4%	N/A	N/A	N/A	N/A	9.4%
	Post-burn leach 1*	N/A	3.7%	3.0%	3.0%	3.0%	5.0%	N/A	13.1%	1.6%
	Post-burn leach 2	N/A	N/A	3.8%	2.5%	N/A	N/A	25.6%	12.6%	4.9%
	SUM (MDA = 0)	N/A	3.7%	2.0%	1.9%	3.0%	5.0%	25.6%	12.0%	1.6%
Segment #2	Decon	N/A	25.6%	3.0%	3.0%	N/A	N/A	N/A	N/A	2.0%
	Pre-burn leach 1	N/A	N/A	3.0%	3.0%	N/A	N/A	N/A	N/A	5.6%
	Pre-burn leach 2	N/A	N/A	4.1%	2.5%	N/A	N/A	N/A	N/A	10.3%
	Post-burn leach 1	N/A	N/A	3.0%	3.0%	15.5%	N/A	N/A	N/A	8.1%
	Post-burn leach 2	N/A	N/A	10.5%	5.0%	N/A	N/A	N/A	N/A	14.5%
	SUM (MDA = 0)	N/A	25.6%	2.1%	2.1%	15.5%	N/A	N/A	N/A	1.8%
Segment #3	Decon	N/A	10.0%	3.0%	3.0%	13.9%	27.0%	N/A	N/A	2.0%
	Pre-burn leach 1	N/A	N/A	3.0%	3.0%	N/A	N/A	N/A	N/A	6.1%
	Pre-burn leach 2	N/A	N/A	2.4%	2.4%	N/A	N/A	N/A	N/A	8.0%
	Post-burn leach 1	N/A	2.9%	2.5%	2.4%	2.4%	4.1%	25.3%	8.0%	2.0%
	Post-burn leach 2	N/A	26.0%	5.5%	3.0%	N/A	N/A	13.6%	16.4%	3.6%
	SUM (MDA = 0)	N/A	2.8%	1.8%	1.8%	2.4%	4.3%	17.3%	7.3%	1.9%

Uncertainty		Ag-110m	Ce-144	Cs-134	Cs-137	Eu-154	Eu-155	Ru-106	Sb-125	Sr-90
Core	Decon	N/A	3.8%	3.0%	3.0%	3.0%	3.0%	3.0%	4.0%	2.0%
	Pre-burn leach 1	N/A	3.0%	3.0%	3.0%	3.0%	3.0%	3.0%	3.0%	2.0%
	Pre-burn leach 2	N/A	10.3%	3.4%	3.0%	3.0%	23.0%	4.0%	3.0%	2.0%
	Post-burn leach 1	N/A	4.0%	3.0%	3.0%	3.0%	3.0%	4.4%	3.0%	2.0%
	Post-burn leach 2	N/A	29.6%	3.7%	3.0%	N/A	N/A	5.0%	3.4%	5.7%
	SUM (MDA = 0)	N/A	2.4%	2.1%	2.1%	1.8%	1.8%	1.9%	1.9%	1.1%
Compact TOTAL (MDA = 0)		N/A	2.1%	1.1%	1.2%	1.6%	1.6%	1.9%	1.8%	1.0%
* This is the measurement error for what was measured in the first pre-burn leach. No attempt to alter the error were made when the inventories were altered to correct for accidental particle damage.										

4.2.2 Compact 5-3 ICP-MS Results

ICP-MS was used to measure actinides in the solutions. Intact TRISO particles will retain all actinides, but exposed kernels, such as in the DTF particles or in damaged TRISO-coated particles, will be subject to leaching during the DLBL process. Table 29 provides results for major isotopes of U and Pu in units of particle equivalents. Additional results in units of mass and compact fraction are summarized in Table 79 and Table 80 of Appendix A.2. Table 30 provides the relative error in these measurements.

Table 29. Particle equivalents for select actinides from ICP-MS of solutions from Compact 5-3 RDLBL.

Particle Equivalents		Pu-239	Pu-240	U-234	U-235	U-236	U-238
Segment #1	Decon	1.72E-02	<4E-02	<1E-01	3.13E-02	1.79E-02	2.05E-02
	Pre-burn leach 1	<2E-02	<1E-01	<4E-01	<6E-03	<1E-02	2.21E-03
	Pre-burn leach 2	<4E-02	<2E-01	<4E-01	<8E-03	<2E-02	<6E-04
	Post-burn leach 1	8.36E-01	8.11E-01	7.16E-01	7.61E-01	8.08E-01	7.66E-01
	Post-burn leach 1*	0	0	0	0	0	0
	Post-burn leach 2	<4E-02	<1E-01	<4E-01	<6E-03	<2E-02	<6E-04
	SUM (MDA = 0)	8.53E-01	8.11E-01	7.16E-01	7.92E-01	8.26E-01	7.89E-01
	SUM (MDA = 0)*	1.72E-02	0	0	3.13E-02	1.79E-02	2.27E-02
Segment #2	Decon	1.80E-02	<4E-02	<1E-01	2.31E-02	2.25E-02	2.25E-02
	Pre-burn leach 1	<4E-02	<1E-01	<4E-01	<8E-03	<1E-02	1.62E-03
	Pre-burn leach 2	<4E-02	<1E-01	<4E-01	<8E-03	<1E-02	<6E-04
	Post-burn leach 1	<4E-02	<1E-01	<4E-01	<8E-03	<1E-02	<6E-04
	Post-burn leach 2	<4E-02	<8E-02	<4E-01	<8E-03	<1E-02	<6E-04
	SUM (MDA = 0)	1.80E-02	0.00E+00	0.00E+00	2.31E-02	2.25E-02	2.41E-02
Segment #3	Decon	4.36E-02	4.27E-02	<2E-01	9.37E-02	8.99E-02	9.13E-02
	Pre-burn leach 1	<4E-02	<8E-02	<4E-01	<8E-03	<2E-02	1.36E-03
	Pre-burn leach 2	<8E-02	<1E-01	<4E-01	<8E-03	<4E-02	<6E-04
	Post-burn leach 1	1.02E+00	1.05E+00	8.94E-01	9.75E-01	1.00E+00	9.87E-01
	Post-burn leach 2	<8E-02	<1E-01	<1E+00	<8E-03	<4E-02	3.05E-03
	SUM (MDA = 0)	1.06E+00	1.09E+00	8.94E-01	1.07E+00	1.09E+00	1.08E+00

Particle Equivalents		Pu-239	Pu-240	U-234	U-235	U-236	U-238
Core	Decon	8.72E+00	9.04E+00	1.04E+01	1.03E+01	1.05E+01	9.95E+00
	Pre-burn leach 1	6.81E+00	7.15E+00	6.89E+00	6.78E+00	6.89E+00	6.62E+00
	Pre-burn leach 2	8.67E-02	<1E-01	<4E-01	1.17E-01	1.13E-01	1.12E-01
	Post-burn leach 1	4.44E-01	5.42E-01	8.31E-01	8.08E-01	8.19E-01	8.00E-01
	Post-burn leach 2	<8E-02	<8E-02	<4E-01	5.18E-02	<4E-02	1.99E-02
	SUM (MDA = 0)	1.61E+01	1.67E+01	1.81E+01	1.81E+01	1.83E+01	1.75E+01
Compact TOTAL (MDA = 0)		17.99	18.64	19.71	19.97	20.27	19.40
Compact TOTAL (MDA = 0)*		17.16	17.83	18.99	19.21	19.47	18.63
* Corrected for apparent particle damage in Segment 1 post-burn leach 1.							

Table 30. Relative error for select actinides from ICP-MS of solutions from Compact 5-3 RDLBL.

Error (%)		Pu-239	Pu-240	U-234	U-235	U-236	U-238
Segment #1	Decon	16%	N/A	N/A	14%	17%	5%
	Pre-burn leach 1	N/A	N/A	N/A	N/A	N/A	20%
	Pre-burn leach 2	N/A	N/A	N/A	N/A	N/A	N/A
	Post-burn leach 1*	5%	13%	17%	7%	5%	5%
	Post-burn leach 2	0%	0%	0%	0%	0%	0%
	SUM (MDA = 0)	16%	N/A	N/A	14%	17%	5%
Segment #2	Decon	13%	N/A	N/A	14%	12%	5%
	Pre-burn leach 1	0%	0%	0%	0%	0%	12%
	Pre-burn leach 2	0%	0%	0%	0%	0%	0%
	Post-burn leach 1	0%	0%	0%	0%	0%	0%
	Post-burn leach 2	0%	0%	0%	0%	0%	0%
	SUM (MDA = 0)	13%	N/A	N/A	14%	12%	5%
Segment #3	Decon	11%	25%	0%	7%	7%	5%
	Pre-burn leach 1	0%	0%	0%	0%	0%	20%
	Pre-burn leach 2	0%	0%	0%	0%	0%	0%
	Post-burn leach 1	9%	9%	25%	5%	5%	5%
	Post-burn leach 2	0%	0%	0%	0%	0%	7%
	SUM (MDA = 0)	8%	9%	25%	5%	5%	5%

Error (%)		Pu-239	Pu-240	U-234	U-235	U-236	U-238
Core	Decon	5%	5%	9%	5%	5%	5%
	Pre-burn leach 1	5%	5%	14%	5%	5%	5%
	Pre-burn leach 2	11%	0%	0%	9%	23%	5%
	Post-burn leach 1	11%	13%	17%	7%	7%	5%
	Post-burn leach 2	0%	0%	0%	15%	0%	9%
	SUM (MDA = 0)	3%	3%	7%	3%	3%	3%
Compact TOTAL (MDA = 0)		3%	3%	9%	3%	3%	3%
* This is the measurement error for what was measured in the first pre-burn leach. No attempts to alter the error were made when the inventories were altered to correct for accidental particle damage.							

4.2.3 Compact 5-3 Discussion

No notable difficulties were encountered mounting Compact 5-3 to the deconsolidation rod or during the deconsolidation itself. Looking at the total amount of actinides measured from the RDLBL suggests that only about 20 particles in the compact had exposed kernels; however, it does appear that a driver particle was broken during the Segment 1 DLBL. It is believed that the particle had an intact SiC coating that was broken at some point between the end of the second pre-burn leach and the end of the first post-burn leach. About 0.02 particle equivalents of actinides were detected in the Segment 1 deconsolidation solution, and no actinides were detected in the pre-burn leaches. Then, approximately 0.8 particle equivalents of actinides such as U-235 and U-238 were measured in the first post-burn leach of Segment 1. Similarly, the only time Ce-144 was detected was in the same solution when 0.93 particle equivalents were measured.^b This evidence alone would point to a particle that had at least one PyC layer intact before the burn, but that particle may or may not have had an intact SiC layer prior to the first burn leach. However, evidence from other gamma-emitters measured from Segment 1 work suggests it is possible that the SiC layer was intact before the first burn leach. No detectable Eu-154 and very little Sr-90 were detected in the pre-burn leaches and about 0.8 to 1.0 particle equivalents of Eu-154 and Sr-90, respectively, in the first post-burn leach solution. Some Cs-134 and Cs-137 was detected prior to the burn steps, but the amount of Cs measured increased from about 0.01 particle equivalents in the second pre-burn leach to 0.4 and 0.6 particle equivalents of Cs-134 and Cs-137, respectively, in the first post-burn leach. This suggests the particle in question retained significant Cs, Eu, and Sr before its SiC layer was broken during the burn, allowing these nuclides to be leached. The alternative that cannot be ruled out is that this particle had a SiC layer that failed in-pile; however, applying the SiC failure rates observed in AGR-1 to AGR-3/4, the probability of a SiC failure here in Compact 5-3 is low ($\leq 3.1E-5$ at 95% confidence).

A correction to better estimate the concentration of fission products and actinides in the compact matrix and OPyC layers in Compact 5-3, Segment 1, was applied as follows. Here, if the inventory of a given nuclide in Segment 1, Burn-Leach 1, was ≥ 1 particle equivalent, a single particle equivalent was subtracted from that inventory. If the inventory of a given nuclide in Segment 1, Burn-Leach 1, was < 1 particle equivalent, that value was set to zero. The values in Table 27 and Table 29 report the results both with and without such a correction.

^b In this campaign of as-irradiated compact RDLBL, the Ce, Ru, and U values tend to agree; however, the Ru quantity tends to be less than the Ce and U quantities. This may be from under-recovery of the Ru, as stated earlier. It is not known why the quantities of Ru-106 measured for Compacts 5-3 and 5-4 are only about 50% of the U and Ce quantities measured in those same compacts.

4.3 Compact 5-4

This compact was deconsolidated in three radial segments, and the remaining core was deconsolidated in a single step. Thus, four distinct volumes of Compact 5-4 were analyzed. The compact appeared normal prior to beginning the deconsolidation, with some light scuffing around the rim of the unbonded end of the compact. The bonded end of the compact also had a couple areas that appeared to have minor scuffs around the rim. The compact remained bonded to the rod for the entire deconsolidation. There were no indications that any TRISO-coated driver particles were damaged during the radial deconsolidation or the leach-burn leach processes.

4.3.1 Compact 5-4 Gamma-Emitter and Sr-90 Results

The total amounts of selected gamma-emitting fission products and beta-emitting Sr-90 measured in the compact outside of the driver-fuel SiC layer for each segment of the radial deconsolidation are summarized in Table 31 in terms of the number of particle-equivalent inventories. Additional results in units of activity and the fraction of the compact inventory are given in Table 81 and Table 82 of Appendix A3. Table 32 gives the relative error for the Compact 5-4 values summarized in the body and appendix.

Table 31. Particle-equivalent inventories measured in the solutions from the radial deconsolidation of Compact 5-4. All values were decay-corrected to EOI + 1 day and compared to physics predictions at the same reference date.

Particle Equivalents		Ag-110m	Ce-144	Cs-134	Cs-137	Eu-154	Eu-155	Ru-106	Sb-125	Sr-90
Segment #1	Decon	<4E+00	<1E-02	3.89E-01	5.92E-01	<2E-02	<8E-02	<1E-01	<1E-01	3.38E-03
	Pre-burn leach 1	<4E+00	<6E-03	4.23E-02	5.96E-02	<2E-02	<8E-02	<6E-02	<4E-02	1.43E-03
	Pre-burn leach 2	<4E+00	<6E-03	4.26E-03	6.48E-03	<2E-02	<8E-02	<2E-02	<2E-02	8.11E-04
	Post-burn leach 1	<4E+00	<6E-03	2.51E-02	3.46E-02	<1E-02	<8E-02	<6E-02	<4E-02	5.74E-04
	Post-burn leach 2	<4E+00	<6E-03	<8E-04	4.58E-04	<2E-02	<8E-02	<1E-02	<2E-02	2.16E-04
	SUM (MDA = 0)	0	0	4.61E-01	6.93E-01	0	0	0	0	6.42E-03
Segment #2	Decon	<6E+00	3.51E-02	3.36E-01	5.29E-01	2.79E-02	3.83E-02	2.97E-02	<8E-02	1.83E-02
	Pre-burn leach 1	<1E+00	<4E-03	5.67E-02	8.95E-02	<8E-03	<1E-02	<8E-03	<2E-02	8.06E-04
	Pre-burn leach 2	<2E+00	<6E-03	1.17E-02	1.60E-02	<1E-02	<4E-02	<2E-02	<2E-02	3.10E-04
	Post-burn leach 1	<2E+00	<6E-03	3.19E-02	4.46E-02	<1E-02	<4E-02	<2E-02	<4E-02	2.41E-03
	Post-burn leach 2	<1E+00	<4E-03	<6E-04	8.82E-04	<1E-02	<2E-02	<1E-02	<1E-02	8.49E-04
	SUM (MDA = 0)	0	3.51E-02	4.36E-01	6.80E-01	2.79E-02	3.83E-02	2.97E-02	0	2.27E-02
Segment #3	Decon	<6E+00	1.34E-01	5.97E-01	9.63E-01	8.88E-02	1.02E-01	4.48E-02	9.98E-02	8.11E-02
	Pre-burn leach 1	<4E+00	<1E-02	9.32E-02	1.36E-01	<2E-02	<8E-02	<6E-03	<8E-02	3.68E-03
	Pre-burn leach 2	<2E+00	<6E-03	9.24E-03	1.35E-02	<1E-02	<4E-02	<2E-02	<4E-02	2.77E-04
	Post-burn leach 1	<4E+00	<1E-02	9.22E-02	1.30E-01	6.19E-02	5.17E-02	<8E-02	<8E-02	2.60E-03
	Post-burn leach 2	<2E+00	<4E-03	1.01E-03	1.86E-03	<1E-02	<4E-02	<1E-02	<2E-02	4.47E-04
	SUM (MDA = 0)	0	1.34E-01	7.93E-01	1.24E+00	1.51E-01	1.54E-01	4.48E-02	9.98E-02	8.81E-02
Core	Decon	<6E+00	2.12E+00	7.15E-01	1.32E+00	1.67E+00	1.90E+00	8.97E-01	8.53E-01	2.01E+00
	Pre-burn leach 1	<4E+01	1.66E+01	1.98E+00	3.49E+00	1.16E+01	1.22E+01	8.48E+00	<1E+00	7.65E+00
	Pre-burn leach 2	<2E+01	3.60E-01	3.86E-02	4.78E-02	2.21E-01	<4E-01	1.21E+00	4.12E-01	3.76E+00
	Post-burn leach 1	<2E+01	1.15E+00	3.85E-01	4.78E-01	3.21E+00	3.24E+00	5.45E-01	8.47E+00	1.02E+01
	Post-burn leach 2	<2E+01	<6E-02	9.01E-03	1.25E-02	<8E-02	<1E-01	<8E-02	3.25E-01	8.80E-03
	SUM (MDA = 0)	0	2.02E+01	3.13E+00	5.34E+00	1.67E+01	1.73E+01	1.11E+01	1.01E+01	2.37E+01
Compact TOTAL (MDA = 0)		0	20.39	4.82	7.96	16.91	17.50	11.21	10.16	23.79

Table 32. Relative error in the Compact 5-4 RDLBL results. The errors in the “sum” rows were computed by propagating the error from all the RDLBL steps.

Uncertainty		Ag-110m	Ce-144	Cs-134	Cs-137	Eu-154	Eu-155	Ru-106	Sb-125	Sr-90
Segment #1	Decon	N/A	N/A	3.0%	3.0%	N/A	N/A	N/A	N/A	2.0%
	Pre-burn leach 1	N/A	N/A	3.0%	3.0%	N/A	N/A	N/A	N/A	5.1%
	Pre-burn leach 2	N/A	N/A	6.3%	3.0%	N/A	N/A	N/A	N/A	7.0%
	Post-burn leach 1	N/A	N/A	3.0%	3.0%	N/A	N/A	N/A	N/A	7.1%
	Post-burn leach 2	N/A	N/A	N/A	12.4%	N/A	N/A	N/A	N/A	13.2%
	SUM (MDA = 0)	N/A	N/A	2.6%	2.6%	N/A	N/A	N/A	N/A	1.9%
Segment #2	Decon	N/A	8.0%	3.0%	3.0%	7.0%	13.2%	19.3%	N/A	2.0%
	Pre-burn leach 1	N/A	N/A	3.0%	3.0%	N/A	N/A	N/A	N/A	4.8%
	Pre-burn leach 2	N/A	N/A	4.0%	3.0%	N/A	N/A	N/A	N/A	13.0%
	Post-burn leach 1	N/A	N/A	3.0%	3.0%	N/A	N/A	N/A	N/A	4.0%
	Post-burn leach 2	N/A	N/A	N/A	6.0%	N/A	N/A	N/A	N/A	9.5%
	SUM (MDA = 0)	N/A	8.0%	2.4%	2.4%	7.0%	13.2%	19.3%	N/A	1.7%
Segment #3	Decon	N/A	5.0%	3.0%	3.0%	5.7%	18.5%	25.0%	6.4%	2.0%
	Pre-burn leach 1	N/A	N/A	3.0%	3.0%	N/A	N/A	N/A	N/A	3.0%
	Pre-burn leach 2	N/A	N/A	3.4%	3.0%	N/A	N/A	N/A	N/A	11.6%
	Post-burn leach 1	N/A	N/A	3.0%	3.0%	3.0%	24.2%	N/A	N/A	3.0%
	Post-burn leach 2	N/A	N/A	12.9%	5.3%	N/A	N/A	N/A	N/A	9.3%
	SUM (MDA = 0)	N/A	5.0%	2.3%	2.4%	3.6%	14.7%	25.0%	6.4%	1.8%
Core	Decon	N/A	3.9%	2.4%	2.5%	2.4%	4.3%	3.3%	7.1%	2.0%
	Pre-burn leach 1	N/A	4.0%	3.0%	3.0%	3.0%	4.4%	3.4%	N/A	2.0%
	Pre-burn leach 2	N/A	11.1%	5.7%	5.0%	14.6%	N/A	7.3%	18.5%	2.0%
	Post-burn leach 1	N/A	16.7%	3.0%	3.0%	3.0%	6.7%	17.7%	3.0%	2.0%
	Post-burn leach 2	N/A	N/A	15.6%	9.0%	N/A	N/A	N/A	15.4%	7.5%
	SUM (MDA = 0)	N/A	3.4%	2.0%	2.1%	2.2%	3.4%	2.8%	2.8%	1.1%
Compact TOTAL (MDA = 0)		N/A	3.4%	1.4%	1.5%	2.2%	3.3%	2.8%	2.7%	1.1%

4.3.2 Compact 5-4 ICP-MS Results

ICP-MS was used to measure actinides in the RDLBL solutions. Intact TRISO particles will retain all actinides, but exposed kernels in the DTF particles will be subject to leaching during the RDLBL process. Table 33 provides results for major isotopes of U and Pu in units of particle equivalents. Additional results in units of mass and compact fraction are in Table 83 and Table 84 of Appendix A3, respectively. Table 34 provides the relative error in these measurements.

Table 33. Particle equivalents for select actinides from ICP-MS of solutions from Compact 5-4 RDLBL.

Particle Equivalents		Pu-239	Pu-240	U-234	U-235	U-236	U-238
Segment #1	Decon	1.39E-02	<2E-02	<1E-01	1.73E-02	1.19E-02	1.35E-02
	Pre-burn leach 1	<4E-02	<4E-02	<2E-01	5.58E-03	<1E-02	2.10E-03
	Pre-burn leach 2	<4E-02	<6E-02	<4E-01	<8E-03	<1E-02	1.29E-03
	Post-burn leach 1	<2E-02	<6E-02	<4E-01	<8E-03	<1E-02	1.11E-03
	Post-burn leach 2	<4E-02	<6E-02	<4E-01	<8E-03	<2E-02	1.04E-03
	SUM (MDA = 0)	1.39E-02	0.00E+00	0.00E+00	2.29E-02	1.19E-02	1.91E-02
Segment #2	Decon	4.48E-02	4.26E-02	<1E-01	6.39E-02	6.04E-02	6.15E-02
	Pre-burn leach 1	<2E-02	<4E-02	<4E-01	<8E-03	<1E-02	2.03E-03
	Pre-burn leach 2	<4E-02	<6E-02	<4E-01	<8E-03	<2E-02	4.57E-04
	Post-burn leach 1	7.29E-02	<6E-02	<4E-01	2.22E-02	<2E-02	1.32E-02
	Post-burn leach 2	<4E-02	<4E-02	<2E-01	5.94E-03	<1E-02	7.14E-04
	SUM (MDA = 0)	1.18E-01	4.26E-02	0.00E+00	9.20E-02	6.04E-02	7.79E-02
Segment #3	Decon	1.12E-01	1.16E-01	1.54E-01	1.47E-01	1.44E-01	1.43E-01
	Pre-burn leach 1	<4E-02	<6E-02	<4E-01	1.26E-02	<2E-02	5.88E-03
	Pre-burn leach 2	<2E-02	<6E-02	<4E-01	<8E-03	<1E-02	3.71E-04
	Post-burn leach 1	<2E-02	<4E-02	<2E-01	<6E-03	<1E-02	2.22E-03
	Post-burn leach 2	<4E-02	<6E-02	<4E-01	<8E-03	<2E-02	5.96E-04
	SUM (MDA = 0)	1.12E-01	1.16E-01	1.54E-01	1.59E-01	1.44E-01	1.52E-01
Core	Decon	1.90E+00	1.95E+00	2.74E+00	2.72E+00	2.65E+00	2.64E+00
	Pre-burn leach 1	1.21E+01	1.24E+01	1.67E+01	1.68E+01	1.68E+01	1.61E+01
	Pre-burn leach 2	2.29E+00	2.36E+00	<4E-01	3.25E-01	3.21E-01	3.21E-01
	Post-burn leach 1	7.03E-01	7.98E-01	<4E-01	1.20E-01	8.34E-02	1.21E-01
	Post-burn leach 2	<4E-02	<6E-02	<4E-01	<8E-03	<2E-02	5.90E-04
	SUM (MDA = 0)	1.70E+01	1.75E+01	1.94E+01	2.00E+01	1.98E+01	1.92E+01
Compact TOTAL (MDA = 0)		17.21	17.71	19.58	20.25	20.03	19.46

Table 34. Relative error in the Compact 5-4 ICP-MS results given in the preceding table.

Error (%)		Pu-239	Pu-240	U-234	U-235	U-236	U-238
Segment #1	Decon	12%	N/A	N/A	11%	12%	5%
	Pre-burn leach 1	N/A	N/A	N/A	30%	N/A	9%
	Pre-burn leach 2	N/A	N/A	N/A	N/A	N/A	26%
	Post-burn leach 1	N/A	N/A	N/A	N/A	N/A	14%
	Post-burn leach 2	N/A	N/A	N/A	N/A	N/A	28%
	SUM (MDA = 0)	12%	N/A	N/A	11%	12%	4%

Error (%)		Pu-239	Pu-240	U-234	U-235	U-236	U-238
Segment #2	Decon	17%	20%	N/A	9%	9%	5%
	Pre-burn leach 1	N/A	N/A	N/A	N/A	N/A	13%
	Pre-burn leach 2	N/A	N/A	N/A	N/A	N/A	27%
	Post-burn leach 1	22%	N/A	N/A	18%	N/A	10%
	Post-burn leach 2	N/A	N/A	N/A	15%	N/A	17%
	SUM (MDA = 0)	15%	20%	N/A	7%	9%	4%
Segment #3	Decon	10%	7%	21%	7%	7%	5%
	Pre-burn leach 1	N/A	N/A	N/A	14%	N/A	7%
	Pre-burn leach 2	N/A	N/A	N/A	N/A	N/A	18%
	Post-burn leach 1	N/A	N/A	N/A	N/A	N/A	20%
	Post-burn leach 2	N/A	N/A	N/A	N/A	N/A	26%
	SUM (MDA = 0)	10%	7%	21%	7%	7%	5%
Core	Decon	5%	5%	9%	5%	5%	5%
	Pre-burn leach 1	5%	5%	9%	5%	5%	5%
	Pre-burn leach 2	7%	7%	N/A	7%	10%	5%
	Post-burn leach 1	11%	14%	N/A	9%	6%	5%
	Post-burn leach 2	N/A	N/A	N/A	N/A	N/A	32%
	SUM (MDA = 0)	4%	4%	8%	4%	4%	4%
Compact TOTAL (MDA = 0)		4%	4%	9%	4%	4%	4%

4.3.3 Compact 5-4 Discussion

Looking at the total amount of Ce-144 and actinides measured from the RDLBL suggests that only the 20 DTF particles had exposed kernels. Comparing these Compact 5-4 results to those for Compact 5-3 indicates similar behavior between the two with the exception of the kernel that was leached during the Segment 1 first post-burn leach.

4.4 Compact 7-3

As was done with most AGR-3/4 compacts, Compact 7-3 was transferred from HFEF to AL via a pneumatic rabbit; however, Compact 7-3 was damaged when it arrived at AL, and a significant amount of the compact had chipped off, exposing particles embedded in the matrix (see Figure 12). Given that the fuel in AGR-3/4 Capsule 7 had the highest irradiation temperatures of any fuel irradiated in the AGR program at the time, it was decided that the radial deconsolidation would be performed despite the pre-deconsolidation damage. If the TRISO-coated driver particles near the damage survived intact, then the data from the compact would be useful for the original goals of measuring fission-product concentration profiles. If they did not survive, this should be apparent in the analysis of the DLBL solutions. The results in the following sections indicate that there was indeed no failure or damage to the driver particles prior to the start of the deconsolidation.

4.4.1 Compact 7-3 Gamma-Emitter and Sr-90 Results

The amount of selected gamma-emitting fission products and beta-emitting Sr-90 measured in the compact outside of the driver-fuel SiC layer for the two radial segments and the center segment from the deconsolidation are summarized in Table 35 in terms of the number of particle-equivalent inventories. Table 85 and Table 86 in Appendix A4 gives the same results in units of activity and the fraction of the compact inventory of fission products. Table 36 gives the relative error for these results.

There was one driver particle that seems to have been fully intact until it was broken during the second post-burn leach of the first of two radial segments deconsolidated from this compact. A correction can be applied to the data to account for this particle damage, and results in the following sections will be reported with and without the application of this correction. The correction to better estimate the concentration of fission products and actinides in the compact matrix and OPyC layers in Compact 7-3, Segment 1, was applied as follows. Here, if the inventory of a given nuclide in Segment 1 burn leach 2 was ≥ 1 particle equivalent, a single particle equivalent was subtracted from that inventory. If the inventory of a given nuclide in Segment 1 burn leach 2 was < 1 particle equivalent, that value was set to zero. The values in Table 35 (and those in the Appendix) report the results both with and without this correction.

Table 35. Particle-equivalent inventories measured in the solutions from the radial deconsolidation of Compact 7-3. All values were decay-corrected to EOI + 1 day and compared to physics predictions at the same reference date.

Particle Equivalents		Ag-110m	Ce-144	Cs-134	Cs-137	Eu-154	Eu-155	Ru-106	Sb-125	Sr-90
Segment #1	Decon	<1E+1	<4E-2	7.46E-3	1.58E-2	2.85E+0	2.71E+0	<8E-2	1.26E-1	2.91E+0
	Pre-burn leach 1	<2E+1	<6E-2	<8E-3	2.49E-2	3.20E+0	3.14E+0	<2E-1	<2E-1	1.43E+0
	Pre-burn leach 2	<1E+1	<6E-2	<4E-3	2.87E-3	2.44E-1	2.41E-1	<1E-1	<1E-1	7.09E-2
	Post-burn leach 1	<4E+1	3.69E-1	3.03E-2	4.20E-2	1.24E+1	1.20E+1	<2E-1	4.26E-1	7.44E+0
	Post-burn leach 2	<4E+1	1.15E+0	5.92E-1	6.57E-1	6.75E-1	7.04E-1	1.00E+0	6.58E-1	9.85E-1
	Post-burn leach 2*	<4E+01	1.48E-01	0	0	0	0	4.47E-03	0	0
	SUM (MDA = 0)	0	1.52E+0	6.30E-1	7.43E-1	1.93E+1	1.88E+1	1.00E+0	1.21E+0	1.28E+1
	SUM (MDA = 0)*	0	5.16E-1	3.78E-2	8.56E-2	1.87E+1	1.81E+1	4.47E-3	5.51E-1	1.18E+1
Segment #2	Decon	<1E+1	<4E-2	2.10E-2	3.88E-2	2.45E+0	2.30E+0	<8E-2	<1E-1	2.26E+0
	Pre-burn leach 1	<4E+1	<6E-2	9.03E-2	1.05E-1	2.75E+0	2.65E+0	<2E-1	<4E-1	1.24E+0
	Pre-burn leach 2	<2E+1	<6E-2	2.77E-2	3.13E-2	1.84E-1	2.67E-1	<1E-1	<2E-1	6.14E-2
	Post-burn leach 1	<4E+1	3.02E-1	1.32E-1	1.49E-1	1.21E+1	1.16E+1	<2E-1	<6E-1	7.02E+0
	Post-burn leach 2	<2E+1	<6E-2	4.18E-2	4.87E-2	<8E-2	<1E-1	<1E-1	<2E-1	3.33E-2
	SUM (MDA = 0)	0	3.02E-1	3.12E-1	3.72E-1	1.75E+1	1.68E+1	0	0	1.06E+1
Core	Decon	<6E+1	4.11E+0	2.03E+0	3.86E+0	3.19E+0	4.19E+0	6.33E+0	<1E+0	9.42E+0
	Pre-burn leach 1	<1E+2	3.28E+0	7.75E-1	1.49E+0	3.10E+0	3.42E+0	9.06E+0	<1E+0	3.79E+0
	Pre-burn leach 2	<1E+2	1.90E-1	1.85E-2	2.39E-2	<2E-1	<8E-1	<6E-1	<4E-1	1.41E-1
	Post-burn leach 1	<1E+2	1.23E+1	6.27E-1	7.31E-1	1.31E+1	1.30E+1	1.11E+0	2.48E+0	1.06E+1
	Post-burn leach 2	<2E+2	<4E-1	1.27E-1	1.50E-1	<4E-1	<1E+0	<8E-1	<1E+0	5.77E-2
	SUM (MDA = 0)	0	1.99E+1	3.58E+0	6.26E+0	1.94E+1	2.06E+1	1.65E+1	2.48E+0	2.40E+1
Compact TOTAL (MDA = 0)		0	21.74	4.52	7.37	56.22	56.16	17.50	3.69	47.45
Compact TOTAL (MDA = 0)*		0	20.74	3.93	6.72	55.54	55.45	16.50	3.03	46.46
* Corrected for apparent TRISO particle damage in Segment 1 post-burn leach 2.										

Table 36. Relative error in the Compact 7-3 RDLBL results. The errors in the “sum” rows were computed by propagating the error from all the RDLBL steps.

Uncertainty		Ag-110m	Ce-144	Cs-134	Cs-137	Eu-154	Eu-155	Ru-106	Sb-125	Sr-90
Segment #1	Decon	N/A	N/A	12.5%	5.0%	3.0%	4.0%	N/A	22.5%	2.0%
	Pre-burn leach 1	N/A	N/A	N/A	7.0%	3.0%	5.7%	N/A	N/A	2.0%
	Pre-burn leach 2	N/A	N/A	N/A	23.6%	12.9%	21.9%	N/A	N/A	2.0%
	Post-burn leach 1	N/A	14.3%	9.0%	5.3%	3.0%	4.0%	N/A	20.0%	2.0%
	Post-burn leach 2	N/A	8.4%	3.0%	3.0%	6.7%	22.9%	11.4%	21.9%	2.0%
	SUM (MDA = 0)	N/A	10.5%	2.9%	2.7%	2.0%	2.9%	11.4%	21.5%	1.4%
Segment #2	Decon	N/A	N/A	5.0%	3.0%	3.0%	4.0%	N/A	N/A	2.0%
	Pre-burn leach 1	N/A	N/A	4.0%	3.0%	3.0%	5.8%	N/A	N/A	2.0%
	Pre-burn leach 2	N/A	N/A	7.4%	5.0%	12.5%	15.0%	N/A	N/A	2.0%
	Post-burn leach 1	N/A	26.9%	3.7%	3.0%	3.0%	4.0%	N/A	N/A	2.0%
	Post-burn leach 2	N/A	N/A	5.7%	4.0%	N/A	N/A	N/A	N/A	3.0%
	SUM (MDA = 0)	N/A	26.9%	2.2%	1.6%	2.2%	3.0%	N/A	N/A	1.4%
Core	Decon	N/A	15.1%	3.0%	3.0%	3.7%	8.2%	6.0%	N/A	2.0%
	Pre-burn leach 1	N/A	9.3%	3.0%	3.0%	6.4%	12.4%	7.0%	N/A	2.0%
	Pre-burn leach 2	N/A	25.2%	19.3%	11.4%	N/A	N/A	N/A	N/A	2.0%
	Post-burn leach 1	N/A	11.0%	3.0%	3.0%	3.0%	6.0%	18.0%	12.1%	2.0%
	Post-burn leach 2	N/A	N/A	12.1%	5.9%	N/A	N/A	N/A	N/A	3.0%
	SUM (MDA = 0)	N/A	7.7%	1.9%	2.0%	2.3%	4.6%	4.6%	12.1%	1.2%
Compact TOTAL (MDA = 0)		N/A	7.4%	1.6%	1.7%	1.3%	2.1%	4.6%	19.9%	0.8%

4.4.2 Compact 7-3 ICP-MS Results

Table 37 summarizes the actinides measured in the RDLBL solutions from Compact 7-3, and Table 38 gives the relative error for these results. These results are also presented in units of mass and compact fraction in Table 87 and Table 88, respectively. The results include both uncorrected values and values corrected for a particle that was accidentally broken during the Segment 1 post-burn leach 2 phase of the experiment. The same logic applied to the gamma and Sr-90 results from Section 4.4.1 was applied here; namely, if the inventory of a given nuclide in Segment 1 burn leach 2 was ≥ 1 particle equivalent, a single particle equivalent was subtracted from that inventory. If the inventory of a given nuclide in segment 1 burn leach 2 was < 1 particle equivalent, that value was set to zero.

Table 37. Particle equivalents for select actinides from ICP-MS of solutions from Compact 7-3 RDLBL.

		Particle Equivalents					
		Pu-239	Pu-240	U-234	U-235	U-236	U-238
Segment #1	Decon	<8E-3	<1E-2	<4E-2	7.53E-3	5.09E-3	5.84E-3
	Pre-burn leach 1	<4E-2	<6E-2	<1E-1	3.01E-2	<8E-3	1.00E-2
	Pre-burn leach 2	<2E-2	<4E-2	<1E-1	9.30E-3	<6E-3	4.80E-3
	Post-burn leach 1	4.21E-1	8.59E-1	<1E-1	6.57E-2	5.15E-2	5.03E-2
	Post-burn leach 2	1.13E+0	1.20E+0	1.11E+0	1.14E+0	1.08E+0	1.06E+0
	Post-burn leach 2*	1.27E-1	1.96E-1	1.07E-1	1.39E-1	8.11E-2	6.33E-2
	SUM (MDA = 0)	1.55E+0	2.05E+0	1.11E+0	1.25E+0	1.14E+0	1.13E+0
	SUM (MDA = 0)*	5.47E-1	1.05E+0	1.07E-1	2.51E-1	1.38E-1	1.34E-1
Segment #2	Decon	2.98E-2	2.24E-2	1.02E-1	1.04E-1	9.74E-2	9.73E-2
	Pre-burn leach 1	2.86E-2	2.47E-2	<1E-1	3.01E-2	5.68E-3	7.57E-3
	Pre-burn leach 2	3.96E-2	2.19E-2	<1E-1	8.97E-3	<4E-3	2.80E-3
	Post-burn leach 1	3.60E-1	7.26E-1	<1E-1	4.61E-2	4.37E-2	4.22E-2
	Post-burn leach 2	<2E-2	<2E-2	<1E-1	3.90E-3	<4E-3	1.76E-3
	SUM (MDA = 0)	4.58E-1	7.95E-1	1.02E-1	1.93E-1	1.47E-1	1.52E-1
	Core	8.28E+0	6.80E+0	1.54E+1	1.56E+1	1.49E+1	1.44E+1
Core	Pre-burn leach 1	4.73E+0	4.52E+0	4.33E+0	4.54E+0	4.25E+0	4.19E+0
	Pre-burn leach 2	9.60E-2	1.24E-1	<4E-2	1.43E-2	9.31E-3	1.34E-2
	Post-burn leach 1	4.42E+0	7.02E+0	1.22E+0	1.19E+0	1.13E+0	1.13E+0
	Post-burn leach 2	1.31E-1	1.44E-1	<1E-1	1.34E-2	<4E-3	4.38E-2
	SUM (MDA = 0)	1.77E+1	1.86E+1	2.09E+1	2.13E+1	2.03E+1	1.98E+1
	Compact TOTAL (MDA = 0)		19.67	21.45	22.12	22.78	21.58
Compact TOTAL (MDA = 0)*		18.67	20.45	21.12	21.78	20.58	20.05

* Corrected for apparent particle damage in Segment 1 post-burn leach 2.

Table 38. Relative error in the Compact 7-3 ICP-MS results.

		Error (%)					
		Pu-239	Pu-240	U-234	U-235	U-236	U-238
Segment #1	Decon	N/A	N/A	N/A	15%	15%	5%
	Pre-burn leach 1	N/A	N/A	N/A	9%	N/A	9%
	Pre-burn leach 2	N/A	N/A	N/A	23%	N/A	5%
	Post-burn leach 1	7%	7%	N/A	7%	11%	5%
	Post-burn leach 2	5%	11%	17%	5%	5%	5%
	SUM (MDA = 0)	6%	6%	17%	4%	5%	3%
Segment #2	Decon	12%	19%	17%	5%	5%	5%
	Pre-burn leach 1	15%	33%	0%	7%	16%	5%
	Pre-burn leach 2	10%	35%	0%	19%	0%	8%
	Post-burn leach 1	9%	7%	0%	15%	12%	5%
	Post-burn leach 2	0%	0%	0%	30%	0%	12%
	SUM (MDA = 0)	7%	6%	17%	5%	5%	4%

		Error (%)					
		Pu-239	Pu-240	U-234	U-235	U-236	U-238
Core	Decon	5%	5%	5%	5%	5%	5%
	Pre-burn leach 1	5%	5%	5%	5%	5%	5%
	Pre-burn leach 2	13%	17%	0%	13%	27%	5%
	Post-burn leach 1	5%	5%	13%	5%	5%	5%
	Post-burn leach 2	8%	10%	0%	8%	0%	8%
	SUM (MDA = 0)	3%	3%	4%	4%	4%	4%
Compact TOTAL (MDA = 0)		3%	3%	5%	4%	4%	4%

4.4.3 Compact 7-3 Discussion

As shown in Figure 12, Compact 7-3 suffered a chip and a loss of some matrix material and some particles prior to the start of the deconsolidation. If this event caused damage to any particles, it was not obvious from the results. Segment 1 did not show any signs of damaged particles except for the one particle that is believed to have been accidentally broken during the second post-burn leach, where 1.15 particle equivalents of Ce-144, 1.00 particle equivalents of Ru-106, and 1.06 particle equivalents of U-238 were measured. If a particle had been damaged by the chip prior to deconsolidation, it would have shown up in the deconsolidation or pre-burn leaches before the post-burn leaches. The second segment had only 0.15 particle equivalents of U-238 and about 0.3 particle equivalents of Ce-144 and Cs-134; thus, no particle failures occurred in Segment 2. If a TRISO-coated particle or two had been damaged in the core of the compact, it was not obvious because the total fission-product and actinide inventories measured in the Compact 7-3 RDLBL are consistent with the inventories in 20 DTF particles plus the one driver particle that failed in the Segment 1 post-burn leach 2. After accounting for that accidentally damaged particle, Table 37 shows that a total of 20.05 particle equivalents of U-238 were measured in Compact 7-3. The Ce-144 balance came in a little higher at 20.74 ± 1.4 particle equivalents.

The fact that 55.5 and 46.5 particle equivalents of Eu-154 and Sr-90, respectively, were measured in this RDLBL is evidence of diffusion of these nuclides through intact TRISO-coated driver particles into the surrounding compact matrix in addition to the contribution from the DTF particles. Some diffusion of Eu-154 and Sr-90 through intact TRISO coatings, especially at temperatures of about 1200°C and higher have been noted in AGR-2 (Stempien et al. 2021) and in the AGR-3/4 mass balance (Stempien et al. 2018). Compact 7-3 had a TAVA irradiation temperature of 1376°C, sufficiently high to see significant release from particles into the compact matrix. Furthermore, from measuring the irradiation test train components in Capsule 7 (e.g., the graphite surrounding the fuel, the capsule shell, and the spacers), it is apparent that about 3% of the Eu-154 in the capsule was released from the compacts, despite DTF particles' making up only about 1% of the particles in the capsule (Stempien et al. 2018). This corroborates the assertion that TRISO-coated particles also contribute to the Eu-154 source in Capsule 7 fuel. The DTF kernels are likely not completely depleted of Sr-90 and Eu-154; therefore, it cannot be assumed that all the Eu-154 and Sr-90 in the core is in the matrix and OPyC.

4.5 Compact 8-3

Compact 8-3 was deconsolidated in just two radial segments because it fell off the rod during the radial deconsolidation of the second segment, and then the remaining core was deconsolidated in a single step. There was an indication that one TRISO-coated driver particle was damaged during the second pre-burn leach of Segment 2, which is discussed in Section 4.5.3. Additionally, the volume of material removed in Segment 1 was very small and could not be determined from the image-analysis method (see Section 3.5). Therefore, when volumetric concentrations were calculated for Compact 8-3 (see Section 5.5), the inventories from the summation of Segments 1 and 2 were divided by the volume difference between the pre-deconsolidation dimensions and the end of Segment 2.

4.5.1 Compact 8-3 Gamma-Emitter and Sr-90 Results

The total amounts of selected fission products measured in the compact outside of the driver-fuel SiC layer for each segment of the radial deconsolidation are summarized in Table 39 in terms of the number of particle-equivalent inventories. Additional results in units of activity and fraction of the calculated compact inventory are shown in Table 89 and Table 90 of Appendix A5. Table 40 gives the relative error for the values summarized in all these tables. The values in these tables report the results both with and without a correction for the driver particle that was broken in the second pre-burn leach in Segment 2. This correction was made according to the following logic. If the inventory of a given nuclide in Segment 2 pre-burn leach 2 was ≥ 1 particle equivalent, a single particle equivalent was subtracted from that inventory. If the inventory of a given nuclide in Segment 2 pre-burn leach 2 was < 1 particle equivalent, that value was set to zero.

Table 39. Particle-equivalent inventories measured in the solutions from the radial deconsolidation of Compact 8-3. All values were decay-corrected to EOI + 1 day and compared to physics predictions at the same reference date.

Particle Equivalents		Ag-110m	Ce-144	Cs-134	Cs-137	Eu-154	Eu-155	Ru-106	Sb-125	Sr-90
Segment #1	Decon	<6E+00	<2E-02	7.21E-03	2.24E-02	3.39E-01	3.33E-01	6.31E-02	3.17E-02	7.55E-01
	Pre-burn leach 1	<2E+01	<6E-02	2.18E-02	2.54E-02	2.48E-01	2.87E-01	<1E-01	<1E-01	2.21E-01
	Pre-burn leach 2	<4E+01	1.87E-01	1.57E-02	2.11E-02	1.15E-01	1.01E-01	1.70E-01	1.36E-01	1.89E-01
	Post-burn leach 1	<1E+01	<4E-02	4.43E-03	1.09E-02	6.92E-01	6.74E-01	<8E-02	<1E-01	8.23E-01
	Post-burn leach 2	<1E-02	<2E-05	1.14E-06	1.67E-06	<3E-05	<6E-05	<4E-05	<6E-05	3.75E-06
	SUM (MDA = 0)	0	1.87E-01	4.92E-02	7.98E-02	1.39E+00	1.39E+00	2.33E-01	1.67E-01	1.99E+00
Segment #2	Decon	<1E+01	1.13E-01	2.26E-02	7.21E-02	1.04E+00	1.04E+00	2.71E-01	<1E-01	1.41E+00
	Pre-burn leach 1	<2E+01	<6E-02	1.31E-02	1.79E-02	7.68E-01	7.45E-01	<1E-01	<1E-01	4.70E-01
	Pre-burn leach 2	<1E+01	1.22E+00	6.16E-01	6.69E-01	6.48E-01	6.71E-01	1.07E+00	5.29E-01	1.10E+00
	Pre-burn leach 2*	<1E+01	2.21E-01	0	0	0	0	7.33E-02	0	1.02E-01
	Post-burn leach 1	<4E+01	1.29E-01	2.55E-01	2.72E-01	3.55E+00	3.57E+00	<2E-01	<2E-01	3.08E+00
	Post-burn leach 2	<2E+01	<4E-02	4.78E-02	5.13E-02	4.23E-02	<1E-01	<8E-02	<1E-01	3.21E-02
	SUM (MDA = 0)	0	1.46E+00	9.55E-01	1.08E+00	6.05E+00	6.03E+00	1.34E+00	5.29E-01	6.09E+00
	SUM (MDA = 0)*	0	4.63E-01	3.39E-01	4.13E-01	5.40E+00	5.36E+00	3.44E-01	0	5.09E+00
Core	Decon	<2E+01	3.77E+00	5.36E-01	1.74E+00	4.68E+00	5.13E+00	4.50E+00	6.96E-01	6.95E+00
	Pre-burn leach 1	<4E+01	4.08E+00	5.24E-01	1.68E+00	4.07E+00	4.51E+00	8.82E+00	4.54E-01	4.04E+00
	Pre-burn leach 2	<2E+01	2.65E-01	1.90E-02	2.80E-02	5.29E-01	5.03E-01	3.87E-01	2.16E-01	3.48E-01
	Post-burn leach 1	<6E+01	1.29E+01	2.58E-02	3.69E-02	3.96E+01	3.84E+01	6.54E-01	2.88E+00	2.91E+01
	Post-burn leach 2	<2E+01	<4E-02	1.31E-02	1.53E-02	6.97E-02	6.91E-02	3.07E-01	1.94E-01	4.31E-02
	SUM (MDA = 0)	0	2.10E+01	1.12E+00	3.50E+00	4.89E+01	4.86E+01	1.47E+01	4.44E+00	4.05E+01
Compact TOTAL (MDA = 0)		0	22.63	2.12	4.66	56.39	56.02	16.25	5.13	48.58
Compact TOTAL (MDA = 0)*		0	21.66	1.51	3.99	55.75	55.36	15.29	4.61	47.58

* Corrected for apparent particle damage in Segment 2 pre-burn leach 2.

Table 40. Relative error in the Compact 8-3 RDLBL results. The errors in the “sum” rows were computed by propagating the error from all the RDLBL steps.

Uncertainty		Ag-110m	Ce -144	Cs-134	Cs-137	Eu-154	Eu-155	Ru-106	Sb-125	Sr-90
Segment #1	Decon	N/A	N/A	5.9%	3.4%	3.4%	6.9%	15.7%	25.0%	2.0%
	Pre-burn leach 1	N/A	N/A	9.3%	5.4%	17.2%	18.3%	N/A	N/A	2.0%
	Pre-burn leach 2	N/A	22.9%	11.8%	5.8%	11.0%	19.0%	11.0%	17.0%	2.0%
	Post-burn leach 1	N/A	N/A	10.9%	7.3%	4.8%	7.6%	N/A	N/A	2.0%
	Post-burn leach 2	N/A	N/A	24.0%	18.3%	N/A	N/A	N/A	N/A	2.0%
	SUM (MDA = N/A)	N/A	22.9%	5.6%	2.7%	4.1%	5.7%	9.1%	14.6%	1.2%
Segment #2	Decon	N/A	23.5%	5.2%	3.0%	3.0%	6.2%	13.3%	N/A	2.0%
	Pre-burn leach 1	N/A	N/A	11.8%	5.5%	4.2%	11.6%	N/A	N/A	2.0%
	Pre-burn leach 2	N/A	13.7%	3.0%	3.0%	3.3%	10.2%	7.7%	15.2%	2.0%
	Post-burn leach 1	N/A	25.1%	3.0%	3.0%	3.0%	4.7%	N/A	N/A	2.0%
	Post-burn leach 2	N/A	N/A	4.2%	3.4%	21.3%	N/A	N/A	N/A	2.0%
	SUM (MDA = N/A)	N/A	11.8%	2.1%	2.0%	1.9%	3.5%	6.7%	15.2%	1.2%
Core	Decon	N/A	5.4%	3.0%	3.0%	3.0%	3.7%	3.0%	11.3%	2.0%
	Pre-burn leach 1	N/A	9.7%	3.0%	3.0%	3.0%	5.9%	3.4%	21.4%	2.0%
	Pre-burn leach 2	N/A	13.6%	7.9%	4.2%	5.4%	14.1%	17.7%	11.3%	2.0%
	Post-burn leach 1	N/A	6.2%	11.9%	11.7%	3.0%	3.0%	16.3%	5.7%	2.0%
	Post-burn leach 2	N/A	N/A	9.2%	5.9%	2N/A	25.0%	12.3%	11.0%	2.3%
	SUM (MDA = N/A)	N/A	4.3%	2.0%	2.1%	2.5%	2.5%	2.4%	4.7%	1.5%
Compact TOTAL (MDA = N/A)		N/A	4.1%	1.4%	1.6%	2.1%	2.2%	2.2%	4.4%	1.3%

4.5.2 Compact 8-3 ICP-MS Results

ICP-MS was used to measure actinides in the deconsolidation solutions. Intact TRISO particles will retain all actinides, but exposed kernels, such as in the DTF particles or in a damaged TRISO-coated particle, will be subject to leaching during the DLBL process. Table 41 provides results for major isotopes of U and Pu in units of particle equivalents. Additional results in units of mass and compact fraction are given in Table 91 and Table 92 of Appendix A5. Table 42 provides the relative error in these results. The results are presented both with and without a correction for the particle that was accidentally broken during the second pre-burn leach in Segment 2. The same logic applied to the corrections in Section 4.5.1 was applied here.

Table 41. Particle equivalents for select actinides from ICP-MS of solutions from Compact 8-3 RDLBL.

Particle Equivalents		Pu-239	Pu-240	U-234	U-235	U-236	U-238
Segment #1	Decon	5.63E-02	3.05E-02	1.50E-01	1.57E-01	1.45E-01	1.42E-01
	Pre-burn leach 1	<1E-02	<4E-02	<1E-01	6.19E-03	<4E-03	4.08E-03
	Pre-burn leach 2	1.76E-01	1.83E-01	1.81E-01	1.83E-01	1.83E-01	1.80E-01
	Post-burn leach 1	2.94E-02	2.69E-02	1.00E-02	1.46E-02	5.04E-03	9.79E-03
	Post-burn leach 2	2.75E-03	1.71E-03	<4E-03	3.44E-03	5.87E-04	1.29E-03
	SUM (MDA = 0)	2.65E-01	2.42E-01	3.41E-01	3.64E-01	3.34E-01	3.37E-01

Particle Equivalents		Pu-239	Pu-240	U-234	U-235	U-236	U-238
Segment #2	Decon	2.57E-01	1.57E-01	5.25E-01	6.31E-01	5.07E-01	4.16E-01
	Pre-burn leach 1	1.58E-02	1.24E-02	<2E-02	1.85E-02	1.18E-02	1.44E-02
	Pre-burn leach 2	1.10E+00	1.15E+00	1.19E+00	1.34E+00	1.18E+00	9.47E-01
	Pre-burn leach 2*	1.02E-01	1.45E-01	1.92E-01	3.38E-01	1.82E-01	0
	Post-burn leach 1	1.45E-01	2.57E-01	2.63E-02	2.97E-02	2.25E-02	2.67E-02
	Post-burn leach 2	5.50E-03	6.13E-03	<2E-02	1.22E-03	<4E-04	8.79E-04
	SUM (MDA = 0)	1.52E+00	1.58E+00	1.74E+00	2.02E+00	1.72E+00	1.41E+00
	SUM (MDA = 0)*	5.24E-01	5.77E-01	7.44E-01	1.02E+00	7.23E-01	4.58E-01
Core	Decon	5.69E+00	5.05E+00	9.98E+00	7.77E+00	7.98E+00	1.15E+01
	Pre-burn leach 1	8.04E+00	7.08E+00	8.95E+00	9.47E+00	8.27E+00	1.07E+01
	Pre-burn leach 2	1.26E-01	1.85E-01	3.64E-02	1.81E-02	1.11E-02	1.32E-02
	Post-burn leach 1	4.93E+00	8.00E+00	3.22E-01	2.27E-01	1.93E-01	2.03E-01
	Post-burn leach 2	2.57E-02	4.43E-02	2.80E-02	7.02E-03	2.55E-03	8.57E-03
	SUM (MDA = 0)	1.88E+01	2.04E+01	1.93E+01	1.75E+01	1.65E+01	2.24E+01
Compact TOTAL (MDA = 0)		20.60	22.18	21.40	19.87	18.51	24.13
Compact TOTAL (MDA = 0)*		19.60	21.18	20.40	18.87	17.51	23.19
* Corrected for apparent particle damage in Segment 2 pre-burn leach 2.							

Table 42. Relative error in the Compact 8-3 ICP-MS results given in the preceding tables.

Error (%)		Pu-239	Pu-240	U-234	U-235	U-236	U-238
Segment #1	Decon	5%	7%	9%	5%	5%	5%
	Pre-burn leach 1	N/A	N/A	N/A	11%	N/A	7%
	Pre-burn leach 2	7%	10%	17%	5%	5%	5%
	Post-burn leach 1	9%	22%	30%	5%	17%	7%
	Post-burn leach 2	20%	24%	N/A	13%	30%	7%
	SUM (MDA = 0)	5%	8%	10%	3%	4%	3%
Segment #2	Decon	5%	5%	5%	5%	5%	5%
	Pre-burn leach 1	13%	13%	N/A	7%	5%	5%
	Pre-burn leach 2	5%	5%	5%	5%	5%	5%
	Post-burn leach 1	5%	5%	12%	5%	5%	5%
	Post-burn leach 2	8%	16%	N/A	14%	N/A	8%
	SUM (MDA = 0)	4%	4%	4%	4%	4%	4%
Core	Decon	5%	5%	5%	5%	5%	5%
	Pre-burn leach 1	5%	5%	5%	5%	5%	5%
	Pre-burn leach 2	5%	5%	18%	19%	5%	5%
	Post-burn leach 1	5%	5%	9%	5%	5%	19%
	Post-burn leach 2	10%	9%	16%	5%	20%	5%
	SUM (MDA = 0)	3%	3%	3%	4%	3%	4%
Compact TOTAL (MDA = 0)		3%	3%	3%	3%	3%	3%

4.5.3 Compact 8-3 Discussion

The inventory of fission products in the second leaches (i.e., the second pre-burn or second post-burn leaches) is usually less than 20% of that dissolved in the first leach (unless coatings are broken in the second leach process) because the first leach effectively collects much of that inventory (Stempien et al. 2021). However, a sudden increase in the inventory of certain fission products (i.e., Ce-144 and Ru-106) and actinides in a second leach could suggest a particle was completely or partially damaged by the process. There were two instances of this in the RDLBL of Compact 8-3. In the first instance, the inventories of Ce, Ru, and actinides in the second pre-burn leach of Segment 1 were considerably higher than in the deconsolidation solution and the first pre-burn leach. The amounts equate to about 0.20 particle equivalents. The post-burn leaches have much lower values than this. It is not clear exactly what these 0.20 particle equivalents represent. It does not seem to be a normal TRISO particle that failed (in-pile) or was broken (in PIE) because significant additional fission products and actinides were not measured in the post-burn leaches. One hypothesis is that this was a particle with an undersized kernel with damaged coatings.

The second instance was observed in the second pre-burn leach of Segment 2, where about 1 particle-equivalent of Ce-144, Ru-106, and U-238 was measured. These are very similar to the inventories measured after a particle was broken during the second post-burn leach of the Compact 7-3 first segment (see Section 4.4). The inventory of Cs-134, Cs-137, and Eu-154 also jumped from less than 0.1 particle equivalents in the deconsolidation solution and first pre-burn leach to >0.6 particle equivalents in the second pre-burn leach. The Sr-90 inventory was about 1.1 particle equivalents in the second pre-burn leach. Typically, a second leach contains <20% of each element dissolved in the first leaches unless TRISO coatings are damaged by the process (Stempien et al. 2021). All of this suggests the inventories of Cs, Eu, and Sr in the second pre-burn leach were dominated by the one accidentally broken particle. A correction (described in Section 4.5.1) was applied to attempt to subtract out the inventory from this single particle failure. Instances of kernels being leached in second pre-burn leaches are not unique to AGR-3/4. There were cases like this in AGR-1 Compact 5-1-1 (Demkowicz et al. 2015) and AGR-2 Compacts 2-2-3 and 2-3-1 (Hunn et al. 2018, Stempien et al. 2021). In those instances, particles with in-pile SiC failures and intact OPyC layers that subsequently broke in the pre-burn leaches were deemed to have been the source of the uranium in those pre-burn leaches. Here in AGR-3/4, there was insufficient evidence to confirm in-pile SiC failures. Another hypothesis is that a particle could have been partially mechanically damaged in the deconsolidation process (e.g., the OPyC and SiC were broken but the IPyC initially survived), and then the remainder of the TRISO coating was completely damaged in a subsequent pre-burn leach, allowing kernel leaching.

From the core DLBL solutions, it appears that some damaged driver particles were present, but it is difficult to determine exactly how many were damaged or whether the damage was accidental and had occurred during the RDLBL or had occurred in-pile. It is possible that a TRISO particle was broken when the compact fell off the rod, after which deconsolidation of the second segment was stopped, or that a particle was broken when the compact diameter was measured three times by calipers after it had fallen off. Historically, this particle design has a low probability for in-pile damage (Demkowicz et al. 2015). In the compact core, the measured particle equivalents of Ce-144, U-235, and U-238 were 21.0, 17.5, and 22.4, respectively. The other Pu and U isotopes listed in Table 41 have core inventories ranging from 16.5 to 20.4 particle equivalents. Given the inventories measured in the core, it is possible up to two or three TRISO particles were damaged. However, the 20 DTF particles present in the core, which are already contributing approximately 20 particle equivalents of actinides and Ce-144, mean it cannot be determined at which step of the core leach-burn-leach process any TRISO particle damage would have been detectable in the DLBL solutions. Thus, no attempts to correct for possible TRISO-particle damage in the core were made.

It is not clear why the total inventory of U-238 measured in the Compact 8-3 deconsolidation is about 3.5 particle equivalents more than the measured inventory of U-235 and 2.5 particle equivalents more than the measured inventory of Pu-239. This difference in the measured U-238 and Pu-239 inventories is consistent across six of the eight compacts in this report, however. Generally, the ratio of particle equivalents of Pu-239 to particle equivalents of U-238 is about 0.8–0.9, and for Compact 8-3 this ratio is 0.85. Most compacts had U-235:U-238

particle-equivalent ratios between 1.03 and 1.11, but for Compacts 8-3 and 10-3 that ratio was different, at 0.81 and 0.85, respectively.

4.6 Compact 10-3

Compact 10-3 was irradiated with a temperature and burnup history similar to that of Compact 3-3. The average irradiation temperatures of Compact 10-3 were also similar to those of Compact 8-3, but at a little lower EOI burnup. Three radial segments were obtained from Compact 10-3 in addition to the core. This means four distinct volumes of this compact were analyzed via RDLBL. However, the compact fell off the rod three times. Elevated values for certain fission products and actinides were observed due to the accidental damage. Unfortunately, the results suggest 10 or more TRISO-coated particles were damaged at various stages of the RDLBL.

4.6.1 Compact 10-3 Gamma-Emitter and Sr-90 Results

The total inventories of selected gamma-emitting fission products and beta-emitting Sr-90 measured in the compact outside of the driver-fuel SiC layer for each segment of the radial deconsolidation of Compact 10-3 are summarized in Table 43 in terms of the number of particle-equivalent inventories. Additional results in units of activity and fraction of the compact inventory are shown in Table 93 and Table 94 of Appendix A6. Table 44 summarizes the relative errors for these results.

Table 43. Particle-equivalent inventories measured in the solutions from the radial deconsolidation of Compact 10-3. All values were decay-corrected to EOI + 1 day.

		Ag-110m	Ce-144	Cs-134	Cs-137	Eu-154	Eu-155	Ru-106	Sb-125	Sr-90
Segment #1	Decon	<4E+01	2.81E+0	1.28E+0	1.64E+0	1.32E+0	1.37E+0	2.22E+0	1.33E+0	6.23E+0
	Pre-burn leach 1	<1E+02	3.46E+0	1.69E+0	2.61E+0	9.39E-1	1.37E+0	2.19E+0	<6E-01	2.01E+0
	Pre-burn leach 2	<1E+02	1.08E+0	5.86E-1	8.95E-1	4.03E-1	5.58E-1	8.71E-1	<4E-01	9.79E-1
	Post-burn leach 1	<8E+01	<2E-01	5.20E-1	6.60E-1	2.47E+0	2.80E+0	<2E-01	1.32E+0	1.17E+1
	Post-burn leach 2	<2E+01	<2E-02	2.28E-2	3.09E-2	6.94E-2	9.40E-2	3.26E-2	2.02E-1	7.89E-1
	SUM (MDA = 0)	N/A	7.35	4.10	5.84	5.21	6.19	5.31	2.85	21.74
Segment #2	Decon	<1E+01	5.13E-2	5.63E-2	9.07E-2	8.57E-2	9.54E-2	3.08E-2	2.20E-2	5.21E-1
	Pre-burn leach 1	<6E+01	1.33E+0	1.25E+0	1.71E+0	6.19E-1	8.15E-1	1.31E+0	<4E-01	3.37E-1
	Pre-burn leach 2	<6E+01	8.33E-1	2.90E-1	3.75E-1	4.30E-1	5.12E-1	6.47E-1	<2E-01	1.93E-1
	Post-burn leach 1	<1E+02	<2E-01	2.69E-1	3.47E-1	2.16E+0	2.43E+0	<2E-01	9.39E-1	4.09E+0
	Post-burn leach 2	<4E+01	<4E-02	1.10E-2	1.41E-2	9.93E-3	<4E-02	<4E-02	1.15E-1	8.82E-3
	SUM (MDA = 0)	N/A	2.21	1.88	2.53	3.30	3.86	1.99	1.08	5.15
Segment #3	Decon	<8E+00	7.70E-2	2.47E-2	8.03E-2	9.41E-2	1.32E-1	5.90E-2	1.82E-2	5.47E-1
	Pre-burn leach 1	<2E+01	3.17E-2	2.88E-3	8.24E-3	3.99E-2	5.85E-2	3.85E-2	3.70E-2	4.75E-2
	Pre-burn leach 2	<1E+01	<4E-02	7.92E-4	8.21E-4	9.25E-3	<4E-02	<4E-02	1.70E-2	9.60E-3
	Post-burn leach 1	<1E+02	8.45E-1	2.48E-1	4.19E-1	6.32E-1	7.81E-1	6.75E-1	4.85E-1	1.00E+0
	Post-burn leach 2	<4E+01	<8E-02	6.05E-2	9.30E-2	1.46E-2	<6E-02	<2E-01	3.85E-2	1.58E-2
	SUM (MDA = 0)	N/A	0.95	0.34	0.60	0.79	0.97	0.77	0.60	1.62

		Ag-110m	Ce-144	Cs-134	Cs-137	Eu-154	Eu-155	Ru-106	Sb-125	Sr-90
Core	Decon	<1E+02	7.23E+0	5.51E-1	2.34E+0	2.02E+0	3.38E+0	6.49E+0	1.50E+0	1.24E+1
	Pre-burn leach 1	<1E+02	5.08E+0	7.79E-1	1.49E+0	2.12E+0	2.51E+0	7.28E+0	1.07E+0	6.63E-2
	Pre-burn leach 2	<6E+01	3.75E-1	2.25E-1	3.23E-1	2.76E-1	3.16E-1	3.90E-1	2.69E-1	1.77E-2
	Post-burn leach 1	<2E+02	7.06E+0	5.04E-1	7.18E-1	9.16E+0	1.05E+1	5.77E-1	3.92E+0	1.48E-1
	Post-burn leach 2	<6E+01	<8E-02	1.60E-2	1.97E-2	8.57E-2	1.23E-1	1.12E-1	4.24E-1	4.06E-3
	SUM (MDA = 0)	N/A	19.74	2.07	4.89	13.67	16.84	14.84	7.18	12.65
Compact TOTAL (MDA = 0)		N/A	30.26	8.39	13.86	22.97	27.86	22.92	11.70	41.17

Table 44. Relative error for the RDLBL results from Compact 10-3. The errors in the “sum” rows were computed by propagating the error from all the RDLBL steps.

Uncertainty		Ag-110m	Ce-144	Cs-134	Cs-137	Eu-154	Eu-155	Ru -106	Sb-125	Sr-90
Segment #1	Decon	N/A	6.0%	3.0%	3.0%	3.0%	6.0%	3.0%	4.5%	2.0%
	Pre-burn leach 1	N/A	20.7%	3.1%	3.0%	3.0%	6.7%	8.9%	N/A	2.0%
	Pre-burn leach 2	N/A	19.0%	3.1%	3.0%	3.4%	14.9%	13.0%	N/A	2.0%
	Post-burn leach 1	N/A	N/A	3.0%	3.0%	3.0%	5.0%	N/A	5.1%	2.0%
	Post-burn leach 2	N/A	N/A	3.9%	3.0%	5.6%	7.0%	11.0%	6.1%	2.0%
	SUM (MDA = 0)	N/A	10.4%	1.7%	1.7%	1.7%	3.3%	4.4%	3.2%	1.2%
Segment #2	Decon	N/A	27.1%	3.0%	3.0%	3.0%	13.5%	17.0%	10.0%	2.0%
	Pre-burn leach 1	N/A	18.2%	3.0%	3.0%	5.7%	8.5%	13.6%	N/A	2.0%
	Pre-burn leach 2	N/A	20.1%	3.5%	4.3%	4.9%	25.7%	18.0%	N/A	2.0%
	Post-burn leach 1	N/A	N/A	3.5%	4.2%	3.0%	8.5%	N/A	11.7%	2.0%
	Post-burn leach 2	N/A	N/A	6.6%	3.6%	10.0%	N/A	N/A	12.9%	2.6%
	SUM (MDA = 0)	N/A	13.3%	2.2%	2.2%	2.3%	6.6%	10.7%	10.3%	1.6%
Segment #3	Decon	N/A	11.8%	3.0%	3.0%	3.0%	4.8%	19.6%	22.0%	2.0%
	Pre-burn leach 1	N/A	13.0%	7.6%	3.0%	4.8%	7.4%	8.4%	7.0%	2.0%
	Pre-burn leach 2	N/A	N/A	8.0%	6.6%	6.0%	N/A	N/A	9.0%	2.3%
	Post-burn leach 1	N/A	13.7%	3.0%	3.0%	3.0%	11.7%	5.3%	3.0%	2.0%
	Post-burn leach 2	N/A	N/A	3.0%	3.0%	9.0%	N/A	N/A	15.0%	2.0%
	SUM (MDA = 0)	N/A	12.2%	2.3%	2.2%	2.4%	9.4%	4.9%	2.8%	1.4%
Core	Decon	N/A	4.0%	3.0%	3.0%	3.0%	4.7%	3.4%	9.0%	2.0%
	Pre-burn leach 1	N/A	7.7%	3.0%	3.0%	3.0%	4.4%	3.0%	5.9%	2.0%
	Pre-burn leach 2	N/A	10.5%	3.1%	3.0%	3.0%	8.7%	16.2%	12.2%	2.0%
	Post-burn leach 1	N/A	6.1%	3.1%	3.0%	3.0%	3.4%	7.0%	3.0%	2.0%
	Post-burn leach 2	N/A	N/A	3.2%	3.1%	5.6%	7.6%	14.1%	3.0%	2.0%
	SUM (MDA = 0)	N/A	3.3%	1.6%	1.8%	2.1%	2.4%	2.2%	2.7%	2.0%
Compact TOTAL (MDA = 0)		N/A	21.1%	3.9%	3.9%	4.3%	12.2%	12.8%	11.5%	3.2%

4.6.2 Compact 10-3 ICP-MS Results

ICP-MS was used to measure major isotopes of Pu and U in the RDLBL solutions. Table 45 provides results in units of particle equivalents, and Table 46 gives the relative error in these measurements. Additional results in units of mass and compact fraction are summarized in Table 94 and Table 95 of Appendix A6.

Table 45. Particle equivalents for select actinides from ICP-MS of solutions from Compact 10-3 RDLBL.

Particle Equivalents		Pu-239	Pu-240	U-234	U-235	U-236	U-238
Segment #1	Decon	2.61E+0	2.54E+0	3.04E+0	3.17E+0	2.70E+0	2.93E+0
	Pre-burn leach 1	2.77E+0	2.63E+0	3.00E+0	3.07E+0	2.85E+0	2.76E+0
	Pre-burn leach 2	9.58E-1	9.06E-1	1.16E+0	1.17E+0	1.11E+0	1.15E+0
	Post-burn leach 1	1.01E+0	1.07E+0	9.17E-1	9.21E-1	8.68E-1	8.95E-1
	Post-burn leach 2	3.33E-2	2.43E-2	2.16E-2	2.22E-2	1.49E-2	1.79E-2
	SUM (MDA = 0)	7.38	7.17	8.14	8.36	7.54	7.76
Segment #2	Decon	5.78E-2	5.52E-2	9.78E-2	9.69E-2	9.42E-2	9.77E-2
	Pre-burn leach 1	1.78E+0	1.72E+0	1.86E+0	1.96E+0	1.77E+0	1.84E+0
	Pre-burn leach 2	8.54E-1	8.44E-1	9.38E-1	9.25E-1	8.99E-1	9.34E-1
	Post-burn leach 1	3.73E-1	4.72E-1	2.10E-1	2.06E-1	1.96E-1	1.87E-1
	Post-burn leach 2	8.76E-3	9.59E-3	3.43E-3	3.69E-3	2.03E-3	3.06E-3
	SUM (MDA = 0)	3.07	3.11	3.11	3.19	2.96	3.07
Segment #3	Decon	8.80E-2	7.17E-2	3.55E-1	3.41E-1	3.42E-1	3.53E-1
	Pre-burn leach 1	3.58E-2	3.16E-2	8.12E-2	8.16E-2	7.68E-2	7.52E-2
	Pre-burn leach 2	2.41E-3	2.08E-3	<8E-04	4.09E-4	2.78E-4	4.26E-4
	Post-burn leach 1	9.74E-1	9.71E-1	9.95E-1	9.55E-1	9.71E-1	9.66E-1
	Post-burn leach 2	3.38E-3	3.78E-3	1.41E-3	1.40E-3	1.34E-3	1.31E-3
	SUM (MDA = 0)	1.10	1.08	1.43	1.38	1.39	1.40
Core	Decon	1.26E+1	9.41E+0	1.57E+1	1.45E+1	1.80E+1	1.90E+1
	Pre-burn leach 1	6.14E+0	6.30E+0	6.41E+0	5.75E+0	7.29E+0	7.56E+0
	Pre-burn leach 2	1.50E-1	1.65E-1	7.11E-2	6.51E-2	6.77E-2	6.95E-2
	Post-burn leach 1	2.44E+0	3.63E+0	2.65E-1	2.17E-1	2.31E-1	2.83E-1
	Post-burn leach 2	3.76E-3	5.12E-3	<8E-04	3.68E-4	2.96E-4	5.35E-4
	SUM (MDA = 0)	21.4	19.5	22.4	20.5	25.6	26.9
Compact TOTAL (MDA = 0)		32.9	30.9	35.1	33.5	37.5	39.1

Table 46. Relative error in the Compact 10-3 U and Pu results given in Table 45.

Error (%)		Pu-239	Pu-240	U-234	U-235	U-236	U-238
Segment #1	Decon	5%	5%	5%	7%	9%	7%
	Pre-burn leach 1	5%	9%	5%	5%	7%	5%
	Pre-burn leach 2	5%	7%	5%	5%	7%	5%
	Post-burn leach 1	5%	5%	5%	5%	7%	5%
	Post-burn leach 2	5%	5%	12%	5%	7%	5%
	SUM (MDA = 0)	3%	4%	3%	3%	4%	3%

	Error (%)	Pu-239	Pu-240	U-234	U-235	U-236	U-238
Segment #2	Decon	5%	5%	5%	5%	5%	7%
	Pre-burn leach 1	5%	9%	5%	5%	7%	5%
	Pre-burn leach 2	7%	5%	5%	5%	7%	5%
	Post-burn leach 1	5%	10%	5%	7%	7%	5%
	Post-burn leach 2	10%	18%	30%	5%	8%	5%
	SUM (MDA = 0)	4%	5%	3%	3%	5%	3%
Segment #3	Decon	5%	5%	5%	5%	5%	5%
	Pre-burn leach 1	15%	7%	5%	5%	5%	5%
	Pre-burn leach 2	5%	12%	N/A	5%	16%	5%
	Post-burn leach 1	7%	9%	5%	5%	5%	5%
	Post-burn leach 2	10%	12%	8%	7%	7%	5%
	SUM (MDA = 0)	6%	8%	4%	4%	4%	4%
Core	Decon	5%	5%	5%	5%	5%	5%
	Pre-burn leach 1	5%	5%	5%	5%	5%	5%
	Pre-burn leach 2	5%	5%	5%	5%	5%	5%
	Post-burn leach 1	5%	5%	5%	5%	5%	5%
	Post-burn leach 2	16%	10%	N/A	7%	15%	5%
	SUM (MDA = 0)	3%	3%	4%	4%	4%	4%
Compact TOTAL (MDA = 0)		2%	2%	3%	2%	3%	3%

4.6.3 Compact 10-3 Discussion

Compact 10-3 fell off the rod several times, as discussed in Section 3.6. The elevated quantities of Ce-144 and actinides measured in the DLBL solutions confirmed that some of the TRISO-coated driver particles were damaged. This makes it impossible to distinguish the fission-product inventories that originated in the DTF particles from those that were introduced from accidental damage to some of the driver particles. About 30 particle equivalents of Ce-144 (Table 43) and approximately 39 particle equivalents of U-238 (Table 45) were detected in total. In addition, 31–37 particle equivalents of the other actinides (Pu-239, Pu-240, U-234, U-235, and U-236) were also detected. With only 20 DTF particles in the compact, the radiochemical analysis suggests there were 11–19 TRISO-coated driver particles that were damaged during RDLBL. This case is similar to what was encountered with Compact 3-3.

The most-viable correction that could potentially be made is for Segment 3. The measurements made for Segments 1, 2, and the core are not salvageable. Some information from Segment 2 may be useful, but only if the nuclides measured in the deconsolidation solution are retained, and the erroneous inventory in Segment 1 is not added to that of Segment 2. Given the inability to determine the volume for Segment 1 (see Sections 3.6 and 5.6), the volume of Segment 2 is only estimated with a low degree of certainty. A correction for damaged particles in Segment 3 could be made by retaining only the measurements from the deconsolidation and the two pre-burn leaches. In doing this, the true inventory would be somewhat underestimated, but the effects of particles damaged during DLBL would be avoided.

In addition to the inability to determine a deconsolidated volume for Segment 1, there are seemingly too many damaged particles in Segment 1 and the core to make corrections with much confidence. In the core, it is unusual to have such a large difference in the U-238 and U-235 values, making it impossible to determine how many damaged particles to correct for. Because corrections could not be applied for the numerous damaged particles, the radial fission-product concentration profiles in the compact matrix will be presented in Section 5.6 for information only, and this compact will be excluded from the fission-product concentration-profile comparisons with other compacts.

4.7 Compact 12-1

Three radial segments were obtained from Compact 12-1 in addition to the core; however, the compact fell off the rod while the deconsolidation apparatus was being positioned for video collection after the third radial segment had been completed. Using calipers, the compact was measured once at three locations along its length.

4.7.1 Compact 12-1 Gamma-Emitter and Sr-90 Results

The amounts of selected gamma-emitting fission products and beta-emitting Sr-90 measured in the compact outside of the driver fuel SiC layer for each segment of the radial deconsolidation are summarized in Table 47 in terms of the number of particle-equivalent inventories. The results are also expressed in units of activity and the fraction of the compact inventory in Table 97 and Table 98 of Appendix A7, respectively. Table 48 gives the relative error for the values summarized in these tables. Table 47 shows the measured inventories of select fission products both with and without corrections for broken TRISO particles. The corrections were applied according to the same logic employed earlier (e.g., Section 4.4.1).

Table 47. Particle-equivalent inventories measured in the solutions from the radial deconsolidation of Compact 12-1. All values were decay-corrected to EOI + 1 day.

Particle Equivalents		Ag-110m	Ce-144	Cs-134	Cs-137	Eu-154	Eu-155	Ru-106	Sb-125	Sr-90
Segment #1	Decon	<7.3E+0	2.37E+0	1.92E+0	3.06E+0	1.89E+0	2.34E+0	2.64E-1	<3.5E-1	2.24E+0
	Decon*	<7.3E+0	3.72E-1	0.00E+0	1.06E+0	0	3.41E-1	0	<3.5E-1	2.37E-1
	Pre-burn leach 1	<2.7E+1	1.90E-2	3.16E-2	2.75E-1	<1.6E-1	<1.5E-1	1.29E-1	<2.5E-1	3.20E-2
	Pre-burn leach 2	<6.3E+0	4.40E-3	1.09E-3	7.69E-3	<6.5E-2	<1.2E-1	1.92E-2	<3.1E-2	2.34E-3
	Post-burn leach 1	<9.0E+0	<5.9E-3	4.97E-3	3.39E-2	2.22E-1	1.18E-1	<4.6E-2	<7.1E-2	8.22E-3
	Post-burn leach 2	<5.4E+0	<5.9E-3	4.46E-3	1.49E-2	<8.2E-2	<1.5E-1	<3.5E-2	<3.5E-2	3.89E-3
	Sum (MDA = 0)	0	2.40E+0	1.96E+0	3.39E+0	2.11E+0	2.46E+0	4.13E-1	0	2.28E+0
	Sum (MDA = 0)*	0	3.96E-1	4.21E-2	1.39E+0	2.22E-1	4.59E-1	1.48E-1	0	2.84E-1
Segment #2	Decon	<9.0E+0	1.33E+0	1.10E+0	1.83E+0	9.83E-1	1.22E+0	2.16E-1	<1.7E-1	1.38E+0
	Decon*	<9.0E+0	3.35E-1	1.03E-1	8.34E-1	0	2.15E-1	0	<1.7E-1	3.78E-1
	Pre-burn leach 1	<5.4E+0	4.04E-3	9.76E-3	1.99E-2	<8.2E-2	<1.5E-1	3.38E-2	<7.1E-2	4.08E-3
	Pre-burn leach 2	<9.0E+0	<5.9E-3	2.80E-3	1.39E-2	<1.2E-1	<1.5E-1	1.98E-2	<7.1E-2	4.76E-3
	Post-burn leach 1	<1.8E+1	1.12E+0	7.23E-1	1.08E+0	1.05E+0	9.85E-1	6.44E-1	5.72E-1	1.11E+0
	Post-burn leach 1*	<1.8E+1	1.19E-1	0	7.60E-2	5.47E-2	0	0	0	1.14E-1
	Post-burn leach 2	<9.0E+0	2.80E-3	7.58E-3	2.01E-2	<1.2E-1	<1.5E-1	2.49E-2	<7.1E-2	1.02E-2
	Sum (MDA = 0)	0	2.46E+0	1.85E+0	2.96E+0	2.04E+0	2.20E+0	9.38E-1	5.72E-1	2.51E+0
	Sum (MDA=0)*	0	4.61E-1	1.23E-1	9.64E-1	5.47E-2	2.15E-1	7.85E-2	0	5.12E-1

Particle Equivalents		Ag-110m	Ce-144	Cs-134	Cs-137	Eu-154	Eu-155	Ru-106	Sb-125	Sr-90
Segment #3	Decon	<2.7E+1	1.96E+0	1.25E+0	2.05E+0	1.48E+0	1.62E+0	2.67E-1	<7.1E-2	2.18E+0
	Decon*	<2.7E+1	9.62E-1	2.53E-1	1.05E+0	4.85E-1	6.24E-1	0	<7.1E-2	1.18E+0
	Pre-burn leach 1	<2.7E+0	2.19E-2	1.85E-2	4.09E-2	<5.0E-2	<4.4E-2	5.31E-2	<3.1E-2	2.47E-2
	Pre-burn leach 2	<2.7E+0	<1.5E-3	2.87E-3	2.18E-2	<5.0E-2	<4.4E-2	1.18E-2	<2.5E-2	1.04E-2
	Post-burn leach 1	<5.4E+0	4.64E-3	9.25E-2	1.57E-1	2.49E-1	1.39E-1	6.14E-2	<7.1E-2	1.14E-2
	Post-burn leach 2	<2.7E+0	<1.5E-3	1.37E-2	2.68E-2	1.81E-1	1.15E-1	2.13E-2	<3.1E-2	8.18E-3
	Sum (MDA = 0)	0	1.99E+0	1.38E+0	2.30E+0	1.92E+0	1.88E+0	4.15E-1	0	2.23E+0
	Sum (MDA=0)*	0	9.89E-1	3.81E-1	1.30E+0	9.15E-1	8.79E-1	1.48E-1	0	1.23E+0
Core	Decon	<3.6E+1	1.19E+1	4.34E+0	7.32E+0	8.14E+0	9.25E+0	4.53E+0	4.19E+0	8.10E+0
	Pre-burn leach 1	<3.6E+1	1.60E+0	1.21E+0	1.82E+0	1.24E+0	9.60E-1	7.19E+0	2.54E+0	1.31E+0
	Pre-burn leach 2	<1.8E+1	5.88E-2	2.03E-1	2.55E-1	<1.5E-1	<2.9E-1	1.68E-1	6.85E-1	4.75E-2
	Post-burn leach 1	<2.7E+1	1.48E+0	8.88E-1	1.30E+0	2.75E+0	2.10E+0	1.10E+0	4.31E+0	1.87E+0
	Post-burn leach 2	<1.8E+1	1.34E-2	2.02E-2	3.66E-2	<1.3E-1	<2.9E-1	3.62E-1	4.49E-1	2.50E-2
	Sum (MDA = 0)	0	1.50E+1	6.66E+0	1.07E+1	1.21E+1	1.23E+1	1.34E+1	1.22E+1	1.14E+1
Compact TOTAL (MDA = 0)		0	21.86	11.85	19.39	18.19	18.85	15.13	12.75	18.38
Compact TOTAL (MDA = 0)*		0	16.86	7.21	14.39	13.32	13.86	13.74	12.18	13.38
* Corrected for apparent TRISO particle damage										

Table 48. Relative error in the Compact 12-1 results. The errors in the “sum” rows were computed by propagating the error from all the RDLBL steps.

Uncertainty		Ag-110m	Ce-144	Cs-134	Cs-137	Eu-154	Eu-155	Ru-106	Sb-125	Sr-90
Segment #1	Decon	N/A	3.0%	3.0%	3.0%	3.0%	6.0%	12.0%	N/A	2.0%
	Pre-burn leach 1	N/A	29.0%	13.0%	4.0%	N/A	N/A	29.0%	N/A	2.0%
	Pre-burn leach 2	N/A	21.0%	42.0%	7.0%	N/A	N/A	20.0%	N/A	3.0%
	Post-burn leach 1	N/A	N/A	6.0%	6.0%	3.0%	9.0%	N/A	N/A	2.0%
	Post-burn leach 2	N/A	N/A	5.0%	7.0%	N/A	N/A	N/A	N/A	2.0%
	SUM (MDA = 0)	N/A	3.0%	2.9%	2.7%	2.7%	5.7%	12.3%	N/A	2.0%
Segment #2	Decon	N/A	5.0%	3.0%	6.0%	3.0%	8.0%	8.0%	N/A	2.0%
	Pre-burn leach 1	N/A	21.0%	9.0%	7.0%	N/A	N/A	7.0%	N/A	3.0%
	Pre-burn leach 2	N/A	N/A	5.0%	7.0%	N/A	N/A	7.0%	N/A	2.0%
	Post-burn leach 1	N/A	5.0%	3.0%	6.0%	5.0%	11.0%	6.0%	8.0%	2.0%
	Post-burn leach 2	N/A	29.0%	12.0%	7.0%	N/A	N/A	26.0%	N/A	N/A
	SUM (MDA = 0)	N/A	3.5%	2.1%	4.3%	3.0%	6.6%	4.6%	8.0%	1.4%
Segment #3	Decon	N/A	4.0%	3.0%	4.0%	3.0%	5.0%	5.0%	N/A	2.0%
	Pre-burn leach 1	N/A	31.0%	6.0%	4.0%	N/A	N/A	15.0%	N/A	2.0%
	Pre-burn leach 2	N/A	N/A	22.0%	5.0%	N/A	N/A	28.0%	N/A	2.0%
	Post-burn leach 1	N/A	36.0%	3.0%	4.0%	8.0%	20.0%	12.0%	N/A	2.0%
	Post-burn leach 2	N/A	N/A	7.0%	4.0%	10.0%	19.0%	32.0%	N/A	2.0%
	SUM (MDA = 0)	N/A	4.0%	2.7%	3.6%	2.7%	4.7%	4.6%	N/A	2.0%

Uncertainty		Ag-110m	Ce-144	Cs-134	Cs-137	Eu-154	Eu-155	Ru-106	Sb-125	Sr-90
Core	Decon	N/A	3.0%	3.0%	3.0%	3.0%	3.0%	3.0%	3.0%	2.0%
	Pre-burn leach 1	N/A	4.0%	3.0%	3.0%	3.0%	15.0%	3.0%	3.0%	2.0%
	Pre-burn leach 2	N/A	4.0%	3.0%	3.0%	N/A	N/A	9.0%	4.0%	2.0%
	Post-burn leach 1	N/A	4.0%	3.0%	3.0%	3.0%	7.0%	3.0%	3.0%	2.0%
	Post-burn leach 2	N/A	13.0%	4.0%	3.0%	N/A	N/A	4.0%	4.0%	2.0%
	SUM (MDA = 0)	N/A	2.4%	2.1%	2.1%	2.1%	2.8%	1.9%	1.6%	1.5%
Compact TOTAL (MDA = 0)		N/A	1.8%	1.3%	1.5%	1.5%	2.2%	1.8%	1.6%	1.0%

4.7.2 Compact 12-1 ICP-MS Results

ICP-MS was used to measure actinides in the RDLBL solutions. Table 49 provides results for U and Pu in units of mass, compact fraction, and particle equivalents.^c For Compact 12-1, only total U and Pu were measured at AL, and the isotopics were not determined. Table 49 also includes corrected values, which account for particles damaged during radial deconsolidation. Table 50 provides the relative error in these measurements.

Table 49. Uranium and plutonium measured from radial deconsolidation of Compact 12-1.

		Mass (μg)		Compact Fraction		Particle Equivalents	
		Pu Total	U Total	Pu Total	U Total	Pu Total	U Total
Segment #1	Decon	4.82	454	9.77E-4	1.09E-3	1.87	2.08
	Decon*	0	18.06	0	4.32E-5	0	0.08
	Pre-burn leach 1	<0.09	<4	<1.8E-5	<9.6E-6	<0.03	<0.02
	Pre-burn leach 2	<2	<0.09	<4.1E-4	<2.2E-7	<0.79	<4.2E-4
	Post-burn leach 1	0.07	<2	1.46E-5	<4.8E-6	2.80E-2	<0.01
	Post-burn leach 2	<5	<1	<1.0E-3	<2.4E-6	<1.92	<4.6E-3
	SUM (MDA = 0)	4.89	454	9.91E-4	1.09E-3	1.90	2.08
	SUM (MDA=0)*	0.07	18.06	1.46E-5	4.32E-5	0.03	0.08
Segment #2	Decon	2.13	239	4.32E-4	5.71E-4	0.83	1.10
	Decon*	0	21.90	0	5.00E-5	0	0.10
	Pre-burn leach 1	<7	2.60	<1.4E-3	6.22E-6	<2.69	1.19E-2
	Pre-burn leach 2	<7	6.63	<1.4E-3	1.58E-5	<2.69	3.04E-2
	Post-burn leach 1	3.61	252	7.32E-4	6.02E-4	1.40	1.16
	Post-burn leach 1*	1.04	33.90	2.11E-4	8.10E-5	0.40	0.16
	Post-burn leach 2	<6	2.35	<1.2E-3	5.62E-6	<2.30	1.08E-2
	SUM (MDA = 0)	5.74	502.58	1.16E-3	1.20E-3	2.23	2.30
SUM (MDA=0)*	1.04	66.38	2.11E-4	1.59E-4	0.40	0.30	

^c In this instance, these data fit neatly in a single table, and no additional ICP-MS data will be presented in Appendix A7.

		Mass (μg)		Compact Fraction		Particle Equivalents	
		Pu Total	U Total	Pu Total	U Total	Pu Total	U Total
Segment #3	Decon	1.19	236	2.41E-4	5.64E-4	0.46	1.08
	Decon*	0	17.90	0	4.28E-5	0	0.08
	Pre-burn leach 1	0.15	7.16	3.00E-5	1.71E-5	5.76E-2	3.28E-2
	Pre-burn leach 2	0.44	5.99	8.86E-5	1.43E-5	0.17	2.75E-2
	Post-burn leach 1	0.26	3.30	5.31E-5	7.89E-6	0.10	1.51E-2
	Post-burn leach 2	<0.7	1.22	<1.4E-4	2.92E-6	<0.27	5.59E-3
	SUM (MDA = 0)	2.04	253.67	4.13E-4	6.06E-4	0.79	1.16
	SUM (MDA=0)*	0.85	35.57	1.72E-4	8.50E-5	0.33	0.16
Core	Decon	38.0	3260	7.71E-3	7.79E-3	14.78	14.95
	Pre-burn leach 1	8.1	403	1.64E-3	9.63E-4	3.14	1.85
	Pre-burn leach 2	0.2	13.6	3.95E-5	3.25E-5	7.58E-2	6.24E-2
	Post-burn leach 1	3.4	254	6.83E-4	6.07E-4	1.31	1.16
	Post-burn leach 2	<0.08	1.9	<1.6E-5	4.54E-6	<0.03	8.71E-3
	SUM (MDA = 0)	49.65	3932.50	1.01E-2	9.40E-3	19.31	18.03
Compact Total (MDA = 0)		62.31	5143.01	1.26E-2	1.23E-2	24.23	23.58
Compact Total (MDA = 0)*		51.60	4052.51	1.05E-2	9.69E-3	20.07	18.58

* Corrected for accidental TRISO particle damage

Table 50. Relative error in the Compact 12-1 U and Pu measurements given in Table 49.

Uncertainty		Pu Total	U Total
Segment #1	Decon	15%	10%
	Pre-burn leach 1	N/A	N/A
	Pre-burn leach 2	N/A	N/A
	Post-burn leach 1	30%	N/A
	Post-burn leach 2	N/A	N/A
	SUM (MDA = 0)	15%	10%
Segment #2	Decon	15%	5%
	Pre-burn leach 1	N/A	15%
	Pre-burn leach 2	N/A	20%
	Post-burn leach 1	25%	10%
	Post-burn leach 2	N/A	20%
	SUM (MDA = 0)	17%	6%
Segment #3	Decon	35%	20%
	Pre-burn leach 1	35%	20%
	Pre-burn leach 2	15%	15%
	Post-burn leach 1	25%	20%
	Post-burn leach 2	N/A	30%
	SUM (MDA = 0)	21%	19%

Uncertainty		Pu Total	U Total
Core	Decon	5%	10%
	Pre-burn leach 1	15%	10%
	Pre-burn leach 2	30%	15%
	Post-burn leach 1	10%	5%
	Post-burn leach 2	N/A	10%
	SUM (MDA = 0)	3.9%	8.4%
Compact Total (MDA = 0)		3.7%	6.5%

4.7.3 Compact 12-1 Discussion

As discussed in Section 3.7, there were a couple chips on the compact top and bottom rims prior to the start of the Segment 1 radial deconsolidation (Figure 16). This might have damaged some driver particles and affected the results obtained for Segment 1. The data show that 2.08 particle equivalents of U were detected in the deconsolidation solution from Segment 1, suggesting that two driver particles were accidentally broken just before or during the Segment 1 deconsolidation. In Segment 2, 1.1 particle equivalents of U were measured in the deconsolidation solution. About 1.1 particle equivalents of total uranium were detected in the deconsolidation solution from Segment 3.

Seeing damage in these deconsolidation steps could indicate that four particles had failed during irradiation, but this does not seem credible given the relatively low burnup and irradiation temperature of this compact, the performance demonstrated with this AGR-1-type TRISO fuel that had low particle failure rates (Demkowicz et al. 2015), and the amount of Cs recovered. Before any corrections for accidental particle damage were made, this compact had about 11.85 particle equivalents of Cs-134 measured in the RDLBL. This was 59% of the expected DTF-particle inventory of Cs-134. The near-integer quantities of particle equivalents of U measured in Segments 1–3 (see Table 49) coinciding with similar quantities of Cs-134 in the same RDLBL steps (see Table 47) indicate the particles leached in these steps retained $\geq 90\%$ of their predicted inventories. If the particles had failed in pile, more Cs-134 release from those particles would be expected, and the amount of Cs-134 recoverable from such particles might be expected to be more on the order of the 59% indicated from the totals measured in RDLBL (Table 47).

In Segment 2, another 1.16 particle equivalents of U were measured in the first post-burn leach step. This might suggest a driver particle that experienced an in-pile SiC failure; however, a particle with an in-pile SiC layer failure might have a smaller inventory of Cs remaining for recovery than the 0.72 particle equivalents of Cs-134 measured. Limited studies of the apportioning of Cs between the kernels and coatings of intact TRISO particles show that 10-100% of the Cs may reside in the kernel of an intact particle, but on average, about 80% of the Cs-134 was found in the kernels (Demkowicz et al. 2016, Stempien 2020). In that context, a recovery of 0.72 particle equivalents from an accidentally damaged particle is not unreasonable. As has been noted, SiC failures in AGR-1-type TRISO particles were very rare (Demkowicz et al. 2015). Thus, it is believed that a particle was broken during the first post-burn leach in Segment 2. Such a particle might have been partially damaged in a prior step of the Segment 2 RDLBL, and complete damage that allowed leaching of the particle interior did not occur until the first burn-leach step. An uncertainty in this determination is that (as Section 5.9.1 will discuss) the compacts with irradiation temperatures $< 960^\circ\text{C}$ retained notably more Cs-134. It is not impossible that exposed kernels (whether in DTF particles or in a hypothetical in-pile failed TRISO or failed-SiC particle) retained on the order of 70% of their Cs in these AGR-3/4 compacts with the lower irradiation temperatures.

As for the core, the measured uranium corresponded to 18.03 (± 1.5) particle equivalents, suggesting that no additional particle damaged occurred in the core. Thus, despite the use of calipers to measure the compact diameter after it fell off the rod after the third radial segment of deconsolidation, it does not appear that any driver particles were broken. From all the RDLBL steps, the data suggest a total of five TRISO-coated driver particles were accidentally damaged.

With that understanding, two particle-equivalents were subtracted from what was measured in the deconsolidation solution of Segment 1, and one particle-equivalent was subtracted from each of the Segment 2 deconsolidation and first post-burn leach. As for the deconsolidation of Segment 3, the Ce-144 quantity suggests two particles were damaged, but the Cs-134 and U measurements indicate only one particle-equivalent inventory. It was decided that the total uranium and Cs-134 quantities be used as indicators of particle damage here. Thus, one particle equivalent was subtracted from the Segment 3 values based on the apparent failure of a single particle during the Segment 3 deconsolidation. In total, it was estimated that five particles were accidentally damaged in the RDLBL work on Compact 12-1, and the results have been corrected for that damage.

While the amounts of measured Ce-144 in different stages of the DLBL of Compact 12-1 reasonably track with suspected TRISO-particle damage (based on comparisons to the amounts of Cs-134 and total U), the total amount of Ce-144 measured in the compact is a little lower than what was seen in DLBLs of other compacts (e.g., 5-3, 5-4, 7-3, and 8-3). In those other compacts, closer to 20 particle equivalents were measured, even after correcting for suspected TRISO damage, but in Compact 12-1, only about 17 particle equivalents were measured after correcting for suspected TRISO damage. It is not clear why the Ce-144 detected in Compact 12-1 is a little lower given that the other DLBLs of AGR-3/4 compacts demonstrate that it is well retained.

4.8 Compact 12-3

After the first radial segment was deconsolidated from Compact 12-3, the compact was knocked from the rod before any video could be captured for dimensional analysis. The compact was re-attached to the rod so that video could be captured and analyzed; however, because the jig used at the time to attach the compact to the rod was designed for compacts in the as-irradiated state, the compact was not perfectly centered on the rod. Thus, additional radial deconsolidations were not performed. Instead, the compact was then deconsolidated in a single, axial step after only one radial segment had been obtained. The mounting jig was subsequently redesigned to effectively center compacts of any diameter.

Another problem was encountered during the handling of the deconsolidated material. The thimble of the deconsolidated particles and matrix debris from the axial deconsolidation of the core was spilled prior to obtaining a mass of the particles and debris. A portion of the thimble did not spill and was retained in the thimble. The spilled particles and matrix debris were recovered from the tray where the spill occurred. The unspilled portion and the spilled portions were weighed, and the rest of the leach-burn leach process was performed while keeping the spilled and unspilled portions separate in case the spilled material had become contaminated. Table 51 summarizes the masses of each portion of material. The results in the following sections will be presented for both the spilled and unspilled portions.

Table 51. Masses of spilled (and recovered) and unspilled particles and matrix debris from the axial deconsolidation of the core of Compact 12-3.

	Mass (g)
Unspilled, dried particles and debris after deconsolidation, before pre-burn leaching	0.331
Spilled, dried particles and debris after deconsolidation, before pre-burn leaching	0.408
Total	0.740

4.8.1 Compact 12-3 Gamma-Emitter and Sr-90 Results

The amounts of selected gamma-emitting fission products and beta-emitting Sr-90 measured in the compact outside of the driver fuel SiC layer for the one radial segment and the central core are summarized in Table 52 in units of particle-equivalents. The radionuclide inventories measured at each step of the leach-burn leach process are given for both the spilled and unspilled material. A total inventory from summing the contributions of the unspilled and spilled sample streams is also given. Additional results in units of activity and compact fraction are reported in Table 99 and Table 100 of Appendix A8. Table 53 gives the relative error for the values summarized in these tables.

Table 52. Quantity of fission products measured in the solutions from the radial deconsolidation of Compact 12-3. Values are given for both the unspilled and spilled portions from the core deconsolidation. Compact total is sum from all solutions from Segment 1 and the core. All values were decay-corrected to EOI + 1 day.

Particle Equivalents		Ag-110m	Ce-144	Cs-134	Cs-137	Eu-154	Eu-155	Ru-106	Sb-125	Sr-90
Segment #1	Decon	<2.9E+0	<1.7E-3	2.73E-2	4.19E-2	<2.3E-2	<5.0E-2	<2.9E-2	<3.6E-2	1.44E-3
	Pre-burn leach 1	<8.6E+0	<3.3E-3	2.35E-3	9.66E-3	<9.0E-2	<1.3E-1	<2.9E-2	<3.6E-2	4.78E-3
	Pre-burn leach 2	<8.6E+0	<6.7E-3	<4.4E-3	4.34E-3	<1.1E-1	<1.7E-1	<2.9E-2	<4.0E-2	2.74E-3
	Post-burn leach 1	<8.6E+0	<6.7E-3	<4.4E-3	5.14E-3	3.68E-1	2.22E-1	<2.9E-2	<4.0E-2	4.52E-3
	Post-burn leach 2	<4.4E+0	<3.3E-3	<2.3E-3	7.52E-4	<9.0E-2	<1.2E-1	<1.4E-2	<2.9E-2	9.23E-4
	Total (MDA = 0)	N/A	N/A	2.97E-2	6.18E-2	3.68E-1	2.22E-1	N/A	N/A	1.44E-2
Core	Decon	<95.90	8.63	4.87	7.92	6.44	7.23	3.25	2.50	7.99
	Pre-burn Leach 1 Unspilled	<128.51	3.32	2.27	3.45	2.56	2.63	0.63	1.75	4.09
	Pre-burn Leach 1 Spilled	<172.62	4.40	4.26	7.11	4.51	4.97	1.54	3.75	6.78
	Pre-burn Leach 2 Unspilled	<47.95	<0.02	8.83E-3	1.52E-2	<0.16	<0.27	<0.08	9.66E-2	1.34E-2
	Pre-burn Leach 2 Spilled	<42.20	9.22E-3	1.93E-2	3.07E-2	<0.13	<0.23	3.10E-1	4.72E-1	3.99E-2
	Post-burn Leach 1 Unspilled	<32.61	2.92E-2	8.94E-3	1.47E-2	4.24E-1	1.79E-1	1.85E-1	1.79E-1	8.05E-2
	Post-burn Leach 1 Spilled	<36.44	3.57E-2	4.81E-3	1.05E-2	4.43E-1	2.16E-1	6.58E-2	9.72E-2	9.81E-2
	Post-burn Leach 2 Unspilled	<32.61	1.77E-2	1.30E-2	1.95E-2	<0.13	<0.21	1.11E-1	1.03E-1	2.00E-3
	Post-burn Leach 2 Spilled	<46.03	<0.01	<0.01	1.24E-3	<0.10	<0.21	6.24E-2	<0.06	9.02E-4
	Total (MDA = 0) Unspilled + Decon	N/A	12.00	7.17	11.42	9.42	10.04	4.18	4.63	12.17
	Total (MDA = 0) Spilled Only	N/A	4.44	4.28	7.15	4.95	5.19	1.98	4.32	6.92
	Total (MDA = 0)	N/A	16.44	11.45	18.57	14.37	15.23	6.15	8.95	19.09
Compact TOTAL (MDA = 0)		N/A	16.44	11.48	18.63	14.74	15.45	6.15	8.95	19.11

Table 53. Relative error for the results from the Compact 12-3 RDLBL.

Uncertainty		Ag-110m	Ce-144	Cs-134	Cs-137	Eu-154	Eu-155	Ru-106	Sb-125	Sr-90
Segment #1	Decon	N/A	N/A	4.0%	6.0%	N/A	N/A	N/A	N/A	2.0%
	Pre-burn leach 1	N/A	N/A	19.0%	7.0%	N/A	N/A	N/A	N/A	2.0%
	Pre-burn leach 2	N/A	N/A	N/A	9.0%	N/A	N/A	N/A	N/A	3.0%
	Post-burn leach 1	N/A	N/A	N/A	8.0%	3.0%	9.0%	N/A	N/A	2.0%
	Post-burn leach 2	N/A	N/A	N/A	6.0%	N/A	N/A	N/A	N/A	5.0%
	Total (MDA = 0)	N/A	N/A	4.0%	4.3%	3.0%	9.0%	N/A	N/A	1.1%

Uncertainty		Ag-110m	Ce-144	Cs-134	Cs-137	Eu-154	Eu-155	Ru-106	Sb-125	Sr-90
Core	Decon	N/A	3.0%	3.0%	3.0%	3.0%	3.0%	3.0%	3.0%	1.6%
	Pre-burn Leach 1 Unspilled	N/A	3.7%	3.0%	3.0%	3.6%	8.7%	14.6%	5.6%	2.0%
	Pre-burn Leach 1 Spilled	N/A	4.3%	3.0%	3.0%	3.0%	6.0%	8.7%	4.7%	2.0%
	Pre-burn Leach 2 Unspilled	N/A	N/A	6.5%	3.0%	N/A	N/A	N/A	9.0%	3.0%
	Pre-burn Leach 2 Spilled	N/A	20.2%	7.9%	3.0%	N/A	N/A	7.6%	4.6%	2.0%
	Post-burn Leach 1 Unspilled	N/A	9.7%	13.3%	3.0%	3.0%	18.7%	8.4%	3.0%	2.0%
	Post-burn Leach 1 Spilled	N/A	8.8%	16.0%	3.0%	3.0%	12.8%	18.5%	3.7%	2.0%
	Post-burn Leach 2 Unspilled	N/A	17.1%	11.0%	3.0%	N/A	N/A	12.1%	5.6%	6.6%
	Post-burn Leach 2 Spilled	N/A	N/A	N/A	10.2%	N/A	N/A	30.9%	N/A	10.3%
	Total (MDA = 0) Unspilled + Decon	N/A	2.4%	2.2%	2.3%	2.3%	3.2%	3.3%	2.7%	1.3%
	Total (MDA = 0) Spilled Only	N/A	4.3%	3.0%	3.0%	2.7%	5.8%	6.9%	4.1%	2.0%
	Total (MDA = 0)	N/A	2.1%	1.8%	1.8%	1.8%	2.9%	3.1%	2.4%	1.1%
Compact TOTAL (MDA = 0)		N/A	2.1%	1.8%	1.8%	1.7%	2.8%	3.1%	2.4%	1.1%

4.8.2 Compact 12-3 ICP-MS Results

ICP-MS was used to measure actinides in the RDLBL solutions. Table 54 summarizes results for major isotopes of U and Pu in units of particle equivalents. The radionuclide inventories measured at each step of the leach-burn-leach process are given for both the spilled and unspilled material. A total inventory from summing the contributions of the unspilled and spilled sample streams is also given. Additional results in units of mass and compact fraction are present in Table 101 and Table 102, respectively, in Appendix A8. Table 55 provides the relative error in these measurements.

Table 54. Particle equivalents for select actinides from ICP-MS of solutions from Compact 12-3 RDLBL.

		Particle Equivalents					
		Pu-239	Pu-240	U-234	U-235	U-236	U-238
Segment #1	Decon	<1.7E-2	<2.9E-2	<6.7E-2	<2.7E-3	<1.2E-2	2.84E-3
	Pre-burn leach 1	<3.5E-2	<7.1E-2	<2.1E-1	<1.2E-2	<3.1E-2	<5.4E-3
	Pre-burn leach 2	<4.6E-2	<1.4E-1	<3.1E-1	1.18E-2	<3.8E-2	4.01E-3
	Post-burn leach 1	<4.0E-2	<1.1E-1	<2.7E-1	<1.5E-2	<3.8E-2	9.26E-3
	Post-burn leach 2	<4.0E-2	<1.1E-1	<2.7E-1	<9.2E-3	<3.8E-2	<2.7E-3
	Total (MDA = 0)	N/A	N/A	N/A	1.18E-2	N/A	1.61E-2

Particle Equivalents							
		Pu-239	Pu-240	U-234	U-235	U-236	U-238
Core	Decon	7.99	7.06	8.79	8.88	8.72	8.34
	Pre-burn Leach 1 Unspilled	2.65	2.51	3.73	3.90	3.82	3.83
	Pre-burn Leach 1 Spilled	8.30	7.70	7.95	8.18	6.94	6.79
	Pre-burn Leach 2 Unspilled	<2.3E-2	<7.1E-2	<6.7E-2	1.25E-2	9.55E-3	1.12E-2
	Pre-burn Leach 2 Spilled	1.73E-1	<1.1E-1	<3.5E-2	2.29E-2	2.40E-2	7.53E-3
	Post-burn Leach 1 Unspilled	2.86E-2	<4.8E-2	<3.5E-2	1.76E-2	1.61E-2	1.61E-2
	Post-burn Leach 1 Spilled	2.39E-2	<3.6E-2	<3.1E-2	1.22E-2	1.17E-2	1.14E-2
	Post-burn Leach 2 Unspilled	<1.9E-2	<7.1E-2	<6.7E-2	9.64E-3	<1.0E-2	8.86E-3
	Post-burn Leach 2 Spilled	<1.2E-1	<3.6E-1	<6.7E-1	<3.1E-3	<7.7E-2	<5.4E-4
	Total Unspilled + Decon (MDA = 0)	10.67	9.56	12.52	12.83	12.56	12.20
	Total Spilled (MDA = 0)	8.50	7.70	7.95	8.22	6.98	6.81
	Total Spilled + Unspilled (MDA) = 0	19.17	17.27	20.47	21.04	19.54	19.01
Grand Compact Total (MDA = 0)		19.17	17.27	20.47	21.05	19.54	19.02

Table 55. Relative error in ICP-MS results for Compact 12-3.

		Pu-239	Pu-240	U-234	U-235	U-236	U-238
Segment #1	Decon	N/A	N/A	N/A	N/A	N/A	10%
	Pre-burn leach 1	N/A	N/A	N/A	N/A	N/A	N/A
	Pre-burn leach 2	N/A	N/A	N/A	15%	N/A	20%
	Post-burn leach 1	N/A	N/A	N/A	N/A	N/A	10%
	Post-burn leach 2	N/A	N/A	N/A	N/A	N/A	N/A
	Total (MDA = 0)	N/A	N/A	N/A	15%	N/A	7.8%
Core	Decon	5.0%	7.0%	5.0%	5.0%	5.0%	5.0%
	Pre-burn Leach 1 Unspilled	7.1%	11.9%	11.9%	5.0%	5.0%	5.0%
	Pre-burn Leach 1 Spilled	5.0%	7.0%	7.1%	5.0%	5.0%	5.0%
	Pre-burn Leach 2 Unspilled	N/A	N/A	N/A	21.9%	20.0%	13.4%
	Pre-burn Leach 2 Spilled	20.0%	N/A	N/A	10.3%	20.0%	15.7%
	Post-burn Leach 1 Unspilled	25.1%	N/A	N/A	14.3%	15.2%	7.1%
	Post-burn Leach 1 Spilled	35.0%	N/A	N/A	10.5%	14.3%	5.0%
	Post-burn Leach 2 Unspilled	N/A	N/A	N/A	15.3%	N/A	10.0%
	Post-burn Leach 2 Spilled	N/A	N/A	N/A	N/A	N/A	N/A
	Total Unspilled + Decon (MDA = 0)	4.1%	6.1%	5.0%	3.8%	3.8%	3.8%

		Pu-239	Pu-240	U-234	U-235	U-236	U-238
	Total Spilled (MDA = 0)	4.9%	7.0%	7.1%	5.0%	5.0%	5.0%
	Total Spilled + Unspilled (MDA) = 0	3.2%	4.6%	4.1%	3.0%	3.0%	3.0%
Grand Compact Total (MDA = 0)		3.2%	4.6%	4.1%	3.0%	3.0%	3.0%

4.8.3 Compact 12-3 Discussion

When a compact detaches from the deconsolidation rod, there is always concern that TRISO-coated driver particles could be damaged. Section 3.8 showed some images taken after Compact 12-3 had become detached from the deconsolidation rod. While a small amount of material from the compact appears to be adhered to the epoxy after detachment, no particles were obviously embedded in any of that material. Looking at the total amounts of fission products and actinides in the RDLBL solutions from Segment 1 and the core, there appears to be little or no damage to TRISO particles in the compact because the quantities of U-235, U-238, and Pu-239 are near 20 particle equivalents at 21.05 ± 0.63 , 19.02 ± 0.57 , and 19.1 ± 0.61 particle equivalents, respectively. The total Ce-144 is a little low, at 16.4 ± 0.34 particle equivalents. For compacts with minimal complications during RDLBL (e.g., Compacts 5-3, 5-4, and 7-3), the ratio of measured Ce-144:U-235 is typically closer to 1. While every attempt to recover all the spilled Compact 12-3 material was made, a small amount may have been lost. The material that was spilled and recovered fell onto a clean cloth, but it had a higher likelihood of being exposed to contamination as a result of the spill. Given that the quantities of fission products measured in these samples are reasonable for an AGR-3/4 compact containing 20 DTF particles, it is not obvious that the results are strongly biased by contamination or by the potential loss of some material when it was spilled. With no compelling evidence for accidental TRISO particle damage or contamination, no adjustments or corrections were made to the results.

5. RADIAL URANIUM AND FISSION-PRODUCT-CONCENTRATION PROFILES

The RDLBL process allows determination of the fission-product content within specific segments or volumes, of the compact. For the purpose of processing and presenting the data, it was assumed that material was removed from the compacts in an azimuthally uniform manner as the compacts rotated in the RDLBL apparatus. The volumes and radial boundaries of the segments were presented in Section 3. The fission-product inventories in each segment were presented for each compact in Section 4. In this section, the fission-product and actinide inventories were normalized by the segment volume to give concentrations, which were plotted at the radial middle of each segment to give radial fission-product-concentration profiles. The radial concentration profiles for selected fission products are presented in units of fraction/mm³, particle equivalents/mm³, and Bq/mm³. With units of fraction/mm³ and particle equivalents/mm³, easy comparisons of the relative amounts of different isotopes can be made. Results given in units of radioactivity/mm³ are included for easier comparison to some earlier AGR-3/4 reports and papers (Stempien 2021, Humrickhouse et al. 2016, Humrickhouse et al. 2018, Riet 2022).

5.1 Compact 3-3 Radial Fission-Product Profiles

The RDLBL process for Compact 3-3 generated fission-product inventories for four radial segments and the core of the compact. Table 56 gives the concentrations for select fission products and U-238 within each segment of the compact. The volume and average radius of each segment were given previously in Table 15. Table 57 gives the relative error on the concentration by propagating the measurement error on the compact's dimensions and the measurement error of the fission-product activities and actinide masses. Figure 20 and Figure 21 plot the radial-concentration profiles for selected fission products in Compact 3-3 in units of particle equivalents/mm³ and Bq/mm³, respectively. Figure 22 compares the concentration profile of Ce-144 to that of U-238.

As Section 4.1.3 discussed, a number of the TRISO-coated driver particles were damaged during the deconsolidation step of the radial segments, and this makes it impossible to distinguish the actinide and radionuclide inventory released from the DTF particles from that contributed by accidental damage to the driver particles. If accidental particle damage had occurred at some stage after the deconsolidation, effective corrections would be more readily applied; however, a number of these particles were damaged during the deconsolidation, and corrections were not applied here. Segments 2 and 3 appear to have one broken particle each in their deconsolidation steps. Segment 4 may have an additional broken particle in its deconsolidation step. The concentrations in Segment 1 and the core are impacted by more widespread accidental damage incurred to 3–4 and 7–8 TRISO particles, respectively.

Table 56. Radial fission product and U-238 concentrations expressed in several units for Compact 3-3.

Units	Segment	Ag-110m	Ce-144	Cs-134	Cs-137	Eu-154	Eu-155	Ru-106	Sb-125	Sr-90	U-238
Bq /mm ³	1	N/A	4.81E+5	1.99E+4	3.70E+4	1.52E+3	1.20E+3	7.71E+4	7.91E+2	1.99E+4	N/A
	2	N/A	2.33E+4	1.50E+3	5.32E+3	8.31E+2	6.78E+2	3.59E+4	2.00E+2	1.66E+4	
	3	N/A	4.07E+4	2.60E+3	7.79E+3	7.84E+2	7.03E+2	6.35E+4	2.01E+2	1.90E+4	
	4	N/A	1.99E+5	1.81E+4	4.82E+4	2.06E+3	1.84E+3	3.21E+5	1.50E+3	7.64E+4	
	Core	N/A	1.59E+6	2.67E+4	3.96E+4	2.07E+3	1.69E+3	2.38E+5	3.09E+3	6.07E+4	
Fraction /mm ³	1	N/A	4.96E-6	2.83E-6	5.79E-6	6.65E-6	7.84E-6	3.81E-6	1.60E-6	3.57E-6	8.29E-6
	2	N/A	2.41E-7	2.13E-7	8.33E-7	3.64E-6	4.42E-6	1.78E-6	4.05E-7	2.98E-6	2.09E-6
	3	N/A	4.20E-7	3.70E-7	1.22E-6	3.44E-6	4.58E-6	3.14E-6	4.08E-7	3.40E-6	5.04E-6
	4	N/A	2.06E-6	2.58E-6	7.54E-6	9.06E-6	1.20E-5	1.59E-5	3.04E-6	1.37E-5	2.76E-6
	Core	N/A	1.65E-5	3.80E-6	6.19E-6	9.09E-6	1.10E-5	1.17E-5	6.26E-6	1.09E-5	1.79E-5
Particle Equivalents /mm ³	1	N/A	9.52E-3	5.44E-3	1.11E-2	1.28E-2	1.50E-2	7.31E-3	3.07E-3	6.84E-3	1.59E-2
	2	N/A	4.61E-4	4.09E-4	1.60E-3	6.99E-3	8.47E-3	3.41E-3	7.77E-4	5.72E-3	4.02E-3
	3	N/A	8.05E-4	7.10E-4	2.34E-3	6.60E-3	8.78E-3	6.02E-3	7.83E-4	6.53E-3	9.66E-3
	4	N/A	3.95E-3	4.95E-3	1.45E-2	1.74E-2	2.30E-2	3.05E-2	5.82E-3	2.63E-2	5.30E-3
	Core	N/A	3.16E-2	7.29E-3	1.19E-2	1.74E-2	2.11E-2	2.25E-2	1.20E-2	2.09E-2	3.42E-2

Table 57. Relative error for the Compact 3-3 fission product and U-238 concentrations given in Table 56.

	Ag-110m	Ce-144	Cs-134	Cs-137	Eu-154	Eu-155	Ru-106	Sb-125	Sr-90	U-238
1	N/A	16%	15%	15%	15%	16%	16%	16%	15%	17%
2	N/A	24%	24%	24%	24%	24%	24%	25%	24%	26%
3	N/A	39%	38%	39%	38%	38%	39%	40%	38%	39%
4	N/A	31%	29%	30%	29%	30%	30%	31%	29%	30%
Core	N/A	4%	4%	4%	4%	5%	4%	5%	4%	5%

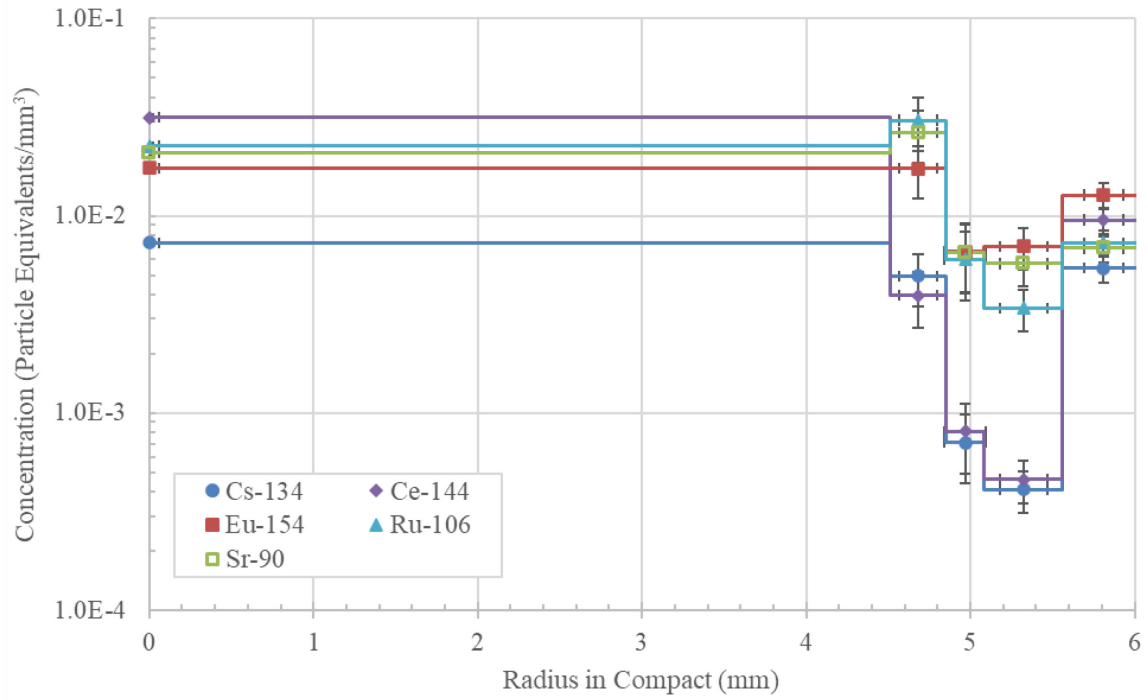


Figure 20. Compact 3-3 fission-product radial-concentration profiles in units of particle equivalents/mm³.

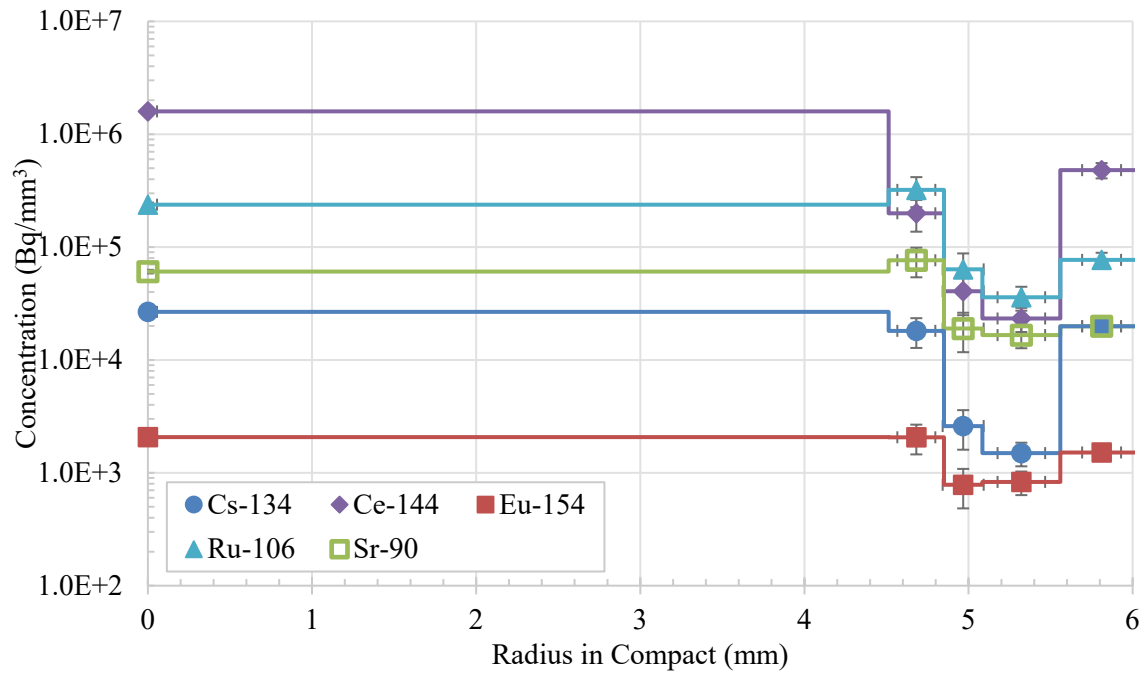


Figure 21. Compact 3-3 fission-product radial-concentration profiles in units of Bq/mm³.

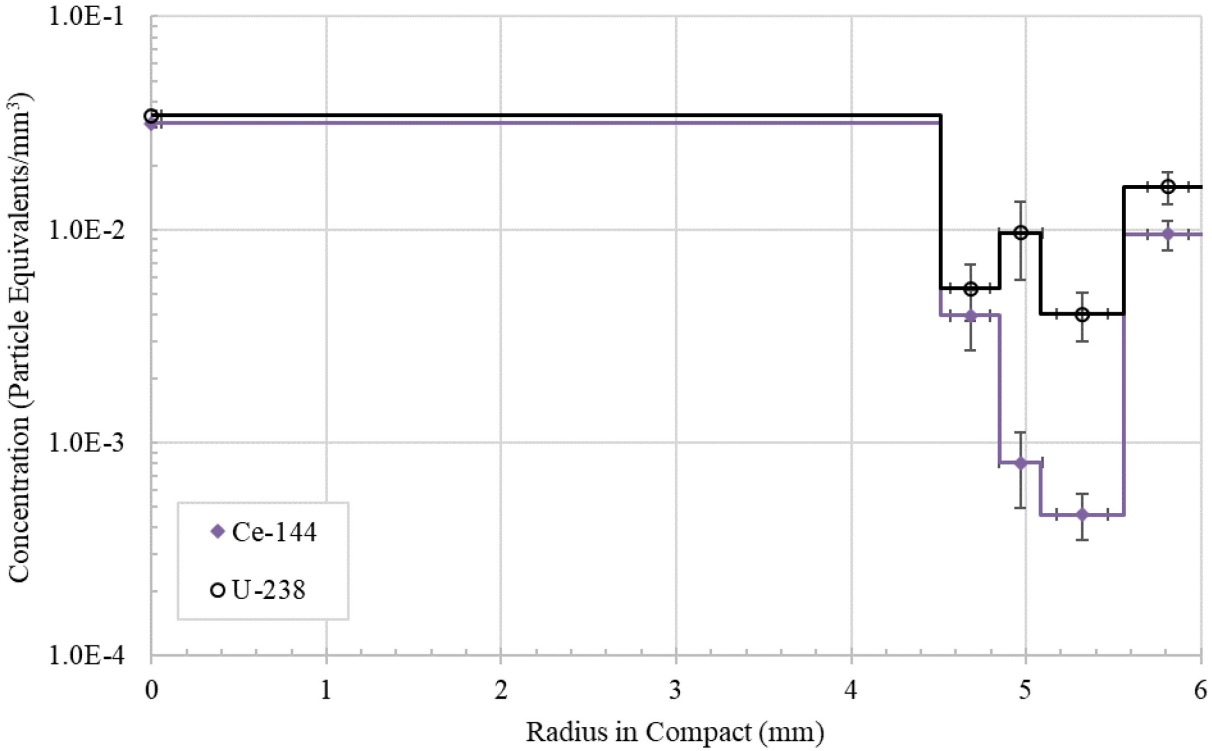


Figure 22. Comparison of U-238 and Ce-144 radial-concentration profiles in Compact 3-3.

5.2 Compact 5-3 Radial Fission-Product Profiles

The RDLBL process for Compact 5-3 generated fission-product inventories for three radial segments and the core of the compact. Table 58 gives the concentrations for select fission products and U-238 within each segment of the compact. The volume and average radius of each segment were given previously in Table 16. As detailed in Section 4.2.3, a TRISO-coated driver particle was accidentally broken during the first-post-burn leach of Segment 1. The concentrations before and after correcting Segment 1 for this broken particle are both given in Table 58. Table 59 gives the relative error on the concentration by accounting for the measurement error on the compact's dimensions and the measurement error of the fission-product activity and U-238 mass.

Figure 23 and Figure 24 give the radial-concentration profiles (corrected for accidental particle damage) for selected fission products in Compact 5-3 in units of particle equivalents/mm³ and Bq/mm³, respectively. The concentrations of Ce-144 and Eu-154 decrease along the radius from the core to the outer layer. The concentration of Sr-90 decreases with increasing radius except at the outermost layer (Segment 1). In contrast, the Cs-134 concentration increases with increasing radius. Figure 25 shows the concentration profiles for Ce-144 and U-238, which are similar (within the error). From the core to Segment 2, the concentration decreases. In Segment 1, the correction for accidental particle damage in the Segment 1 post-burn leach 1 reduced the 0.933 particle equivalents of Ce-144 detected to zero because all the Ce-144 in that segment was attributed to what was suspected to be one particle damaged in the first-post-burn leach of Segment 1. In the outermost segment, Segment 1, the U-238 concentration is a little higher than in Segment 2; however, they are statistically similar within the calculated errors.

Table 58. Radial fission product and U-238 concentrations expressed in several units for each segment of Compact 5-3.

Units	Segment	Ag-110m	Ce-144	Cs-134	Cs-137	Eu-154	Eu-155	Ru-106	Sb-125	Sr-90	U-238
Bq /mm ³	1	N/A	8.01E+5	8.27E+4	7.85E+4	1.83E+3	1.38E+3	2.67E+3	2.06E+3	5.11E+4	N/A
	1*	N/A	0	5.03E+4	4.43E+4	0	0	2.67E+3	1.84E+2	1.55E+3	
	2	N/A	5.29E+3	1.70E+4	1.92E+4	2.96E+1	N/A	N/A	N/A	2.70E+2	
	3	N/A	1.65E+5	1.90E+4	2.19E+4	3.74E+2	3.02E+2	3.95E+3	4.16E+2	1.83E+4	
	Core	N/A	1.27E+6	1.21E+4	2.11E+4	2.62E+3	2.08E+3	1.59E+5	3.88E+3	8.06E+4	
Fraction /mm ³	1	N/A	7.22E-6	8.19E-6	1.05E-5	5.87E-6	6.79E-6	1.01E-7	3.45E-6	7.98E-6	6.11E-6
	1*	N/A	0	5.91E-6	0	0	0	1.01E-7	3.09E-7	2.43E-7	1.76E-7
	2	N/A	4.77E-8	1.68E-6	2.57E-6	9.50E-8	N/A	N/A	N/A	4.22E-8	1.00E-7
	3	N/A	1.49E-6	1.88E-6	2.93E-6	1.20E-6	1.48E-6	1.49E-7	6.97E-7	2.85E-6	1.34E-6
	Core	N/A	1.15E-5	1.19E-6	2.82E-6	8.43E-6	1.02E-5	6.00E-6	6.51E-6	1.26E-5	1.09E-5
Particle Equivalents /mm ³	1	N/A	1.38E-2	1.57E-2	2.01E-2	1.13E-2	1.30E-2	1.93E-4	6.62E-3	1.53E-2	1.17E-2
	1*	N/A	0	9.55E-3	1.13E-2	0	0	1.93E-4	5.92E-4	4.66E-4	3.37E-4
	2	N/A	9.15E-5	3.23E-3	4.93E-3	1.82E-4	N/A	N/A	N/A	8.09E-5	1.93E-4
	3	N/A	2.85E-3	3.61E-3	5.61E-3	2.31E-3	2.84E-3	2.85E-4	1.34E-3	5.47E-3	2.56E-3
	Core	N/A	2.20E-2	2.29E-3	5.41E-3	1.62E-2	1.96E-2	1.15E-2	1.25E-2	2.42E-2	2.09E-2

* Corrected for accidentally broken particle. This generates a value of zero in some instances.

Table 59. Relative error in the Compact 5-3 concentrations given in Table 58.

Concentration Error	Ag-110m	Ce-144	Cs-134	Cs-137	Eu-154	Eu-155	Ru-106	Sb-125	Sr-90	U-238
1	N/A	38%	38%	38%	38%	38%	46%	40%	38%	38%
2	N/A	43%	34%	34%	38%	N/A	N/A	N/A	34%	35%
3	N/A	9%	9%	9%	9%	9%	19%	11%	9%	10%
Core	N/A	5%	5%	5%	5%	5%	5%	5%	5%	6%

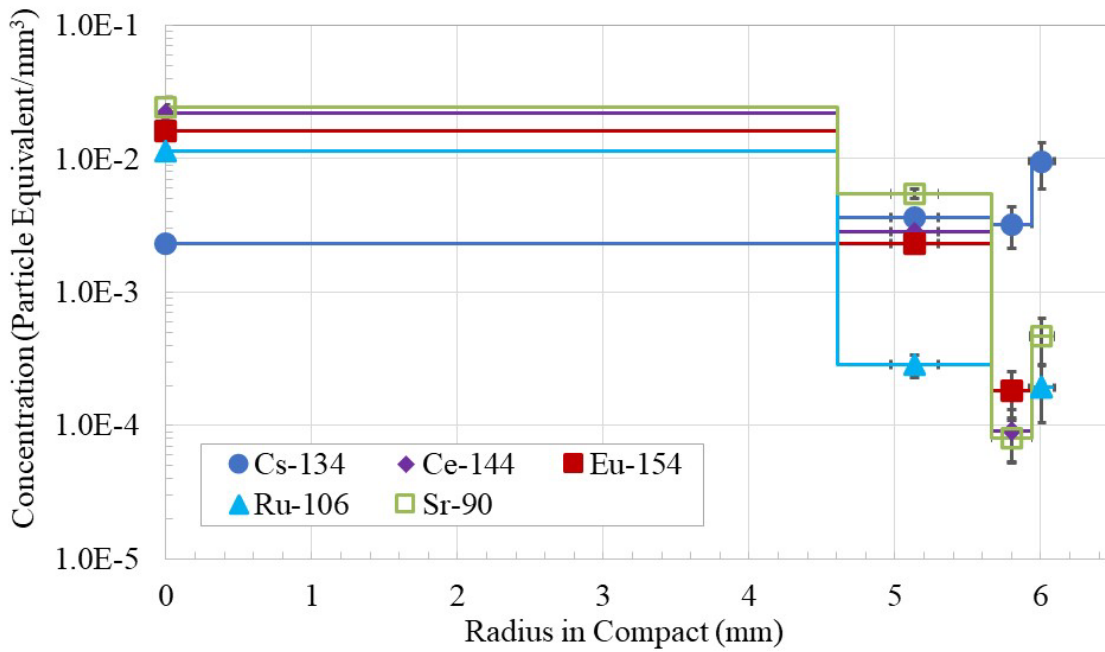


Figure 23. Compact 5-3 fission-product radial-concentration profiles in units of particle equivalents/mm³.

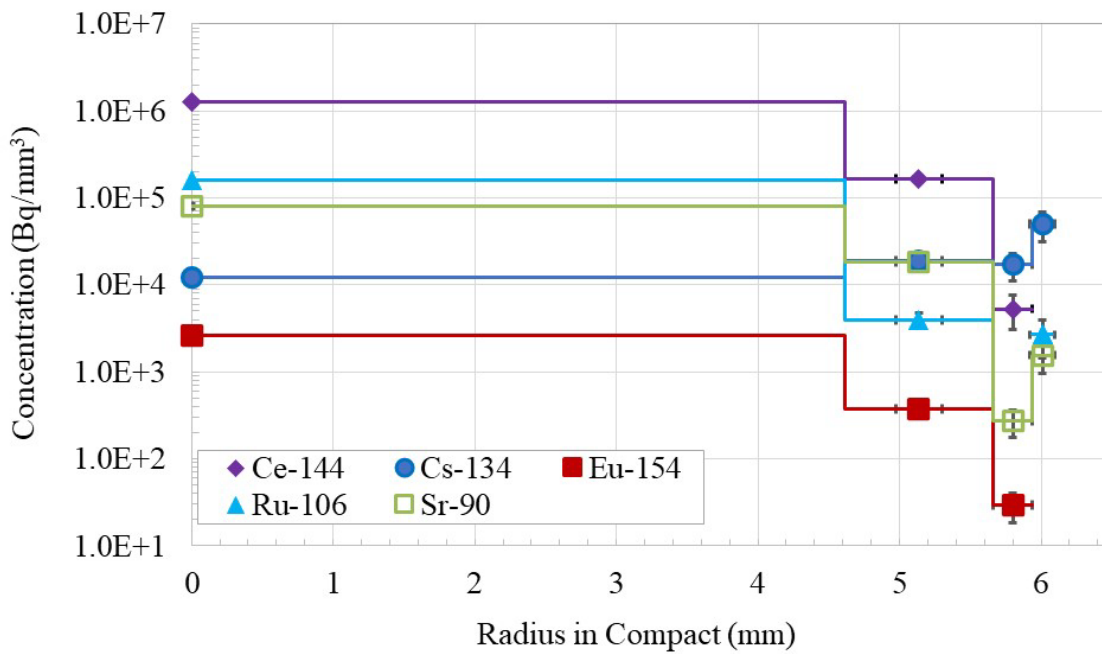


Figure 24. Compact 5-3 fission-product radial-concentration profiles in units of Bq/mm³.

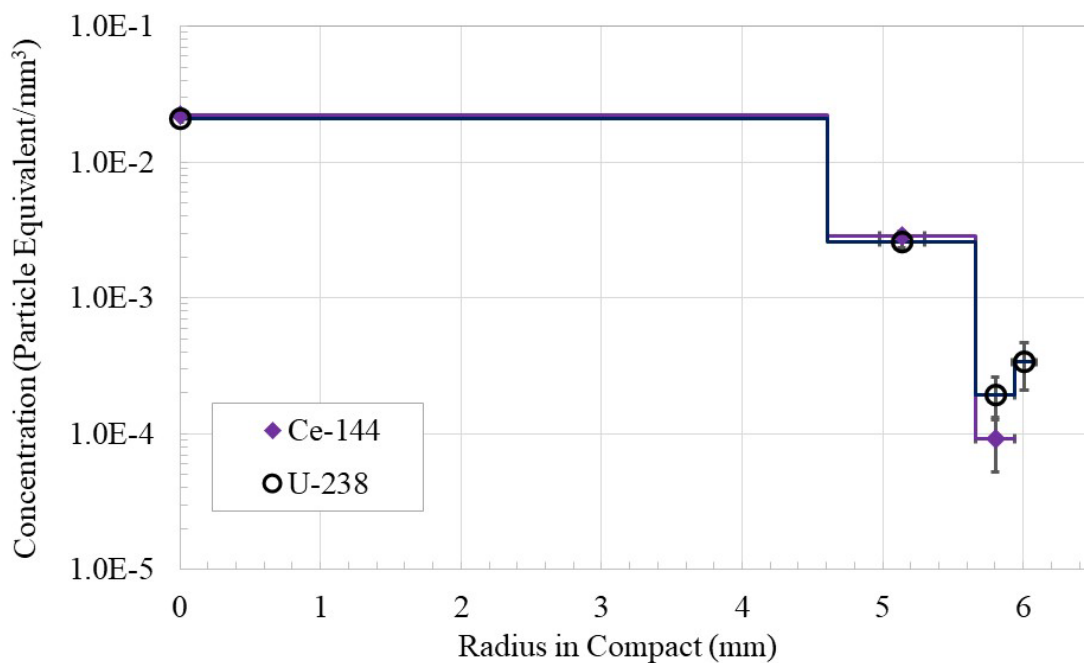


Figure 25. Comparison of Ce-144 and U-238 radial-concentration profiles for Compact 5-3.

5.3 Compact 5-4 Radial Fission-Product Profiles

The radial deconsolidation process for Compact 5-4 generated fission-product inventories for three radial segments and the core of the compact. The compact remained fixed to the deconsolidation rod for the duration of the radial deconsolidation, and there were no indications of in-pile TRISO particle failure or accidental particle damage at any point of the RDLBL. The volumes of each segment and the inner (if applicable) and outer radii of each segment were summarized in Table 17. The inventories of fission products and key actinides in each segment were given in Table 31 and Table 33, respectively. Table 60 gives the concentrations for select fission products and U-238 within each segment of the compact computed by dividing the values in Table 31 and Table 33 by the volumes in Table 17. Table 61 gives the relative error on the concentration by accounting for the measurement error on the compact's dimensions and the measurement error of the analytes.

Figure 26 and Figure 27 give the radial concentration profiles for selected fission products in Compact 5-4 in units of particle equivalents/mm³ and Bq/mm³, respectively. Only Cs, Sr, and actinides were above the detection limits in Segment 1. The units in Figure 26 allow for a comparison of the relative amounts of different isotopes that are present within the four different volumes of Compact 5-4. Most of the selected fission products, as well as U-238, decrease with increasing radius. The exception is Cs-134, which has higher a concentration in Segment 1 than in Segments 2 or 3. The Cs-134 concentration in Segment 1 (near the surface) is about the same as it is in the core. Figure 28 shows the concentration profiles for Ce-144 and U-238, which are similar, and decrease with increasing radius.

Table 60. Radial fission-product and U-238 concentrations expressed in several units for each segment of Compact 5-4.

Units	Segment	Ag-110m	Ce-144	Cs-134	Cs-137	Eu-154	Eu-155	Ru-106	Sb-125	Sr-90	U-238
Bq/mm ³	1	N/A	N/A	2.32E+4	2.60E+4	N/A	N/A	N/A	N/A	2.05E+2	N/A
	2	N/A	7.53E+3	8.48E+3	9.86E+3	1.69E+1	1.52E+1	1.55E+3	N/A	2.81E+2	
	3	N/A	1.93E+4	1.03E+4	1.21E+4	6.09E+1	4.08E+1	1.56E+3	7.75E+1	7.28E+2	
	core	N/A	1.61E+6	2.25E+4	2.86E+4	3.74E+3	2.54E+3	2.15E+5	4.32E+3	1.08E+5	
Fraction/mm ³	1	N/A	N/A	2.30E-6	3.46E-6	N/A	N/A	N/A	N/A	3.20E-8	9.52E-8
	2	N/A	6.76E-8	8.41E-7	1.31E-6	5.38E-8	7.38E-8	5.72E-8	N/A	4.38E-8	1.50E-7
	3	N/A	1.73E-7	1.02E-6	1.60E-6	1.94E-7	1.98E-7	5.77E-8	1.29E-7	1.14E-7	1.96E-7
	core	N/A	1.44E-5	2.23E-6	3.81E-6	1.19E-5	1.23E-5	7.93E-6	7.17E-6	1.69E-5	1.37E-5
Particle Equivalents /mm ³	1	N/A	N/A	4.41E-3	6.63E-3	N/A	N/A	N/A	N/A	6.14E-5	1.83E-4
	2	N/A	1.30E-4	1.61E-3	2.51E-3	1.03E-4	1.42E-4	1.10E-4	N/A	8.39E-5	2.88E-4
	3	N/A	3.31E-4	1.96E-3	3.07E-3	3.72E-4	3.80E-4	1.11E-4	2.47E-4	2.18E-4	3.77E-4
	core	N/A	2.76E-2	4.27E-3	7.30E-3	2.29E-2	2.37E-2	1.52E-2	1.38E-2	3.23E-2	2.63E-2

Table 61. Relative error in the Compact 5-4 concentrations given in Table 60.

	Ag-110m	Ce-144	Cs-134	Cs-137	Eu-154	Eu-155	Ru-106	Sb-125	Sr-90	U-238
1	N/A	N/A	33%	33%	N/A	N/A	N/A	N/A	33%	33%
2	N/A	19%	18%	18%	19%	22%	26%	N/A	18%	18%
3	N/A	9%	8%	8%	8%	16%	26%	10%	8%	9%
Core	N/A	6%	6%	6%	6%	6%	6%	6%	6%	7%

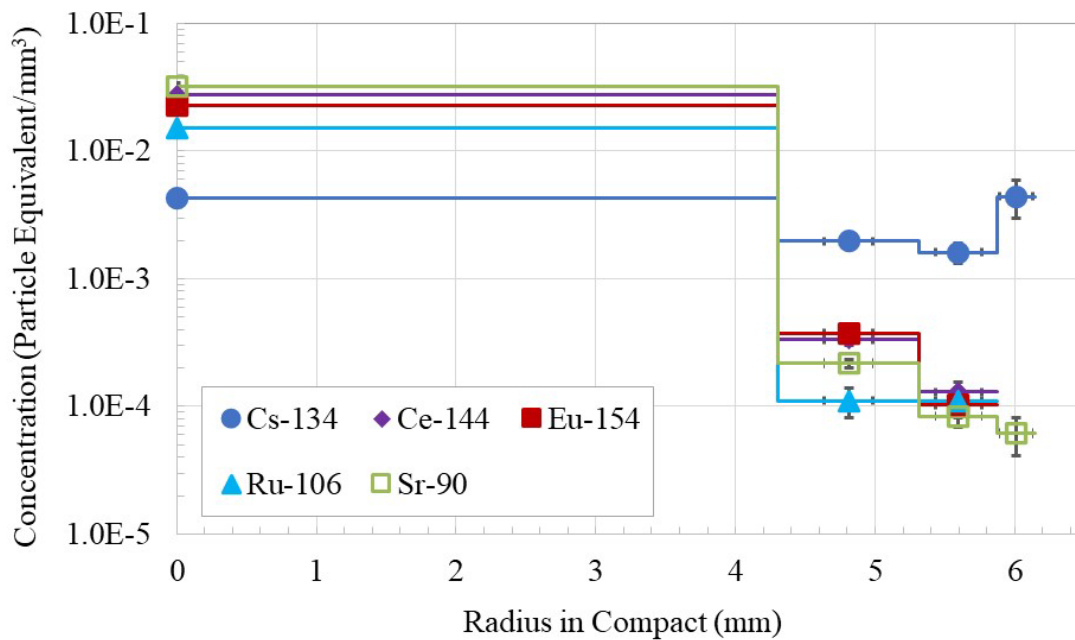


Figure 26. Compact 5-4 fission-product radial-concentration profiles in units of particle equivalents/mm³.

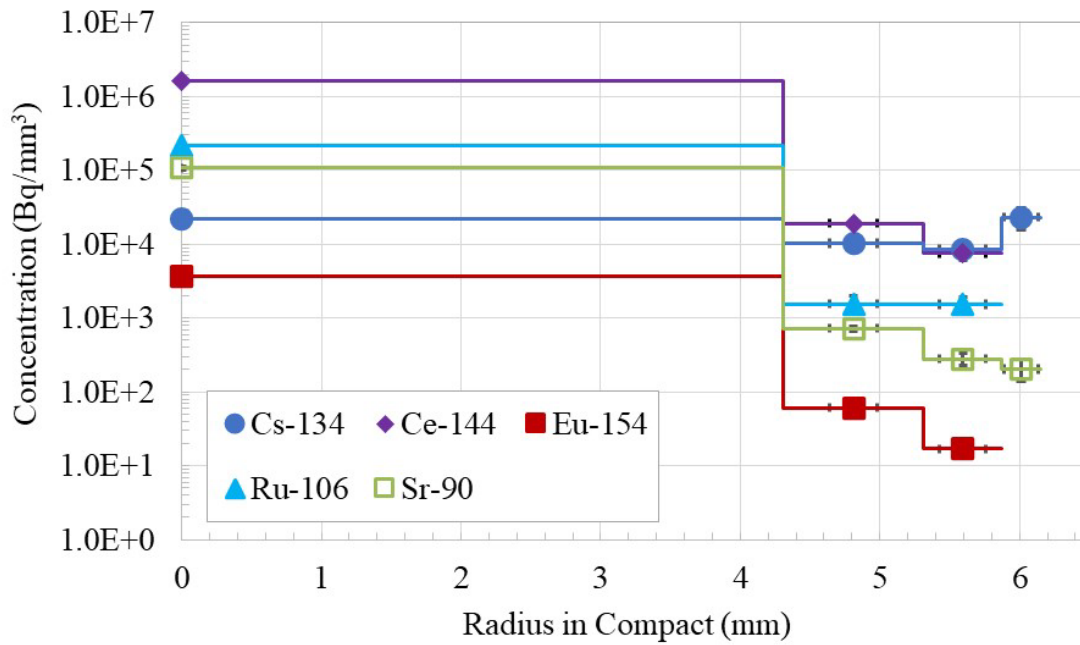


Figure 27. Compact 5-4 fission-product radial-concentration profiles in units of Bq/mm³.

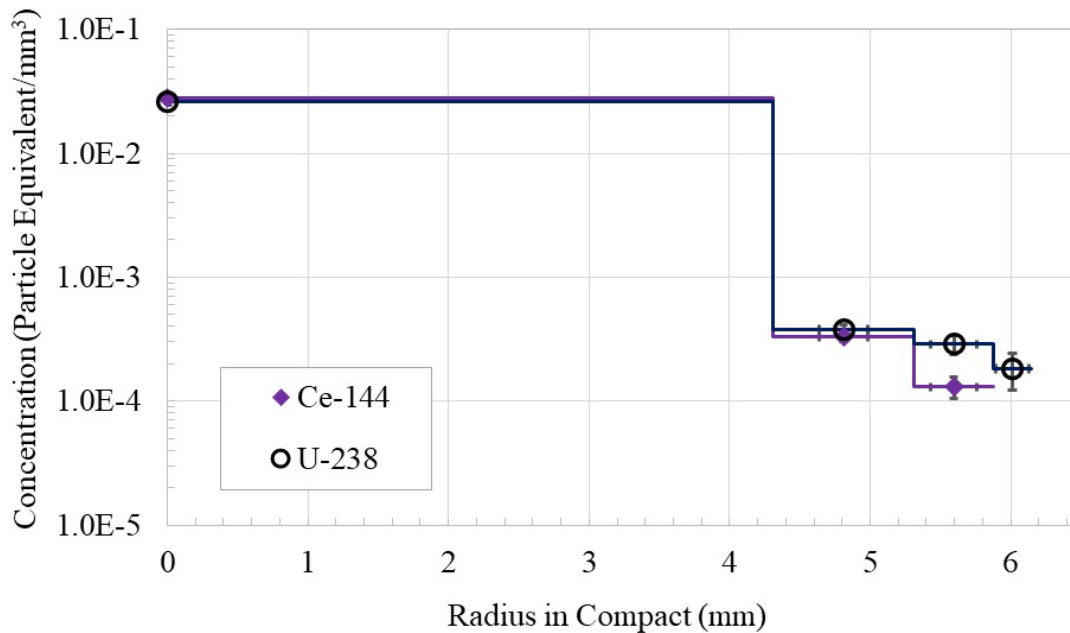


Figure 28. Comparison of Ce-144 and U-238 radial-concentration profiles for Compact 5-4.

5.4 Compact 7-3 Radial Fission-Product Profiles

The radial deconsolidation process for Compact 7-3 generated fission-product inventories for two radial segments and the core of the compact. The dimensions from the radial deconsolidation were given in Table 18.

The inventories of fission products and actinides were given in Table 35 and Table 37, respectively. Table 62 gives the concentrations for select fission products and U-238 within each segment of the compact, including uncorrected and corrected values, the latter of which account for one damaged particle in Segment 1 post-burn leach 2. Table 64 gives the error on the concentration by accounting for the measurement error on the compact’s dimensions and the measurement error of the fission-product activity and U-238 mass.

Figure 29 and Figure 30 give the radial-concentration profiles for selected fission products in Compact 7-3 in units of particle equivalents/mm³ and Bq/mm³, respectively. Figure 31 shows the concentration profiles for Ce-144 and U-238. The Cs-134 concentration decreases with increasing radius. Both Ce-144 and Cs-134 decrease sharply from the core to Segment 2, but the Ce-144 concentration increases again at the outermost segment (Segment 1). The Eu-154 and Sr-90 concentrations are similar and do not vary much from the core to the surface. However, the Eu-154 trend shows a small increase in concentration with increasing radius, and the Sr-90 concentration, after a small decrease from the Core to Segment 2, increases slightly in Segment 1. The Ru-106 nuclide was not detected in Segment 2, but its Segment 1 concentration is several orders of magnitude less than in the core. There is an increase in concentration from Segment 2 to Segment 1 for Eu, Sr, and Ce shown in Figure 12. The U-238 concentration at the outer layer (Segment 1) does not follow this increasing trend, which indicates there was no failure or damage to the driver particles prior to the start of the deconsolidation. Because Capsule 7 had the highest irradiation temperatures, the increased concentration of some nuclides at the outer segment (Segment 1) may be related to fission-product diffusion inside the compact from the high irradiation temperature.

Other hypotheses could explain why concentrations might go up at the compact surface. These include trapping at features or microstructures unique to the compact surface that may have been a consequence of the fabrication process or how those features evolved with irradiation. It is possible that very thin first segments are susceptible to a possible artifact of the RDLBL process. This artifact might conceivably arise if material had been removed but the compact was still experiencing the early “flaking” phase of the deconsolidation where the compact appears to increase in diameter even as material is being deconsolidated (Helmreich 2015, Stempien 2017). In that case, the volume of material removed may be underestimated, and the inventory in Segment 1 is then normalized by a smaller volume than it should be.

Table 62. Radial fission product and U-238 concentrations expressed in several units for Compact 7-3.

Units	Segment	Ag-110m	Ce-144	Cs-134	Cs-137	Eu-154	Eu-155	Ru-106	Sb-125	Sr-90	U-238
Bq/mm ³	1	N/A	2.17E+5	8.21E+3	7.18E+3	7.69E+3	4.94E+3	3.45E+4	9.31E+2	1.06E+5	N/A
	1*	N/A	7.39E+4	4.92E+2	8.27E+2	7.43E+3	4.76E+3	8.15E+2	4.24E+2	9.77E+4	
	2	N/A	4.10E+4	3.85E+3	3.41E+3	6.60E+3	4.19E+3	N/A	N/A	8.30E+4	
	Core	N/A	1.94E+6	3.18E+4	4.12E+4	5.26E+3	3.70E+3	3.86E+5	1.30E+3	1.35E+5	
Fraction/mm ³	1	N/A	1.94E-6	8.07E-7	9.51E-7	2.47E-5	2.40E-5	5.72E-9	1.55E-6	1.64E-5	1.45E-6
	1*	N/A	6.61E-7	4.84E-8	1.10E-7	2.39E-5	2.31E-5	5.72E-9	7.06E-7	1.52E-5	1.72E-7
	2	N/A	3.67E-7	3.79E-7	4.51E-7	2.12E-5	2.04E-5	N/A	N/A	1.29E-5	1.84E-7
	Core	N/A	1.74E-5	3.12E-6	5.46E-6	1.69E-5	1.80E-5	1.44E-5	2.17E-6	2.09E-5	1.72E-5
Particle Equivalents/mm ³	1	N/A	3.72E-3	1.55E-3	1.82E-3	4.75E-2	4.61E-2	2.47E-3	2.97E-3	3.15E-2	2.79E-3
	1*	N/A	1.27E-3	9.28E-5	2.10E-4	4.58E-2	4.44E-2	1.10E-5	1.35E-3	2.91E-2	3.30E-4
	2	N/A	7.03E-4	7.27E-4	8.66E-4	4.07E-2	3.91E-2	N/A	N/A	2.47E-2	3.53E-4
	Core	N/A	3.33E-2	5.99E-3	1.05E-2	3.24E-2	3.45E-2	2.76E-2	4.15E-3	4.02E-2	3.31E-2

* Corrected for accidental damage of one TRISO particle in the Segment 1 post-burn leach 2.

Table 63. Error for the Compact 7-3 fission product concentrations given in Table 62.

Concentration Error	Ag-110m	Ce-144	Cs-134	Cs-137	Eu-154	Eu-155	Ru-106	Sb-125	Sr-90	U-238
---------------------	---------	--------	--------	--------	--------	--------	--------	--------	-------	-------

1	N/A	13%	7%	7%	7%	8%	13%	23%	7%	8%
2	N/A	28%	8%	8%	8%	8%	N/A	N/A	8%	9%
Core	N/A	10%	7%	7%	7%	8%	8%	14%	7%	4%

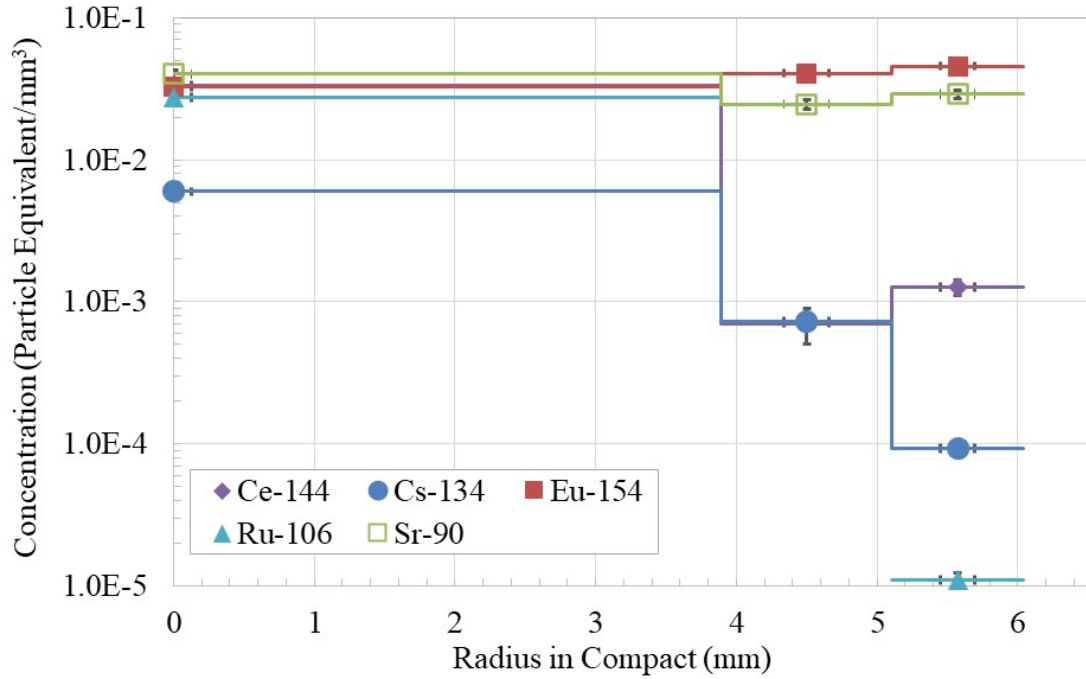


Figure 29. Compact 7-3 fission-product radial-concentration profiles in units of particle equivalents/mm³.

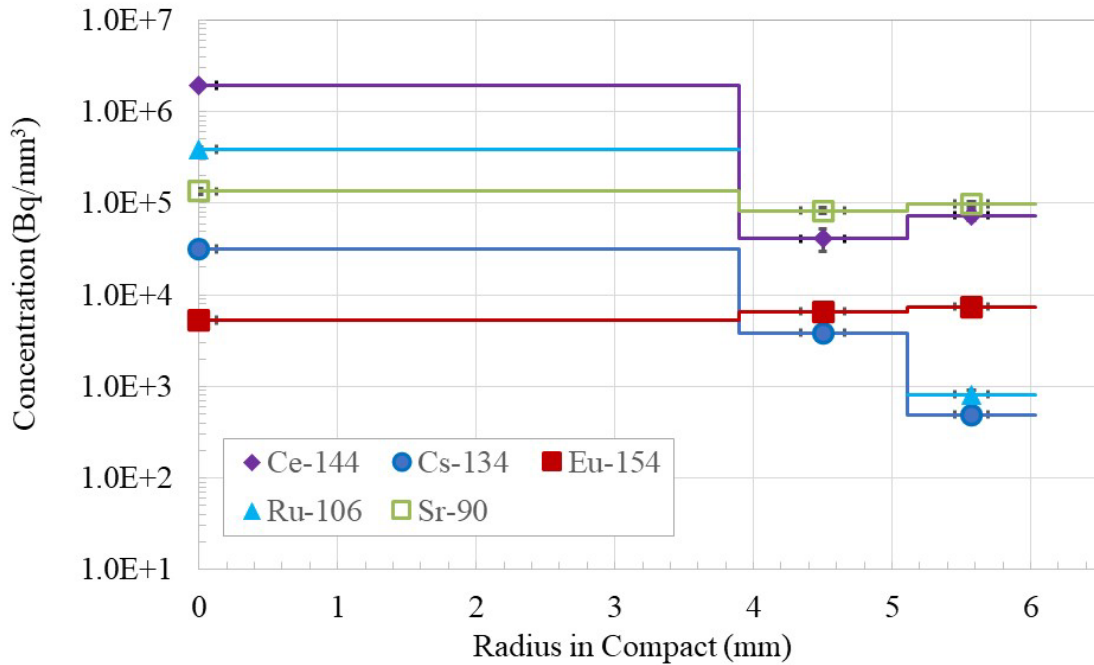


Figure 30. Compact 7-3 fission-product radial-concentration profiles in units of Bq/mm³.

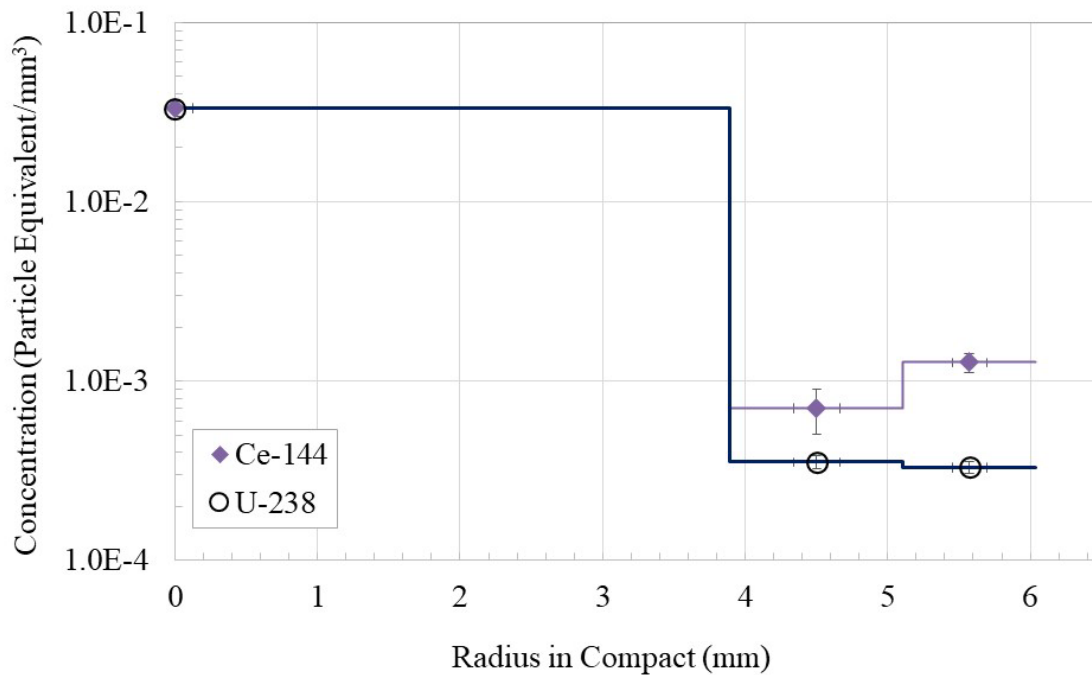


Figure 31. Comparison of U-238 and Ce-144 radial-concentration profiles in Compact 7-3.

5.5 Compact 8-3 Radial Fission Product Profiles

The radial deconsolidation process for Compact 8-3 generated two radial segments and a central core. Fines and particles were collected from the first segment; therefore, material was indeed removed during the first segment of the radial deconsolidation. However, the image analysis revealed that the compact radius after the first segment was statistically the same as that of the compact prior to the start of radial deconsolidation (see Table 19). Because a distinct physical volume could not be established for the first segment, the fission-product and actinide inventories measured in the solutions from the first and second segments (see Table 39 and Table 41, respectively) were added together. These sums were then normalized by the volume difference between the start of the RDLBL and the end of the second segment to give the fission-product concentration.

Table 64 gives the concentrations for select fission products and U-238 within each segment of the compact. There was an indication that one TRISO-coated driver particle was damaged during the second pre-burn leach step of Segment 2, and Table 64 presents values both uncorrected and corrected for that accidental damage. Table 65 gives the error on the concentration by accounting for the measurement error on the compact's dimensions and the measurement error of the fission-product activity and U-238 mass.

Figure 32 and Figure 33 give the radial concentration profiles for selected fission products in Compact 8-3 in units of particle equivalents/mm³ and Bq/mm³, respectively. The concentrations of Cs-134 are higher outside the core. The Eu-154, and Sr-90 concentrations are slightly higher outside of the core, and concentrations of Ce-144 and Ru-106 are highest in the core. Figure 34 shows the concentration profiles for Ce-144 and U-238, which are closely matched.

Table 64. Radial fission product and U-238 concentrations for Compact 8-3.

Units	Segment	Ag-110m	Ce-144	Cs-134	Cs-137	Eu-154	Eu-155	Ru-106	Sb-125	Sr-90	U-238
Bq/ mm ³	1+2	N/A	5.70E+5	3.01E+4	2.71E+4	6.95E+3	4.60E+3	1.27E+5	1.28E+3	1.61E+5	N/A
	1+2*	N/A	2.25E+5	1.17E+4	1.15E+4	6.35E+3	4.18E+3	1.27E+5	3.08E+2	1.41E+5	
	Core	N/A	9.29E+5	4.28E+3	1.04E+4	5.85E+3	3.85E+3	1.51E+5	1.04E+3	1.03E+5	
Fraction/ mm ³	1+2	N/A	5.25E-6	3.20E-6	3.71E-6	2.37E-5	2.36E-5	5.01E-6	2.21E-6	2.57E-5	1.14E-6
	1+2*	N/A	2.07E-6	1.24E-6	1.58E-6	2.16E-5	2.15E-5	1.84E-6	5.33E-7	2.26E-5	5.23E-7
	Core	N/A	8.54E-6	4.55E-7	1.42E-6	1.99E-5	1.98E-5	5.97E-6	1.81E-6	1.65E-5	3.95E-7
Particle Equivalents /mm ³	1+2	N/A	1.01E-2	6.13E-3	7.09E-3	4.54E-2	4.53E-2	9.62E-3	4.25E-3	4.93E-2	2.18E-3
	1+2*	N/A	3.97E-3	2.37E-3	3.01E-3	4.15E-2	4.12E-2	3.52E-3	1.02E-3	4.32E-2	1.00E-3
	Core	N/A	1.64E-2	8.73E-4	2.73E-3	3.82E-2	3.79E-2	1.15E-2	3.46E-3	3.16E-2	7.57E-4

* Corrected for accidental particle damage during the second pre-burn leach step of Segment 2.

Table 65. Uncertainty for the Compact 8-3 fission product and U-238 concentrations given in Table 64.

Concentration Error	Ag-110m	Ce-144	Cs-134	Cs-137	Eu-154	Eu-155	Ru-106	Sb-125	Sr-90	U-238
Segments 1+2	N/A	33%	21%	20%	20%	21%	23%	29%	20%	21%
Core	N/A	5%	3%	3%	4%	4%	4%	5%	3%	4%

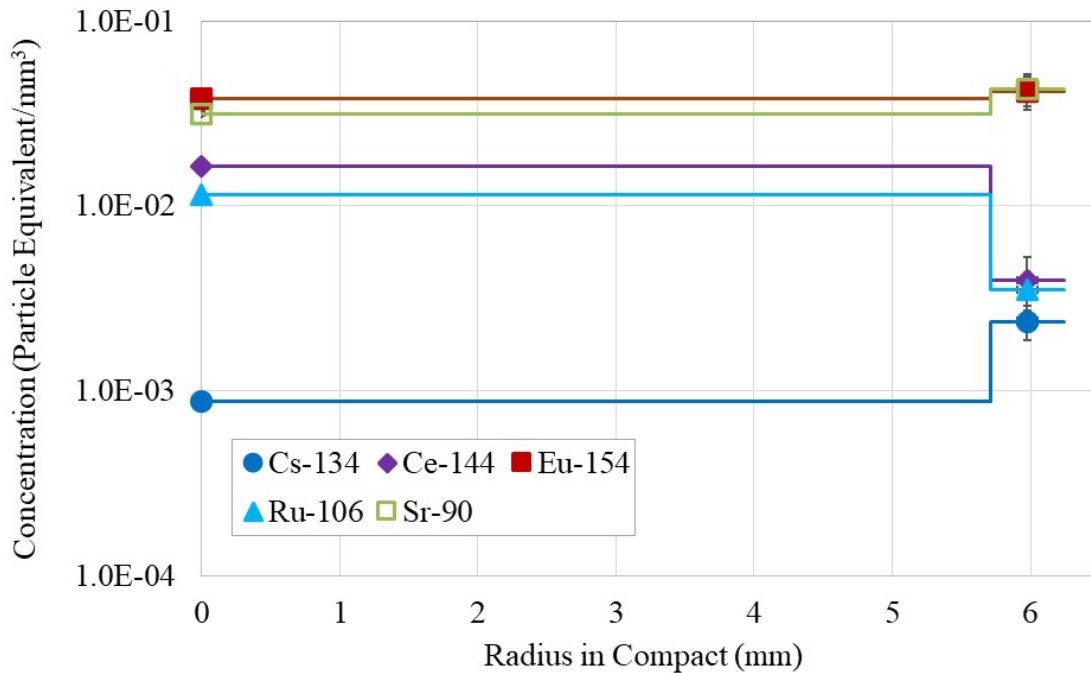


Figure 32. Compact 8-3 fission-product radial-concentration profiles in units of particle equivalent/mm³.

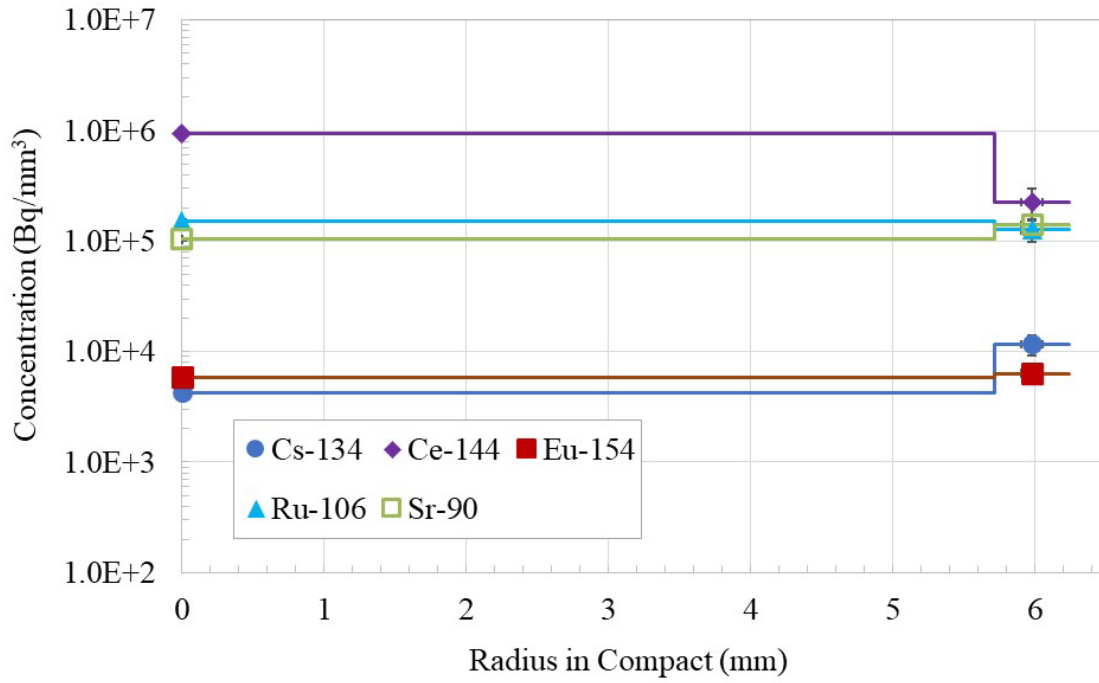


Figure 33. Compact 8-3 fission-product radial-concentration profiles in units of Bq/mm³.

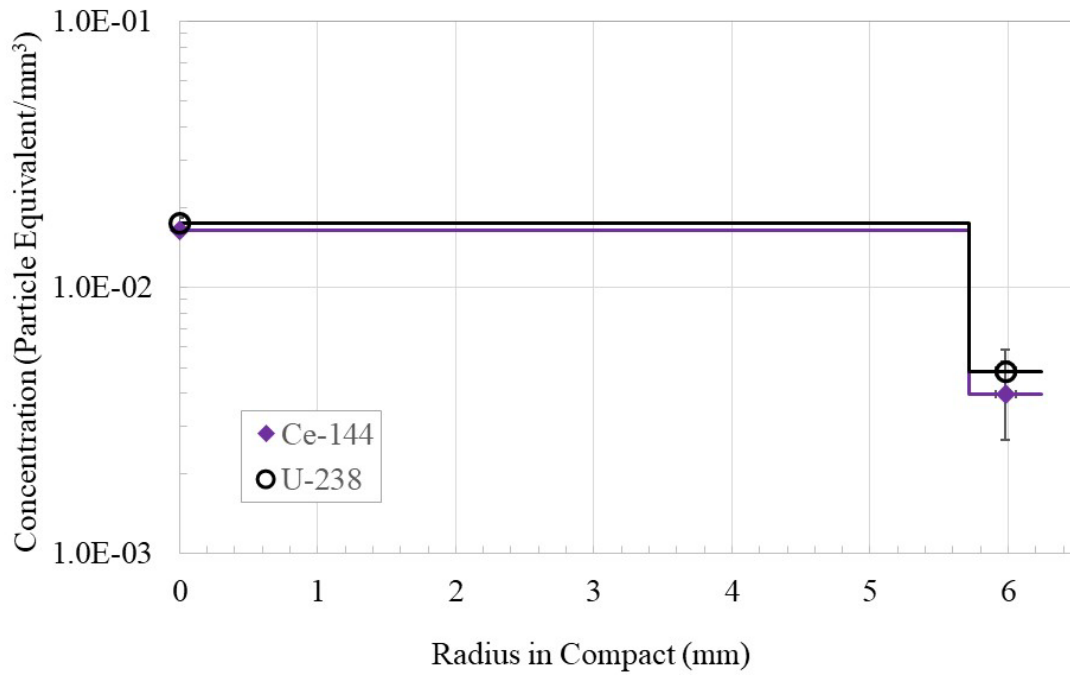


Figure 34. Comparison of U-238 and Ce-144 radial-concentration profiles in Compact 8-3.

5.6 Compact 10-3 Radial Fission-Product Profiles

The radial deconsolidation process for Compact 10-3 generated fission-product inventories for three radial segments and the core of the compact. However, the diameter reduction from the radial deconsolidation of Segment 1 was only 0.076 ± 0.11 mm. Because a distinct physical volume could not be established for Segment 1, the fission-product and actinide inventories measured in the solutions from the first and second segments (see Table 43 and Table 45, respectively) were added together. These sums were then normalized by the volume difference between the start of the RDLBL and the end of the second segment to give the fission-product and actinide concentrations. Table 66 gives the concentrations for select fission products and U-238 within each segment of the compact. Table 67 gives the error on the concentration by accounting for the measurement error on the compact's dimensions and the measurement error of the fission-product activity and U-238 mass. Figure 35 and Figure 36 give the radial-concentration profiles for selected fission products in Compact 10-3 in units of Bq/mm^3 and particle equivalent/ mm^3 , respectively. Figure 37 compares the concentration profiles of Ce-144 and U-238. As discussed in Section 4.6, somewhere between 11 and 19 particles were accidentally damaged during the RDLBL of Compact 10-3, and meaningful corrections could not be made. However, a correction for Segment 3 could be attempted for comparisons to models or to other Capsule 10 compacts (see Section 4.6.3). In the present section, the concentrations were not corrected, and all are elevated compared to what would be expected if there were no accidental damage. The results from the combination of Segments 1 and 2 show that there were at least 11 damaged particles. These results from Compact 10-3 may have only limited usefulness as a result.

Table 66. Radial fission-product and U-238 concentrations for each segment of Compact 10-3. Not corrected for accidental particle damage.

Units	Segment	Ag-110m	Ce-144	Cs-134	Cs-137	Eu-154	Eu-155	Ru-106	Sb-125	Sr-90	U-238
Bq/mm^3	1+2	N/A	9.73E+5	5.34E+4	7.25E+4	3.08E+3	2.49E+3	1.71E+5	2.35E+3	1.30E+5	N/A
	3	N/A	2.93E+5	6.70E+3	1.20E+4	5.15E+2	4.39E+2	4.63E+4	9.09E+2	2.87E+4	
	Core	N/A	7.24E+5	4.92E+3	1.17E+4	1.06E+3	9.08E+2	1.06E+5	1.31E+3	2.66E+4	
Fraction/ mm^3	1+2	N/A	1.08E-5	9.12E-6	1.23E-5	1.60E-5	1.88E-5	9.68E-6	5.23E-6	2.50E-5	1.49E-5
	3	N/A	3.24E-6	1.15E-6	2.04E-6	2.68E-6	3.30E-6	2.63E-6	2.03E-6	5.52E-6	4.74E-6
	Core	N/A	8.00E-6	8.41E-7	1.98E-6	5.54E-6	6.83E-6	6.02E-6	2.91E-6	5.13E-6	1.09E-5
Particle Equivalent/ mm^3	1+2	N/A	2.06E-2	1.75E-2	2.36E-2	3.08E-2	3.60E-2	1.86E-2	1.00E-2	4.80E-2	2.86E-2
	3	N/A	6.22E-3	2.20E-3	3.92E-3	5.15E-3	6.33E-3	5.04E-3	3.89E-3	1.06E-2	9.10E-3
	Core	N/A	1.54E-2	1.61E-3	3.80E-3	1.06E-2	1.31E-2	1.15E-2	5.59E-3	9.84E-3	2.09E-2

Table 67. Error in the Compact 10-3 radial fission-product concentrations given in Table 66.

Concentration Error	Ag-110m	Ce-144	Cs-134	Cs-137	Eu-154	Eu-155	Ru-106	Sb-125	Sr-90	U-238
1+2	N/A	52%	50%	50%	50%	51%	51%	51%	50%	45%
3	N/A	38%	36%	36%	36%	37%	37%	36%	36%	32%
Core	N/A	4%	2%	2%	3%	3%	3%	3%	2%	4%

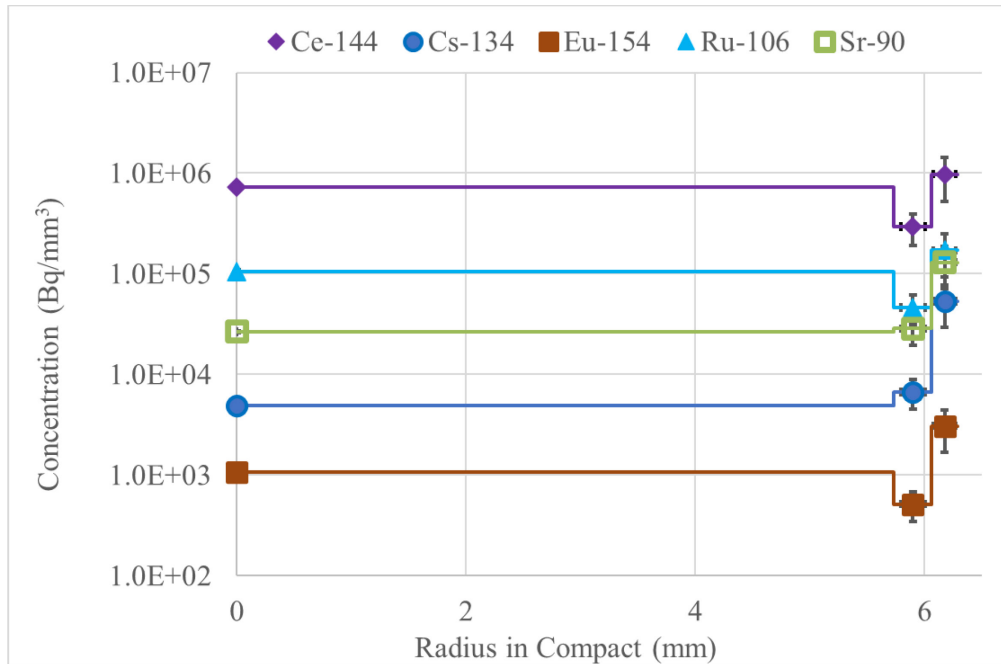


Figure 35. Radial concentrations of fission products in Compact 10-3 (uncorrected for particles accidentally broken) in units of Bq/mm³.

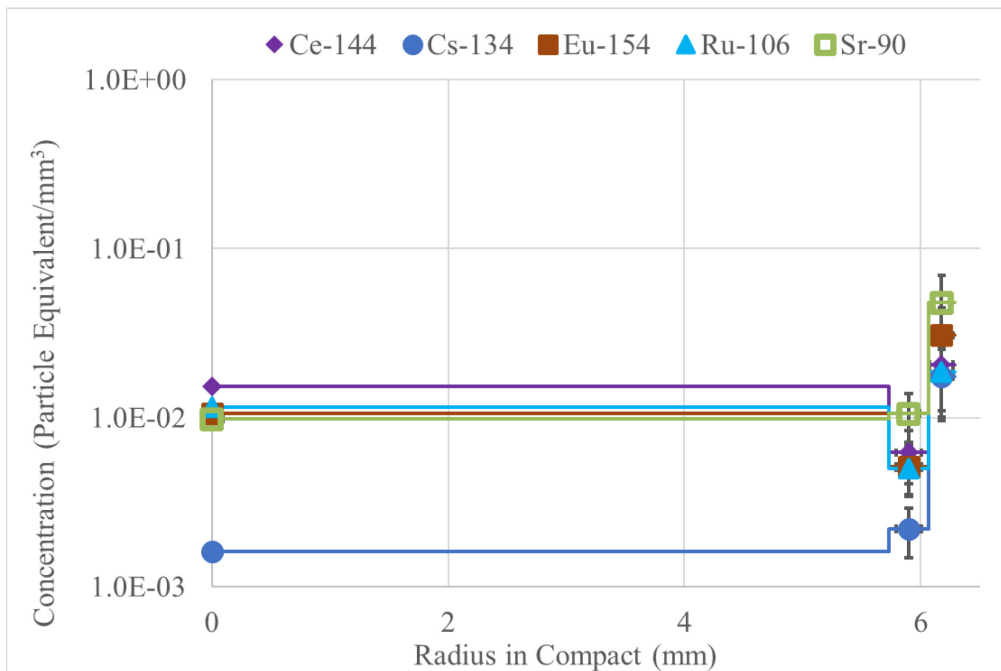


Figure 36. Radial concentrations of fission products in Compact 10-3 (uncorrected for particles accidentally broken) in units of particle equivalents/mm³.

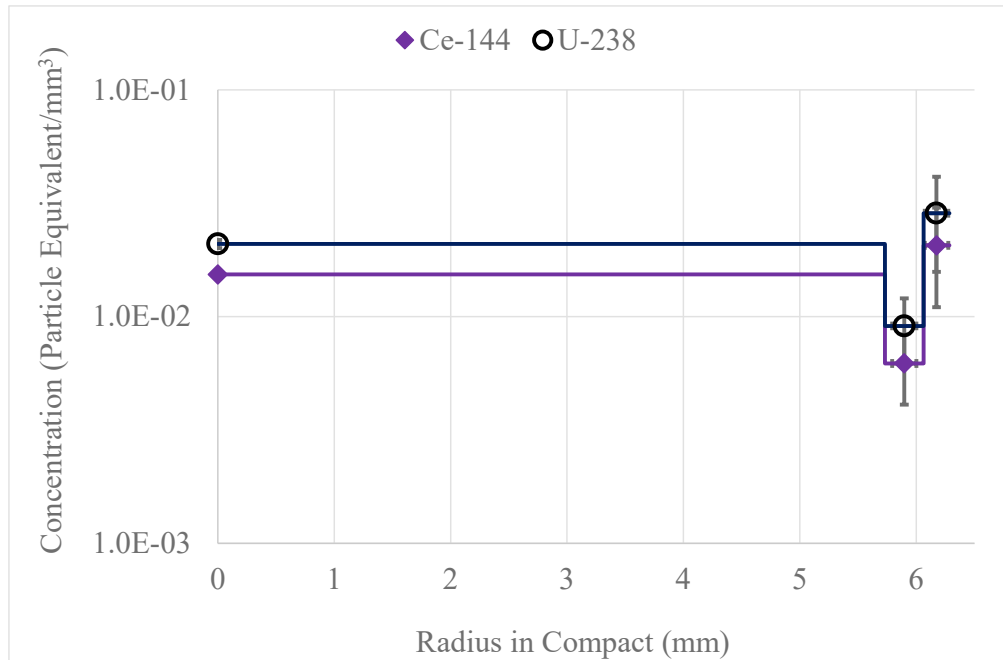


Figure 37. Comparison of Ce-144 and U-238 radial-concentration profiles (uncorrected for particles accidentally broken) in Compact 10-3.

5.7 Compact 12-1 Radial Fission-Product Profiles

The radial-deconsolidation process for Compact 12-1 generated fission-product inventories for three radial segments and the core of the compact. Table 68 gives concentrations for select fission products and uranium within each segment of the compact, including both uncorrected and corrected values, which account for damaged driver particles as discussed in Section 4.7.3. (In this particular compact, the uranium isotopics were not determined. Only the total amount of the uranium element was determined.) Table 69 gives the error on the concentration by accounting for the measurement error on the compact's dimensions (Table 21) and the measurement error of the fission product and uranium inventories (Table 48 and Table 50). Figure 38 and Figure 39 give the radial concentration profiles for selected fission products in Compact 12-1 in units of particle equivalent/mm³ and Bq/mm³, respectively. Figure 40 compares the concentration profiles of Ce-144 and total uranium.

The corrections applied involve subtracting two particle equivalents from what was measured in the deconsolidation solution of Segment 1, and one particle-equivalent from the deconsolidation and first post-burn leach of Segment 2. One particle equivalent was subtracted from the Segment 3 values based on the apparent failure of a single particle during the Segment 3 deconsolidation.

Table 68. Radial fission-product and uranium concentrations for each segment of Compact 12-1.

Units	Segment	Ag-110m	Ce-144	Cs-134	Cs-137	Eu-154	Eu-155	Ru-106	Sb-125	Sr-90	Total U
Bq /mm ³	1	N/A	3.46E+5	7.54E+3	3.00E+4	2.75E+2	3.62E+2	7.68E+3	N/A	1.87E+4	N/A
	1*	N/A	5.72E+4	1.62E+2	1.23E+4	2.89E+1	6.75E+1	2.76E+3	N/A	2.33E+3	
	2	N/A	1.16E+6	2.31E+4	8.53E+4	8.64E+2	1.05E+3	5.68E+4	1.14E+3	6.71E+4	
	2*	N/A	2.17E+5	1.54E+3	2.78E+4	2.32E+1	1.03E+2	4.75E+3	0	1.37E+4	
	3	N/A	1.27E+5	2.35E+3	9.00E+3	1.10E+2	1.22E+2	3.42E+3	N/A	8.11E+3	
	3*	N/A	6.33E+4	6.47E+2	5.08E+3	5.28E+1	5.73E+1	1.22E+3	N/A	4.47E+3	
	Core	N/A	4.49E+5	5.30E+3	1.97E+4	3.27E+2	3.75E+2	5.15E+4	1.54E+3	1.93E+4	
Fraction /mm ³	1	N/A	7.24E-6	5.93E-6	1.02E-5	6.38E-6	7.43E-6	1.25E-6	N/A	6.90E-6	6.30E-6
	1*	N/A	1.20E-6	1.27E-7	4.20E-6	6.70E-7	1.39E-6	4.48E-7	N/A	8.58E-7	2.50E-7
	2	N/A	2.42E-5	1.82E-5	2.92E-5	2.00E-5	2.16E-5	9.23E-6	5.63E-6	2.47E-5	2.27E-5
	2*	N/A	4.53E-6	1.21E-6	9.49E-6	5.38E-7	2.12E-6	7.72E-7	0	5.03E-6	2.99E-6
	3	N/A	2.66E-6	1.85E-6	3.07E-6	2.56E-6	2.52E-6	5.55E-7	N/A	2.99E-6	1.56E-6
	3*	N/A	1.32E-6	5.10E-7	1.74E-6	1.23E-6	1.18E-6	1.98E-7	N/A	1.65E-6	2.18E-7
	Core	N/A	9.39E-6	4.17E-6	6.72E-6	7.58E-6	7.70E-6	8.36E-6	7.62E-6	7.10E-6	1.13E-5
Particle Equivalents /mm ³	1	N/A	1.39E-2	1.14E-2	1.96E-2	1.22E-2	1.43E-2	2.39E-3	N/A	1.32E-2	1.21E-2
	1*	N/A	2.29E-3	2.44E-4	8.05E-3	1.28E-3	2.66E-3	8.59E-4	N/A	1.64E-3	4.80E-4
	2	N/A	4.64E-2	3.48E-2	5.59E-2	3.84E-2	4.15E-2	1.77E-2	1.08E-2	4.74E-2	4.35E-2
	2*	N/A	8.69E-3	2.32E-3	1.82E-2	1.03E-3	4.06E-3	1.48E-3	0	9.65E-3	5.74E-3
	3	N/A	5.11E-3	3.55E-3	5.90E-3	4.92E-3	4.82E-3	1.07E-3	N/A	5.73E-3	2.99E-3
	3*	N/A	2.54E-3	9.77E-4	3.33E-3	2.35E-3	2.26E-3	3.79E-4	N/A	3.16E-3	4.19E-4
	Core	N/A	1.80E-2	8.00E-3	1.29E-2	1.45E-2	1.48E-2	1.60E-2	1.46E-2	1.36E-2	2.16E-2
* Corrected for TRISO particles accidentally damaged during DLBL.											

Table 69. Error in the Compact 12-1 radial fission-product and uranium concentrations given in Table 68.

Uncertainty of Concentrations	Ag-110m	Ce-144	Cs-134	Cs-137	Eu-154	Eu-155	Ru-106	Sb-125	Sr-90	Total U
1	N/A	20.7%	20.7%	20.7%	20.7%	21.3%	23.9%	N/A	20.6%	22.8%
2	N/A	102.7%	102.7%	102.7%	102.7%	102.9%	102.7%	103.0%	102.7%	102.8%
3	N/A	10.7%	10.3%	10.5%	10.3%	11.0%	10.9%	N/A	10.1%	21.1%
Core	N/A	4.6%	4.5%	4.5%	4.5%	4.8%	4.4%	4.3%	4.2%	9.2%

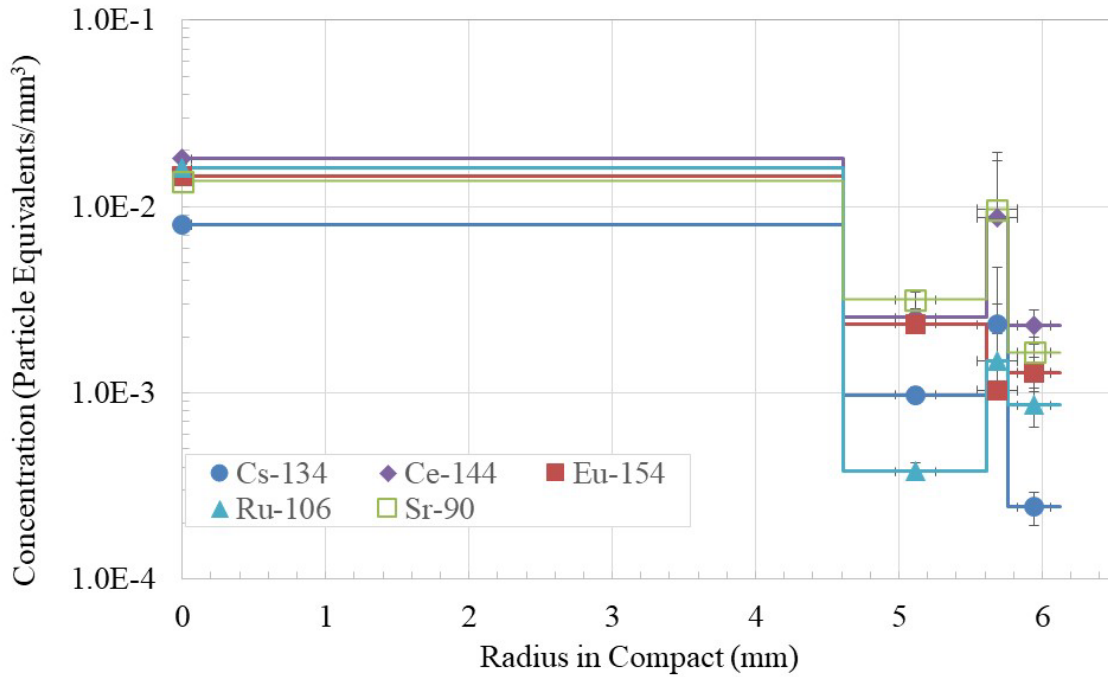


Figure 38. Radial concentrations of fission products in Compact 12-1 in units of particle equivalents/mm³. Note the lower bounds of error bars in Segment 2 are at zero and not shown in this log-normal plot.

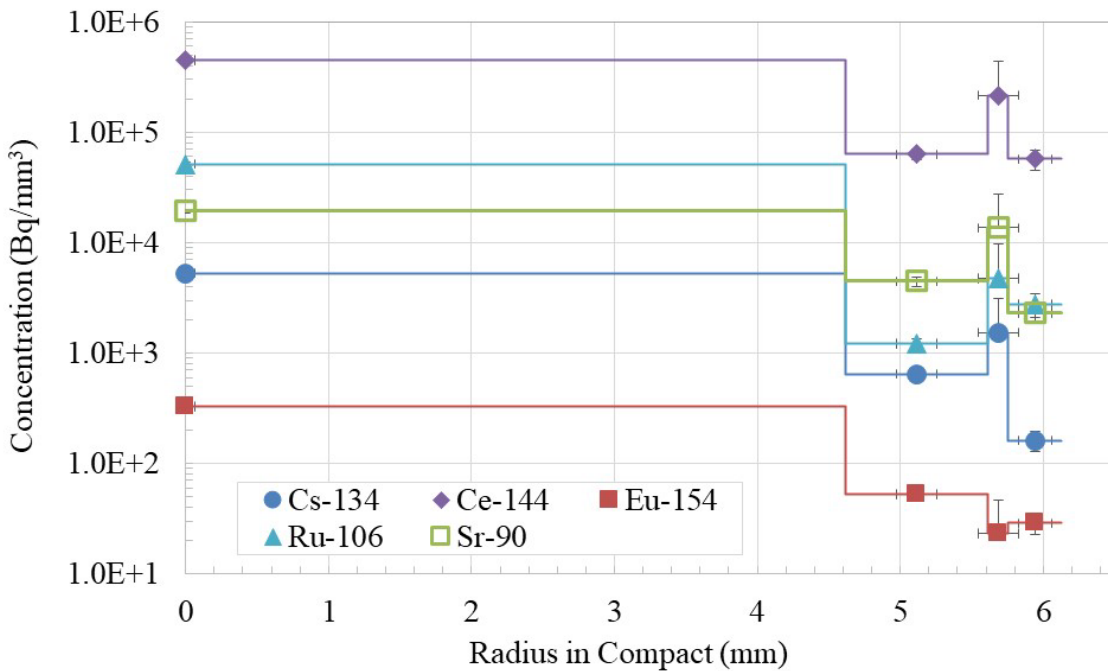


Figure 39. Radial concentrations of fission products in Compact 12-1 in units of Bq/mm³. Note the lower bounds of error bars in Segment 2 are at zero and not shown in this log-normal plot.

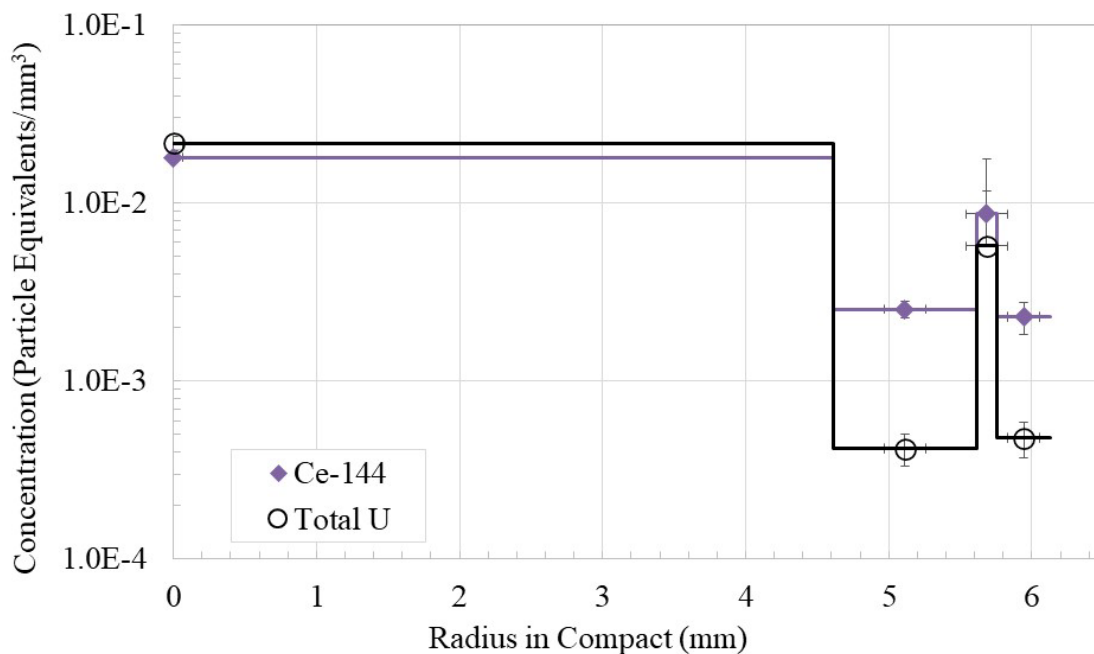


Figure 40. Comparison of Ce-144 and total-uranium radial-concentration profiles in Compact 12-1. Note the lower bounds of error bars in Segment 2 are at zero and not shown in the figure.

5.8 Compact 12-3 Radial Fission-Product Profiles

The radial-deconsolidation process for Compact 12-3 generated fission-product inventories for one radial segment and the core of the compact. Section 4.8 described the challenges encountered during the RDLBL of Compact 12-3; however, with no compelling evidence for accidental TRISO particle damage or contamination, no adjustments or corrections were made to the results. Table 70 gives the concentrations for select fission products and U-238 within each segment of the compact. Table 71 gives the error on the concentration by accounting for the measurement error on the compact’s dimensions (Table 22) and the measurement error of the fission-product and U-238 inventories (Table 53). Figure 41 and Figure 42 give the radial concentration profiles for selected fission products in Compact 12-3 in units of particle equivalent/mm³ and Bq/mm³, respectively. Figure 43 compares the concentration profiles of Ce-144 and U-238.

Table 70. Radial fission-product and U-238 concentrations for each segment of Compact 12-3.

Units	Segment	Ag-110m	Ce-144	Cs-134	Cs-137	Eu-154	Eu-155	Ru-106	Sb-125	Sr-90	U-238
Bq/ mm ³	1	N/A	N/A	1.01E+2	5.77E+2	4.22E+1	3.40E+1	N/A	N/A	1.26E+2	N/A
	Core	N/A	2.75E+5	4.26E+3	1.89E+4	1.79E+2	2.53E+2	1.20E+4	6.10E+2	1.82E+4	
Fraction/ mm ³	1	N/A	N/A	1.07E-7	2.23E-7	1.33E-6	8.04E-7	N/A	N/A	5.20E-8	5.82E-8
	Core	N/A	6.47E-6	4.51E-6	7.31E-6	5.65E-6	5.99E-6	2.42E-6	3.52E-6	7.51E-6	7.48E-6
Particle Equivalents/ mm ³	1	N/A	N/A	2.06E-4	4.28E-4	2.55E-3	1.54E-3	N/A	N/A	9.98E-5	1.12E-4
	Core	N/A	1.24E-2	8.64E-3	1.40E-2	1.08E-2	1.15E-2	4.64E-3	6.76E-3	1.44E-2	1.43E-2

Table 71. Uncertainties in the Compact 12-3 concentrations given in Table 70.

Concentration Error	Ag-110m	Ce-144	Cs-134	Cs-137	Eu-154	Eu-155	Ru-106	Sb-125	Sr-90	U-238
1	N/A	N/A	21.4%	21.4%	21.2%	22.9%	N/A	N/A	21.0%	22.4%
Core	N/A	3.1%	2.9%	2.9%	2.9%	3.7%	3.9%	3.3%	2.5%	3.8%

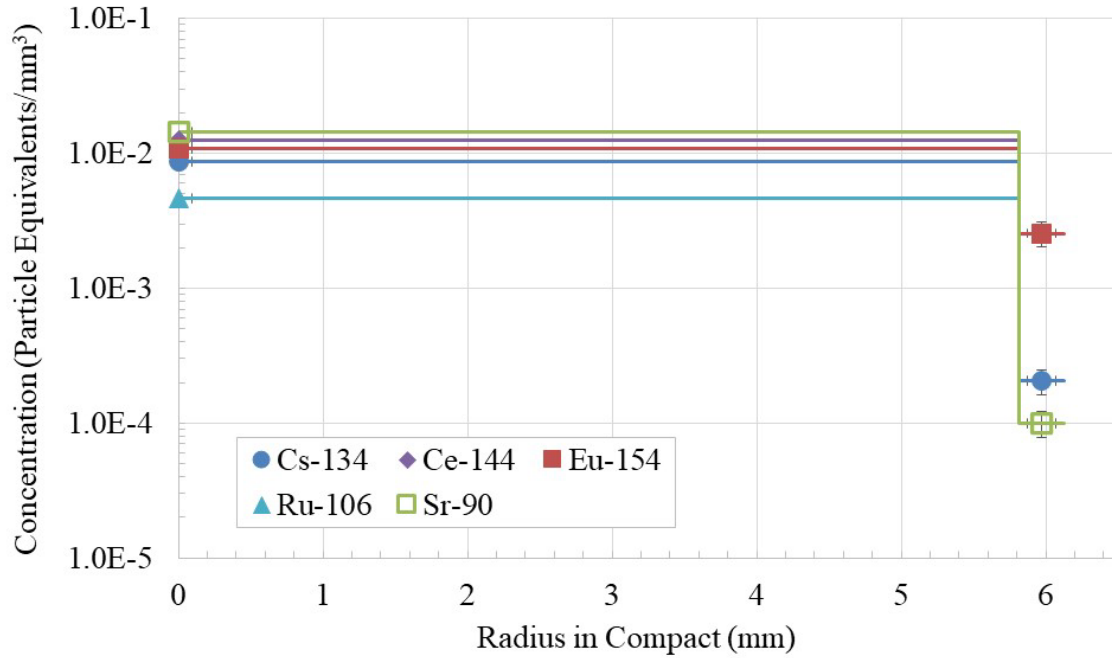


Figure 41. Compact 12-3 fission-product radial-concentration profiles in units of particle equivalents/mm³.

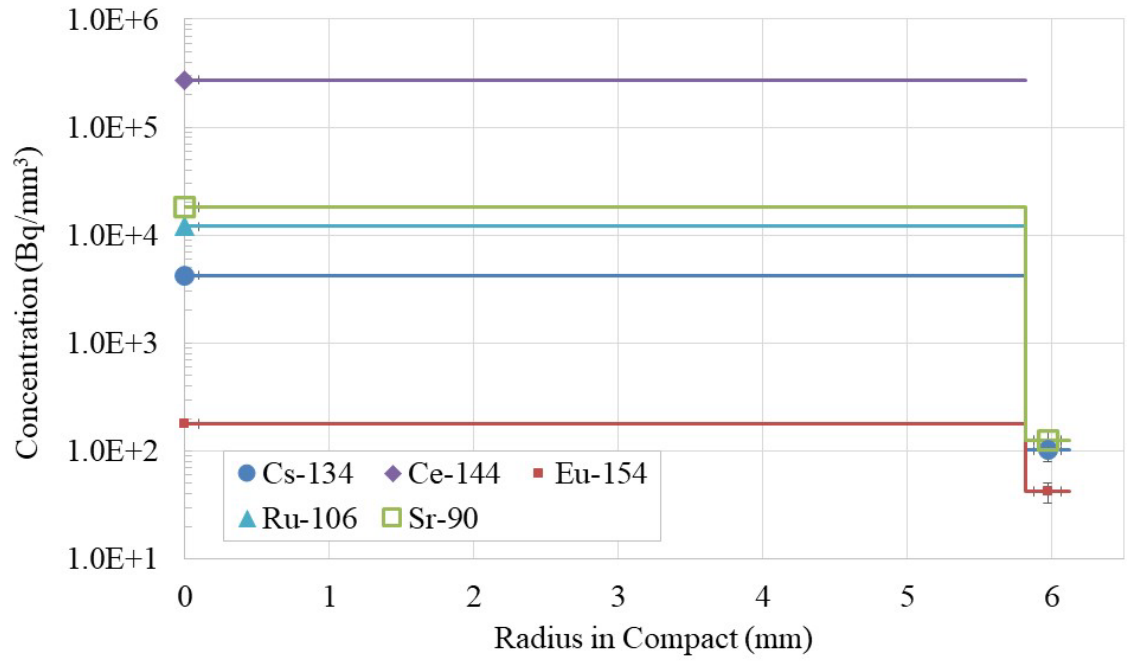


Figure 42. Compact 12-3 fission-product radial-concentration profiles in units of Bq/mm³.

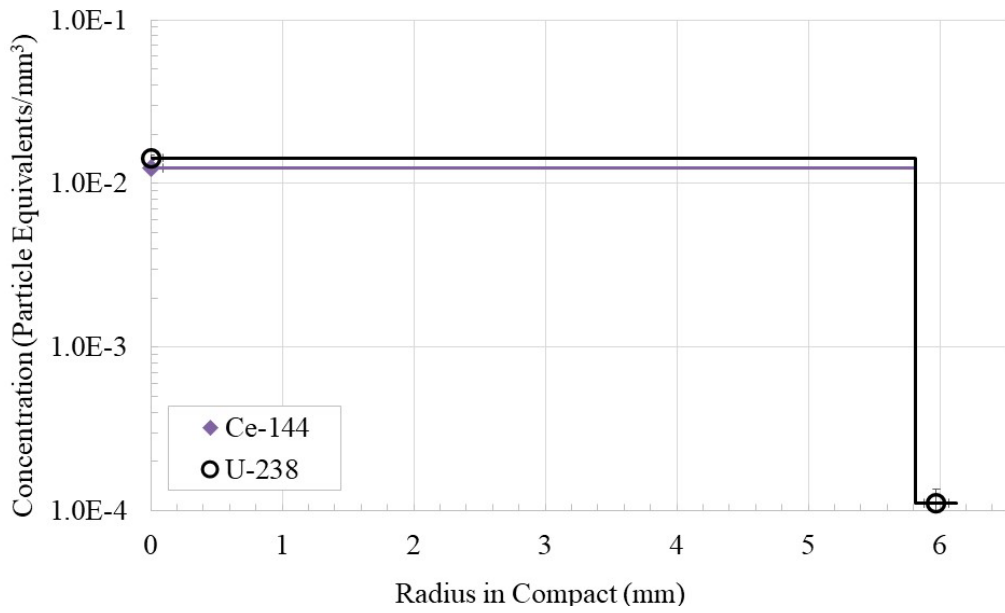


Figure 43. Comparison of Ce-144 and U-238 radial-concentration profiles for Compact 12-3.

5.9 Comparisons of Fission-Product Inventories and Radial Concentration Profiles

This section discusses the general transport trends and comparisons among different compacts that went through RDLBL. Four compacts (1-4, 1-3, 7-4, and 8-4) that went through as-irradiated RDLBL at ORNL (Hunn et al. 2020, Helmreich et al. 2021, Helmreich et al. 2022) are also included for comparison. Note Compacts 3-3 and 10-3 have been excluded from this discussion because multiple particles were accidentally damaged during RDLBL, and effective corrections for the accidental damage could not be made. However, as stated in Sections 4.6.3 and 5.6, it may be possible to correct Segment 3 from Compact 10-3, but the other segments and the core cannot be corrected. Accidental particle damage occurred frequently during the RDLBL processes, and Table 72 summarizes the compacts that were affected and whether reasonable corrections for that accidental damage could be made.

Table 72. List of all as-irradiated AGR-3/4 compacts analyzed at INL and ORNL and whether corrections were applied to their results to account for accidental particle damage.

Compact	Damage	Corrected?
3-3	Up to ~14 particles at various stages of Segment 1 and Core	No ^a
5-3	Segment 1, post-burn leach 1: 1 particle	Yes ^b
5-4	None	N/A ^c
7-3	Segment 1, post-burn leach 2: 1 particle	Yes
8-3	Segment 2, pre-burn leach 2: 1 particle	Yes
10-3	Segments 1, 2, 3 and core: 10-20 particles	No ^d
12-1	Segment 1 decon: 2 particles. Segments 2 and 3 decons, Segment 2 post-burn leach 1: 1 particle each	Yes
12-3	None indicated, but some thimble material was spilled	N/A
1-4	Segment 1, post-burn leach 1: 1 particle	Yes
7-4	Segment 1, deconsolidation: 1 particle	Yes
8-4	None	N/A
1-3	None	N/A

a. Denotes a compact where numerous particles were damaged, and no corrections could be made.

b. Denotes a compact where at least one particle was damaged, and a correction was applied.

c. Denotes a compact where there were no signs of accidental damage.

d. No correction applied, but a correction could be applied to Segment 3 in Compact 10-3.

5.9.1 Total Fission-Product Inventories from RDLBL

The total inventories of key fission products (e.g., Ce-144, Ru-106, U-238, Eu-154, Sr-90, Cs-134, and Cs-137) and U measured from RDLBL are given as a function of compact TAVA temperature in Figure 44 through Figure 46. For comparison, the capsule mass balances (Stempien 2018)^d were divided by four (the number of compacts per capsule) to estimate the total quantity released from an average compact in each capsule. This was plotted in the figures versus the TAVA temperature averaged over all compacts in each capsule.

^d The AGR-3/4 capsule mass balances are the total inventories of fission products measured outside of the fuel in each capsule. They are composed of the sum-total inventories from the inner ring, outer ring, sink ring, and hardware (foils, felts, spacers, and through tubes).

Figure 44 shows that the Ce-144 and U-238 (or total U in the case of Compact 12-1) inventories match well with each other and tend to cluster around 20 particle equivalents, the number of DTF particles per compact. Most often, about 15 particle equivalents of Ru-106 were detected in the RDLBLs, indicating incomplete recovery of this nuclide. There is no strong trend in the RDLBL inventories of Ce, Ru, or U versus irradiation temperature. Most of these nuclides were measured in RDLBL, and little or none was measured outside of the fuel, indicating they are retained in the fuel compact despite the presence of 20 DTF particles per compact. In Capsules 1, 7, and 12, no Ce-144 was measured outside of the fuel, and in the other capsules, the Ce-144 mass balances were less than 0.1 particle equivalent outside of the fuel. No Ru-106 was measured outside of the fuel in Capsules 3 and 5. Where Ru-106 was measured outside of the fuel, it was ≤ 0.005 particle equivalents per compact per capsule.

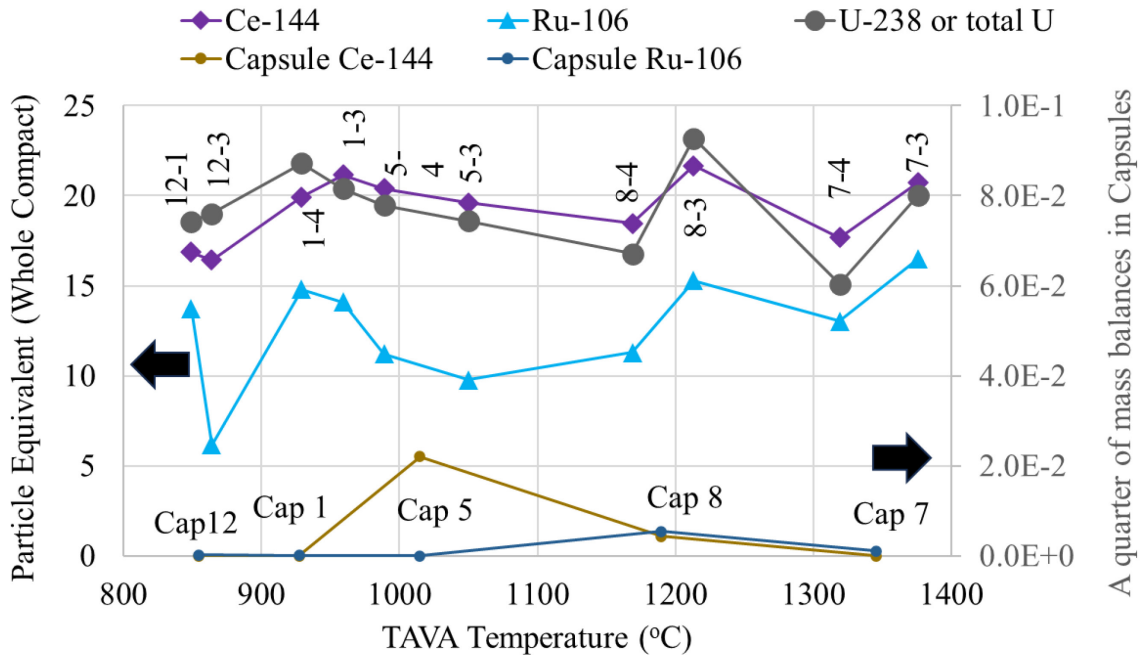


Figure 44. Compact RDLBL and capsule mass-balance inventories as a function of calculated compact TAVA irradiation temperatures. The total U value is plotted here for Compact 12-1 (see Section 4.7.2), but U-238 is plotted for all other compacts.

Figure 45 shows some variations in the Eu-154 and Sr-90 inventories in the compacts outside of the TRISO-coated driver particles as a function of compact-TAVA temperature. Among the three coldest compacts subjected to as-irradiated RDLBL, the Eu-154 and Sr-90 content increases with increasing temperature from 849–929°C. At a TAVA of 864°C, the Eu-154 and Sr-90 inventories measured in the Compact 12-3 RDLBL were 14.7 and 19.1 particle equivalents, respectively. This represents a decent recovery of the inventories originating in the 20 DTF particles in that compact. The Eu-154 and Sr-90 inventories in Compact 1-4 (TAVA 929°C) were 17.4 and 24.6 particle equivalents (after correction for one damaged driver particle), respectively. This suggests that the Sr-90 release through intact driver particles just becomes noticeable around this temperature. From a TAVA of 929°C for Compact 1-4 to 1050°C for Compact 5-3, the Sr-90 and Eu-154 inventories in the four compacts spanning that range are similar, i.e., relatively insensitive to temperature. From 1050 to 1213°C, the Sr-90 and Eu-154 inventories detected from RDLBL increase strongly as release through TRISO-coated driver particles' SiC layers, and retention in the OPyC layers and surrounding compact matrix became noticeable, reaching in excess of 40 particle equivalents. From 1213°C to the compact with the highest TAVA in this study at 1376°C, the inventory of Sr-90 and Eu-154 in the RDLBs was relatively constant. The corresponding mass balances for each capsule tend to mirror the temperature dependence of the RDLBL results, which indicates consistency between the two complementary sets of measurements. The capsule mass balances have a larger increase above 1200°C than the

RDLBL results. This shows that there is an increase in overall diffusive release through intact TRISO coatings and a concomitant increase in the release of these nuclides from the compacts.

Some release of Sr-90 and Eu-154 through intact TRISO coatings has been noted previously (Stempien et al. 2021; Stempien, Cai, and Demkowicz 2023). Fortunately, much of the Sr-90 and Eu-154 released through the TRISO coatings is retained in the OPyC and compact matrix (Stempien et al. 2021; Stempien, Cai, and Demkowicz 2023). A notable increase in the amount of Sr-90 and Eu-154 released through intact coatings has been observed for irradiation temperatures greater than about 1200°C (Stempien et al. 2018; Stempien et al. 2021; Stempien, Cai, and Demkowicz 2023). However, there was a gap in the data between about 1100 and 1250°C regarding Eu-154 and Sr-90 release through intact particles and retention in the OPyC and compact matrix. The AGR-3/4 RDLBL results fill in that temperature gap, and indicate the release becomes observable above the level of 20 DTF kernels at lower irradiation temperatures, at least as low as about 1150°C if not somewhere between about 1050 and 1150°C.

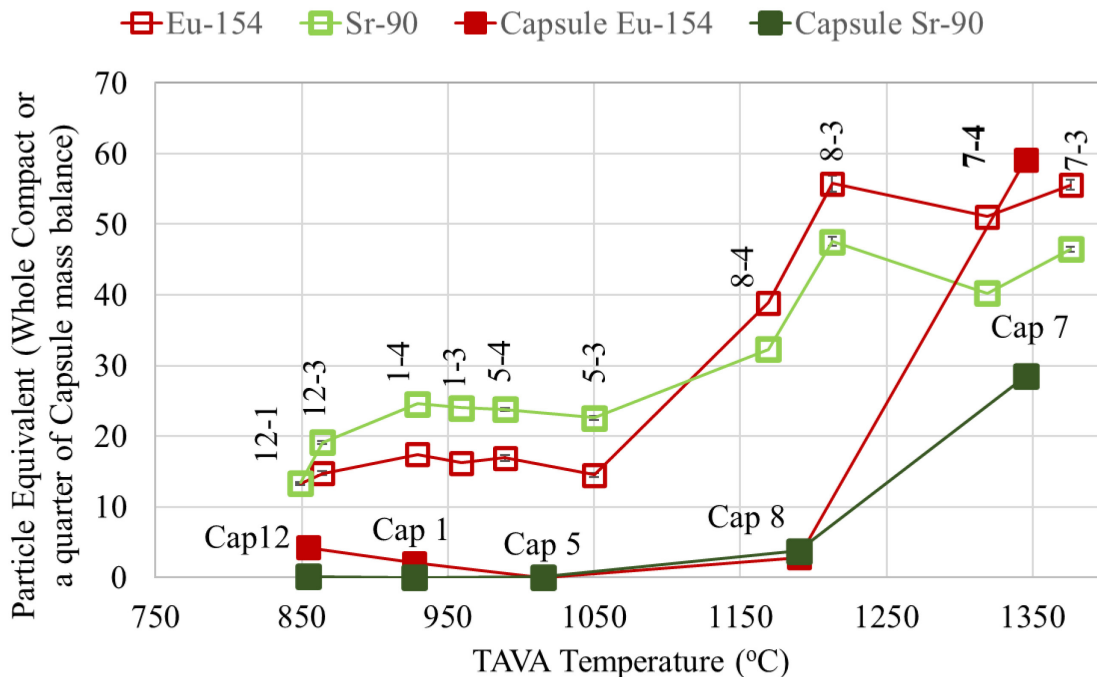


Figure 45. Total RDLBL inventories of Eu-154 and Sr-90 in AGR-3/4 fuel compacts outside of the SiC layer of TRISO-coated driver-fuel particles as a function of TAVA temperature. The error bars are included for compacts analyzed at INL; however, they are smaller than the symbols used in the plot. The capsule mass balances (Stempien et al. 2018) were divided by four to represent the nuclide release from an average compact in each capsule. The Sr-90 and Eu-154 values overlap in Compact 12-1 (refer to Table 47).

Cesium is a nuclide that is well retained by intact SiC layers. Typically, Cs-134 is the preferred indicator of Cs release from the fuel because it tends to be less susceptible to bias from hot-cell contamination than the longer-lived isotope, Cs-137. Evidence of this bias is that the blank solutions prepared with each analysis had higher Cs-137:Cs-134 ratios than the ratios for the RDLBL solutions in nearly every case. There were no failed-SiC or failed TRISO particles in AGR-1 Capsules 1–4, and Cs-134 was below the detection limits outside of the fuel in those capsules (Demkowicz et al. 2013). Despite three failed-SiC particles in AGR-1 Capsule 5, and one failed-SiC particle in AGR-1 Capsule 6, the amount of Cs-134 detected outside of the fuel was about 0.6 particle equivalents for those two capsules (Demkowicz et al. 2015). In AGR-2, including the contributions from five failed-SiC particles and one defective particle in Capsule 2, the two failed TRISO particles in Capsule 5, and the one failed-SiC and two failed TRISO particles in Capsule 6, the Cs-134 inventories outside the UCO fuel compacts in AGR-2 were 0.3, 0.2, and 0.2 particle equivalents, respectively (Stempien et al. 2021). With an

estimated 49,200 particles per AGR-1 capsule and 38,112 particles per AGR-2 capsule, it is apparent that intact fuel retains this Cs, and the capsule mass balances indicate that compacts with failed-SiC or failed TRISO particles still retain some of the Cs in the exposed kernels or compact matrix. Therefore, in AGR-3/4, the Cs inventories measured in RDLBL are dominated by the inventories originating from the DTF particles.

One of the first things to note about the plots of Cs-134 and Cs-137 inventories versus irradiation temperature in Figure 46 is that the measured Cs-137 inventories are higher than the Cs-134 inventories in all but one case (where they are roughly equivalent). This is attributed to the effects of hot-cell contamination where the presence of long-lived Cs-137 from previous activities can bias the measured Cs-137 inventory higher than the Cs-134 inventories.

The second feature of note in Figure 46 is the increase in compact-RDLBL inventory from the coldest compact (Compact 12-1) to the next coldest compact (Compact 12-3) to the two Capsule 1 compacts (1-4 and 1-3). It is not clear what transport mechanism would account for this, and it is not clear how much of this is a genuine effect versus an uncertainty introduced during the analysis. For example, the Capsule 1 and 12 mass balances do not complement the temperature dependence suggested from DLBL of the Capsules 1 and 12 compacts. Assuming Cs-134 data to be more reliable than the Cs-137 data, the trend in Cs-134 capsule mass balance versus temperature shows an increase in out-of-compact inventory (capsule mass balance) from the cooler Capsule 12 to the warmer Capsule 1. This makes intuitive sense for a thermally driven transport process. While we have only examined two of the four compacts in each of Capsules 12 and 1, on average the compact-RDLBL inventories of Cs-134 would have to decrease from the Capsule 12 compacts to the Capsule 1 compacts for there to be an increase in the capsule mass-balance inventory going from Capsule 12 to Capsule 1. That is not the case.

Between the Capsule 1 and 12 RDLBLs, it is notable that the Cs-134:Cs-137 ratios for Compacts 12-1 and 12-3 (done at INL) are smaller by 20–350% than they are for 1-4 and 1-3 (done at ORNL). This could be caused either by higher Cs-137 contamination in the work at INL or from anomalously low Cs-134 in the INL results. The corrections applied to Compact 12-1 were based on the assumption that particles accidentally broken during RDLBL were of average size. If the affected particles were significantly larger or smaller than average, the corrections may under- or over-estimate the corrected values. The potential over- or under-correction for damaged particles still would not account for the difference between the Capsule 12 and Capsule 1 RDLBLs, however.

The Cs-134 RDLBL inventory drops sharply from about 15 particles for Compact 1-3 (TAVA 959°C) to 5 particle equivalents for Compact 5-4 (TAVA 989°C). Accordingly, the capsule mass balances (the inventories measured outside of the fuel) increase sharply from 1.3 particle equivalents in Capsule 1 to 16 particle equivalents for Capsule 5. This demonstrates a sharp increase in Cs release from fuel compacts with exposed kernels at temperatures >960°C. The Cs-134 RDLB inventories are similar for Compacts 5-4 (at 989°C) and 5-3 (at 1050°C). For irradiation temperatures from 989–1376°C, the amount of Cs measured in the RDLBLs of these AGR-3/4 fuel compacts ranges from 0.6 to 4.8 particle equivalents. In that temperature range, the Cs-134 inventories measured at 989 and 1376°C are similar, and the minimum measured Cs-134 quantity of 0.6 particle equivalents occurs at 1169°C.

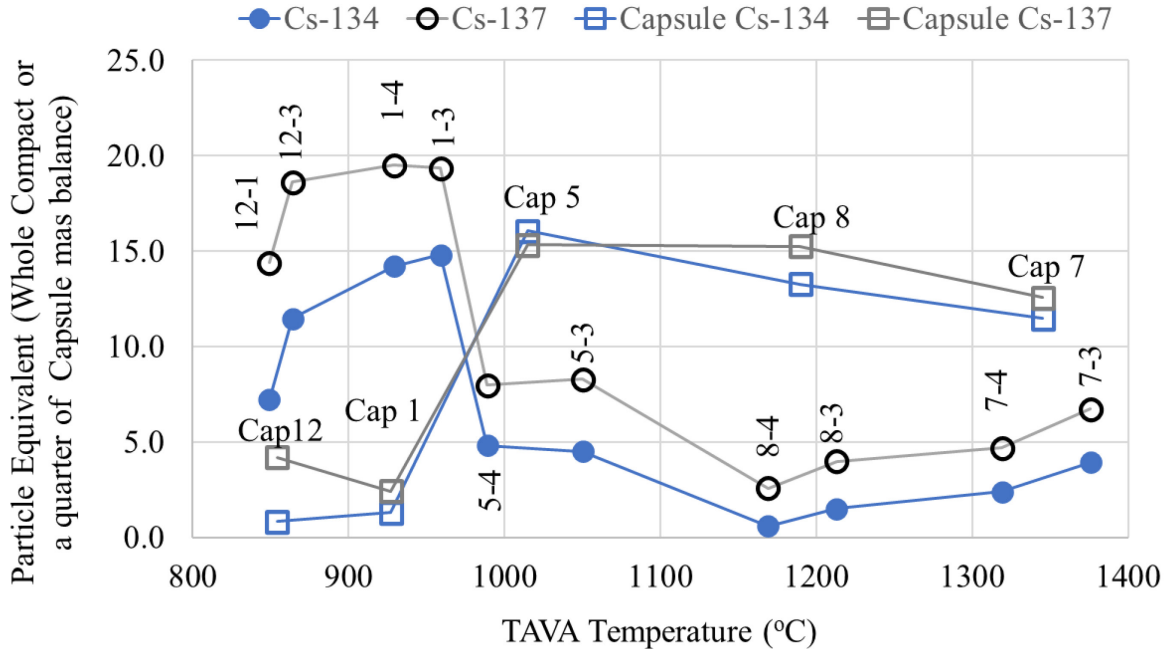


Figure 46. Particle equivalents of Cs-134 and Cs-137 as function of compact TAVA temperature. The particle equivalent of capsule components shown in the figure is a quarter of the total value for easy comparison because there were four compacts in each capsule.

5.9.2 Radial Fission-Product Concentration Profiles

Radial concentration profiles for U-238, Ce-144, Eu-154, Sr-90, and Cs-134 are presented in Figure 47 through Figure 51 for as-irradiated compacts analyzed at INL and those analyzed and reported previously at ORNL (Hunn et al. 2020, Helmreich et al. 2021, Helmreich et al. 2022).^e The reader should also refer back to Sections 4.1–4.8 and 5.1–5.8, which give the relative error on these concentrations. In some cases, segment-to-segment differences may not be statistically significant.

As Figure 47 and Figure 48 show, the concentrations of U-238 and Ce-144 generally decrease with increasing radius. The core always had a higher concentration than any segment outside of the core. From the core to the adjacent segment, there tended to be a sharp drop in concentration. Outside the core, the U-238 concentration profiles among the radial segments were often flat, but Compacts 1-4 and 5-4 had the most noticeable decreases in U-238 from Segment 3 to Segment 1. The Ce-144 concentrations tended to decrease more than U-238 from the innermost radial segment (e.g., Segment 3) to the outermost radial segment (i.e., Segment 1).

In some cases (i.e., Compacts 5-3, 7-4, 8-4, and 12-1), the U-238 concentration had a local maximum in one of the radial segments. In some instances, like with Compacts 5-3 and 12-1, the U-238 concentration differences between the local maximum and adjacent radial segments are small and not statistically significant. The errors in the concentrations in Compacts 7-4 and 8-4 were not available (Helmreich 2021), but the difference between the local maxima and adjacent segments may be significant if the errors in those ORNL measurements are similar to those determined in the INL measurements reported here.

Artifacts of accidental particle damage that occurred during the RDLBL may influence these local maxima as well. For example, Compact 5-3 had one particle that was accidentally damaged in Segment 1 (see Section 4.2.3). After a correction was applied for that damage, the mean U-238 concentration in Segment 1 was marginally higher than that of Segment 2, but those values had overlapping error. There were no indications of accidental

^e Recall that Compacts 3-3 and 10-3 are excluded from this discussion due to the excessive driver particle damage they suffered during RDLBL.

particle damage in the Compact 8-4 RDLBL, but the U-238 concentration in Segment 2 ($3.29\text{E-}3$ particle equivalents/ mm^3) was slightly higher than that in Segment 3 ($2.75\text{E-}3$ particle equivalents/ mm^3). Compact 7-4 had about 1.3 particle equivalents of Ce-144, U-235, and U-236 in Segment 1, but about two particle equivalents of U-238, Pu-239, and Pu-240 (Helmreich et al. 2021). The correction to Compact 7-4 Segment 1 was to subtract one particle equivalent, so the higher U-238 concentration in Segment 1 compared to Segment 2 may be artificial due to inadequate correction. Compact 12-1 had five damaged particles as discussed in Section 4.7.3. Two of those were damaged in two different stages of the Segment-2 RDLBL. Two particle equivalents were subtracted from the Segment 2 inventories; however, the concentrations of several nuclides, including U-238 and Ce-144, are still at a local maximum in Compact 12-1, Segment 2. The data suggest the possibility that the particle damaged during the first post-burn leach of Compact 12-1 Segment 2 could have had a kernel 10–16% larger than an average kernel. If that were the case, attempting to correct for that damaged particle by subtracting only one particle equivalent would still leave 0.1–0.16 particle equivalents uncorrected. In Compact 12-1 Segment 2, 0.16 particle equivalents are 50–100% of the inventory in that segment. Thus, there may be significant uncertainty in the true concentration of that segment.^f

The compacts with higher TAVA irradiation temperatures ($\geq 1169^\circ\text{C}$) tend to have higher Ce-144 concentrations in their outermost segment than those with lower irradiation temperatures. Compacts with no detectable Ce-144 in Segment 1 are 12-3, 5-4, and 5-3,^g which had TAVA temperatures of 846, 989, and 1050°C , respectively. The compacts with the lowest measurable Ce-144 concentrations in their first segments, Compacts 1-3 and 1-4, had TAVA temperatures of 959 and 929°C , respectively. The next three compacts in order of increasing Segment 1 Ce-144 concentrations are 8-4, 7-4, and 7-3, which had TAVA temperatures of 1169, 1319, and 1376°C , respectively.

The compacts with the highest Ce-144 concentrations at the compact periphery are 8-3 and 12-1; however, there may be considerable uncertainty in these because of difficulties encountered during their RDLBLs. The Compact 8-3 Segment 1 and 2 inventories had to be combined when it was impossible to determine the volume of material removed from Segment 1 (see Section 4.5). This could result in an overestimate of the concentration via an underestimate of the volume of material removed. Compact 8-3 Segment 2 had a particle that was accidentally damaged. Based on the inventory of Ce-144 and actinides measured in that segment, it is possible that particle was in excess of 20% larger than an average particle. If that were the case, then subtracting one particle equivalent still leads to an overestimate of the Ce-144 in that segment. Similarly, Compact 12-1 had at five particles damaged during RDLBL, two of which occurred in Segment 1 and could have artificially inflated the Ce-144 content in that segment despite attempts to correct for it.

^f A similar effect may have occurred in Segment 1 from Compact 7-3 where the particle damaged in Segment 1 may have been 6–14% larger than average depending on which nuclide from the Segment 1 post-burn leach 2 is considered. Compact 7-3 did not have a local maximum of U-238, but it did have a local maximum of Ce-144 in Segment 1.

^g Only after correcting for accidental particle damage in the Segment-1 post-burn-leach 1 process did Compact 5-3 have no measurable Ce-144 in Segment 1.

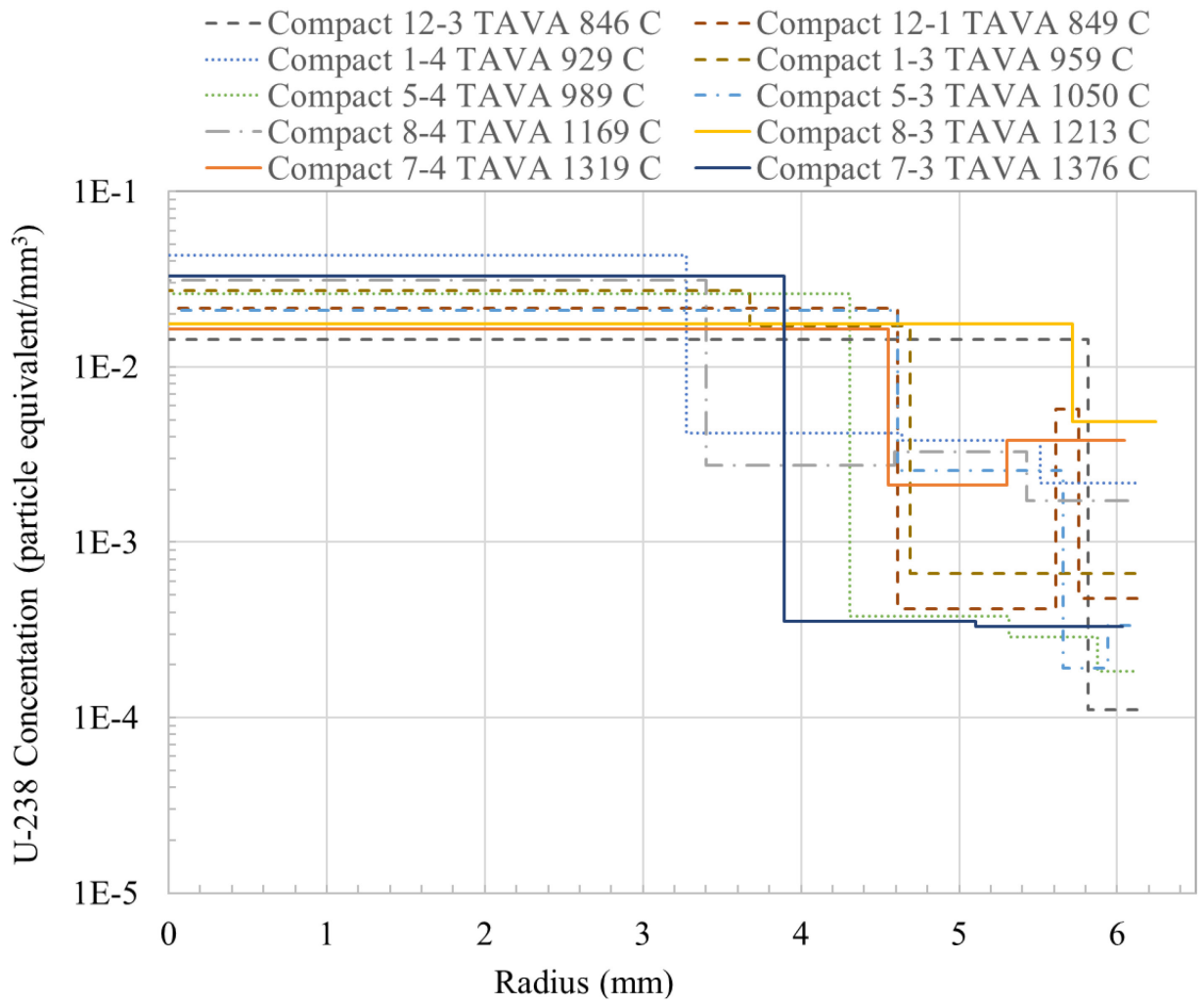


Figure 47. The AGR-3/4 compact radial-concentration profiles for U-238.

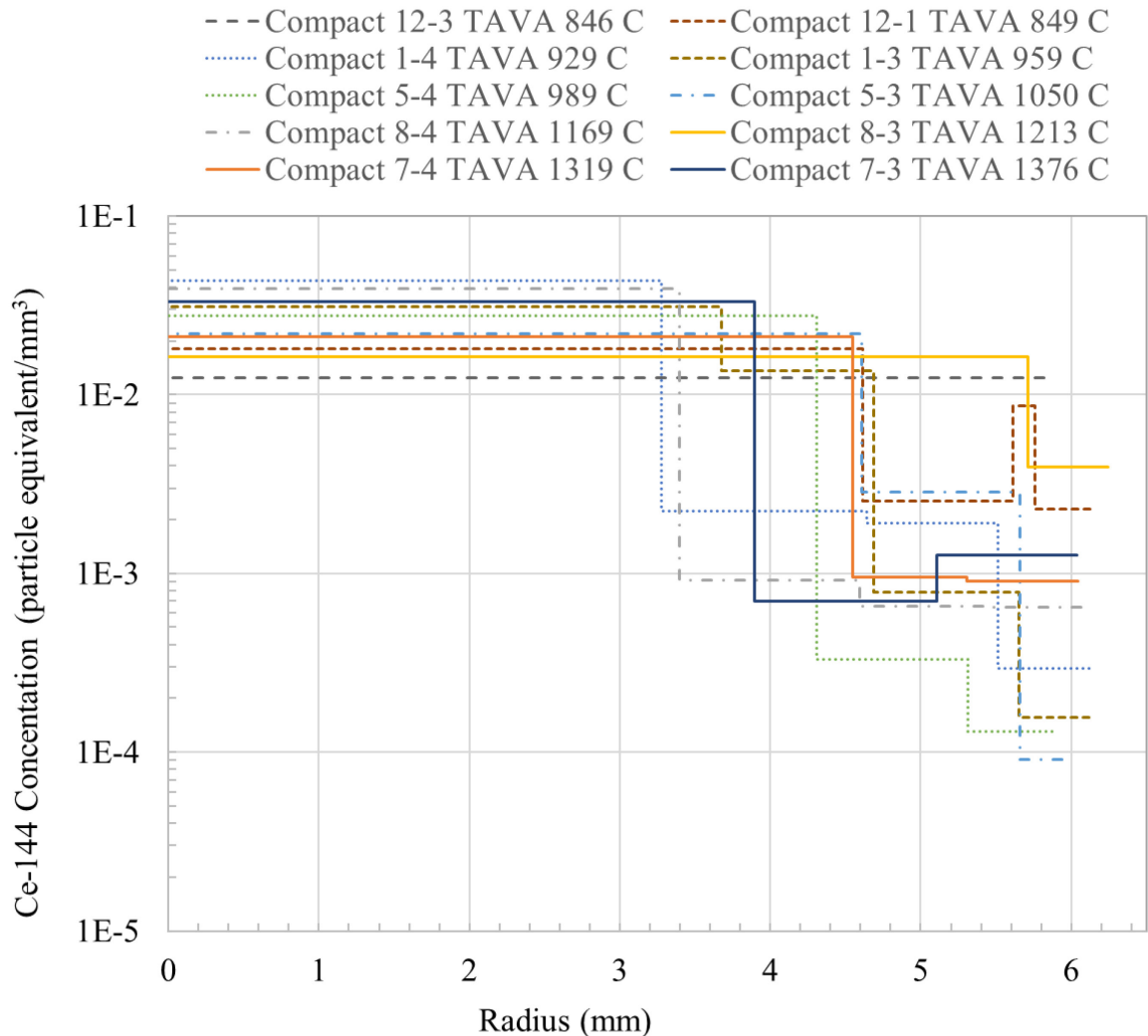


Figure 48. The AGR-3/4 compact radial-concentration profiles for Ce-144.

The radial Eu-154 concentration profiles for the as-irradiated AGR-3/4 compacts subjected to RDLBL are shown in Figure 49. The three hottest compacts to undergo this process, Compacts 7-3, 7-4, and 8-3 (with TAVA temperatures of 1376, 1319, and 1213°C, respectively), exhibit flat or gently increasing Eu-154 concentrations with increasing radii. Compact 8-4 (with a TAVA temperature of 1169°C) is the highest-irradiation-temperature compact to have a decrease in concentration with increasing radius, but there is little difference in the concentrations of its first and second segments. In some cases, the error in the concentrations may be substantial. For example, the Segment 1 concentrations errors are commonly 20–40%; therefore, not all concentration differences are statistically significant (e.g., the differences between the Eu-154 concentrations in the radial profiles of Compacts 7-3 and 8-3). All other compacts (with TAVA temperatures of between 846 and 1050°C) have relatively sharp decreases in concentration from the core to the outer segments.

Interestingly, Compacts 5-3 and 5-4 were the only ones to have no measurable Eu-154 in their first (outermost) segments. These compacts had TAVA temperatures of 1050 and 989°C, respectively. Compacts colder than these (i.e., 12-3, 12-1, 1-3, 1-4), with TAVA temperatures 846–959°C, had intermediate concentrations of Eu-154 in their outermost segments. These concentrations lie between those of the hotter compacts ($\geq 1213^\circ\text{C}$) and those of the intermediate-temperature compacts (989–1050°C). This could be evidence that a little more compact release of Eu-154 that originated in the DTF particles started at temperatures of about 989°C. Once temperatures reached and exceeded 1169°C, the enhanced diffusion of Eu-154 through intact TRISO

coatings overwhelmed the contribution from the DTF particles, but even then, most of that was still retained in the matrix until compact-TAVA temperatures reached and exceeded 1319°C.

The observations surrounding the Eu-154 concentration profiles in Figure 49, are consistent with those made regarding the total RDLBL inventories in the previous section. In Section 5.9.1, Figure 45 showed that compacts from Capsules 12, 1, and 5 had the lowest total RDLBL inventories of measurable Eu-154, and compacts from Capsules 8 and 7 had the highest. In the cooler compacts, the total Eu-154 inventories measured were all less than 20 particle equivalents, suggesting little or no release of Eu-154 through intact TRISO-coated driver particles. With temperatures increasing to 1169°C for Compact 8-4, the Eu-154 inventory in the compact outside of the driver fuel was about 40 particle equivalents. This increased to greater than 50 particle equivalents for temperatures $\geq 1213^\circ\text{C}$ for Compact 8-3 and the Capsule 7 compacts. The compacts with higher measurable inventories from RDLBL (Figure 45) are the hotter ones, which are the same ones that have flatter Eu-154 concentration profiles (Figure 49).

The Sr-90 radial-concentration profiles shown in Figure 50 are very similar to those of Eu-154. This is also consistent with the total Sr-90 inventories measured from RDLBL (see Figure 45), where the measured Sr-90 and Eu-154 quantities varied together according to fuel-irradiation temperature.

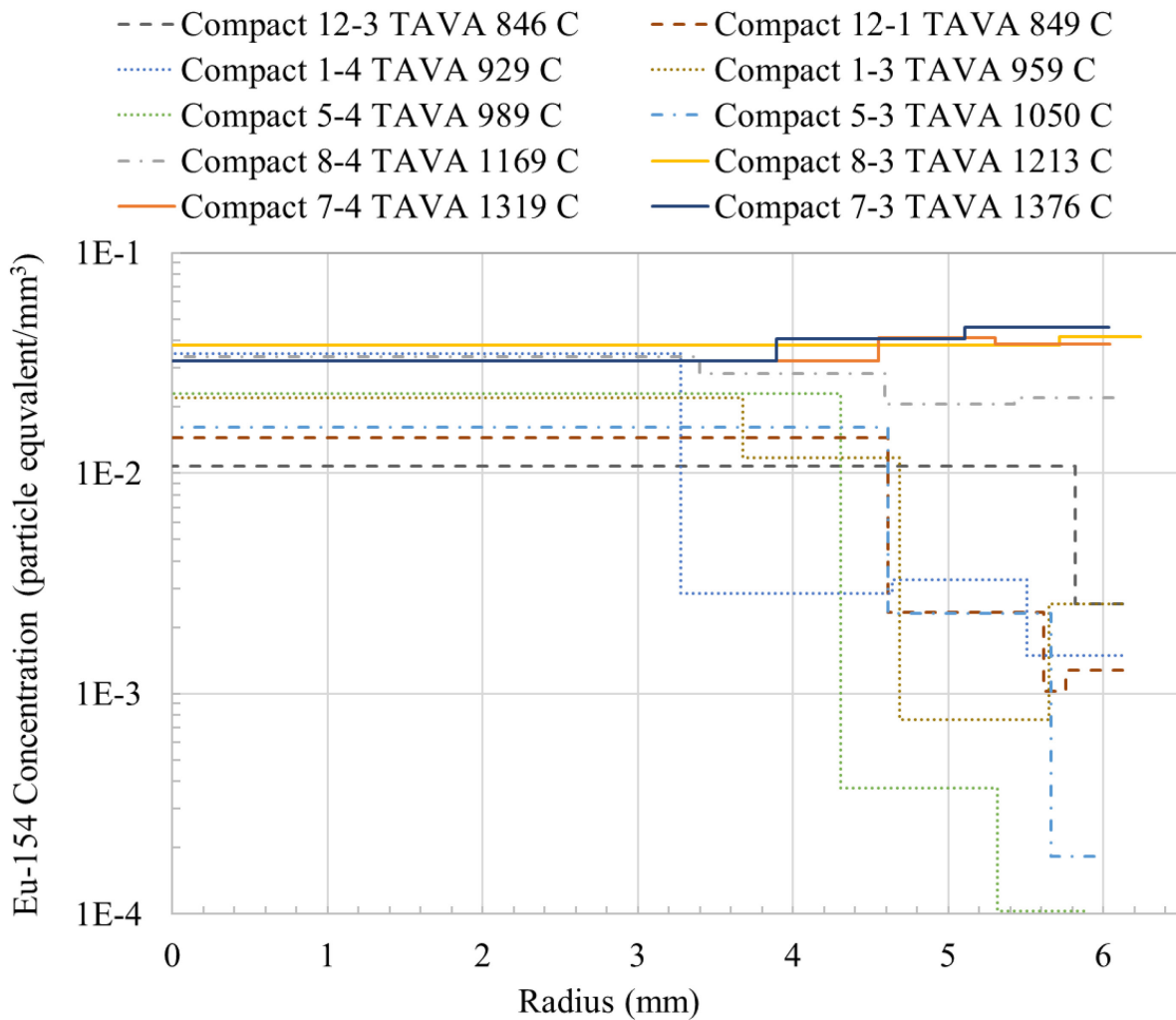


Figure 49. Radial-concentration profiles for Eu-154 in AGR-3/4 compacts.

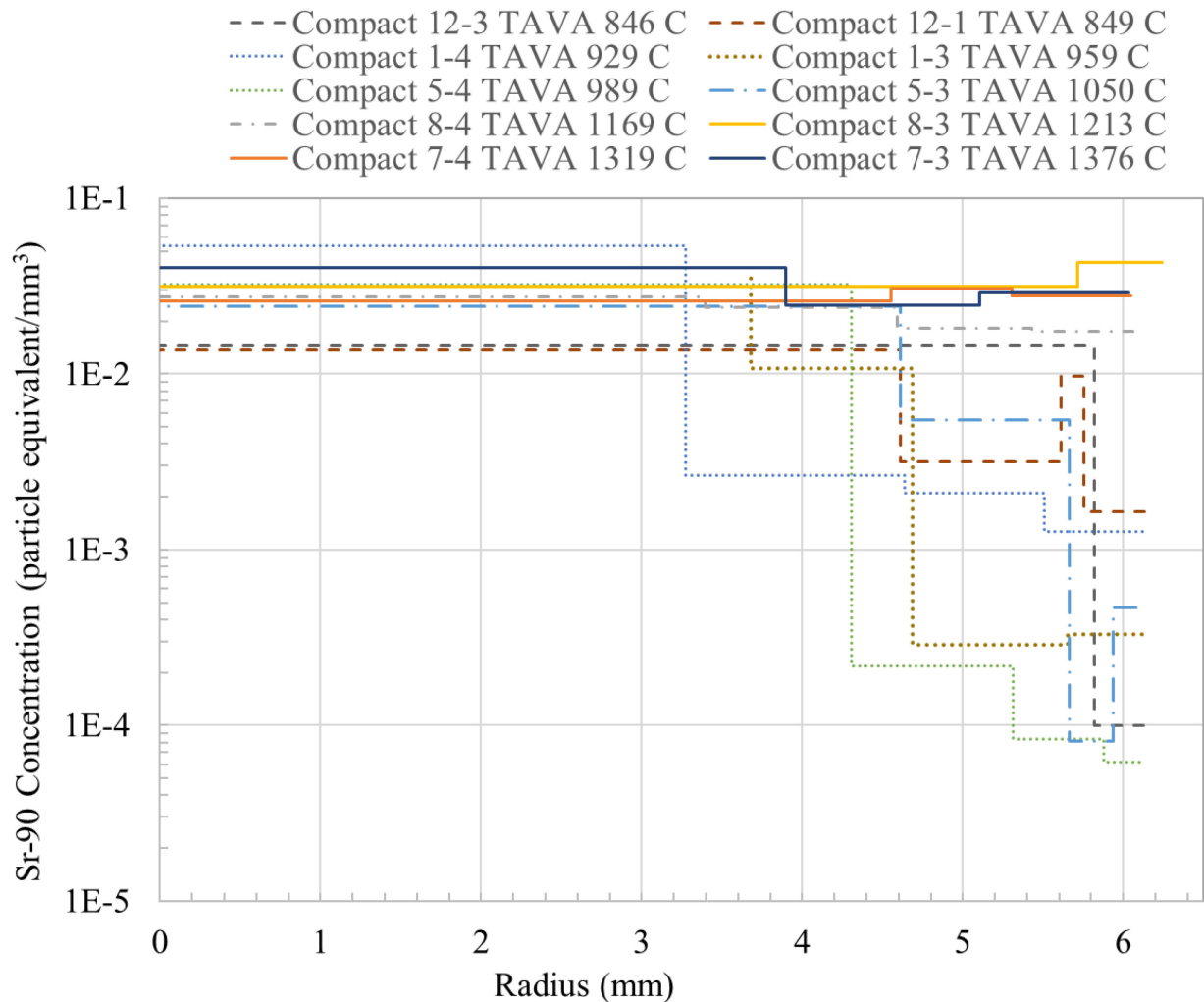


Figure 50. The concentration of Sr-90 particle equivalents as function of compact radius.

Figure 46 showed that, unlike Eu-154 and Sr-90, which were detected in higher quantities as the compact irradiation temperature increased, the total quantity of Cs-134 measured in the compacts via RDLBL was sharply *lower* as compact TAVA irradiation temperatures increased from 959°C for Compact 1-3 to 989°C for Compact 5-4. This is the result of Cs-134 from the DTF particles being driven out of the compacts to the irradiation capsule components more rapidly for TAVA irradiation temperatures $\geq 989^\circ\text{C}$. The time-average peak irradiation temperatures also help to explain this sudden increase in Cs-134 release. While the TAVA temperature for Compact 5-4 was only 30°C hotter than Compact 1-3, the time-average peak temperature in Compact 5-3 was 106°C hotter.

In keeping with the increased release of Cs-134 from compacts with higher irradiation temperatures shown in Figure 46, Figure 51 shows that the three overall lowest concentrations of Cs-134 were measured in Compacts 7-3, 7-4, and 8-4 (TAVA 1376, 1319, and 1169°C, respectively). (Any Cs-134 in the outermost segment of Compact 7-4 was below detection.) Three of the four lowest Cs-134 core concentrations were also among compacts with TAVA irradiation temperatures ranging from 1169 to 1376°C. The four coolest compacts (12-3, 12-1, 1-4, and 1-3) had TAVA temperatures ranging from 846 to 959°C, and they also had the highest core concentrations of Cs-134. Among the segments just outside of the compact cores, Compacts 1-3, and 1-4 had some of the highest concentrations, indicating some Cs-134 transport beyond the compact core at these temperatures; however, release from the compact altogether averaged less than 1.5 particle equivalents per compact until a TAVA temperature of 989°C in Capsule 5, where the compact release jumped to an average of

about 5 particle equivalents per compact. Compacts like 5-3 and 5-4, with TAVA temperatures of 1050 and 989°C, respectively, had core concentrations in the middle of the data set with relatively flat Cs-134 profiles, suggesting there is significant transport of Cs-134 from the core to the compact periphery. Both Compacts 5-3 and 5-4 have higher Cs-134 concentrations in Segment 1 than in Segment 2. It is not clear why this would be. Compact 5-4 had no apparent particle damage caused by RDLBL, and Compact 5-3 was corrected for one particle damaged during Segment 1 RDLBL.

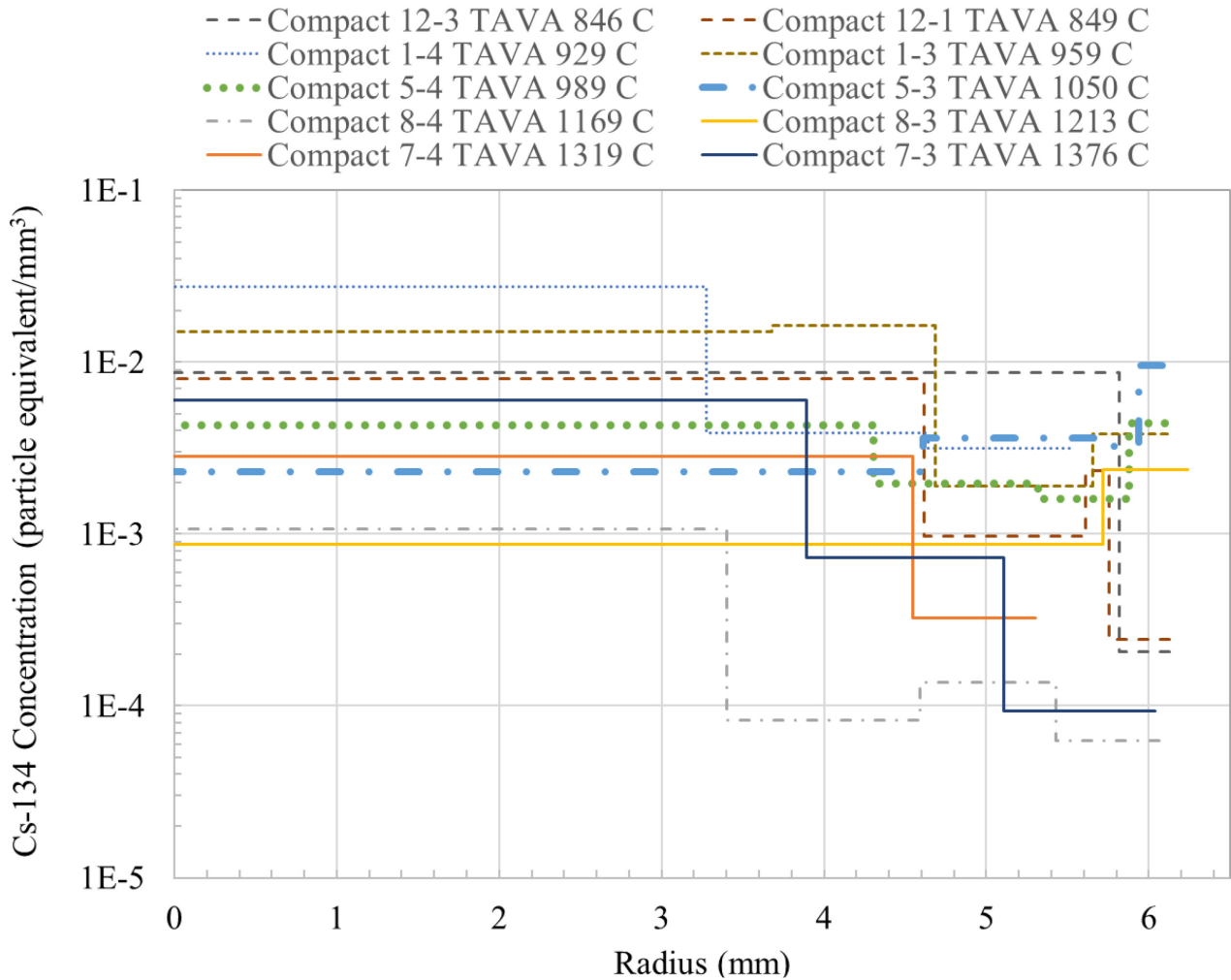


Figure 51. The concentration of Cs-134 particle equivalents as function of compact radius. There is no data point for the outermost segment of Compact 7-4 because any Cs-134 there was below detection.

6. SUMMARY AND CONCLUSIONS

The AGR-3/4 experiment was specifically designed to investigate the migration of fission products in fuel-compact graphitic-matrix and reactor-graphite components. The experiment consisted of fuel compacts containing roughly 1898 TRISO-coated driver-fuel particles and 20 DTF particles aligned along the compact center to intentionally release fission products during irradiation to migrate through and out of the compact.

Eight as-irradiated AGR-3/4 fuel compacts were subjected to destructive post-irradiation examination via RDLBL at INL. The details of that work and the sets of results were reported here. Another four compacts underwent as-irradiated DLBL at ORNL and were reported previously (Hunn et al. 2020, Helmreich et al. 2021, Helmreich et al. 2022). The RDLBL process deconsolidated the compacts in multiple, radial steps, followed by a final single-step axial deconsolidation. The samples generated at each step were analyzed for isotopes of key

fission products (e.g., Ag, Ce, Cs, Eu, Ru, Sr) and actinides (i.e., U and Pu).^h After each deconsolidation step, the compact volume was assessed, and this was used to normalize the measured quantity of nuclides of interest to give a volumetric concentration as a function of radial position within the compact.

The total inventories of measured fission products and actinides and the radial concentration profiles were compared among the eight compacts deconsolidated at INL and the four examined at ORNL. The AGR-3/4 irradiation-capsule mass balances were also considered because they show the inventory of fission products released from the fuel compacts, while the RDLBL shows the inventory of fission products retained in the fuel compacts outside of the SiC layer of intact TRISO-coated particles.

Irradiation temperature was found to affect the inventories and radial distributions of fission products in the AGR-3/4 compacts. Within the OPyC and matrix, the total inventories of nuclides least impacted by irradiation temperature were Ce-144, Ru-106, and isotopes of U and Pu. The measured Ce and U inventories were very similar in all compacts, regardless of irradiation temperature, and tended to cluster around 20 particle equivalents, equal to the number of DTF particles per compact. Most often, about 15 particle equivalents of Ru-106 were detected in the RDLBLs, indicating incomplete recovery of this nuclide.

While the temperature did not significantly impact the total inventories of Ce-144, Ru-106, and isotopes of U and Pu, measured in RDLBL, the shapes of the radial concentration profiles of these nuclides were affected by irradiation temperature. The Ce-144 and U concentrations had similar radial concentration profiles, and the general trend of Ce-144 and U concentrations decreasing with increasing radius was followed for compacts spanning the range of irradiation temperatures. It was observed that compacts with higher irradiation temperatures more often had higher Ce-144 concentrations in their outermost segments than did compacts with lower irradiation temperatures. Of the Ce, Ru, U, and Pu measured in AGR-3/4, most was measured in the core of the as-irradiated-compact RDLBLs and not in the capsule mass balance. Thus, these nuclides are well retained in the fuel compact in or near the exposed DTF kernels. This is consistent with earlier results showing that Ce and Ru remain in the kernel (e.g., Stempien 2020 and Demkowicz et al. 2016).

The common observation that Eu and Sr behave similarly was reinforced in the RDLBL results presented in this report. The inventories measured from RDLBL and the radial-concentration profiles of these two species were comparable. For AGR-3/4 fuel compacts with irradiation temperatures from 846 to 1050°C, the Sr-90 RDLBL inventories ranged from about 18.5 to 25.5 particle equivalents, and the Eu-154 inventories ranged from about 14.5 to 18.5 particle equivalents. Within that temperature range, the Sr and Eu inventories showed no discernable temperature dependence, but the concentration profiles, for which conclusions are presented in the next paragraph, showed some temperature-dependent behavior in that realm. From 1050 to 1169°C, the RDLBL inventories increased sharply and exceeded 20 particle equivalents, indicating significant release of Eu and Sr through intact driver particles with retention within the compact matrix and OPyC. Between 1213 and 1376°C, the Eu and Sr inventories plateaued at 3.5 and 2.0 times higher than they were at 1050°C, respectively. From the mass balances, however, the inventories of these nuclides outside the fuel compacts increased sharply between 1190 and 1345°C. This behavior shows that diffusive release of Eu and Sr through intact TRISO coatings accelerates above 1050°C, but it is still largely retained in the compact until 1190°C. Above 1190°C, diffusive release through intact coatings continues to increase, and so does the release from the compact altogether.

A few characteristics of Eu and Sr concentration profiles were observed. The three hottest compacts to undergo RDLBL (with TAVA temperatures ranging from 1213 to 1376°C), exhibited flat or even gently increasing Eu and Sr concentrations with increases in radius. These were associated with diffusive release through intact coatings, and for $T \geq 1319^\circ\text{C}$ there was greater release from the compacts altogether. Below 1319°C, the evidence shows that most of the Sr and Eu that exists outside of SiC coatings is still retained in the OPyC and compact matrix. A compact with a TAVA irradiation temperature of 1169°C was the highest-temperature compact to show a significant radial decrease in Eu and Sr concentration with increasing radius. Thus, at 1169°C, there was enhanced radial transport of Eu and Sr, but much of it was still retained in the compact matrix and

^h Because of the relatively low fission-yield and half-life (~2/3 y), Ag-110m was not detected in any of the RDLBL samples.

OPyC. For compacts with TAVA temperatures between 846 and 1050°C, the Eu and Sr concentrations had relatively sharp decreases from the core to the outer segments, indicating more limited radial transport. Within that temperature range, compacts with TAVA temperatures from 989 to 1050°C had the lowest peripheral concentrations of Eu and Sr out of all compacts, and compacts with TAVA < 959 had outer-segment concentrations situated at intermediate concentrations. To account for this, it is hypothesized that the Eu and Sr originating in the DTF particles was transported more readily to the compact periphery, with a perhaps little more total compact release, from 989 to 1050°C. Below this temperature, these species tended to reside closer to the DTF particles.

The total quantities of Cs-134 measured in the compacts via RDLBL were sharply lower as compact TAVA irradiation temperatures increased from 959 to 989°C. This was the result of Cs-134 from the DTF particles being driven out of the compacts to the irradiation capsule components more rapidly for TAVA irradiation temperatures $\geq 989^\circ\text{C}$. Below that temperature, much of the Cs remains in the compact despite the presence of 20 DTF particles per compact. The capsule mass balances corroborated this finding, and the radial fission-product concentration profiles from the compacts provided additional details on this behavior. The concentration profiles showed evidence of Cs-134 transport radially outward in the cooler compacts (TAVA < 989°C), but this Cs was largely retained in the compacts. Generally, the compacts with the hottest irradiation temperatures had the lowest Cs-134 concentrations in the compact core and in the outer segments.

The RDLBL technique proved challenging to implement and employ in a hot-cell environment. The compact was often dislodged from the deconsolidation rod. This happened by accidental contact. It also happened when the epoxy/compact bond was exposed to the deconsolidation acid for too long. Keeping that bond out of the acid was important for maintaining the bond. There were several cases of accidental particle damage caused by the RDLBL process, and while attempts were made to correct for this damage, accidental damage likely increased the uncertainty in the results.

There were some instances where the concentration of a given nuclide increased with increasing compact radius or there was an increase in the concentration at the outermost segment of the compact. It was unclear why this might be. Hypotheses include trapping at features or microstructures unique to the compact surface that may have been the consequence of the fabrication process or the evolution of those features under irradiation. Or perhaps fronts of fission products that originated in the DTF particles are being driven out of the compact as this DTF-source is depleted. It is also possible that very thin first segments are susceptible to a possible artifact of the RDLBL process. This artifact might conceivably arise if material was removed, but the compact was still in the early flaking phase of the deconsolidation where the compact appears to increase in diameter even as material is being deconsolidated. In that case, the volume of material removed may be underestimated, and the inventory in Segment 1 is then normalized by a smaller volume than it should be. Given the impracticality of taking video during the deconsolidation for dimensional analysis (as was done during out-of-cell trials with unirradiated samples) the potential for flaking could not be evaluated on the irradiated samples.

The data collected here will be used in comparisons to a detailed fission-product transport model of the AGR-3/4 experiment (Riet 2023, Riet and Stempien 2022). Refinements are being made to that model, with the goal of fitting it to the body of AGR-3/4 data to extract new diffusivities of key fission products in graphitic matrix and nuclear graphite.

RDLBLs have been performed on a group of AGR-3/4 compacts that were subjected to post-irradiation heating tests in the INL FACS furnace at temperatures ranging from 1200 to 1600°C. These will be useful for examining fission-product release as a function of temperature, including temperatures greater than the irradiation temperature. Another group of AGR-3/4 compacts was reirradiated for about five days in the Neutron Radiography Reactor at INL and then subjected to FACS testing at temperatures ranging from 1000 to 1600°C before RDLBL. The primary motivation for those tests was to measure the rates of release of short-lived fission products Xe-133 and I-131. Preparing reports of these results is in progress, and the long-lived fission-product inventories and concentration profiles from those tests will be compared with the as-irradiated DLBL results reported here.

7. REFERENCES

- Collin, B. P. 2015a. "AGR-3/4 Irradiation Test Final As-Run Report." INL/EXT-15-35550, Rev. 0, Idaho National Laboratory, Idaho Falls, ID. <https://doi.org/10.2172/1468992>.
- Collin, B. P. 2015b. "AGR-3/4 Irradiation Experiment Test Plan." PLN-3867, Rev. 1, Idaho National Laboratory, Idaho Falls, ID. https://art.inl.gov/trisofuels/TRISO%20Fuels%20Documents/AGR-3-4/PLN-3867_AGR-3-4_Irradiation_Experiment_Test_Plan.pdf.
- Demkowicz, P. A., J. D. Hunn, R. N. Morris, I. van Rooyen, T. Gerczak, J. M. Harp, and S. A. Ploger. 2015. "AGR-1 Post Irradiation Examination Final Report." INL/EXT-15-36407, Idaho National Laboratory, Idaho Falls, ID. <https://doi.org/10.2172/1236801>.
- Demkowicz, P. A., P. L. Winston, J. M. Harp, and S. A. Ploger. 2016. "AGR-1 Compact 5-3-1 Post-Irradiation Examination Results." INL/EXT-15-36354, Idaho National Laboratory, Idaho Falls, ID. <https://inldigitallibrary.inl.gov/sites/sti/sti/7363989.pdf>.
- Demkowicz, P. A., J. M. Harp, P. L. Winston, and S. A. Ploger. 2013. "Analysis of Fission Products on the AGR-1 Capsule Components." INL/EXT-13-28483, Idaho National Laboratory, Idaho Falls, ID. <https://art.inl.gov/trisofuels/Lists/References/Attachments/7/Analysis%20of%20Fission%20Products%20on%20the%20AGR%201%20Capsule%20Components,%20INL-EXT%2013%2028483.pdf>.
- Hawkes, G. 2016. "AGR-3/4 Daily As-Run Thermal Analyses." ECAR-2807, Rev. 1, Idaho National Laboratory, Idaho Falls, ID.
- Helmreich, G., F. C. Montgomery, and J. D. Hunn. 2015. "Development of a Radial Deconsolidation Method." ORNL/TM-2015/699, Oak Ridge National Laboratory, Oak Ridge, TN. <https://doi.org/10.2172/1235005>.
- Helmreich, G., J. D. Hunn, F. Montgomery, and D. Skitt. 2022. "Radial Deconsolidation and Leach-Burn-Leach of AGR-3/4 Compacts 1-3, 4-3, 10-1, and 10-2." ORNL/TM-2022/2586, Oak Ridge National Laboratory, Oak Ridge, TN. <https://doi.org/10.2172/1887677>.
- Helmreich, G., J. D. Hunn, F. C. Montgomery, and D. Skitt. 2021. "Radial Deconsolidation and Leach-Burn-Leach of AGR-3/4 Compacts 8-4 and 7-4." ORNL/TM-2021/2178, Oak Ridge National Laboratory, Oak Ridge, TN. <https://www.osti.gov/servlets/purl/1820768>.
- Humrickhouse, P. W., J. D. Stempien, J. M. Harp, P. A. Demkowicz, and D. A. Petti. 2018. "Preliminary Estimation of Fission Product Diffusion Coefficients from AGR-3/4 Data." Proceedings of the High Temperature Reactor, HTR 2018, Warsaw, Poland, Paper HTR 2018-3096. https://inis.iaea.org/collection/NCLCollectionStore/_Public/54/061/54061987.pdf.
- Humrickhouse, P. W., B. P. Collin, G. L. Hawkes, J. M. Harp, P. A. Demkowicz, and D. A. Petti. 2016. "Modeling and Analysis of Fission Product Transport in the AGR-3/4 Experiment." HTR 2016, Paper 18693, Las Vegas, NV. <https://www.osti.gov/servlets/purl/1358376>.
- Hunn, J. D., and R. A. Lowden. 2007. "Data Compilation for AGR-3/4 Driver Fuel Coated Particle Composite LEU03-09T." ORNL/TM-2007/019, Oak Ridge National Laboratory, Oak Ridge, TN. <https://doi.org/10.2172/931362>.
- Hunn, J. D., R. N. Morris, C. A. Baldwin, F. C. Montgomery, C. M. Silva, and T. J. Gerczak. 2013. "AGR-1 Irradiated Compact 4-4-2 PIE Report: Evaluation of As-Irradiated Fuel Performance with Leach Burn Leach, IMGA, Materialography, and X-ray Tomography." ORNL/TM-2013/236, Oak Ridge National Laboratory, Oak Ridge, TN. <https://info.ornl.gov/sites/publications/Files/Pub141765.pdf>.
- Hunn, J. D., R. A. Lowden, J. H. Miller, B. C. Jolly, M. P. Trammell, A. K. Kercher, F. C. Montgomery, and C. M. Silva. 2014. "Fabrication and Characterization of Driver Fuel Particles, Designed-to-Fail Fuel Particles, and Fuel Compacts for the US AGR-3/4 Irradiation Test." *Nuclear Engineering and Design* 271:123–130. <https://doi.org/10.1016/j.nucengdes.2013.11.020>.

- Hunn, J. D., C. A. Baldwin, T. J. Gerczak, F. C. Montgomery, R. N. Morris, C. M. Silva, P. A. Demkowicz, J. M. Harp, and S. A. Ploger. 2016. "Detection and Analysis of Particles with Failed SiC in AGR-1 Fuel Compacts." *Nuclear Engineering and Design* 306:36–46. <https://doi.org/10.1016/j.nucengdes.2015.12.011>.
- Hunn, J. D., C. A. Baldwin, F. C. Montgomery, T. J. Gerczak, R. N. Morris, G. W. Helmreich, P. A. Demkowicz, J. M. Harp, and J. D. Stempien. 2018. "Initial Examination of Fuel Compacts and TRISO Particles from the US AGR-2 Irradiation Test." *Nuclear Engineering and Design*, 329: 89-101.
- Hunn, J. D., F. C. Montgomery, D. J. Skitt, and G. W. Helmreich. 2020. "Radial Deconsolidation and Leach-Burn-Leach of AGR-3/4 Compacts 1-4 and 10-4." ORNL/TM-2020/1707, Oak Ridge National Laboratory, Oak Ridge, TN. <https://doi.org/10.2172/1709104>.
- Hunn, J. D. and J. H. Miller. 2009. "Data Compilation for AGR-3/4 Designed-to-Fail (DTF) Fuel Particle Batch LEU04-02DTF." ORNL/TM-2008/193, Oak Ridge National Laboratory, Oak Ridge, TN. <https://doi.org/10.2172/940336>.
- Idaho National Laboratory. 2022. "Technical Program Plan for INL Advanced Reactor Technologies Advanced Gas Reactor Fuel Development and Qualification Program." PLN-3636, INL/MIS-10- 20662, Rev. 11, Idaho National Laboratory, Idaho Falls, ID. <https://www.osti.gov/servlets/purl/1776792>.
- INL. 2017a. "MFC 752 AGR-3/4 Radial Deconsolidation Assembly." DWG-800150, Idaho National Laboratory, Idaho Falls, ID.
- INL. 2017b. "MFC 752 AGR-3/4 Radial Deconsolidation Stage Assembly." DWG-800151, Idaho National Laboratory, Idaho Falls, ID.
- INL. 2017c. "MFC 752 AGR-3/4 Radial Deconsolidation Drag Paddle Assembly." DWG-800152, Idaho National Laboratory, Idaho Falls, ID.
- INL. 2017d. "MFC 752 AGR-3/4 Radial Deconsolidation Glue Fixture Assembly." DWG-800153, Idaho National Laboratory, Idaho Falls, ID.
- Harp, J. M., J. D. Stempien, and P. A. Demkowicz. 2021. "Gamma Spectrometry Examination of the AGR-3/4 Irradiation." INL/EXT-20-58254, Idaho National Laboratory, Idaho Falls, ID. <https://doi.org/10.2172/1844232>.
- Hunn, J., M. P. Trammell, and F. C. Montgomery. 2011. "Data Compilation for AGR-3/4 Designed-to-Fail (DTF) Fuel Compact Lot (LEU03-10T-OP2/LEU03-07DTF-OP1)-Z." ORNL/TM-2011/124, Oak Ridge National Laboratory, Oak Ridge, TN.
- Kercher, A. K. and J. D. Hunn. 2006. "Results from ORNL Characterization of Nominal 350 μm LEUCO Kernels (LEU03) from the BWXT G73V-20-69303 Composite." ORNL/TM-2006/552, Oak Ridge National Laboratory, Oak Ridge, TN. <https://info.ornl.gov/sites/publications/files/Pub3190.pdf>.
- Kercher, A. K., B. C. Jolly, F. C. Montgomery, G. W. C. Silva, and J. D. Hunn. 2011. "Data Compilation for AGR-3/4 Designed-to-Fail (DTF) Fuel Particle Batch LEU03-07DTF," ORNL/TM-2011/109, Oak Ridge National Laboratory, Oak Ridge, TN. <https://doi.org/10.2172/1649083>.
- Riet, A. A. 2022. "Reconstruction of Fission Product Distribution from Tomographic Scans in TRISO Fuel Graphitic Matrix and Nuclear Grade Graphites." INL/RPT-22-67635, Idaho National Laboratory, Idaho Falls, ID. <https://www.osti.gov/biblio/1875923>.
- Riet, A. A. and J. D. Stempien. 2022. "Comparison of AGR-3/4 Fission Product Transport Model to Measurements and Extraction of Diffusivities via Analytical Fits." INL/RPT-22-69040, Idaho National Laboratory, Idaho Falls, ID. <https://www.osti.gov/biblio/1906455>.
- Riet, A. A. 2023. "Status of Modifications to the AGR-3/4 Fission Product Transport Model." INL/RPT-23-74853, Idaho National Laboratory, Idaho Falls, ID. https://inldigitallibrary.inl.gov/sites/sti/sti/Sort_68062.pdf

- Stempien, J. D., L. Cai, and P. A. Demkowicz. 2023. "AGR TRISO Fuel Fission Product Release Data Summary." INL/RPT-23-74651, Idaho National Laboratory, Idaho Falls, ID. <https://www.osti.gov/biblio/2202411>.
- Stempien, J. D., J. D. Hunn, R. N. Morris, T. J. Gerczak, and P. A. Demkowicz. 2021. "AGR-2 TRISO Fuel Post-Irradiation Examination Final Report." INL/EXT-21-64279, Idaho National Laboratory, Idaho Falls, ID. <https://www.osti.gov/biblio/1822447>.
- Stempien, J. D. 2021. "Measurement of Fission Product Concentration Profiles in AGR-3/4 TRISO Fuel Graphitic Matrix and Nuclear Graphites." INL/EXT-21-62863, Idaho National Laboratory, Idaho Falls, ID. <https://www.osti.gov/biblio/1811841>.
- Stempien, J. D., 2020. "AGR-2 Compact 6-4-1 Post-Irradiation Examination Results." INL/EXT-18-45418, Idaho National Laboratory, Idaho Falls, ID. <https://www.osti.gov/biblio/1897106>.
- Stempien, J. D. 2017. "Radial Deconsolidation and Leach-burn-leach of AGR-3/4 Compacts 3-3, 12-1, and 12-3." INL/EXT-17-43182, Idaho National Laboratory, Idaho Falls, ID. <https://doi.org/10.2172/1408764>.
- Stempien, J. D., F. J. Rice, P. L. Winston, and J. M. Harp. 2016. "AGR-3/4 Irradiation Test Train Disassembly and Component Metrology First Look Report." INL/EXT-16-38005, Rev. 1, Idaho National Laboratory, Idaho Falls, ID. <https://doi.org/10.2172/1364232>.
- Stempien, J. D., P. A. Demkowicz, J. M. Harp, and P. L. Winston. 2018. "AGR-3/4 Experiment Preliminary Mass Balance." INL/EXT-18-46049, Idaho National Laboratory, Idaho Falls, ID. <https://doi.org/10.2172/1558760>.
- Sterbentz, J. W. 2015. "JMOCUP As-Run Daily Physics Depletion Calculation for the AGR-3/4 TRISO Particle Experiment in ATR Northeast Flux Trap." Rev. 1, ECAR-2753, Idaho National Laboratory, Idaho Falls, ID. <https://www.osti.gov/biblio/1774808>.

Appendix A
Additional RDLBL Data

Page intentionally left blank

Appendix A

Additional RDLBL Data

The tables in this appendix present the RDLBL data for selected fission products in units of activity (Bq) and compact fraction. This appendix also documents selected actinides by mass (μg) and compact fraction. These tables summarize the same results as the particle-equivalent tables in Section 5, but different units are used here. As the prior sections of this report have discussed, TRISO-coated driver particles were accidentally damaged in some steps of the RDLBL of some compacts. Where possible, corrections were made to account for that accidental damage. In those cases, the tables list both the corrected and uncorrected results. In some instances, accidental damage was so widespread that corrections could not be reasonably made. This was the case for Compacts 3-3 and 10-3. The reader must refer to the earlier sections in the body of the report to properly interpret and use the data summarized in this appendix.

A-1. Compact 3-3

Table 73. Activities of fission products measured in the solutions from RDLBL of Compact 3-3. All values were decay-corrected to EOI + 1 day. See Section 4.1 for a discussion of this compact, which had many particles damaged during RDLBL of Segment 1 and DLBL of the core, but could not be corrected due to the number of particles affected.

Activity (Bq)		Ag-110m	Ce-144	Cs-134	Cs-137	Eu-154	Eu-155	Ru-106	Sb-125	Sr-90
Segment #1	Decon	<3.7E+4	4.59E+7	2.98E+5	5.60E+5	8.48E+4	6.15E+4	7.88E+6	1.34E+5	9.38E+5
	Pre-burn leach 1	<1.1E+5	2.62E+5	6.83E+5	8.89E+5	2.00E+4	1.22E+4	9.09E+5	<2.6E+4	3.54E+6
	Pre-burn leach 2	<1.5E+5	6.06E+7	1.89E+6	4.74E+6	7.83E+4	6.65E+4	8.83E+6	<3.7E+4	2.73E+4
	Post-burn leach 1	<1.5E+5	3.18E+6	1.65E+6	2.18E+6	1.61E+5	1.35E+5	<1.1E+6	4.63E+4	3.03E+4
	Post-burn leach 2	<3.7E+4	<7.4E+4	2.67E+4	8.11E+4	2.58E+3	<1.9E+3	<7.4E+4	<7.4E+3	1.38E+4
	SUM (MDA = 0)	0	1.10E+8	4.55E+6	8.45E+6	3.46E+5	2.75E+5	1.76E+7	1.81E+5	4.55E+6
Segment #2	Decon	<3.7E+4	2.30E+6	2.32E+5	5.88E+5	3.93E+4	3.18E+4	6.25E+6	1.83E+4	1.34E+6
	Pre-burn leach 1	<3.7E+4	<1.9E+5	5.73E+3	3.04E+4	1.40E+4	1.01E+4	6.90E+5	<7.4E+3	1.91E+5
	Pre-burn leach 2	<3.7E+4	5.92E+5	5.70E+4	3.92E+5	<3.3E+3	<7.4E+3	3.49E+5	7.23E+3	1.81E+5
	Post-burn leach 1	<7.4E+4	1.84E+6	8.86E+3	4.58E+4	1.15E+5	9.57E+4	<2.2E+5	1.50E+4	1.64E+6
	Post-burn leach 2	<3.7E+4	<7.4E+4	<2.6E+3	2.31E+4	<1.9E+3	<3.7E+3	<1.1E+5	<3.7E+3	2.30E+4
	SUM (MDA = 0)	0	4.73E+6	3.03E+5	1.08E+6	1.69E+5	1.38E+5	7.29E+6	4.06E+4	3.37E+6
Segment #3	Decon	<3.7E+4	3.06E+6	2.35E+5	6.36E+5	1.75E+4	1.87E+4	5.80E+6	1.92E+4	9.44E+5
	Pre-burn leach 1	<3.0E+4	<7.4E+4	7.75E+3	8.12E+4	5.39E+3	4.31E+3	2.55E+5	<7.4E+3	7.78E+4
	Pre-burn leach 2	<3.0E+4	<7.4E+4	1.36E+3	1.67E+4	<1.9E+3	<3.7E+3	<1.1E+4	<3.7E+3	1.85E+4
	Post-burn leach 1	<3.7E+4	4.64E+5	1.92E+3	4.74E+3	2.97E+4	2.56E+4	<1.1E+5	<3.7E+3	4.52E+5
	Post-burn leach 2	<2.6E+4	3.58E+5	1.44E+3	4.50E+3	2.21E+4	1.85E+4	<7.4E+4	<3.7E+3	3.18E+5
	SUM (MDA = 0)	0	3.88E+6	2.48E+5	7.44E+5	7.48E+4	6.71E+4	6.06E+6	1.92E+4	1.81E+6

Activity (Bq)		Ag-110m	Ce-144	Cs-134	Cs-137	Eu-154	Eu-155	Ru-106	Sb-125	Sr-90
Segment #4	Decon	<3.7E+5	2.55E+7	2.31E+6	6.08E+6	2.01E+5	1.85E+5	4.06E+7	1.83E+5	8.96E+6
	Pre-burn leach 1	<3.7E+4	<1.9E+5	6.86E+3	5.90E+4	1.24E+4	9.33E+3	4.59E+5	<7.4E+3	1.55E+5
	Pre-burn leach 2	<2.6E+4	<7.4E+4	<1.1E+3	2.45E+3	6.31E+3	4.54E+3	<7.4E+4	<3.7E+3	2.30E+4
	Post-burn leach 1	<2.6E+4	<1.9E+5	<2.6E+3	2.87E+3	4.43E+4	3.57E+4	<7.4E+4	7.99E+3	6.13E+5
	Post-burn leach 2	<1.9E+4	<3.7E+4	<1.1E+3	3.12E+3	<1.1E+3	<7.4E+2	<3.7E+4	<2.2E+3	1.11E+4
	SUM (MDA = 0)	0	2.55E+7	2.31E+6	6.15E+6	2.64E+5	2.35E+5	4.11E+7	1.91E+5	9.77E+6
Core	Decon	<2.2E+5	2.68E+8	5.02E+6	1.16E+7	2.67E+5	2.90E+5	4.86E+7	4.97E+5	1.60E+7
	Pre-burn leach 1	<7.4E+5	3.94E+8	1.05E+7	1.26E+7	4.13E+5	2.56E+5	1.31E+8	5.02E+5	1.38E+7
	Pre-burn leach 2	<1.5E+5	2.78E+7	2.37E+6	3.00E+6	4.47E+4	2.89E+4	4.67E+6	1.40E+5	1.64E+6
	Post-burn leach 1	<3.0E+5	5.76E+8	3.14E+6	3.97E+6	9.13E+5	7.61E+5	3.33E+6	1.24E+6	1.67E+7
	Post-burn leach 2	<7.4E+4	5.23E+6	2.25E+5	3.05E+5	1.56E+4	1.01E+4	2.02E+6	8.64E+4	1.73E+5
	SUM (MDA = 0)	0	1.27E+9	2.13E+7	3.15E+7	1.65E+6	1.35E+6	1.90E+8	2.46E+6	4.84E+7
Compact TOTAL (MDA = 0)		0	1.42E+9	2.87E+7	4.80E+7	2.51E+6	2.06E+6	2.62E+8	2.89E+6	6.79E+7

Table 74. Fraction (M/C) of the compact inventory of fission products measured in the solutions from RDLBL of Compact 3-3. All values were decay-corrected to EOI + 1 day. See Section 4.1 for a discussion of this compact, which had many particles damaged during RDLBL of Segment 1 and DLBL of the core, but could not be corrected due to the number of particles affected.

Compact Fraction		Ag-110m	Ce-144	Cs-134	Cs-137	Eu-154	Eu-155	Ru-106	Sb-125	Sr-90
Segment #1	Decon	<5.2E-4	4.74E-4	4.25E-5	8.77E-5	3.72E-4	4.01E-4	3.90E-4	2.72E-4	1.68E-4
	Pre-burn leach 1	<1.6E-3	2.70E-6	9.74E-5	1.39E-4	8.79E-5	7.93E-5	4.49E-5	<5.2E-5	6.35E-4
	Pre-burn leach 2	<2.1E-3	6.25E-4	2.69E-4	7.42E-4	3.44E-4	4.33E-4	4.36E-4	<7.5E-5	4.90E-6
	Post-burn leach 1	<2.1E-3	3.28E-5	2.35E-4	3.42E-4	7.05E-4	8.78E-4	<5.5E-5	9.38E-5	5.44E-6
	Post-burn leach 2	<5.2E-4	<7.6E-7	3.81E-6	1.27E-5	1.13E-5	<1.2E-5	<3.7E-6	<1.5E-5	2.47E-6
	SUM (MDA = 0)	0	1.13E-3	6.48E-4	1.32E-3	1.52E-3	1.79E-3	8.71E-4	3.66E-4	8.16E-4
Segment #2	Decon	<5.2E-4	2.37E-5	3.30E-5	9.21E-5	1.72E-4	2.07E-4	3.09E-4	3.72E-5	2.41E-4
	Pre-burn leach 1	<5.2E-4	<1.9E-6	8.16E-7	4.76E-6	6.16E-5	6.59E-5	3.41E-5	<1.5E-5	3.42E-5
	Pre-burn leach 2	<5.2E-4	6.11E-6	8.13E-6	6.13E-5	<1.5E-5	<4.8E-5	1.73E-5	1.46E-5	3.26E-5
	Post-burn leach 1	<1.0E-3	1.90E-5	1.26E-6	7.16E-6	5.06E-4	6.23E-4	<1.1E-5	3.04E-5	2.94E-4
	Post-burn leach 2	<5.2E-4	<7.6E-7	<3.7E-7	3.62E-6	<8.1E-6	<2.4E-5	<5.5E-6	<7.5E-6	4.13E-6
	SUM (MDA = 0)	0	4.88E-5	4.32E-5	1.69E-4	7.40E-4	8.96E-4	3.60E-4	8.22E-5	6.05E-4
Segment #3	Decon	<5.2E-4	3.16E-5	3.35E-5	9.96E-5	7.70E-5	1.22E-4	2.87E-4	3.89E-5	1.69E-4
	Pre-burn leach 1	<4.2E-4	<7.6E-7	1.10E-6	1.27E-5	2.36E-5	2.81E-5	1.26E-5	<1.5E-5	1.40E-5
	Pre-burn leach 2	<4.2E-4	<7.6E-7	1.93E-7	2.62E-6	<8.1E-6	<2.4E-5	<5.5E-7	<7.5E-6	3.32E-6
	Post-burn leach 1	<5.2E-4	4.78E-6	2.73E-7	7.42E-7	1.30E-4	1.67E-4	<5.5E-6	<7.5E-6	8.10E-5
	Post-burn leach 2	<3.7E-4	3.70E-6	2.05E-7	7.04E-7	9.71E-5	1.20E-4	<3.7E-6	<7.5E-6	5.71E-5
	SUM (MDA = 0)	0	4.01E-5	3.53E-5	1.16E-4	3.28E-4	4.37E-4	2.99E-4	3.89E-5	3.25E-4

Compact Fraction		Ag-110m	Ce-144	Cs-134	Cs-137	Eu-154	Eu-155	Ru-106	Sb-125	Sr-90
Segment #4	Decon	<5.2E-3	2.63E-4	3.29E-4	9.52E-4	8.81E-4	1.21E-3	2.01E-3	3.72E-4	1.61E-3
	Pre-burn leach 1	<5.2E-4	<1.9E-6	9.77E-7	9.24E-6	5.43E-5	6.07E-5	2.27E-5	<1.5E-5	2.78E-5
	Pre-burn leach 2	<3.7E-4	<7.6E-7	<1.6E-7	3.83E-7	2.77E-5	2.96E-5	<3.7E-6	<7.5E-6	4.14E-6
	Post-burn leach 1	<3.7E-4	<1.9E-6	<3.7E-7	4.49E-7	1.94E-4	2.33E-4	<3.7E-6	1.62E-5	1.10E-4
	Post-burn leach 2	<2.6E-4	<3.8E-7	<1.6E-7	4.88E-7	<4.9E-6	<4.8E-6	<1.8E-6	<4.5E-6	1.99E-6
	SUM (MDA = 0)	0	2.63E-4	3.30E-4	9.63E-4	1.16E-3	1.53E-3	2.03E-3	3.88E-4	1.75E-3
Core	Decon	<3.1E-3	2.77E-3	7.16E-4	1.82E-3	1.17E-3	1.89E-3	2.40E-3	1.01E-3	2.87E-3
	Pre-burn leach 1	<1.0E-2	4.06E-3	1.50E-3	1.98E-3	1.81E-3	1.67E-3	6.47E-3	1.02E-3	2.48E-3
	Pre-burn leach 2	<2.1E-3	2.86E-4	3.38E-4	4.70E-4	1.96E-4	1.88E-4	2.31E-4	2.84E-4	2.95E-4
	Post-burn leach 1	<4.2E-3	5.94E-3	4.47E-4	6.22E-4	4.00E-3	4.96E-3	1.64E-4	2.51E-3	3.00E-3
	Post-burn leach 2	<1.0E-3	5.40E-5	3.20E-5	4.78E-5	6.83E-5	6.56E-5	9.98E-5	1.75E-4	3.11E-5
	SUM (MDA = 0)	0	1.31E-2	3.03E-3	4.94E-3	7.25E-3	8.77E-3	9.37E-3	4.99E-3	8.68E-3
Compact TOTAL (MDA = 0)		0	1.46E-2	4.09E-3	7.51E-3	1.10E-2	1.34E-2	1.29E-2	5.87E-3	1.22E-2

Table 75. Masses for select actinides from ICP-MS analyses of solutions from Compact 3-3 RDLBL. See Section 4.1 for a discussion of this compact, which had many particles damaged during RDLBL of Segment 1 and DLBL of the core, but could not be corrected due to the number of particles affected.

		Mass (µg)					
		Pu-239	Pu-240	U-234	U-235	U-236	U-238
Segment #1	Decon	<7	<1	<3	18.4	<6	188
	Pre-burn leach 1	<34	<6	<17	<22	<3	<15
	Pre-burn leach 2	<23	<4	<12	40.3	8.39	461
	Post-burn leach 1	<29	<5	<14	<18	<3	<12
	Post-burn leach 2	<31	<5	<15	<19	<3	<13
	Total (MDA = 0)	0	0	0	58.7	8.39	649
Segment #2	Decon	<7	<1	<3	14.7	4.03	146
	Pre-burn leach 1	<30	<5	<15	<19	<3	<13
	Pre-burn leach 2	<35	<6	<17	<22	<4	<19
	Post-burn leach 1	<27	<5	<14	<17	<3	<12
	Post-burn leach 2	<33	<5	<16	<21	<3	<14
	Total (MDA = 0)	0	0	0	14.7	4.03	146
Segment #3	Decon	1.39	0.37	0.21	15.2	4.58	160
	Pre-burn leach 1	<0.3	<0.02	<0.1	0.31	<0.06	2.06
	Pre-burn leach 2	<0.3	<0.02	<0.2	<0.1	<0.08	1.35
	Post-burn leach 1	<0.3	<0.05	<0.1	<0.1	<0.07	1.13
	Post-burn leach 2	<22	<4	<11	<14	<2	<10
	Total (MDA = 0)	1.39	0.37	0.21	15.5	4.58	165

		Mass (µg)					
		Pu-239	Pu-240	U-234	U-235	U-236	U-238
Segment #4	Decon	1.17	0.32	<0.2	10.9	3.31	116
	Pre-burn leach 1	<0.6	<0.3	<0.7	<0.7	<0.3	3.95
	Pre-burn leach 2	<0.5	<0.2	<0.6	<0.6	<0.2	<0.9
	Post-burn leach 1	<0.5	<0.2	<0.6	<0.5	<0.2	0.98
	Post-burn leach 2	<0.1	<0.07	<0.07	<0.1	<0.04	<0.2
	Total (MDA = 0)	1.17	0.32	0	10.9	3.31	121
Core	Decon	30.1	9.67	<6	288	88.5	3060
	Pre-burn leach 1	28.3	10.4	<10	169	51.4	1770
	Pre-burn leach 2	0.72	0.30	<0.04	1.88	0.62	21.9
	Post-burn leach 1	10.8	5.55	<0.06	2.35	<0.8	25.0
	Post-burn leach 2	0.17	<0.08	<0.02	<0.09	<0.1	<0.6
	Total (MDA = 0)	70.1	25.9	0	461	141	4877
Compact Total (MDA) = 0		72.7	26.6	0.21	561	161	5957

Table 76. Compact fractions for select actinides from ICP-MS of solutions from Compact 3-3 RDLBL. See Section 4.1 for a discussion of this compact, which had many particles damaged during RDLBL of Segment 1 and DLBL of the core, but could not be corrected due to the number of particles affected.

		Compact Fraction					
		Pu-239	Pu-240	U-234	U-235	U-236	U-238
Segment #1	Decon	<1.4E-3	<5.6E-4	<6.6E-3	5.93E-4	<6.0E-4	5.49E-4
	Pre-burn leach 1	<6.7E-3	<3.3E-3	<3.8E-2	<7.1E-4	<3.0E-4	<4.4E-5
	Pre-burn leach 2	<4.6E-3	<2.2E-3	<2.7E-2	1.30E-3	8.45E-4	1.35E-3
	Post-burn leach 1	<5.7E-3	<2.8E-3	<3.1E-2	<5.8E-4	<3.0E-4	<3.5E-5
	Post-burn leach 2	<6.1E-3	<2.8E-3	<3.3E-2	<6.1E-4	<3.0E-4	<3.8E-5
	Total (MDA = 0)	0	0	0	1.89E-3	8.45E-4	1.89E-3
Segment #2	Decon	<1.4E-3	<5.6E-4	<6.6E-3	4.72E-4	4.06E-4	4.25E-4
	Pre-burn leach 1	<5.9E-3	<2.8E-3	<3.3E-2	<6.1E-4	<3.0E-4	<3.8E-5
	Pre-burn leach 2	<6.9E-3	<3.3E-3	<3.8E-2	<7.1E-4	<4.0E-4	<5.5E-5
	Post-burn leach 1	<5.4E-3	<2.8E-3	<3.1E-2	<5.5E-4	<3.0E-4	<3.5E-5
	Post-burn leach 2	<6.5E-3	<2.8E-3	<3.5E-2	<6.8E-4	<3.0E-4	<4.1E-5
	Total (MDA = 0)	0	0	0	4.72E-4	4.06E-4	4.25E-4
Segment #3	Decon	2.76E-4	2.08E-4	4.58E-4	4.89E-4	4.61E-4	4.67E-4
	Pre-burn leach 1	<5.9E-5	<1.1E-5	<2.2E-4	1.01E-5	<6.0E-6	6.01E-6
	Pre-burn leach 2	<5.9E-5	<1.1E-5	<4.4E-4	<3.2E-6	<8.1E-6	3.95E-6
	Post-burn leach 1	<5.9E-5	<2.8E-5	<2.2E-4	<3.2E-6	<7.0E-6	3.31E-6
	Post-burn leach 2	<4.4E-3	<2.2E-3	<2.4E-2	<4.5E-4	<2.0E-4	<2.9E-5
	Total (MDA = 0)	2.76E-4	2.08E-4	4.58E-4	4.99E-4	4.61E-4	4.81E-4

		Compact Fraction					
		Pu-239	Pu-240	U-234	U-235	U-236	U-238
Segment #4	Decon	2.32E-4	1.77E-4	<4.4E-4	3.51E-4	3.33E-4	3.39E-4
	Pre-burn leach 1	<1.2E-4	<1.7E-4	<1.5E-3	<2.3E-5	<3.0E-5	1.15E-5
	Pre-burn leach 2	<9.9E-5	<1.1E-4	<1.3E-3	<1.9E-5	<2.0E-5	<2.6E-6
	Post-burn leach 1	<9.9E-5	<1.1E-4	<1.3E-3	<1.6E-5	<2.0E-5	2.85E-6
	Post-burn leach 2	<2.0E-5	<3.9E-5	<1.5E-4	<3.2E-6	<4.0E-6	<5.8E-7
	Total (MDA = 0)	2.32E-4	1.77E-4	0	3.51E-4	3.33E-4	3.53E-4
Core	Decon	5.97E-3	5.40E-3	<1.3E-2	9.28E-3	8.91E-3	8.93E-3
	Pre-burn leach 1	5.61E-3	5.81E-3	<2.2E-2	5.44E-3	5.17E-3	5.17E-3
	Pre-burn leach 2	1.43E-4	1.70E-4	<8.9E-5	6.05E-5	6.25E-5	6.39E-5
	Post-burn leach 1	2.14E-3	3.10E-3	<1.3E-4	7.57E-5	<8.1E-5	7.30E-5
	Post-burn leach 2	3.31E-5	<4.5E-5	<4.4E-5	<2.9E-6	<1.0E-5	<1.8E-6
	Total (MDA = 0)	1.39E-2	1.45E-2	0	1.49E-2	1.41E-2	1.42E-2
Compact Total (MDA = 0)		1.44E-2	1.49E-2	4.58E-4	1.81E-2	1.62E-2	1.74E-2

A-2. Compact 5-3

Table 77. Activities of fission products measured in the solutions from RDLBL of Compact 5-3. All values were decay-corrected to EOI + 1 day. For Segment 1 post-burn leach 1, Segment 1 sum, and compact sum, the data include both uncorrected and corrected values, as discussed in Section 4.2.

Activity (Bq)		Ag-110m	Ce-144	Cs-134	Cs-137	Eu-154	Eu-155	Ru-106	Sb-125	Sr-90
Segment #1	Decon	<3E+05	<3E+06	2.94E+06	2.49E+06	<4E+03	<1E+04	<1E+06	<7E+04	1.92E+04
	Pre-burn leach 1	<2E+05	<7E+05	3.84E+05	4.23E+05	<3E+03	<4E+03	<7E+05	<2E+04	5.86E+03
	Pre-burn leach 2	<1E+05	<7E+05	5.04E+04	5.39E+04	<3E+03	<7E+03	<4E+05	<1E+04	2.22E+03
	Post-burn leach 1	<7E+05	5.40E+07	2.18E+06	2.31E+06	1.23E+05	9.33E+04	<3E+06	1.26E+05	3.41E+06
	Post-burn leach 1 - corrected	<7E+05	0	0	0	0	0	<3E+06	0	7.29E+04
	Post-burn leach 2	<1E+05	<7E+05	1.64E+04	1.25E+04	<2E+03	<7E+03	1.80E+05	1.24E+04	4.63E+03
	SUM (MDA = 0)	0	5.40E+07	5.57E+06	5.29E+06	1.23E+05	9.33E+04	1.80E+05	1.39E+05	3.44E+06
	SUM (MDA = 0) - corrected	0	0	3.39E+06	2.98E+06	0	0	1.80E+05	1.24E+04	1.05E+05
Segment #2	Decon	<2E+05	6.63E+05	1.38E+06	1.62E+06	<2E+03	<7E+03	<1E+06	<3E+04	2.63E+04
	Pre-burn leach 1	<2E+05	<7E+05	2.74E+05	2.94E+05	<3E+03	<7E+03	<1E+06	<3E+04	3.94E+03
	Pre-burn leach 2	<1E+05	<7E+05	4.44E+04	4.43E+04	<2E+03	<4E+03	<4E+05	<1E+04	1.01E+03
	Post-burn leach 1	<3E+05	<7E+05	4.27E+05	4.43E+05	3.70E+03	<7E+03	<1E+06	<3E+04	1.95E+03
	Post-burn leach 2	<1E+05	<3E+05	5.07E+03	5.81E+03	<1E+03	<4E+03	<2E+05	<4E+03	6.24E+02
	SUM (MDA = 0)	0	6.63E+05	2.13E+06	2.41E+06	3.70E+03	0	0	0	3.38E+04

Activity (Bq)		Ag-110m	Ce-144	Cs-134	Cs-137	Eu-154	Eu-155	Ru-106	Sb-125	Sr-90
Segment #3	Decon	<3E+05	2.90E+06	3.45E+06	4.20E+06	7.16E+03	9.12E+03	<2E+06	<4E+04	5.63E+05
	Pre-burn leach 1	<1E+05	<7E+05	3.30E+05	3.55E+05	<3E+03	<7E+03	<1E+06	<3E+04	3.00E+03
	Pre-burn leach 2	<1E+05	<7E+05	4.32E+04	4.70E+04	<2E+03	<4E+03	<4E+05	<1E+04	1.02E+03
	Post-burn leach 1	<4E+05	6.65E+07	4.18E+06	4.63E+06	1.51E+05	1.19E+05	1.10E+06	1.57E+05	7.15E+06
	Post-burn leach 2	<2E+05	3.53E+05	3.32E+04	3.60E+04	<3E+03	<7E+03	5.67E+05	1.87E+04	8.13E+03
	SUM (MDA = 0)	0	6.97E+07	8.04E+06	9.27E+06	1.58E+05	1.28E+05	1.67E+06	175780.67	7.72E+06
Core	Decon	<1E+06	5.52E+08	6.41E+06	1.16E+07	9.80E+05	7.96E+05	5.78E+07	1.09E+06	2.40E+07
	Pre-burn leach 1	<1E+06	4.49E+08	2.41E+06	4.43E+06	6.86E+05	5.43E+05	6.22E+07	5.41E+05	2.15E+07
	Pre-burn leach 2	<2E+05	2.27E+06	1.02E+05	1.20E+05	1.15E+04	6.69E+03	4.46E+06	2.15E+05	4.35E+05
	Post-burn leach 1	<7E+05	6.06E+07	1.13E+06	1.45E+06	5.17E+05	4.00E+05	7.54E+06	1.28E+06	2.15E+07
	Post-burn leach 2	<2E+05	3.64E+05	4.21E+04	6.31E+04	<3E+03	<7E+03	1.27E+06	1.23E+05	3.66E+04
	SUM (MDA = 0)	0	1.06E+09	1.01E+07	1.77E+07	2.19E+06	1.74E+06	1.33E+08	3.25E+06	6.75E+07
Compact TOTAL (MDA = 0)		0	1.19E+09	2.58E+07	3.47E+07	2.48E+06	1.97E+06	1.35E+08	3.56E+06	7.87E+07
Compact TOTAL (MDA = 0) - corrected		0	1.13E+09	2.37E+07	3.23E+07	2.36E+06	1.87E+06	1.35E+08	3.44E+06	7.54E+07

Table 78. Fraction (M/C) of the compact inventory of fission products measured in the solutions from RDLBL of Compact 5-3. All values were decay-corrected to EOI + 1 day. For Segment 1 post-burn leach 1, segment 1 sum, and compact sum, the data include both uncorrected and corrected values, as discussed in Section 4.2.

Compact Fraction		Ag-110m	Ce-144	Cs-134	Cs-137	Eu-154	Eu-155	Ru-106	Sb-125	Sr-90
Segment #1	Decon	<3E-03	<2E-05	2.91E-04	3.33E-04	<1E-05	<7E-05	<4E-05	<1E-04	2.99E-06
	Pre-burn leach 1	<2E-03	<7E-06	3.81E-05	5.64E-05	<8E-06	<2E-05	<3E-05	<3E-05	9.15E-07
	Pre-burn leach 2	<1E-03	<7E-06	4.99E-06	7.20E-06	<1E-05	<4E-05	<1E-05	<2E-05	3.46E-07
	Post-burn leach 1	<6E-03	4.86E-04	2.16E-04	3.08E-04	3.95E-04	4.57E-04	<1E-04	2.12E-04	5.33E-04
	Post-burn leach 1 corrected	<6E-03	0	0	0	0	0	<1E-04	0	1.14E-05
	Post-burn leach 2	<1E-03	<7E-06	1.63E-06	1.66E-06	<7E-06	<4E-05	6.77E-06	2.08E-05	7.23E-07
	SUM (MDA = 0)	0	4.86E-04	5.52E-04	7.06E-04	3.95E-04	4.57E-04	6.77E-06	2.32E-04	5.38E-04
	SUM (MDA = 0) corrected	0	0	3.36E-04	3.98E-04	0	0	6.77E-06	2.08E-05	1.64E-05
Segment #2	Decon	<2E-03	5.97E-06	1.37E-04	2.17E-04	<7E-06	<4E-05	<4E-05	<4E-05	4.10E-06
	Pre-burn leach 1	<2E-03	<7E-06	2.71E-05	3.93E-05	<1E-05	<4E-05	<4E-05	<4E-05	6.15E-07
	Pre-burn leach 2	<1E-03	<7E-06	4.40E-06	5.92E-06	<7E-06	<2E-05	<1E-05	<2E-05	1.57E-07
	Post-burn leach 1	<2E-03	<7E-06	4.23E-05	5.91E-05	1.19E-05	<4E-05	<4E-05	<4E-05	3.05E-07
	Post-burn leach 2	<1E-03	<3E-06	5.03E-07	7.76E-07	<5E-06	<2E-05	<8E-06	<6E-06	9.74E-08
	SUM (MDA = 0)	0	5.97E-06	2.11E-04	3.22E-04	1.19E-05	0	0	0	5.28E-06

Compact Fraction		Ag-110m	Ce-144	Cs-134	Cs-137	Eu-154	Eu-155	Ru-106	Sb-125	Sr-90
Segment #3	Decon	<3E-03	2.62E-05	3.42E-04	5.61E-04	2.30E-05	4.47E-05	<8E-05	<6E-05	8.79E-05
	Pre-burn leach 1	<1E-03	<7E-06	3.27E-05	4.74E-05	<1E-05	<4E-05	<4E-05	<4E-05	4.68E-07
	Pre-burn leach 2	<1E-03	<7E-06	4.28E-06	6.27E-06	<7E-06	<2E-05	<1E-05	<2E-05	1.59E-07
	Post-burn leach 1	<3E-03	5.99E-04	4.14E-04	6.18E-04	4.86E-04	5.82E-04	4.15E-05	2.64E-04	1.12E-03
	Post-burn leach 2	<2E-03	3.18E-06	3.29E-06	4.81E-06	<8E-06	<4E-05	2.14E-05	3.14E-05	1.27E-06
	SUM (MDA = 0)	0	6.28E-04	7.96E-04	1.24E-03	5.09E-04	6.27E-04	6.29E-05	2.95E-04	1.21E-03
Core	Decon	<1E-02	4.97E-03	6.35E-04	1.55E-03	3.15E-03	3.90E-03	2.18E-03	1.83E-03	3.75E-03
	Pre-burn leach 1	<1E-02	4.05E-03	2.39E-04	5.91E-04	2.20E-03	2.66E-03	2.34E-03	9.08E-04	3.36E-03
	Pre-burn leach 2	<2E-03	2.04E-05	1.01E-05	1.60E-05	3.69E-05	3.28E-05	1.68E-04	3.60E-04	6.80E-05
	Post-burn leach 1	<6E-03	5.46E-04	1.12E-04	1.94E-04	1.66E-03	1.96E-03	2.84E-04	2.15E-03	3.37E-03
	Post-burn leach 2	<2E-03	3.28E-06	4.17E-06	8.42E-06	<8E-06	<4E-05	4.79E-05	2.06E-04	5.72E-06
	SUM (MDA = 0)	0	9.59E-03	1.00E-03	2.36E-03	7.05E-03	8.55E-03	5.02E-03	5.45E-03	1.05E-02
Compact TOTAL (MDA = 0)		0	1.07E-02	2.56E-03	4.62E-03	7.97E-03	9.64E-03	5.09E-03	5.98E-03	1.23E-02
Compact TOTAL (MDA = 0) corrected		0	1.02E-02	2.34E-03	4.32E-03	7.57E-03	9.18E-03	5.09E-03	5.77E-03	1.18E-02

Table 79. Masses for select actinides from ICP-MS of solutions from Compact 5-3 RDLBL. For Segment 1 post-burn-leach 1, Segment 1 sum, and compact sum, the data include both uncorrected and corrected values, as discussed in Section 4.2.

Mass (µg)		Pu-239	Pu-240	U-234	U-235	U-236	U-238
Segment #1	Decon	0.04	<3E-02	<2E-02	0.38	0.10	3.62
	Pre-burn leach 1	<6E-02	<9E-02	<7E-02	<6E-02	<7E-02	0.39
	Pre-burn leach 2	<1E-01	<2E-01	<1E-01	<1E-01	<1E-01	<1E-01
	Post-burn leach 1	2.17	0.82	0.16	9.26	4.61	135.33
	Post-burn leach 1 corrected	0	0	0	0	0	0
	Post-burn leach 2	<8E-02	<1E-01	<1E-01	<8E-02	<1E-01	<1E-01
	SUM (MDA = 0)	2.22	0.82	0.16	9.64	4.71	139.34
	SUM (MDA = 0) corrected	0.04	0	0	0.38	0.10	4.01
Segment #2	Decon	0.05	<3E-02	<3E-02	0.28	0.13	3.97
	Pre-burn leach 1	<9E-02	<1E-01	<1E-01	<1E-01	<6E-02	0.29
	Pre-burn leach 2	<9E-02	<1E-01	<1E-01	<1E-01	<6E-02	<1E-01
	Post-burn leach 1	<9E-02	<1E-01	<1E-01	<1E-01	<6E-02	<1E-01
	Post-burn leach 2	<8E-02	<8E-02	<9E-02	<1E-01	<5E-02	<1E-01
	SUM (MDA = 0)	0.05	0.00	0.00	0.28	0.13	4.26

	Mass (μg)	Pu-239	Pu-240	U-234	U-235	U-236	U-238
Segment #3	Decon	0.11	0.04	<5E-02	1.14	0.51	16.13
	Pre-burn leach 1	<1E-01	<7E-02	<1E-01	<9E-02	<1E-01	0.24
	Pre-burn leach 2	<2E-01	<1E-01	<1E-01	<1E-01	<2E-01	<1E-01
	Post-burn leach 1	2.65	1.06	0.19	11.87	5.72	174.33
	Post-burn leach 2	<2E-01	<1E-01	<2E-01	<1E-01	<2E-01	0.54
	SUM (MDA = 0)	2.77	1.11	0.19	13.01	6.23	191.24
Core	Decon	22.67	9.14	2.25	125.67	60.00	1756.67
	Pre-burn leach 1	17.70	7.23	1.49	82.53	39.33	1170.00
	Pre-burn leach 2	0.23	<9E-02	<1E-01	1.43	0.64	19.80
	Post-burn leach 1	1.15	0.55	0.18	9.83	4.68	141.33
	Post-burn leach 2	<2E-01	<8E-02	<9E-02	0.63	<2E-01	3.51
	SUM (MDA = 0)	41.75	16.92	3.92	220.09	104.65	3091.31
Compact TOTAL (MDA = 0)		46.78	18.85	4.27	243.01	115.72	3426.16
Compact TOTAL (MDA = 0) Corrected		44.60	18.03	4.11	233.76	111.11	3290.82

Table 80. Compact fractions for select actinides from ICP-MS of solutions from Compact 5-3 RDLBL. For Segment 1 post-burn leach 1, Segment 1 sum, and compact sum, the data include both uncorrected and corrected values, as discussed in Section 4.2

	Compact Fraction	Pu-239	Pu-240	U-234	U-235	U-236	U-238
Segment #1	Decon	8.96E-06	<2E-05	<5E-05	1.63E-05	9.33E-06	1.07E-05
	Pre-burn leach 1	<1E-05	<5E-05	<2E-04	<3E-06	<6E-06	1.15E-06
	Pre-burn leach 2	<2E-05	<1E-04	<2E-04	<4E-06	<9E-06	<3E-07
	Post-burn leach 1	4.36E-04	4.23E-04	3.73E-04	3.97E-04	4.21E-04	4.00E-04
	Post-burn leach 1 Corrected	0	0	0	0	0	0
	Post-burn leach 2	<2E-05	<5E-05	<2E-04	<3E-06	<9E-06	<3E-07
	SUM (MDA = 0)	4.45E-04	4.23E-04	3.73E-04	4.13E-04	4.30E-04	4.11E-04
	SUM (MDA = 0) Corrected	8.96E-06	0	0	1.63E-05	9.33E-06	1.18E-05
Segment #2	Decon	9.40E-06	<2E-05	<7E-05	1.21E-05	1.18E-05	1.17E-05
	Pre-burn leach 1	<2E-05	<5E-05	<2E-04	<4E-06	<5E-06	8.45E-07
	Pre-burn leach 2	<2E-05	<5E-05	<2E-04	<4E-06	<5E-06	<3E-07
	Post-burn leach 1	<2E-05	<5E-05	<2E-04	<4E-06	<5E-06	<3E-07
	Post-burn leach 2	<2E-05	<4E-05	<2E-04	<4E-06	<5E-06	<3E-07
	SUM (MDA = 0)	9.40E-06	0.00E+00	0.00E+00	1.21E-05	1.18E-05	1.26E-05

Compact Fraction		Pu-239	Pu-240	U-234	U-235	U-236	U-238
Segment #3	Decon	2.27E-05	2.23E-05	<1E-04	4.88E-05	4.69E-05	4.76E-05
	Pre-burn leach 1	<2E-05	<4E-05	<2E-04	<4E-06	<9E-06	7.07E-07
	Pre-burn leach 2	<4E-05	<5E-05	<2E-04	<4E-06	<2E-05	<3E-07
	Post-burn leach 1	5.32E-04	5.48E-04	4.66E-04	5.08E-04	5.22E-04	5.15E-04
	Post-burn leach 2	<4E-05	<5E-05	<5E-04	<4E-06	<2E-05	1.59E-06
	SUM (MDA = 0)	5.55E-04	5.71E-04	4.66E-04	5.57E-04	5.69E-04	5.65E-04
Core	Decon	4.55E-03	4.72E-03	5.41E-03	5.38E-03	5.48E-03	5.19E-03
	Pre-burn leach 1	3.55E-03	3.73E-03	3.59E-03	3.54E-03	3.59E-03	3.45E-03
	Pre-burn leach 2	4.52E-05	<5E-05	<2E-04	6.11E-05	5.87E-05	5.85E-05
	Post-burn leach 1	2.31E-04	2.82E-04	4.33E-04	4.21E-04	4.27E-04	4.17E-04
	Post-burn leach 2	<4E-05	<4E-05	<2E-04	2.70E-05	<2E-05	1.04E-05
	SUM (MDA = 0)	8.37E-03	8.73E-03	9.44E-03	9.43E-03	9.56E-03	9.13E-03
Compact TOTAL (MDA = 0)		9.38E-03	9.72E-03	1.03E-02	1.04E-02	1.06E-02	1.01E-02
Compact TOTAL (MDA = 0) Corrected		8.94E-03	9.30E-03	9.90E-03	1.00E-02	1.01E-02	9.71E-03

A-3. Compact 5-4

Table 81. Activities of fission products measured in the solutions from RDLBL of Compact 5-4. All values were decay-corrected to EOI + 1 day. No accidental particle damage occurred during RDLBL. See Section 4.3 for a discussion of this compact.

Activity (Bq)		Ag-110m	Ce-144	Cs-134	Cs-137	Eu-154	Eu-155	Ru-106	Sb-125	Sr-90
Segment #1	Decon	<3E+05	<7E+05	2.05E+06	2.32E+06	<4E+03	<7E+03	<2E+06	<3E+04	1.13E+04
	Pre-burn leach 1	<1E+05	<4E+05	2.23E+05	2.34E+05	<3E+03	<7E+03	<7E+05	<1E+04	4.79E+03
	Pre-burn leach 2	<1E+05	<4E+05	2.24E+04	2.54E+04	<3E+03	<7E+03	<4E+05	<7E+03	2.71E+03
	Post-burn leach 1	<1E+05	<4E+05	1.32E+05	1.36E+05	<1E+03	<7E+03	<7E+05	<1E+04	1.92E+03
	Post-burn leach 2	<1E+05	<4E+05	<4E+03	1.80E+03	<3E+03	<7E+03	<2E+05	<7E+03	7.23E+02
	SUM (MDA = 0)	0	0	2.42E+06	2.72E+06	0	0	0	0	2.15E+04
Segment #2	Decon	<4E+05	2.04E+06	1.77E+06	2.08E+06	4.57E+03	4.11E+03	4.19E+05	<2E+04	6.14E+04
	Pre-burn leach 1	<7E+04	<2E+05	2.98E+05	3.51E+05	<1E+03	<1E+03	<1E+05	<7E+03	2.70E+03
	Pre-burn leach 2	<1E+05	<3E+05	6.17E+04	6.27E+04	<2E+03	<4E+03	<3E+05	<7E+03	1.04E+03
	Post-burn leach 1	<1E+05	<3E+05	1.68E+05	1.75E+05	<2E+03	<4E+03	<4E+05	<1E+04	8.06E+03
	Post-burn leach 2	<7E+04	<2E+05	<3E+03	3.46E+03	<1E+03	<3E+03	<1E+05	<3E+03	2.84E+03
	SUM (MDA = 0)	0	2.04E+06	2.30E+06	2.67E+06	4.57E+03	4.11E+03	4.19E+05	0	7.60E+04
Segment #3	Decon	<3E+05	7.80E+06	3.14E+06	3.78E+06	1.45E+04	1.10E+04	6.31E+05	3.14E+04	2.71E+05
	Pre-burn leach 1	<3E+05	<7E+05	4.90E+05	5.34E+05	<4E+03	<7E+03	<7E+04	<3E+04	1.23E+04
	Pre-burn leach 2	<1E+05	<4E+05	4.86E+04	5.29E+04	<2E+03	<4E+03	<4E+05	<1E+04	9.26E+02
	Post-burn leach 1	<2E+05	<7E+05	4.85E+05	5.09E+05	1.01E+04	5.54E+03	<1E+06	<3E+04	8.70E+03
	Post-burn leach 2	<1E+05	<3E+05	5.33E+03	7.31E+03	<2E+03	<4E+03	<2E+05	<7E+03	1.50E+03
	SUM (MDA = 0)	0	7.80E+06	4.17E+06	4.88E+06	2.46E+04	1.65E+04	6.31E+05	3.14E+04	2.95E+05

Activity (Bq)		Ag-110m	Ce-144	Cs-134	Cs-137	Eu-154	Eu-155	Ru-106	Sb-125	Sr-90
Core	Decon	<3E+05	1.23E+08	3.76E+06	5.16E+06	2.73E+05	2.04E+05	1.27E+07	2.68E+05	6.71E+06
	Pre-burn leach 1	<3E+06	9.65E+08	1.04E+07	1.37E+07	1.90E+06	1.30E+06	1.20E+08	<4E+05	2.56E+07
	Pre-burn leach 2	<1E+06	2.09E+07	2.03E+05	1.88E+05	3.62E+04	<3E+04	1.71E+07	1.29E+05	1.26E+07
	Post-burn leach 1	<1E+06	6.69E+07	2.03E+06	1.87E+06	5.26E+05	3.48E+05	7.69E+06	2.66E+06	3.43E+07
	Post-burn leach 2	<1E+06	<3E+06	4.74E+04	4.89E+04	<1E+04	<1E+04	<1E+06	1.02E+05	2.94E+04
	SUM (MDA = 0)	0	1.18E+09	1.65E+07	2.10E+07	2.74E+06	1.86E+06	1.57E+08	3.16E+06	7.91E+07
Compact TOTAL (MDA = 0)		0	1.19E+09	2.54E+07	3.12E+07	2.77E+06	1.88E+06	1.58E+08	3.19E+06	7.95E+07

Table 82. Fraction (M/C) of the compact inventory of fission products measured in the solutions from RDLBL of Compact 5-4. All values were decay-corrected to EOI + 1 day. No accidental particle damage occurred during RDLBL. See Section 4.3 for a discussion of this compact.

Compact Fraction		Ag-110m	Ce-144	Cs-134	Cs-137	Eu-154	Eu-155	Ru-106	Sb-125	Sr-90
Segment #1	Decon	<2E-03	<7E-06	2.03E-04	3.09E-04	<1E-05	<4E-05	<7E-05	<6E-05	1.76E-06
	Pre-burn leach 1	<1E-03	<3E-06	2.21E-05	3.11E-05	<9E-06	<4E-05	<3E-05	<2E-05	7.47E-07
	Pre-burn leach 2	<1E-03	<3E-06	2.22E-06	3.38E-06	<8E-06	<4E-05	<1E-05	<1E-05	4.23E-07
	Post-burn leach 1	<1E-03	<3E-06	1.31E-05	1.80E-05	<5E-06	<4E-05	<3E-05	<2E-05	2.99E-07
	Post-burn leach 2	<9E-04	<3E-06	<4E-07	2.39E-07	<8E-06	<4E-05	<7E-06	<1E-05	1.13E-07
	SUM (MDA = 0)	0	0	2.40E-04	3.61E-04	0	0	0	0	3.35E-06
Segment #2	Decon	<3E-03	1.83E-05	1.75E-04	2.76E-04	1.46E-05	2.00E-05	1.55E-05	<4E-05	9.57E-06
	Pre-burn leach 1	<6E-04	<2E-06	2.95E-05	4.66E-05	<4E-06	<7E-06	<4E-06	<1E-05	4.20E-07
	Pre-burn leach 2	<9E-04	<3E-06	6.12E-06	8.34E-06	<6E-06	<2E-05	<1E-05	<1E-05	1.62E-07
	Post-burn leach 1	<1E-03	<3E-06	1.66E-05	2.33E-05	<6E-06	<2E-05	<1E-05	<2E-05	1.26E-06
	Post-burn leach 2	<6E-04	<2E-06	<3E-07	4.60E-07	<5E-06	<1E-05	<5E-06	<6E-06	4.43E-07
	SUM (MDA = 0)	0	1.83E-05	2.28E-04	3.55E-04	1.46E-05	2.00E-05	1.55E-05	0	1.18E-05
Segment #3	Decon	<3E-03	6.99E-05	3.11E-04	5.02E-04	4.63E-05	5.34E-05	2.33E-05	5.21E-05	4.23E-05
	Pre-burn leach 1	<2E-03	<7E-06	4.86E-05	7.09E-05	<1E-05	<4E-05	<3E-06	<4E-05	1.92E-06
	Pre-burn leach 2	<1E-03	<3E-06	4.82E-06	7.04E-06	<7E-06	<2E-05	<1E-05	<2E-05	1.44E-07
	Post-burn leach 1	<2E-03	<7E-06	4.81E-05	6.76E-05	3.23E-05	2.69E-05	<4E-05	<4E-05	1.36E-06
	Post-burn leach 2	<9E-04	<2E-06	5.28E-07	9.71E-07	<7E-06	<2E-05	<7E-06	<1E-05	2.33E-07
	SUM (MDA = 0)	0	6.99E-05	4.13E-04	6.49E-04	7.85E-05	8.03E-05	2.33E-05	5.21E-05	4.60E-05
Core	Decon	<3E-03	1.10E-03	3.73E-04	6.86E-04	8.71E-04	9.92E-04	4.68E-04	4.45E-04	1.05E-03
	Pre-burn leach 1	<2E-02	8.65E-03	1.03E-03	1.82E-03	6.06E-03	6.34E-03	4.42E-03	<6E-04	3.99E-03
	Pre-burn leach 2	<9E-03	1.88E-04	2.01E-05	2.49E-05	1.15E-04	<2E-04	6.33E-04	2.15E-04	1.96E-03
	Post-burn leach 1	<9E-03	6.00E-04	2.01E-04	2.49E-04	1.67E-03	1.69E-03	2.84E-04	4.42E-03	5.34E-03
	Post-burn leach 2	<9E-03	<3E-05	4.70E-06	6.50E-06	<4E-05	<7E-05	<4E-05	1.69E-04	4.59E-06
	SUM (MDA = 0)	0	1.05E-02	1.63E-03	2.79E-03	8.72E-03	9.02E-03	5.81E-03	5.25E-03	1.23E-02
Compact TOTAL (MDA = 0)		0	1.06E-02	2.51E-03	4.15E-03	8.82E-03	9.13E-03	5.84E-03	5.30E-03	1.24E-02

Table 83. Masses for select actinides from ICP-MS of solutions from Compact 5-4 RDLBL. No accidental particle damage occurred during RDLBL. See Section 4.3 for a discussion of this compact.

	Mass (μg)	Pu-239	Pu-240	U-234	U-235	U-236	U-238
Segment #1	Decon	0.04	<2E-02	<2E-02	0.21	0.07	2.39
	Pre-burn leach 1	<8E-02	<5E-02	<6E-02	0.07	<6E-02	0.37
	Pre-burn leach 2	<1E-01	<6E-02	<7E-02	<9E-02	<8E-02	0.23
	Post-burn leach 1	<7E-02	<6E-02	<7E-02	<1E-01	<8E-02	0.20
	Post-burn leach 2	<9E-02	<7E-02	<9E-02	<1E-01	<1E-01	0.18
	SUM (MDA = 0)	0.04	0.00	0.00	0.28	0.07	3.36
Segment #2	Decon	0.12	0.04	<2E-02	0.78	0.34	10.83
	Pre-burn leach 1	<7E-02	<5E-02	<7E-02	<9E-02	<8E-02	0.36
	Pre-burn leach 2	<9E-02	<7E-02	<9E-02	<1E-01	<1E-01	0.08
	Post-burn leach 1	0.20	<6E-02	<8E-02	0.27	<9E-02	2.33
	Post-burn leach 2	<9E-02	<5E-02	<6E-02	0.07	<6E-02	0.13
	SUM (MDA = 0)	0.32	0.04	0.00	1.12	0.34	13.73
Segment #3	Decon	0.31	0.12	0.03	1.79	0.82	25.27
	Pre-burn leach 1	<8E-02	<6E-02	<8E-02	0.15	<9E-02	1.04
	Pre-burn leach 2	<7E-02	<6E-02	<7E-02	<1E-01	<8E-02	0.07
	Post-burn leach 1	<6E-02	<5E-02	<6E-02	<8E-02	<7E-02	0.39
	Post-burn leach 2	<8E-02	<6E-02	<8E-02	<1E-01	<9E-02	0.11
	SUM (MDA = 0)	0.31	0.12	0.03	1.94	0.82	26.87
Core	Decon	5.21	2.04	0.59	33.07	15.12	465.00
	Pre-burn leach 1	33.07	13.00	3.62	204.67	95.60	2843.33
	Pre-burn leach 2	6.27	2.47	<9E-02	3.96	1.83	56.60
	Post-burn leach 1	1.93	0.83	<8E-02	1.46	0.48	21.40
	Post-burn leach 2	<8E-02	<6E-02	<8E-02	<1E-01	<9E-02	0.10
	SUM (MDA = 0)	46.48	18.34	4.21	243.15	113.03	3386.44
Compact TOTAL (MDA = 0)		47.14	18.51	4.24	246.49	114.27	3430.39

Table 84. Compact fractions for select actinides from ICP-MS of solutions from Compact 5-4 RDLBL. No accidental particle damage occurred during RDLBL. See Section 4.3 for a discussion of this compact.

	Compact Fraction	Pu-239	Pu-240	U-234	U-235	U-236	U-238
Segment #1	Decon	7.24E-06	<1E-05	<5E-05	9.02E-06	6.22E-06	7.06E-06
	Pre-burn leach 1	<2E-05	<2E-05	<1E-04	2.91E-06	<5E-06	1.09E-06
	Pre-burn leach 2	<2E-05	<3E-05	<2E-04	<4E-06	<7E-06	6.74E-07
	Post-burn leach 1	<1E-05	<3E-05	<2E-04	<4E-06	<7E-06	5.78E-07
	Post-burn leach 2	<2E-05	<3E-05	<2E-04	<4E-06	<9E-06	5.44E-07
	SUM (MDA = 0)	7.24E-06	0	0	1.19E-05	6.22E-06	9.95E-06

Compact Fraction		Pu-239	Pu-240	U-234	U-235	U-236	U-238
Segment #2	Decon	2.33E-05	2.22E-05	<5E-05	3.33E-05	3.15E-05	3.20E-05
	Pre-burn leach 1	<1E-05	<2E-05	<2E-04	<4E-06	<7E-06	1.06E-06
	Pre-burn leach 2	<2E-05	<3E-05	<2E-04	<4E-06	<9E-06	2.38E-07
	Post-burn leach 1	3.80E-05	<3E-05	<2E-04	1.15E-05	<8E-06	6.89E-06
	Post-burn leach 2	<2E-05	<2E-05	<1E-04	3.10E-06	<5E-06	3.72E-07
	SUM (MDA = 0)	6.13E-05	2.22E-05	0	4.80E-05	3.15E-05	4.06E-05
Segment #3	Decon	5.82E-05	6.04E-05	8.01E-05	7.65E-05	7.50E-05	7.47E-05
	Pre-burn leach 1	<2E-05	<3E-05	<2E-04	6.57E-06	<8E-06	3.07E-06
	Pre-burn leach 2	<1E-05	<3E-05	<2E-04	<4E-06	<7E-06	1.93E-07
	Post-burn leach 1	<1E-05	<2E-05	<1E-04	<3E-06	<6E-06	1.16E-06
	Post-burn leach 2	<2E-05	<3E-05	<2E-04	<4E-06	<8E-06	3.11E-07
	SUM (MDA = 0)	5.82E-05	6.04E-05	8.01E-05	8.31E-05	7.50E-05	7.95E-05
Core	Decon	9.92E-04	1.02E-03	1.43E-03	1.42E-03	1.38E-03	1.38E-03
	Pre-burn leach 1	6.29E-03	6.48E-03	8.70E-03	8.77E-03	8.74E-03	8.41E-03
	Pre-burn leach 2	1.19E-03	1.23E-03	<2E-04	1.70E-04	1.68E-04	1.67E-04
	Post-burn leach 1	3.67E-04	4.16E-04	<2E-04	6.24E-05	4.35E-05	6.33E-05
	Post-burn leach 2	<2E-05	<3E-05	<2E-04	<4E-06	<8E-06	3.08E-07
	SUM (MDA = 0)	8.85E-03	9.15E-03	1.01E-02	1.04E-02	1.03E-02	1.00E-02
Compact TOTAL (MDA = 0)		8.97E-03	9.23E-03	1.02E-02	1.06E-02	1.04E-02	1.01E-02

A-4. Compact 7-3

Table 85. Activities of fission products measured in the solutions from RDLBL of Compact 7-3. All values were decay-corrected to EOI + 1 day. Segment 1, post-burn leach 2 was corrected for accidental damage to one particle. See Section 4.4 for a discussion of this compact.

Activity (Bq)		Ag-110m	Ce-144	Cs-134	Cs-137	Eu-154	Eu-155	Ru-106	Sb-125	Sr-90
Segment #1	Decon	<7E+5	<2E+6	3.96E+4	6.22E+4	4.62E+5	2.91E+5	<1E+6	3.94E+4	9.78E+6
	Pre-burn leach 1	<1E+6	<4E+6	<4E+4	9.80E+4	5.19E+5	3.36E+5	<3E+6	<7E+4	4.79E+6
	Pre-burn leach 2	<7E+5	<3E+6	<2E+4	1.13E+4	3.96E+4	2.58E+4	<1E+6	<4E+4	2.38E+5
	Post-burn leach 1	<3E+6	2.15E+7	1.61E+5	1.65E+5	2.00E+6	1.28E+6	<3E+6	1.33E+5	2.50E+7
	Post-burn leach 2	<2E+6	6.69E+7	3.14E+6	2.59E+6	1.09E+5	7.54E+4	1.41E+7	2.06E+5	3.31E+6
	Post-burn leach 2 Corrected	<2E+6	8.61E+6	0	0	0	0	3.32E+5	0	0
	SUM (MDA = 0)	0	8.84E+7	3.34E+6	2.92E+6	3.13E+6	2.01E+6	1.41E+7	3.79E+5	4.31E+7
	SUM (MDA = 0) Corrected	0	3.01E+7	2.00E+5	3.37E+5	3.02E+6	1.94E+6	3.32E+5	1.73E+05	3.98E+7

Activity (Bq)		Ag-110m	Ce-144	Cs-134	Cs-137	Eu-154	Eu-155	Ru-106	Sb-125	Sr-90
Segment #2	Decon	<7E+5	<2E+6	1.11E+5	1.52E+5	3.97E+5	2.47E+5	<1E+6	<3E+4	7.60E+6
	Pre-burn leach 1	<2E+6	<4E+6	4.79E+5	4.12E+5	4.45E+5	2.84E+5	<3E+6	<1E+5	4.17E+6
	Pre-burn leach 2	<1E+6	<3E+6	1.47E+5	1.23E+5	2.99E+4	2.87E+4	<1E+6	<7E+4	2.06E+5
	Post-burn leach 1	<3E+6	1.76E+7	6.98E+5	5.85E+5	1.97E+6	1.24E+6	<4E+6	<2E+5	2.36E+7
	Post-burn leach 2	<1E+6	<4E+6	2.22E+5	1.91E+5	<1E+4	<1E+4	<1E+6	<7E+4	1.12E+5
	SUM (MDA = 0)	0	1.76E+7	1.66E+6	1.46E+6	2.84E+6	1.80E+6	0	0	3.57E+7
Core	Decon	<3E+6	2.40E+8	1.08E+7	1.52E+7	5.16E+5	4.49E+5	8.85E+7	<3E+5	3.16E+7
	Pre-burn leach 1	<7E+6	1.91E+8	4.11E+6	5.87E+6	5.02E+5	3.66E+5	1.27E+8	<4E+5	1.27E+7
	Pre-burn leach 2	<7E+6	1.11E+7	9.81E+4	9.40E+4	<3E+4	<7E+4	<7E+6	<1E+5	4.73E+5
	Post-burn leach 1	<7E+6	7.19E+8	3.33E+6	2.88E+6	2.12E+6	1.39E+6	1.56E+7	7.78E+5	3.55E+7
	Post-burn leach 2	<1E+7	<2E+7	6.76E+5	5.92E+5	<7E+4	<1E+5	<1E+7	<3E+5	1.94E+5
	SUM (MDA = 0)	0	1.16E+9	1.90E+7	2.46E+7	3.14E+6	2.21E+6	2.31E+8	7.78E+5	8.06E+7
Compact TOTAL (MDA = 0)		0	1.27E+9	2.40E+7	2.90E+7	9.11E+6	6.02E+6	2.45E+8	1.16E+6	1.59E+8
Compact TOTAL (MDA = 0) Corrected		0	1.21E+9	2.08E+7	2.64E+7	9.00E+6	5.94E+6	2.31E+8	9.51E+5	1.56E+8

Table 86. Fraction (M/C) of the compact inventory of fission products measured in the solutions from RDLBL of Compact 7-3. All values were decay-corrected to EOI + 1 day. Segment 1, post-burn leach 2 was corrected for accidental damage to one particle. See Section 4.4 for a discussion of this compact.

Compact Fraction		Ag-110m	Ce-144	Cs-134	Cs-137	Eu-154	Eu-155	Ru-106	Sb-125	Sr-90
Segment #1	Decon	<6E-3	<2E-5	3.89E-6	8.24E-6	1.49E-3	1.42E-3	<4E-5	6.55E-5	1.52E-3
	Pre-burn leach 1	<1E-2	<3E-5	<4E-6	1.30E-5	1.67E-3	1.64E-3	<1E-4	<1E-4	7.43E-4
	Pre-burn leach 2	<6E-3	<3E-5	<2E-6	1.50E-6	1.27E-4	1.25E-4	<6E-5	<6E-5	3.70E-5
	Post-burn leach 1	<2E-2	1.92E-4	1.58E-5	2.19E-5	6.44E-3	6.24E-3	<1E-4	2.22E-4	3.88E-3
	Post-burn leach 2	<2E-2	5.98E-4	3.09E-4	3.43E-4	3.52E-4	3.67E-4	5.24E-4	3.43E-4	5.13E-4
	Post-burn leach 2 Corrected	<2E-2	7.70E-5	0	0	0	0	2.33E-6	0	0
	SUM (MDA = 0)	0	7.91E-4	3.29E-4	3.87E-4	1.01E-2	9.79E-3	5.24E-4	6.30E-4	6.69E-3
	SUM (MDA = 0) Corrected	0	2.69E-4	1.97E-5	4.46E-5	9.72E-3	9.42E-3	2.33E-6	2.87E-4	6.18E-3
Segment #2	Decon	<6E-3	<2E-5	1.09E-5	2.02E-5	1.28E-3	1.20E-3	<4E-5	<6E-5	1.18E-3
	Pre-burn leach 1	<2E-2	<3E-5	4.71E-5	5.46E-5	1.43E-3	1.38E-3	<1E-4	<2E-4	6.47E-4
	Pre-burn leach 2	<9E-3	<3E-5	1.44E-5	1.63E-5	9.60E-5	1.39E-4	<6E-5	<1E-4	3.20E-5
	Post-burn leach 1	<2E-2	1.58E-4	6.86E-5	7.75E-5	6.32E-3	6.03E-3	<1E-4	<3E-4	3.66E-3
	Post-burn leach 2	<9E-3	<3E-5	2.18E-5	2.54E-5	<4E-5	<7E-5	<6E-5	<1E-4	1.74E-5
	SUM (MDA = 0)	0	1.58E-4	1.63E-4	1.94E-4	9.13E-3	8.75E-3	0	0	5.54E-3

Core	Decon	<3E-2	2.14E-3	1.06E-3	2.01E-3	1.66E-3	2.19E-3	3.30E-3	<5E-4	4.91E-3
	Pre-burn leach 1	<6E-2	1.71E-3	4.04E-4	7.78E-4	1.61E-3	1.78E-3	4.72E-3	<6E-4	1.98E-3
	Pre-burn leach 2	<6E-2	9.88E-5	9.65E-6	1.25E-5	<1E-4	<4E-4	<3E-4	<2E-4	7.34E-5
	Post-burn leach 1	<6E-2	6.43E-3	3.27E-4	3.81E-4	6.83E-3	6.77E-3	5.80E-4	1.29E-3	5.52E-3
	Post-burn leach 2	<9E-2	<2E-4	6.64E-5	7.84E-5	<2E-4	<5E-4	<4E-4	<6E-4	3.01E-5
	SUM (MDA = 0)	0	1.04E-2	1.87E-3	3.26E-3	1.01E-2	1.07E-2	8.60E-3	1.29E-3	1.25E-2
Compact TOTAL (MDA = 0)		0	1.13E-2	2.36E-3	3.84E-3	2.93E-2	2.93E-2	9.12E-3	1.92E-3	2.47E-2
Compact TOTAL (MDA = 0) Corrected		0	1.08E-2	2.05E-3	3.50E-3	2.90E-2	2.89E-2	8.60E-3	1.58E-3	2.42E-2

Table 87. Masses for select actinides from ICP-MS of solutions from Compact 7-3 RDLBL. Segment 1, post-burn leach 2 was corrected for accidental damage to one particle. See Section 4.4 for a discussion of this compact.

		Mass (µg)					
		Pu-239	Pu-240	U-234	U-235	U-236	U-238
Segment #1	Decon	<2E-02	<1E-02	<9E-03	0.09	0.03	1.03
	Pre-burn leach 1	<9E-02	<5E-02	<3E-02	0.36	<4E-02	1.77
	Pre-burn leach 2	<7E-02	<4E-02	<3E-02	0.11	<3E-02	0.85
	Post-burn leach 1	1.09	0.89	<3E-02	0.79	0.30	8.88
	Post-burn leach 2	2.93	1.24	0.24	13.67	6.20	187.67
	Post-burn leach 2 Corrected	0.33	0.20	0.02	1.67	0.47	11.18
	SUM (MDA = 0)	4.02	2.13	0.24	15.02	6.52	200.19
	SUM (MDA = 0) Corrected	1.42	1.09	0.02	3.02	0.79	23.70
Segment #2	Decon	0.08	0.02	0.02	1.24	0.56	17.17
	Pre-burn leach 1	0.07	0.03	<3E-02	0.36	0.03	1.34
	Pre-burn leach 2	0.10	0.02	<2E-02	0.11	<2E-02	0.49
	Post-burn leach 1	0.94	0.75	<3E-02	0.55	0.25	7.44
	Post-burn leach 2	<5E-02	<2E-02	<2E-02	0.05	<2E-02	0.31
	SUM (MDA = 0)	1.19	0.82	0.02	2.31	0.84	26.75
Core	Decon	21.53	7.05	3.33	187.00	85.47	2540.00
	Pre-burn leach 1	12.30	4.69	0.94	54.47	24.40	738.67
	Pre-burn leach 2	0.25	0.13	<1E-02	0.17	0.05	2.36
	Post-burn leach 1	11.50	7.28	0.27	14.23	6.46	199.00
	Post-burn leach 2	0.34	0.15	<2E-02	0.16	<2E-02	7.73
	SUM (MDA = 0)	45.92	19.29	4.53	256.03	116.38	3487.76
Compact TOTAL (MDA = 0)		51.14	22.25	4.79	273.36	123.75	3714.70
Compact TOTAL (MDA = 0) Corrected		48.54	21.21	4.57	261.36	118.01	3538.20

Table 88. Compact fractions for select actinides from ICP-MS of solutions from Compact 7-3 RDLBL. Segment 1, post-burn leach 2 was corrected for accidental damage to one particle. See Section 4.4 for a discussion of this compact.

		Compact Fraction					
		Pu-239	Pu-240	U-234	U-235	U-236	U-238
Segment #1	Decon	<4E-6	<5E-6	<2E-5	3.93E-6	2.65E-6	3.04E-6
	Pre-burn leach 1	<2E-5	<3E-5	<7E-5	1.57E-5	<4E-6	5.22E-6
	Pre-burn leach 2	<1E-5	<2E-5	<7E-5	4.85E-6	<3E-6	2.50E-6
	Post-burn leach 1	2.19E-4	4.48E-4	<7E-5	3.43E-5	2.68E-5	2.62E-5
	Post-burn leach 2	5.88E-4	6.23E-4	5.77E-4	5.94E-4	5.64E-4	5.54E-4
	Post-burn leach 2 Corrected	6.62E-5	1.02E-4	5.55E-5	7.24E-5	4.23E-5	3.30E-5
	SUM (MDA = 0)	8.07E-4	1.07E-3	5.77E-4	6.52E-4	5.93E-4	5.91E-4
	SUM (MDA = 0) Corrected	2.85E-4	5.50E-4	5.55E-5	1.31E-4	7.18E-5	7.00E-5
Segment #2	Decon	1.56E-5	1.17E-5	5.30E-5	5.40E-5	5.08E-5	5.07E-5
	Pre-burn leach 1	1.49E-5	1.29E-5	<7E-5	1.57E-5	2.96E-6	3.95E-6
	Pre-burn leach 2	2.07E-5	1.14E-5	<5E-5	4.68E-6	<2E-6	1.46E-6
	Post-burn leach 1	1.88E-4	3.79E-4	<7E-5	2.41E-5	2.28E-5	2.20E-5
	Post-burn leach 2	<1E-5	<1E-5	<5E-5	2.03E-6	<2E-6	9.20E-7
	SUM (MDA = 0)	2.39E-4	4.15E-4	5.30E-5	1.00E-4	7.65E-5	7.90E-5
Core	Decon	4.32E-3	3.55E-3	8.01E-3	8.12E-3	7.77E-3	7.50E-3
	Pre-burn leach 1	2.47E-3	2.36E-3	2.26E-3	2.37E-3	2.22E-3	2.18E-3
	Pre-burn leach 2	5.01E-5	6.47E-5	<2E-5	7.47E-6	4.85E-6	6.96E-6
	Post-burn leach 1	2.31E-3	3.66E-3	6.38E-4	6.18E-4	5.87E-4	5.88E-4
	Post-burn leach 2	6.82E-5	7.49E-5	<5E-5	7.00E-6	<2E-6	2.28E-5
	SUM (MDA = 0)	9.21E-3	9.70E-3	1.09E-2	1.11E-2	1.06E-2	1.03E-2
Compact TOTAL (MDA = 0)		1.03E-2	1.12E-2	1.15E-2	1.19E-2	1.12E-2	1.10E-2
Compact TOTAL (MDA = 0) Corrected		9.73E-3	1.07E-2	1.10E-2	1.14E-2	1.07E-2	1.05E-2

A-5. Compact 8-3

Table 89. Activities of fission products measured in the solutions from the RDLBL of Compact 8-3. All values were decay-corrected to EOI + 1 day. Segment 2, pre-burn leach 2 was corrected for accidental damage to one particle. See Section 4.5 for a discussion of this compact.

Activity (Bq)		Ag-110m	Ce -144	Cs-134	Cs-137	Eu-154	Eu-155	Ru -106	Sb-125	Sr-90
Segment #1	Decon	<4E+05	<1E+06	3.5E+04	8.5E+04	5.2E+04	3.4E+04	8.3E+05	9.6E+03	2.5E+06
	Pre-burn leach 1	<1E+06	<3E+06	1.1E+05	9.7E+04	3.8E+04	2.9E+04	<1E+06	<4E+04	7.2E+05
	Pre-burn leach 2	<2E+06	1.1E+07	7.7E+04	8.0E+04	1.8E+04	1.0E+04	2.2E+06	4.1E+04	6.2E+05
	Post-burn leach 1	<7E+05	<2E+06	2.2E+04	4.1E+04	1.1E+05	6.8E+04	<1E+06	<3E+04	2.7E+06
	Post-burn leach 2	<1E+06	<2E+06	1.1E+04	1.2E+04	<7E+03	<1E+04	<1E+06	<3E+04	2.4E+04
	SUM (MDA = 0)	0	1.1E+07	2.5E+05	3.2E+05	2.1E+05	1.4E+05	3.1E+06	5.0E+04	6.5E+06

Activity (Bq)		Ag-110m	Ce-144	Cs-134	Cs-137	Eu-154	Eu-155	Ru-106	Sb-125	Sr-90
Segment #2	Decon	<7E+05	6.4E+06	1.1E+05	2.7E+05	1.6E+05	1.1E+05	3.6E+06	<3E+04	4.6E+06
	Pre-burn leach 1	<1E+06	<4E+06	6.4E+04	6.8E+04	1.2E+05	7.6E+04	<2E+06	<4E+04	1.5E+06
	Pre-burn leach 2	<7E+05	6.9E+07	3.0E+06	2.5E+06	9.9E+04	6.8E+04	1.4E+07	1.6E+05	3.6E+06
	Pre-burn leach 2 - Corrected	<7E+05	1.3E+07	0	0	0	0	9.6E+05	0	3.3E+05
	Post-burn leach 1	<2E+06	7.3E+06	1.3E+06	1.0E+06	5.4E+05	3.6E+05	<2E+06	<7E+04	1.0E+07
	Post-burn leach 2	<1E+06	<2E+06	2.3E+05	2.0E+05	6.5E+03	<1E+04	<1E+06	<3E+04	1.0E+05
	SUM (MDA = 0)	0	8.3E+07	4.7E+06	4.1E+06	9.3E+05	6.1E+05	1.8E+07	1.6E+05	2.0E+07
	SUM (MDA = 0) - Corrected	0	2.6E+07	1.7E+06	1.6E+06	8.3E+05	5.4E+05	4.5E+06	0	1.7E+07
Core	Decon	<1E+06	2.1E+08	2.6E+06	6.6E+06	7.2E+05	5.2E+05	5.9E+07	2.1E+05	2.3E+07
	Pre-burn leach 1	<3E+06	2.3E+08	2.6E+06	6.4E+06	6.2E+05	4.6E+05	1.2E+08	1.4E+05	1.3E+07
	Pre-burn leach 2	<1E+06	1.5E+07	9.3E+04	1.1E+05	8.1E+04	5.1E+04	5.1E+06	6.5E+04	1.1E+06
	Post-burn leach 1	<3E+06	7.3E+08	1.3E+05	1.4E+05	6.1E+06	3.9E+06	8.6E+06	8.7E+05	9.5E+07
	Post-burn leach 2	<1E+06	<2E+06	6.4E+04	5.8E+04	1.1E+04	7.0E+03	4.0E+06	5.9E+04	1.4E+05
	SUM (MDA = 0)	0	1.2E+09	5.5E+06	1.3E+07	7.5E+06	4.9E+06	1.9E+08	1.3E+06	1.3E+08
Compact TOTAL (MDA = 0)		0	1.3E+09	1.0E+07	1.8E+07	8.6E+06	5.7E+06	2.1E+08	1.5E+06	1.6E+08
Compact TOTAL (MDA = 0) Corrected		0	1.2E+09	7.4E+06	1.5E+07	8.5E+06	5.6E+06	2.0E+08	1.4E+06	1.6E+08

Table 90. Fraction (M/C) of the compact inventory of fission products measured in the solutions from RDLBL of Compact 8-3. All values were decay-corrected to EOI + 1 day. Segment 2, pre-burn leach 2 was corrected for accidental damage to one particle. See Section 4.5 for a discussion of this compact.

Compact Fraction		Ag-110m	Ce-144	Cs-134	Cs-137	Eu-154	Eu-155	Ru-106	Sb-125	Sr-90
Segment #1	Decon	<3E-03	<1E-05	3.76E-06	1.17E-05	1.77E-04	1.74E-04	3.29E-05	1.65E-05	3.93E-04
	Pre-burn leach 1	<1E-02	<3E-05	1.14E-05	1.32E-05	1.29E-04	1.50E-04	<6E-05	<6E-05	1.15E-04
	Pre-burn leach 2	<2E-02	9.76E-05	8.21E-06	1.10E-05	6.02E-05	5.28E-05	8.86E-05	7.07E-05	9.86E-05
	Post-burn leach 1	<7E-03	<2E-05	2.31E-06	5.68E-06	3.61E-04	3.51E-04	<4E-05	<6E-05	4.29E-04
	Post-burn leach 2	<1E-02	<2E-05	1.14E-06	1.67E-06	<3E-05	<6E-05	<4E-05	<6E-05	3.75E-06
	SUM (MDA = 0)	0	9.76E-05	2.68E-05	4.33E-05	7.27E-04	7.27E-04	1.22E-04	8.72E-05	1.04E-03
Segment #2	Decon	<7E-03	5.89E-05	1.18E-05	3.76E-05	5.44E-04	5.42E-04	1.41E-04	<5E-05	7.34E-04
	Pre-burn leach 1	<1E-02	<3E-05	6.85E-06	9.31E-06	4.00E-04	3.89E-04	<7E-05	<6E-05	2.45E-04
	Pre-burn leach 2	<7E-03	6.36E-04	3.21E-04	3.49E-04	3.38E-04	3.50E-04	5.59E-04	2.76E-04	5.75E-04
	Pre-burn leach 2 Corrected	<7E-03	1.15E-04	0	0	0	0	3.82E-05	0	5.33E-05
	Post-burn leach 1	<2E-02	6.71E-05	1.33E-04	1.42E-04	1.85E-03	1.86E-03	<9E-05	<1E-04	1.61E-03
	Post-burn leach 2	<1E-02	<2E-05	2.49E-05	2.67E-05	2.20E-05	<6E-05	<4E-05	<6E-05	1.67E-05
	SUM (MDA = 0)	0	7.62E-04	4.98E-04	5.64E-04	3.16E-03	3.14E-03	7.00E-04	2.76E-04	3.18E-03
	SUM (MDA = 0) Corrected	0	2.41E-04	1.77E-04	2.15E-04	2.82E-03	2.79E-03	1.79E-04	0	2.66E-03

Compact Fraction		Ag-110m	Ce-144	Cs-134	Cs-137	Eu-154	Eu-155	Ru-106	Sb-125	Sr-90
Core	Decon	<1E-02	1.96E-03	2.79E-04	9.06E-04	2.44E-03	2.67E-03	2.35E-03	3.63E-04	3.62E-03
	Pre-burn leach 1	<2E-02	2.13E-03	2.73E-04	8.77E-04	2.12E-03	2.35E-03	4.60E-03	2.37E-04	2.10E-03
	Pre-burn leach 2	<1E-02	1.38E-04	9.90E-06	1.46E-05	2.76E-04	2.62E-04	2.02E-04	1.13E-04	1.81E-04
	Post-burn leach 1	<3E-02	6.71E-03	1.34E-05	1.92E-05	2.06E-02	2.00E-02	3.41E-04	1.50E-03	1.52E-02
	Post-burn leach 2	<1E-02	<2E-05	6.85E-06	8.00E-06	3.63E-05	3.60E-05	1.60E-04	1.01E-04	2.25E-05
	SUM (MDA = 0)	0	1.09E-02	5.83E-04	1.82E-03	2.55E-02	2.53E-02	7.65E-03	2.31E-03	2.11E-02
Compact TOTAL (MDA = 0)		0	1.18E-02	1.11E-03	2.43E-03	2.94E-02	2.92E-02	8.47E-03	2.68E-03	2.53E-02
Compact TOTAL (MDA = 0) Corrected		0	1.13E-02	7.87E-04	2.08E-03	2.91E-02	2.89E-02	7.97E-03	2.40E-03	2.48E-02

Table 91. Masses for select actinides from ICP-MS of solutions from Compact 8-3 RDLBL. Segment 2, pre-burn leach 2 was corrected for accidental damage to one particle. See Section 4.5 for a discussion of this compact.

Mass (μg)		Pu-239	Pu-240	U-234	U-235	U-236	U-238
Segment #1	Decon	0.15	0.03	0.03	2.01	0.82	25.07
	Pre-burn leach 1	<3E-02	<3E-02	<2E-02	0.08	<2E-02	0.72
	Pre-burn leach 2	0.46	0.19	0.04	2.34	1.03	31.90
	Post-burn leach 1	0.08	0.03	0.00	0.19	0.03	1.73
	Post-burn leach 2	0.01	0.00	<7E-04	0.04	0.00	0.23
	SUM (MDA = 0)	0.69	0.25	0.08	4.65	1.88	59.65
Segment #2	Decon	0.67	0.16	0.12	8.06	2.86	73.57
	Pre-burn leach 1	0.04	0.01	<5E-03	0.24	0.07	2.55
	Pre-burn leach 2	2.88	1.17	0.26	17.10	6.66	167.67
	Pre-burn leach 2 Corrected	0.27	0.15	0.20	4.32	1.02	0
	Post-burn leach 1	0.38	0.26	0.01	0.38	0.13	4.73
	Post-burn leach 2	0.01	0.01	<4E-03	0.02	<2E-03	0.16
	SUM (MDA = 0)	3.98	1.61	0.38	25.79	9.71	248.67
	SUM (MDA = 0) Corrected	1.37	0.59	0.32	13.01	4.08	81.01
Core	Decon	14.87	5.16	2.20	99.33	44.97	2033.33
	Pre-burn leach 1	21.00	7.24	1.97	121.00	46.60	1890.00
	Pre-burn leach 2	0.33	0.19	0.01	0.23	0.06	2.33
	Post-burn leach 1	12.87	8.17	0.07	2.91	1.09	35.97
	Post-burn leach 2	0.07	0.05	0.01	0.09	0.01	1.52
	SUM (MDA = 0)	49.13	20.81	4.25	223.56	92.73	3963.15
Compact TOTAL (MDA = 0)		53.80	22.67	4.71	254.01	104.33	4271.47
Compact TOTAL (MDA = 0) Corrected		51.19	21.64	4.64	241.23	98.69	4103.81

Table 92. Compact fractions for select actinides from ICP-MS of solutions from Compact 8-3 RDLBL. Segment 2, pre-burn leach 2 was corrected for accidental damage to one particle. See Section 4.5 for a discussion of this compact.

Compact Fraction		Pu-239	Pu-240	U-234	U-235	U-236	U-238
Segment #1	Decon	2.94E-05	1.59E-05	7.83E-05	8.19E-05	7.57E-05	7.38E-05
	Pre-burn leach 1	<6E-06	<2E-05	<5E-05	3.23E-06	<2E-06	2.12E-06
	Pre-burn leach 2	9.20E-05	9.52E-05	9.42E-05	9.53E-05	9.53E-05	9.40E-05
	Post-burn leach 1	1.53E-05	1.40E-05	5.23E-06	7.59E-06	2.63E-06	5.11E-06
	Post-burn leach 2	1.43E-06	8.90E-07	<2E-06	1.79E-06	3.06E-07	6.75E-07
	SUM (MDA = 0)	1.38E-04	1.26E-04	1.78E-04	1.90E-04	1.74E-04	1.76E-04
Segment #2	Decon	1.34E-04	8.18E-05	2.74E-04	3.29E-04	2.65E-04	2.17E-04
	Pre-burn leach 1	8.25E-06	6.45E-06	<1E-05	9.63E-06	6.17E-06	7.52E-06
	Pre-burn leach 2	5.74E-04	5.97E-04	6.21E-04	6.98E-04	6.16E-04	4.94E-04
	Pre-burn leach 2 Corrected	5.30E-05	7.56E-05	1.00E-04	1.76E-04	9.47E-05	0
	Post-burn leach 1	7.54E-05	1.34E-04	1.37E-05	1.55E-05	1.17E-05	1.39E-05
	Post-burn leach 2	2.87E-06	3.20E-06	<9E-06	6.34E-07	<2E-07	4.58E-07
	SUM (MDA = 0)	7.95E-04	8.22E-04	9.09E-04	1.05E-03	8.99E-04	7.33E-04
	SUM (MDA = 0) Corrected	2.73E-04	3.01E-04	3.88E-04	5.31E-04	3.77E-04	2.39E-04
Core	Decon	2.97E-03	2.63E-03	5.20E-03	4.05E-03	4.16E-03	5.99E-03
	Pre-burn leach 1	4.19E-03	3.69E-03	4.67E-03	4.94E-03	4.31E-03	5.57E-03
	Pre-burn leach 2	6.58E-05	9.64E-05	1.90E-05	9.44E-06	5.77E-06	6.87E-06
	Post-burn leach 1	2.57E-03	4.17E-03	1.68E-04	1.19E-04	1.01E-04	1.06E-04
	Post-burn leach 2	1.34E-05	2.31E-05	1.46E-05	3.66E-06	1.33E-06	4.47E-06
	SUM (MDA = 0)	9.81E-03	1.06E-02	1.01E-02	9.12E-03	8.58E-03	1.17E-02
Compact TOTAL (MDA = 0)		1.07E-02	1.16E-02	1.12E-02	1.04E-02	9.65E-03	1.26E-02
Compact TOTAL (MDA = 0) Corrected		1.02E-02	1.10E-02	1.06E-02	9.84E-03	9.13E-03	1.21E-02

A-6. Compact 10-3

Table 93. Activities of fission products measured in the solutions from RDLBL of Compact 10-3. All values were decay-corrected to EOI + 1 day. Between Segments 1 and 2, 10–20 particles were accidentally damaged. With such widespread damage, corrections were not attempted. See Section 4.6 for a discussion of this compact.

Activity (Bq)		Ag-110m	Ce-144	Cs-134	Cs-137	Eu-154	Eu-155	Ru-106	Sb-125	Sr-90
Segment #1	Decon	<1E+06	1.3E+8	3.9E+6	5.0E+6	1.3E+5	9.5E+4	2.0E+7	3.1E+5	1.7E+7
	Pre-burn leach 1	<3E+06	1.6E+8	5.2E+6	8.0E+6	9.4E+4	9.5E+4	2.0E+7	<1E+05	5.4E+6
	Pre-burn leach 2	<3E+06	5.1E+7	1.8E+6	2.7E+6	4.0E+4	3.9E+4	8.0E+6	<7E+04	2.6E+6
	Post-burn leach 1	<2E+06	<7E+06	1.6E+6	2.0E+6	2.5E+5	1.9E+5	<2E+06	3.1E+5	3.2E+7
	Post-burn leach 2	<7E+05	<1E+06	7.0E+4	9.5E+4	6.9E+3	6.5E+3	3.0E+5	4.7E+4	2.1E+6
	SUM (MDA = 0)	0	3.5E+8	1.2E+7	1.8E+7	5.2E+5	4.3E+5	4.9E+7	6.7E+5	5.9E+7

Activity (Bq)		Ag-110m	Ce-144	Cs-134	Cs-137	Eu-154	Eu-155	Ru-106	Sb-125	Sr-90
Segment #2	Decon	<3E+05	2.4E+6	1.7E+5	2.8E+5	8.6E+3	6.6E+3	2.8E+5	5.1E+3	1.4E+6
	Pre-burn leach 1	<2E+06	6.3E+7	3.8E+6	5.2E+6	6.2E+4	5.6E+4	1.2E+7	<7E+04	9.1E+5
	Pre-burn leach 2	<1E+06	3.9E+7	8.8E+5	1.2E+6	4.3E+4	3.6E+4	5.9E+6	<4E+04	5.2E+5
	Post-burn leach 1	<3E+06	<1E+07	8.2E+5	1.1E+6	2.2E+5	1.7E+5	<2E+06	2.2E+5	1.1E+7
	Post-burn leach 2	<1E+06	<1E+06	3.4E+4	4.3E+4	9.9E+2	<2E+03	<4E+05	2.7E+4	2.4E+4
	SUM (MDA = 0)	0	1.0E+8	5.7E+6	7.8E+6	3.3E+5	2.7E+5	1.8E+7	2.5E+5	1.4E+7
Segment #3	Decon	<2E+05	3.6E+6	7.5E+4	2.5E+5	9.4E+3	9.2E+3	5.4E+5	4.3E+3	1.5E+6
	Pre-burn leach 1	<7E+05	1.5E+6	8.8E+3	2.5E+4	4.0E+3	4.1E+3	3.5E+5	8.7E+3	1.3E+5
	Pre-burn leach 2	<4E+05	<1E+06	2.4E+3	2.5E+3	9.3E+2	<3E+03	<4E+05	4.0E+3	2.6E+4
	Post-burn leach 1	<3E+06	4.0E+7	7.6E+5	1.3E+6	6.3E+4	5.4E+4	6.2E+6	1.1E+5	2.7E+6
	Post-burn leach 2	<1E+06	<4E+06	1.8E+5	2.9E+5	1.5E+3	<4E+03	<1E+06	9.0E+3	4.3E+4
	SUM (MDA = 0)	0	4.5E+7	1.0E+6	1.8E+6	7.9E+4	6.7E+4	7.1E+6	1.4E+5	4.4E+6
Core	Decon	<3E+06	3.4E+8	1.7E+6	7.2E+6	2.0E+5	2.3E+5	6.0E+7	3.5E+5	3.4E+7
	Pre-burn leach 1	<3E+06	2.4E+8	2.4E+6	4.6E+6	2.1E+5	1.7E+5	6.7E+7	2.5E+5	1.8E+5
	Pre-burn leach 2	<2E+06	1.8E+7	6.9E+5	9.9E+5	2.8E+4	2.2E+4	3.6E+6	6.3E+4	4.8E+4
	Post-burn leach 1	<7E+06	3.3E+8	1.5E+6	2.2E+6	9.2E+5	7.3E+5	5.3E+6	9.2E+5	4.0E+5
	Post-burn leach 2	<2E+06	<4E+06	4.9E+4	6.0E+4	8.6E+3	8.6E+3	1.0E+6	9.9E+4	1.1E+4
	SUM (MDA = 0)	0	9.3E+8	6.3E+6	1.5E+7	1.4E+6	1.2E+6	1.4E+8	1.7E+6	3.4E+7
Compact TOTAL (MDA = 0)		0	1.4E+9	2.6E+7	4.3E+7	2.3E+6	1.9E+6	2.1E+8	2.7E+6	1.1E+8

Table 94. Fraction (M/C) of the compact inventory of fission products measured in the solutions from the radial deconsolidation of Compact 10-3. All values were decay-corrected to EOI + 1 day. Between Segments 1 and 2, 10–20 particles were accidentally damaged. With such widespread damage, corrections were not attempted. See Section 4.6 for a discussion of this compact.

Compact Fraction		Ag-110m	Ce-144	Cs-134	Cs-137	Eu-154	Eu-155	Ru-106	Sb-125	Sr-90
Segment #1	Decon	<2E-02	1.5E-3	6.6E-4	8.6E-4	6.9E-4	7.2E-4	1.2E-3	6.9E-4	3.3E-3
	Pre-burn leach 1	<5E-02	1.8E-3	8.8E-4	1.4E-3	4.9E-4	7.1E-4	1.1E-3	<3E-04	1.0E-3
	Pre-burn leach 2	<5E-02	5.6E-4	3.1E-4	4.7E-4	2.1E-4	2.9E-4	4.5E-4	<2E-04	5.1E-4
	Post-burn leach 1	<4E-02	<8E-05	2.7E-4	3.4E-4	1.3E-3	1.5E-3	<1E-04	6.9E-4	6.1E-3
	Post-burn leach 2	<1E-02	<1E-05	1.2E-5	1.6E-5	3.6E-5	4.9E-5	1.7E-5	1.1E-4	4.1E-4
	SUM (MDA = 0)	0.0E+0	3.8E-3	2.1E-3	3.0E-3	2.7E-3	3.2E-3	2.8E-3	1.5E-3	1.1E-2
Segment #2	Decon	<5E-03	2.7E-5	2.9E-5	4.7E-5	4.5E-5	5.0E-5	1.6E-5	1.1E-5	2.7E-4
	Pre-burn leach 1	<3E-02	6.9E-4	6.5E-4	8.9E-4	3.2E-4	4.2E-4	6.9E-4	<2E-04	1.8E-4
	Pre-burn leach 2	<3E-02	4.3E-4	1.5E-4	2.0E-4	2.2E-4	2.7E-4	3.4E-4	<8E-05	1.0E-4
	Post-burn leach 1	<5E-02	<1E-04	1.4E-4	1.8E-4	1.1E-3	1.3E-3	<1E-04	4.9E-4	2.1E-3
	Post-burn leach 2	<2E-02	<2E-05	5.7E-6	7.4E-6	5.2E-6	<2E-05	<2E-05	6.0E-5	4.6E-6
	SUM (MDA = 0)	0	1.2E-3	9.8E-4	1.3E-3	1.7E-3	2.0E-3	1.0E-3	5.6E-4	2.7E-3

Compact Fraction		Ag-110m	Ce-144	Cs-134	Cs-137	Eu-154	Eu-155	Ru-106	Sb-125	Sr-90
Segment #3	Decon	<4E-03	4.0E-5	1.3E-5	4.2E-5	4.9E-5	6.9E-5	3.1E-5	9.5E-6	2.9E-4
	Pre-burn leach 1	<1E-02	1.7E-5	1.5E-6	4.3E-6	2.1E-5	3.1E-5	2.0E-5	1.9E-5	2.5E-5
	Pre-burn leach 2	<7E-03	<2E-05	4.1E-7	4.3E-7	4.8E-6	<2E-05	<2E-05	8.9E-6	5.0E-6
	Post-burn leach 1	<5E-02	4.4E-4	1.3E-4	2.2E-4	3.3E-4	4.1E-4	3.5E-4	2.5E-4	5.2E-4
	Post-burn leach 2	<2E-02	<4E-05	3.2E-5	4.8E-5	7.6E-6	<3E-05	<8E-05	2.0E-5	8.2E-6
	SUM (MDA = 0)	0	5.0E-4	1.8E-4	3.1E-4	4.1E-4	5.1E-4	4.0E-4	3.1E-4	8.5E-4
Core	Decon	<5E-02	3.8E-3	2.9E-4	1.2E-3	1.1E-3	1.8E-3	3.4E-3	7.8E-4	6.5E-3
	Pre-burn leach 1	<5E-02	2.6E-3	4.1E-4	7.8E-4	1.1E-3	1.3E-3	3.8E-3	5.6E-4	3.5E-5
	Pre-burn leach 2	<3E-02	2.0E-4	1.2E-4	1.7E-4	1.4E-4	1.6E-4	2.0E-4	1.4E-4	9.2E-6
	Post-burn leach 1	<1E-01	3.7E-3	2.6E-4	3.7E-4	4.8E-3	5.5E-3	3.0E-4	2.0E-3	7.7E-5
	Post-burn leach 2	<3E-02	<4E-05	8.3E-6	1.0E-5	4.5E-5	6.4E-5	5.8E-5	2.2E-4	2.1E-6
	SUM (MDA = 0)	0	1.0E-2	1.1E-3	2.5E-3	7.1E-3	8.8E-3	7.7E-3	3.7E-3	6.6E-3
Compact TOTAL (MDA = 0)		0	1.6E-2	4.4E-3	7.2E-3	1.2E-2	1.5E-2	1.2E-2	6.1E-3	2.1E-2

Table 95. Masses for select actinides from ICP-MS of solutions from Compact 10-3 RDLBL. Between Segments 1 and 2, 10–20 particles were accidentally damaged. With such widespread damage, corrections were not attempted. See Section 4.6 for a discussion of this compact.

Mass (μg)		Pu-239	Pu-240	U-234	U-235	U-236	U-238
Segment #1	Decon	6.8E+0	2.2E+0	7.4E-1	5.7E+1	1.3E+1	5.3E+2
	Pre-burn leach 1	7.2E+0	2.3E+0	7.3E-1	5.5E+1	1.4E+1	5.0E+2
	Pre-burn leach 2	2.5E+0	8.0E-1	2.8E-1	2.1E+1	5.5E+0	2.1E+2
	Post-burn leach 1	2.6E+0	9.4E-1	2.2E-1	1.7E+1	4.3E+0	1.6E+2
	Post-burn leach 2	8.7E-2	2.1E-2	5.3E-3	4.0E-1	7.3E-2	3.2E+0
	SUM (MDA = 0)	1.9E+1	6.3E+0	2.0E+0	1.5E+2	3.7E+1	1.4E+3
Segment #2	Decon	1.5E-1	4.9E-2	2.4E-2	1.8E+0	4.6E-1	1.8E+1
	Pre-burn leach 1	4.6E+0	1.5E+0	4.5E-1	3.6E+1	8.7E+0	3.3E+2
	Pre-burn leach 2	2.2E+0	7.4E-1	2.3E-1	1.7E+1	4.4E+0	1.7E+2
	Post-burn leach 1	9.7E-1	4.2E-1	5.1E-2	3.7E+0	9.6E-1	3.4E+1
	Post-burn leach 2	2.3E-2	8.4E-3	8.4E-4	6.7E-2	1.0E-2	5.5E-1
	SUM (MDA = 0)	8.0E+0	2.7E+0	7.6E-1	5.8E+1	1.5E+1	5.5E+2
Segment #3	Decon	2.3E-1	6.3E-2	8.7E-2	6.2E+0	1.7E+0	6.3E+1
	Pre-burn leach 1	9.3E-2	2.8E-2	2.0E-2	1.5E+0	3.8E-1	1.4E+1
	Pre-burn leach 2	6.3E-3	1.8E-3	<2E-04	7.4E-3	1.4E-3	7.7E-2
	Post-burn leach 1	2.5E+0	8.5E-1	2.4E-1	1.7E+1	4.8E+0	1.7E+2
	Post-burn leach 2	8.8E-3	3.3E-3	3.4E-4	2.5E-2	6.6E-3	2.3E-1
	SUM (MDA = 0)	2.9E+0	9.5E-1	3.5E-1	2.5E+1	6.8E+0	2.5E+2

Core	Decon	3.3E+1	8.3E+0	3.8E+0	2.6E+2	8.9E+1	3.4E+3
	Pre-burn leach 1	1.6E+1	5.5E+0	1.6E+0	1.0E+2	3.6E+1	1.4E+3
	Pre-burn leach 2	3.9E-1	1.5E-1	1.7E-2	1.2E+0	3.3E-1	1.2E+1
	Post-burn leach 1	6.4E+0	3.2E+0	6.5E-2	3.9E+0	1.1E+0	5.1E+1
	Post-burn leach 2	9.8E-3	4.5E-3	<2E-04	6.7E-3	1.9E-3	9.6E-2
	SUM (MDA = 0)	5.6E+1	1.7E+1	5.5E+0	3.7E+2	1.3E+2	4.8E+3
Compact TOTAL (MDA = 0)		8.6E+1	2.7E+1	8.6E+0	6.1E+2	1.8E+2	7.0E+3

Table 96. Compact fraction for select actinides from ICP-MS of solutions from Compact 10-3 RDLBL. Between Segments 1 and 2, 10–20 particles were accidentally damaged. With such widespread damage, corrections were not attempted. See Section 4.6 for a discussion of this compact.

Compact Fraction		Pu-239	Pu-240	U-234	U-235	U-236	U-238
Segment #1	Decon	1.4E-3	1.3E-3	1.6E-3	1.7E-3	1.4E-3	1.5E-3
	Pre-burn leach 1	1.4E-3	1.4E-3	1.6E-3	1.6E-3	1.5E-3	1.4E-3
	Pre-burn leach 2	5.0E-4	4.7E-4	6.1E-4	6.1E-4	5.8E-4	6.0E-4
	Post-burn leach 1	5.3E-4	5.6E-4	4.8E-4	4.8E-4	4.5E-4	4.7E-4
	Post-burn leach 2	1.7E-5	1.3E-5	1.1E-5	1.2E-5	7.7E-6	9.3E-6
	SUM (MDA = 0)	3.8E-3	3.7E-3	4.2E-3	4.4E-3	3.9E-3	4.0E-3
Segment #2	Decon	3.0E-5	2.9E-5	5.1E-5	5.1E-5	4.9E-5	5.1E-5
	Pre-burn leach 1	9.3E-4	9.0E-4	9.7E-4	1.0E-3	9.2E-4	9.6E-4
	Pre-burn leach 2	4.5E-4	4.4E-4	4.9E-4	4.8E-4	4.7E-4	4.9E-4
	Post-burn leach 1	1.9E-4	2.5E-4	1.1E-4	1.1E-4	1.0E-4	9.8E-5
	Post-burn leach 2	4.6E-6	5.0E-6	1.8E-6	1.9E-6	1.1E-6	1.6E-6
	SUM (MDA = 0)	1.6E-3	1.6E-3	1.6E-3	1.7E-3	1.5E-3	1.6E-3
Segment #3	Decon	4.6E-5	3.7E-5	1.8E-4	1.8E-4	1.8E-4	1.8E-4
	Pre-burn leach 1	1.9E-5	1.6E-5	4.2E-5	4.3E-5	4.0E-5	3.9E-5
	Pre-burn leach 2	1.3E-6	1.1E-6	<4E-07	2.1E-7	1.4E-7	2.2E-7
	Post-burn leach 1	5.1E-4	5.1E-4	5.2E-4	5.0E-4	5.1E-4	5.0E-4
	Post-burn leach 2	1.8E-6	2.0E-6	7.3E-7	7.3E-7	7.0E-7	6.8E-7
	SUM (MDA = 0)	5.8E-4	5.6E-4	7.5E-4	7.2E-4	7.3E-4	7.3E-4
Core	Decon	6.6E-3	4.9E-3	8.2E-3	7.6E-3	9.4E-3	9.9E-3
	Pre-burn leach 1	3.2E-3	3.3E-3	3.3E-3	3.0E-3	3.8E-3	3.9E-3
	Pre-burn leach 2	7.8E-5	8.6E-5	3.7E-5	3.4E-5	3.5E-5	3.6E-5
	Post-burn leach 1	1.3E-3	1.9E-3	1.4E-4	1.1E-4	1.2E-4	1.5E-4
	Post-burn leach 2	2.0E-6	2.7E-6	<4E-07	1.9E-7	2.0E-7	2.8E-7
	SUM (MDA = 0)	1.1E-2	1.0E-2	1.2E-2	1.1E-2	1.3E-2	1.4E-2
Compact TOTAL (MDA = 0)		1.7E-2	1.6E-2	1.8E-2	1.7E-2	2.0E-2	2.0E-2

A-7. Compact 12-1

Table 97. Activities of fission products measured in the solutions from RDLBL of Compact 12-1. All values were decay-corrected to EOI + 1 day. Compact 12-1 was corrected at various stages of RDLBL for accidental damage to five particles. See Section 4.7 for a discussion of Compact 12-1.

Activity (Bq)		Ag-110m	Ce-144	Cs-134	Cs-137	Eu-154	Eu-155	Ru-106	Sb-125	Sr-90
Segment #1	Decon	<3.0E+4	5.91E+7	1.27E+6	4.66E+6	4.24E+4	5.94E+4	8.49E+5	<3.7E+4	3.17E+6
	Decon Corrected	<3.0E+4	9.28E+6	0	1.61E+6	0	8.64E+3	0	<3.7E+4	3.36E+5
	Pre-burn leach 1	<1.1E+5	4.73E+5	2.09E+4	4.20E+5	<3.7E+3	<3.7E+3	4.14E+5	<2.6E+4	4.53E+4
	Pre-burn leach 2	<2.6E+4	1.10E+5	7.24E+2	1.17E+4	<1.5E+3	<3.0E+3	6.15E+4	<3.3E+3	3.31E+3
	Post-burn leach 1	<3.7E+4	<1.5E+5	3.29E+3	5.17E+4	4.98E+3	3.00E+3	<1.5E+5	<7.4E+3	1.16E+4
	Post-burn leach 2	<2.2E+4	<1.5E+5	2.95E+3	2.27E+4	<1.9E+3	<3.7E+3	<1.1E+5	<3.7E+3	5.50E+3
	Sum (MDA = 0)	0	5.97E+7	1.30E+6	5.17E+6	4.74E+4	6.24E+4	1.32E+6	0	3.23E+6
	Sum (MDA = 0) Corrected	0	9.87E+6	2.79E+4	2.12E+6	4.98E+3	1.16E+4	4.75E+5	0	4.01E+5
Segment #2	Decon	<3.7E+4	3.33E+7	7.30E+5	2.80E+6	2.21E+4	3.08E+4	6.92E+5	<1.9E+4	1.95E+6
	Decon Corrected	<3.7E+4	8.34E+6	0	1.27E+6	0	5.46E+3	0	<1.9E+4	5.35E+5
	Pre-burn leach 1	<2.2E+4	1.01E+5	6.46E+3	3.04E+4	<1.9E+3	<3.7E+3	1.08E+5	<7.4E+3	5.78E+3
	Pre-burn leach 2	<3.7E+4	<1.5E+5	1.86E+3	2.12E+4	<2.6E+3	<3.7E+3	6.35E+4	<7.4E+3	6.74E+3
	Post-burn leach 1	<7.4E+4	2.79E+7	4.79E+5	1.64E+6	2.37E+4	2.50E+4	2.07E+6	6.03E+4	1.58E+6
	Post-burn leach 2	<3.7E+4	6.98E+4	5.02E+3	3.07E+4	<2.6E+3	<3.7E+3	8.00E+4	<7.4E+3	1.44E+4
	Sum (MDA = 0)	0	6.13E+7	1.22E+6	4.52E+6	4.58E+4	5.58E+4	3.01E+6	6.03E+4	3.55E+6
	Sum (MDA = 0) Corrected	0	3.64E+7	4.92E+5	3.00E+6	2.37E+4	3.05E+4	2.32E+6	6.03E+4	2.14E+6
Segment #3	Decon	<1.1E+5	4.89E+7	8.30E+5	3.13E+6	3.34E+4	4.12E+4	8.58E+5	<7.4E+3	3.08E+6
	Decon Corrected	<1.1E+5	2.40E+7	0	1.60E+6	1.09E+4	1.58E+4	0	<7.4E+3	1.66E+6
	Pre-burn leach 1	<1.1E+4	5.46E+5	1.22E+4	6.24E+4	<1.1E+3	<1.1E+3	1.70E+5	<3.3E+3	3.50E+4
	Pre-burn leach 2	<1.1E+4	<3.7E+4	1.90E+3	3.32E+4	<1.1E+3	<1.1E+3	3.79E+4	<2.6E+3	1.47E+4
	Post-burn leach 1	<2.2E+4	1.16E+5	6.13E+4	2.40E+5	5.60E+3	3.53E+3	1.97E+5	<7.4E+3	1.62E+4
	Post-burn leach 2	<1.1E+4	<3.7E+4	9.05E+3	4.08E+4	4.07E+3	2.92E+3	6.84E+4	<3.3E+3	1.16E+4
	Sum (MDA = 0)	0	4.96E+7	9.14E+5	3.50E+6	4.30E+4	4.77E+4	1.33E+6	0	3.16E+6
	Sum (MDA = 0) Corrected	0	2.46E+7	8.45E+4	1.98E+6	2.06E+4	2.23E+4	4.74E+5	0	1.74E+6
Core	Decon	<1.5E+5	2.96E+8	2.88E+6	1.12E+7	1.83E+5	2.35E+5	1.45E+7	4.42E+5	1.15E+7
	Pre-burn leach 1	<1.5E+5	3.99E+7	8.00E+5	2.78E+6	2.78E+4	2.44E+4	2.31E+7	2.68E+5	1.85E+6
	Pre-burn leach 2	<7.4E+4	1.47E+6	1.35E+5	3.89E+5	<3.3E+3	<7.4E+3	5.38E+5	7.23E+4	6.71E+4
	Post-burn leach 1	<1.1E+5	3.68E+7	5.88E+5	1.99E+6	6.18E+4	5.32E+4	3.54E+6	4.54E+5	2.65E+6
	Post-burn leach 2	<7.4E+4	3.33E+5	1.33E+4	5.59E+4	<3.0E+3	<7.4E+3	1.16E+6	4.74E+4	3.54E+4
	Sum (MDA = 0)	0	3.74E+8	4.41E+6	1.64E+7	2.72E+5	3.12E+5	4.29E+7	1.28E+6	1.61E+7
Compact TOTAL (MDA = 0)	0	5.45E+8	7.85E+6	2.96E+7	4.09E+5	4.78E+5	4.85E+7	1.34E+6	2.60E+7	
Compact TOTAL (MDA = 0) Corrected	0	4.45E+8	5.02E+6	2.35E+7	3.22E+5	3.77E+5	4.61E+7	1.34E+6	2.03E+7	

Table 98. Fraction (M/C) of the compact inventory of fission products measured in the solutions from the radial deconsolidation of Compact 12-1. All values were decay-corrected to EOI + 1 day. Compact 12-1 was corrected at various stages of RDLBL for accidental damage to five particles. See Section 4.7 for a discussion of Compact 12-1.

Compact Fraction		Ag-110m	Ce-144	Cs-134	Cs-137	Eu-154	Eu-155	Ru-106	Sb-125	Sr-90
Segment #1	Decon	<3.8E-3	1.24E-3	1.00E-3	1.59E-3	9.84E-4	1.22E-3	1.38E-4	<1.8E-4	1.17E-3
	Decon Corrected	<3.8E-3	1.94E-4	0	5.51E-4	0	1.78E-4	0	<1.8E-4	1.24E-4
	Pre-burn leach 1	<1.4E-2	9.90E-6	1.65E-5	1.44E-4	<8.6E-5	<7.6E-5	6.73E-5	<1.3E-4	1.67E-5
	Pre-burn leach 2	<3.3E-3	2.30E-6	5.70E-7	4.01E-6	<3.4E-5	<6.1E-5	9.99E-6	<1.6E-5	1.22E-6
	Post-burn leach 1	<4.7E-3	<3.1E-6	2.59E-6	1.77E-5	1.16E-4	6.17E-5	<2.4E-5	<3.7E-5	4.29E-6
	Post-burn leach 2	<2.8E-3	<3.1E-6	2.32E-6	7.74E-6	<4.3E-5	<7.6E-5	<1.8E-5	<1.8E-5	2.03E-6
	Sum (MDA = 0)	0	1.25E-3	1.02E-3	1.77E-3	1.10E-3	1.28E-3	2.15E-4	0	1.19E-3
	Sum (MDA = 0) Corrected	0	2.06E-4	2.19E-5	7.24E-4	1.16E-4	2.39E-4	7.72E-5	0	1.48E-4
Segment #2	Decon	<4.7E-3	6.96E-4	5.75E-4	9.56E-4	5.12E-4	6.34E-4	1.12E-4	<9.1E-5	7.19E-4
	Decon Corrected	<4.7E-3	1.74E-4	0	4.35E-4	0	1.12E-4	0	<9.1E-5	1.97E-4
	Pre-burn leach 1	<2.8E-3	2.10E-6	5.09E-6	1.04E-5	<4.3E-5	<7.6E-5	1.76E-5	<3.7E-5	2.13E-6
	Pre-burn leach 2	<4.7E-3	<3.1E-6	1.46E-6	7.25E-6	<6.0E-5	<7.6E-5	1.03E-5	<3.7E-5	2.48E-6
	Post-burn leach 1	<9.4E-3	5.84E-4	3.77E-4	5.61E-4	5.50E-4	5.13E-4	3.36E-4	2.98E-4	5.81E-4
	Post-burn leach 2	<4.7E-3	1.46E-6	3.95E-6	1.05E-5	<6.0E-5	<7.6E-5	1.30E-5	<3.7E-5	5.31E-6
	Sum (MDA = 0)	0	1.28E-3	9.62E-4	1.55E-3	1.06E-3	1.15E-3	4.89E-4	2.98E-4	1.31E-3
	Sum (MDA = 0) Corrected	0	7.62E-4	3.87E-4	1.02E-3	5.50E-4	6.26E-4	3.77E-4	2.98E-4	7.88E-4
Segment #3	Decon	<1.4E-2	1.02E-3	6.53E-4	1.07E-3	7.74E-4	8.47E-4	1.39E-4	<3.7E-5	1.13E-3
	Decon Corrected	<1.4E-2	5.02E-4	0	5.47E-4	2.53E-4	3.26E-4	0	<3.7E-5	6.13E-4
	Pre-burn leach 1	<1.4E-3	1.14E-5	9.62E-6	2.13E-5	<2.6E-5	<2.3E-5	2.77E-5	<1.6E-5	1.29E-5
	Pre-burn leach 2	<1.4E-3	<7.7E-7	1.50E-6	1.13E-5	<2.6E-5	<2.3E-5	6.16E-6	<1.3E-5	5.43E-6
	Post-burn leach 1	<2.8E-3	2.42E-6	4.83E-5	8.20E-5	1.30E-4	7.26E-5	3.20E-5	<3.7E-5	5.96E-6
	Post-burn leach 2	<1.4E-3	<7.7E-7	7.13E-6	1.40E-5	9.43E-5	6.01E-5	1.11E-5	<1.6E-5	4.26E-6
	Sum (MDA = 0)	0	1.04E-3	7.20E-4	1.20E-3	9.98E-4	9.80E-4	2.16E-4	0	1.16E-3
	Sum (MDA = 0) Corrected	0	5.15E-4	6.65E-5	6.76E-4	4.77E-4	4.58E-4	7.70E-5	0	6.42E-4
Core	Decon	<1.9E-2	6.19E-3	2.27E-3	3.82E-3	4.24E-3	4.83E-3	2.36E-3	2.19E-3	4.22E-3
	Pre-burn leach 1	<1.9E-2	8.35E-4	6.30E-4	9.51E-4	6.45E-4	5.01E-4	3.75E-3	1.33E-3	6.81E-4
	Pre-burn leach 2	<9.4E-3	3.07E-5	1.06E-4	1.33E-4	<7.7E-5	<1.5E-4	8.74E-5	3.57E-4	2.47E-5
	Post-burn leach 1	<1.4E-2	7.70E-4	4.63E-4	6.79E-4	1.43E-3	1.09E-3	5.76E-4	2.25E-3	9.76E-4
	Post-burn leach 2	<9.4E-3	6.97E-6	1.05E-5	1.91E-5	<6.9E-5	<1.5E-4	1.89E-4	2.34E-4	1.31E-5
	Sum (MDA = 0)	0	7.83E-3	3.47E-3	5.60E-3	6.32E-3	6.42E-3	6.97E-3	6.35E-3	5.92E-3
Compact TOTAL (MDA = 0)		0	1.14E-2	6.18E-3	1.01E-2	9.48E-3	9.83E-3	7.89E-3	6.65E-3	9.58E-3
Compact TOTAL (MDA = 0) Corrected		0	9.31E-3	3.95E-3	8.02E-3	7.46E-3	7.74E-3	7.50E-3	6.65E-3	7.50E-3

A-8. Compact 12-3

Table 99. Activities of fission products measured in the solutions from the radial deconsolidation of Compact 12-3. Values are given for both the unspilled and spilled but recovered portions from the core deconsolidation. The compact total is the sum of activity from all solutions from Segment 1 and the core. All values were decay-corrected to EOI + 1 day. There were no indications of accidental damage to any of the particles. See Section 4.8 for a discussion of Compact 12-3.

Activity (Bq)		Ag-110m	Ce-144	Cs-134	Cs-137	Eu-154	Eu-155	Ru-106	Sb-125	Sr-90
Segment #1	Decon	<7.4E+3	<3.7E+4	1.35E+4	5.64E+4	<3.7E+2	<1.1E+3	<7.4E+4	<3.3E+3	1.81E+3
	Pre-burn leach 1	<2.2E+4	<7.4E+4	1.16E+3	1.30E+4	<1.5E+3	<3.0E+3	<7.4E+4	<3.3E+3	6.02E+3
	Pre-burn leach 2	<2.2E+4	<1.5E+5	<2.2E+3	5.84E+3	<1.9E+3	<3.7E+3	<7.4E+4	<3.7E+3	3.46E+3
	Post-burn leach 1	<2.2E+4	<1.5E+5	<2.2E+3	6.92E+3	6.09E+3	4.90E+3	<7.4E+4	<3.7E+3	5.70E+3
	Post-burn leach 2	<1.1E+4	<7.4E+4	<1.1E+3	1.01E+3	<1.5E+3	<2.6E+3	<3.7E+4	<2.6E+3	1.16E+3
	Total (MDA = 0)	N/A	N/A	1.46E+4	8.32E+4	6.09E+3	4.90E+3	N/A	N/A	1.82E+4
Core	Decon	<2.5E+5	1.91E+8	2.40E+6	1.07E+7	1.07E+5	1.59E+5	8.41E+6	2.26E+5	1.01E+7
	Pre-burn Leach 1 Unspilled	<3.3E+5	7.36E+7	1.12E+6	4.64E+6	4.23E+4	5.79E+4	1.64E+6	1.58E+5	5.16E+6
	Pre-burn Leach 1 Spilled	<4.4E+5	9.75E+7	2.10E+6	9.56E+6	7.46E+4	1.10E+5	3.98E+6	3.39E+5	8.55E+6
	Pre-burn Leach 2 Unspilled	<1.2E+5	<3.7E+5	4.35E+3	2.04E+4	<2.7E+3	<5.9E+3	<2.0E+5	8.72E+3	1.69E+4
	Pre-burn Leach 2 Spilled	<1.1E+5	2.04E+5	9.51E+3	4.13E+4	<2.2E+3	<5.2E+3	8.03E+5	4.26E+4	5.03E+4
	Post-burn Leach 1 Unspilled	<8.1E+4	6.48E+5	4.41E+3	1.98E+4	7.02E+3	3.94E+3	4.79E+5	1.62E+4	1.01E+5
	Post-burn Leach 1 Spilled	<9.3E+4	7.91E+5	2.37E+3	1.41E+4	7.33E+3	4.77E+3	1.70E+5	8.77E+3	1.24E+5
	Post-burn Leach 2 Unspilled	<8.1E+4	3.93E+5	6.43E+3	2.63E+4	<2.1E+3	<4.8E+3	2.87E+5	9.33E+3	2.52E+3
	Post-burn Leach 2 Spilled	<1.2E+5	<3.2E+5	<4.1E+3	1.68E+3	<1.7E+3	<4.4E+3	1.62E+5	<5.2E+3	1.14E+3
	Total (MDA = 0) Unspilled + Decon	N/A	2.66E+8	3.53E+6	1.54E+7	1.56E+5	2.21E+5	1.08E+7	4.18E+5	1.53E+7
	Total (MDA = 0) Spilled Only	N/A	9.85E+7	2.11E+6	9.62E+6	8.19E+4	1.14E+5	5.12E+6	3.90E+5	8.72E+6
	Total (MDA = 0)	N/A	3.65E+8	5.65E+6	2.50E+7	2.38E+5	3.36E+5	1.59E+7	8.08E+5	2.41E+7
Compact TOTAL (MDA = 0)		N/A	3.65E+8	5.66E+6	2.51E+7	2.44E+5	3.41E+5	1.59E+7	8.08E+5	2.41E+7

Table 100. Fraction of fission products measured in the solutions from the radial deconsolidation of Compact 12-3 compared to the calculated inventory (M/C). Values are given for both the unspilled and spilled but recovered portions from the core deconsolidation. Compact total is sum of M/Cs from all solutions from Segment 1 and the core. All values were decay-corrected to EOI + 1 day. There were no indications of accidental damage to any of the particles. See Section 4.8 for a discussion of Compact 12-3.

Compact Fraction (M/C)		Ag-110m	Ce-144	Cs-134	Cs-137	Eu-154	Eu-155	Ru-106	Sb-125	Sr-90
Segment #1	Decon	<1.5E-3	<8.7E-7	1.42E-5	2.19E-5	<1.2E-5	<2.6E-5	<1.5E-5	<1.9E-5	7.48E-7
	Pre-burn leach 1	<4.5E-3	<1.7E-6	1.23E-6	5.04E-6	<4.7E-5	<7.0E-5	<1.5E-5	<1.9E-5	2.49E-6
	Pre-burn leach 2	<4.5E-3	<3.5E-6	<2.3E-6	2.26E-6	<5.8E-5	<8.8E-5	<1.5E-5	<2.1E-5	1.43E-6
	Post-burn leach 1	<4.5E-3	<3.5E-6	<2.3E-6	2.68E-6	1.92E-4	1.16E-4	<1.5E-5	<2.1E-5	2.36E-6
	Post-burn leach 2	<2.3E-3	<1.7E-6	<1.2E-6	3.92E-7	<4.7E-5	<6.1E-5	<7.5E-6	<1.5E-5	4.81E-7
	Total (MDA = 0)	N/A	N/A	1.55E-5	3.22E-5	1.92E-4	1.16E-4	N/A	N/A	7.51E-6

Compact Fraction (M/C)		Ag-110m	Ce-144	Cs-134	Cs-137	Eu-154	Eu-155	Ru-106	Sb-125	Sr-90
Core	Decon	<5.0E-2	4.50E-3	2.54E-3	4.13E-3	3.36E-3	3.77E-3	1.69E-3	1.30E-3	4.16E-3
	Pre-burn Leach 1 Unspilled	<6.7E-2	1.73E-3	1.18E-3	1.80E-3	1.33E-3	1.37E-3	3.30E-4	9.14E-4	2.13E-3
	Pre-burn Leach 1 Spilled	<9.0E-2	2.29E-3	2.22E-3	3.70E-3	2.35E-3	2.59E-3	8.02E-4	1.96E-3	3.53E-3
	Pre-burn Leach 2 Unspilled	<2.5E-2	<8.7E-6	4.60E-6	7.90E-6	<8.5E-5	<1.4E-4	<4.1E-5	5.04E-5	7.01E-6
	Pre-burn Leach 2 Spilled	<2.2E-2	4.81E-6	1.01E-5	1.60E-5	<6.9E-5	<1.2E-4	1.62E-4	2.46E-4	2.08E-5
	Post-burn Leach 1 Unspilled	<1.7E-2	1.52E-5	4.66E-6	7.68E-6	2.21E-4	9.32E-5	9.65E-5	9.33E-5	4.20E-5
	Post-burn Leach 1 Spilled	<1.9E-2	1.86E-5	2.51E-6	5.46E-6	2.31E-4	1.13E-4	3.43E-5	5.07E-5	5.12E-5
	Post-burn Leach 2 Unspilled	<1.7E-2	9.24E-6	6.79E-6	1.02E-5	<6.8E-5	<1.1E-4	5.78E-5	5.39E-5	1.04E-6
	Post-burn Leach 2 Spilled	<2.4E-2	<7.5E-6	<4.3E-6	6.49E-7	<5.2E-5	<1.1E-4	3.25E-5	<3.0E-5	4.70E-7
	Total (MDA = 0) Unspilled + Decon	N/A	6.25E-3	3.74E-3	5.95E-3	4.91E-3	5.23E-3	2.18E-3	2.41E-3	6.35E-3
	Total (MDA = 0) Spilled Only	N/A	2.32E-3	2.23E-3	3.73E-3	2.58E-3	2.71E-3	1.03E-3	2.25E-3	3.61E-3
	Total (MDA = 0)	N/A	8.57E-3	5.97E-3	9.68E-3	7.49E-3	7.94E-3	3.21E-3	4.67E-3	9.95E-3
Compact TOTAL (MDA = 0)		N/A	8.57E-3	5.99E-3	9.71E-3	7.69E-3	8.06E-3	3.21E-3	4.67E-3	9.96E-3

Table 101. Masses of select actinides from ICP-MS analysis of Compact 12-3 RDLBL. There were no indications of accidental damage to any of the particles. See Section 4.8 for a discussion of Compact 12-3.

		Mass (µg)					
		Pu-239	Pu-240	U-234	U-235	U-236	U-238
Segment #1	Decon	<0.03	<0.008	<0.02	<0.09	<0.03	5.25E-1
	Pre-burn leach 1	<0.06	<0.02	<0.06	<0.4	<0.08	<1
	Pre-burn leach 2	<0.08	<0.04	<0.09	3.86E-1	<0.1	7.40E-1
	Post-burn leach 1	<0.07	<0.03	<0.08	<0.5	<0.1	1.71E+0
	Post-burn leach 2	<0.07	<0.03	<0.08	<0.3	<0.1	<0.5
	Total (MDA = 0)	N/A	N/A	N/A	3.86E-1	N/A	2.98E+0
Core	Decon	1.38E+1	1.96E+0	2.59E+0	2.91E+2	2.28E+1	1.54E+3
	Pre-burn Leach 1 Unspilled	4.59E+0	6.98E-1	1.10E+0	1.28E+2	9.99E+0	7.07E+2
	Pre-burn Leach 1 Spilled	1.44E+1	2.14E+0	2.34E+0	2.68E+2	1.82E+1	1.25E+3
	Pre-burn Leach 2 Unspilled	<0.04	<0.02	<0.02	4.09E-1	2.50E-2	2.07E+0
	Pre-burn Leach 2 Spilled	2.99E-1	<0.03	<0.01	7.49E-1	6.29E-2	1.39E+0
	Post-burn Leach 1 Unspilled	4.95E-2	<0.01	<0.01	5.75E-1	4.22E-2	2.98E+0
	Post-burn Leach 1 Spilled	4.13E-2	<0.01	<0.01	3.99E-1	3.06E-2	2.10E+0
	Post-burn Leach 2 Unspilled	<0.03	<0.02	<0.02	3.15E-1	<0.03	1.64E+0
	Post-burn Leach 2 Spilled	<0.2	<0.1	<0.2	<0.1	<0.2	<0.1
	Total Unspilled + Decon (MDA = 0)	1.85E+1	2.66E+0	3.69E+0	4.20E+2	3.29E+1	2.25E+3

	Total Spilled (MDA = 0)	1.47E+1	2.14E+0	2.34E+0	2.69E+2	1.83E+1	1.26E+3
	Grand Total (MDA) = 0	3.32E+1	4.80E+0	6.04E+0	6.88E+2	5.12E+1	3.51E+3
Compact Total (MDA = 0)		3.32E+1	4.80E+0	6.04E+0	6.89E+2	5.12E+1	3.51E+3

Table 102. Compact fractions for select actinides from ICP-MS analysis of Compact 12-3 RDLBL. There were no indications of accidental damage to any of the particles. See Section 4.8 for a discussion of Compact 12-3.

		Compact Fraction					
		Pu-239	Pu-240	U-234	U-235	U-236	U-238
Segment #1	Decon	<9.0E-6	<1.5E-5	<3.5E-5	<1.4E-6	<6.0E-6	1.48E-6
	Pre-burn leach 1	<1.8E-5	<3.7E-5	<1.1E-4	<6.4E-6	<1.6E-5	<2.8E-6
	Pre-burn leach 2	<2.4E-5	<7.5E-5	<1.6E-4	6.15E-6	<2.0E-5	2.09E-6
	Post-burn leach 1	<2.1E-5	<5.6E-5	<1.4E-4	<8.0E-6	<2.0E-5	4.83E-6
	Post-burn leach 2	<2.1E-5	<5.6E-5	<1.4E-4	<4.8E-6	<2.0E-5	<1.4E-6
	Total (MDA = 0)	N/A	N/A	N/A	6.15E-6	N/A	8.40E-6
Core	Decon	4.17E-3	3.68E-3	4.58E-3	4.63E-3	4.55E-3	4.35E-3
	Pre-burn Leach 1 Unspilled	1.38E-3	1.31E-3	1.94E-3	2.03E-3	1.99E-3	2.00E-3
	Pre-burn Leach 1 Spilled	4.33E-3	4.02E-3	4.14E-3	4.27E-3	3.62E-3	3.54E-3
	Pre-burn Leach 2 Unspilled	<1.2E-5	<3.7E-5	<3.5E-5	6.52E-6	4.98E-6	5.83E-6
	Pre-burn Leach 2 Spilled	9.00E-5	<5.6E-5	<1.8E-5	1.19E-5	1.25E-5	3.92E-6
	Post-burn Leach 1 Unspilled	1.49E-5	<2.5E-5	<1.8E-5	9.16E-6	8.41E-6	8.40E-6
	Post-burn Leach 1 Spilled	1.24E-5	<1.9E-5	<1.6E-5	6.35E-6	6.09E-6	5.94E-6
	Post-burn Leach 2 Unspilled	<1.0E-5	<3.7E-5	<3.5E-5	5.02E-6	<5.3E-6	4.62E-6
	Post-burn Leach 2 Spilled	<6.0E-5	<1.9E-4	<3.5E-4	<1.6E-6	<4.0E-5	<2.8E-7
	Total Unspilled + Decon (MDA = 0)	5.56E-3	4.99E-3	6.53E-3	6.69E-3	6.55E-3	6.36E-3
	Total Spilled (MDA = 0)	4.43E-3	4.02E-3	4.14E-3	4.28E-3	3.64E-3	3.55E-3
	Grand Total (MDA) = 0	9.99E-3	9.00E-3	1.07E-2	1.10E-2	1.02E-2	9.91E-3
	Compact Total (MDA = 0)		9.99E-3	9.00E-3	1.07E-2	1.10E-2	1.02E-2